1994

Design of rock bolting systems for underground excavations

Dianmin Chen
University of Wollongong

DESIGN OF ROCK BOLTING SYSTEMS FOR UNDERGROUND EXCAVATIONS

A thesis submitted in fulfilment of the requirements for the award of the degree

DOCTOR OF PHILOSOPHY

from

UNIVERSITY OF WOLLONGONG

By

DIANMIN CHEN, B.E.(Honours)

DEPARTMENT OF CIVIL AND MINING ENGINEERING

1994

AFFIRMATION

I hereby declare that the research work described in this thesis is my own work except where specifically indicated and has not been submitted for a degree to any other university or institute.

The following publications have been extracted from the present research.

Singh R. N., Porter I. and **Chen D.**, 1991; Integrated computer aided stability analysis and rock bolting design for underground excavations. Proc. 12th Science and Technology Congress, Turkey, PP245-258.

Porter I. and **Chen D.**, 1992; Stability analysis and rock bolting design in a multiple joint rock mass. Journal of Mining Research, Vol. 1, No. 3, PP7-18.

Chen D., Porter I. and Singh R. N., 1993; Determination of major discontinuity sets for stability analysis in a jointed rock mass. Int. Symp. Application of Computer Methods in Rock Mechanics and Engineering, Xian, China, Vol. 1, PP187-194.

Dianmin Chen

July, 1994

ACKNOWLEDGMENTS

The author would like to express sincere gratitude to Professor R. N. Singh, Head of Department Civil and Mining Engineering, University of Wollongong, for the invitation to work in the Department as a Visiting Fellow and for providing the facilities and support for this PhD project. Sincere appreciation is also due to Dr I. Porter and Professor R. N. Singh for their invaluable supervision, useful discussions and enthusiastic encouragement during the period of the research; without which the research would not have been possible.

The author is indebted to the University of Wollongong for offering two postgraduate research awards without which completion of the project would have been very difficult. The author would also like to thank Pasminco Mining, Broken Hill Operation and CSA Mine, Cobar for providing the sites for the field investigations. Thanks are also extended to the Changsha Institute of Mining Research, China, for providing leave of absence and continual support for the research conducted in Australia.

The author is grateful to all of the staff in the Department of Civil and Mining Engineering and the assistance from Associate Professor N. Aziz and Dr J. Shonhardt is particularly appreciated. The author also wishes to acknowledge fellow PhD candidate Mr M. Tavakoli and honours student Mr S. Graham for their assistance during the site investigations. Appreciation is also due to Mr D. Xu, Mr G. Smith and Mr K. Brooks for their valuable assistance.

Finally, the author would like to record his gratitude to all members of his family, in particular his parents-in-law and his wife, Ruoning Li, for their constant encouragement and selfless support. Special thanks are due to his lovely daughter, Shelley (Xiaomeng) Chen who brought much happiness during this period of intensive study.

ABSTRACT

Stability of underground structures is critical in underground mining. Every effort must be made to preserve stability for the safety of mining operations. There are a number of techniques available for reinforcing unstable rock masses, of which rock bolting is the most widely used. Due to the complexity of geological conditions and the variety of mining methods employed, reinforcement methods also vary widely. Rock bolting systems are designed to effectively utilise the capacity of the support elements and secure the safety of miners and the mining operation.

The focus of this research was a study of discontinuities and their influence on the stability of structures in a rock mass. To determine the jointing system in a rock mass, a three dimensional scanline technique was used to collect the necessary data. This technique was used to eliminate the bias that occurs when using horizontal scanlines. The data were processed statistically and the modified K-mean method is used to cluster the data into groups. The data points in the groups are the elements of the clusters. An assessment system treating the frequency, persistence, type and various mechanical properties of discontinuities was established to determine the major discontinuity sets which have a dominant influence on rock mass behaviour.

When the major discontinuity sets were determined, the stability of the rock mass was then analysed based on an assessment of the competence of the rock mass using a modified geomechanics classification system. The magnitude and direction of the local stress field and the geometry of the opening were taken into

consideration by introducing a correction to the rock mass rating. The initial design for the rock bolting system was then carried out.

Due to the presence of the discontinuities, the rocks are separated into blocks and weathering and infilling can occur between the walls of the discontinuities. The behaviour of a jointed rock mass may be governed by the discontinuities in sets and wedge failure may occur if the discontinuities intersect unfavourably. It is therefore necessary to identify potentially unstable wedges. The traditional stereographic projection technique is one of the most common methods used and the major limitation of which is that it can only provide a graphical solution for those wedges defined by three discontinuity sets. It is also time consuming and tedious. In this project a computer aided stereographic projection technique was developed. The geometry of either tetrahedral or polyhedral wedges can now be determined. The removability of the wedges is then evaluated. If the wedge is removable the number of bolts required may then be calculated.

Based on the initial design and the support requirements of potentially unstable wedges, a final decision on the rock bolting system to stabilise the area of interest can be made. The system developed here assists on-site designers by providing a reliable and on-going method of arriving at the primary roof bolting scheme.

The applicability of the system has been tested and demonstrated in underground excavations at Pasminco Mining Broken Hill Operation and at CSA Mine, Cobar. The results obtained indicated that an enhanced rock bolting system should be adopted in the stopes in the NBHC Mine. The results agreed broadly with the current empirical design used at CSA Mine, Cobar.

This research has shown that the discontinuities in a rock mass have a significant bearing on the rock mass behaviour. The rock bolting design is directly relevant to the safety and effectiveness of an underground mining operation. The design approach resulting from this research will provide a reliable rock bolting system for underground structures in a jointed rock mass.

CONTENTS

LIST OF FIGURES

LIST OF TABLES

NOTATIONS

A	total rock mass rating
$A \cap B$	intersection of A and B
$A \subset B$	A is a subset of B
A_b	cross-sectional area of a bolt, mm^2
A_i, B_i, C_i, D_i	constants associated with orientation of discontinuity planes
$A_r(i)$	area of the i-th sliding face, m^2
B	intact rock strength (IRS) rating
B_l	length of bolts, m
BP	block pyramid
B_s	spacing of bolts, m
C	intact rock strength (IRS) of intact rock specimen
C_F	continuity factor
C_i	cohesion coefficient of the i-th plane
C_m	stress modification coefficient
C_o	distance from the centre of semicircle arch to the origin, m
C_s	stability coefficient
d	diameter of a borehole, mm
DRMS	design rock mass strength, MPa
E	mean value in statistical analysis
E_{ij}^2	variance of the rotation of $\widehat{M}$ about axis μ_k
EP	excavation pyramid
F_c	cohesion force, kN
F_d	difference of F_t and F_w
F_f	friction force, kN
F_F	frequency factor
F_g	gravity, kN
F(i)	frequency of discontinuities in the i-th set
F(i)	i-th force acting on a wedge, kN
F_{max}	frequency of discontinuities in the set with the maximum number of discontinuities
F_s	factor of safety
F_t	resultant force, kN
F_w	total force to anti-sliding, kN
g	order number of a tetrahedral wedge
h	integer

H	height of sidewall, m
H_{mw}	the maximum height of a wedge, m
H_t	height of rock load, m
H_w	height of a wedge, m
H_z	distance from projection level to floor, m
I_o	original angle of the joint asperities arising in the direction of shear
IRMS	in-situ rock mass strength, MPa
IRS	intact rock strength, MPa
JP	joint pyramid
K	constant
K_i	slope of the i-th strike line
$K_i^!$	slope of intersection projection of two planes
$\bar{l}$, $\bar{m}$, $\bar{n}$	direction cosine of a plane
L_1	length of anchoring, m
L_2	length in zone to be stabilised, m
L(i)	mean trace length of discontinuities in the i-th set, m
L_{max}	mean trace length of the discontinuities in the set with the maximum number of discontinuities, m
M	number of clusters in partition P
$\widehat{M}$	a set of three axis in space
n	order number of a discontinuity in a set
N	total number of discontinuity planes
n_1	number of corners of a wedge
N_b	number of bolts
N_c	number of discontinuities forming a wedge
N^c	number of cables designed
n_f	number of forces acting on a wedge
N_g	number of tedrahedral wedges in a polyhedral wedge
N_i	number of possible intersection of every two strike lines
N_j	number of points in cluster j of partition P
N_k	points expected in a spherical quadrilateral
ox(t), oy(t), oz(t)	coordinates of apexes of a wedge
P_A	bolting load of a bolt, kN
P_b	load provided by a bolting system in a unit length of an opening, kN/m
P_i	i-th plane
P_i^n	magnitude of normal reaction force
P_r	rock load, kN
P_s	load capacity of rock bolting system in a unit length of an opening, kN

P_y	yield load provided by a rock bolt, kN
q	order number of a face in a tetrahedral wedge
r	distance from a pole G to the centre of the reference circle
$\vec{r}$	active resultant force, kN
R	radius of reference circle, mm
R_0	radius of semi-circle arch of an opening
R_i	radius of the i-th great circle
R_i, R_j	normal reactions provided by planes i and j, kN
RMR	rock mass rating
RMR'	modified rock mass rating
s	vector of sliding direction
S_P	spacing of discontinuities, m
SP	space pyramid
t	thickness of reinforced rock, m
t	variable used in statistical analysis
v	integer in the Gamma function
V_{poly}	volume of a polyhedral wedge, m^3
$V_{tetr}(g)$	volume of a tedrahedral wedge, m^3
V_w	volume of a wedge, m^3
W	weight of a wedge, kN
W	half width of an excavation, m
$x_1(i)$, $y_1(i)$, $z_1(i)$	coordinates of a point at any discontinuity plane
$x_A(t)$, $y_A(t)$	coordinates of an apex on the projection level
x_{A_1}, y_{A_1}, z_{A_1}	coordinates of a point on the arch roof
$\bar{X}_c$	centroid of a cluster
$x_c(h)$, $y_c(h)$	coordinates of the intersection of two strike lines
xf(i), yf(i), zf(i)	coordinates of corners of a wedge on free face
x_i, y_i	coordinates of the centre of a great circle in Chapter 5
x_i, y_i, z_i	coordinates of a point in the spherical coordinate system in Chapter 3.
X_i, Y_i	coordinates of any pole in the reference circle
$\bar{X}_i$, $\bar{X}_j$	centroids of clusters i and j.
X_j^i	i-th element of cluster j
$x_L(i)$, $y_L(i)$	coordinates of intersection of two great circles
α	direction of acceleration
α_i, β_i	dip and dip direction of the i-th plane
α_i'	dip of the intersection of two planes
β_0	azimuth of the Y axis

ϕ	friction angle of a rock mass
ϕ_o	angle of residual friction on the smooth joint surface
ϕ_i, ϕ_j	friction angles of discontinuity planes i and j
Φ	angle between horizontal level and the line O'A
γ_r	unit weight of rocks, kN/m^3
γ_{ij}	dip angle of intersection of two planes
μ_1, μ_2, μ_3	three axes used in Bingham's distribution
θ_{ab}	angle between the development and the projection of the line ab
θ_i	angle between plunge of a cable and the normal to the sliding face
σ	strength of bolts or cables (shear strength or tensile strength), MPa
σ_{cjs}	integral normal compressive strength on the joint surface, MPa
σ_{cjw}	compressive strength of the joint walls, MPa
σ_h	horizontal stress, MPa
σ_v	vertical stress, MPa
$\Delta\sigma_1$	effective increase in the allowable stress of the rock mass, MPa
$\Delta\sigma_3$	increase in rock mass confinement (minimum principal stress), MPa
τ	shear stress, MPa
τ	variable in statistical analysis
τ_{bond}	average working bond stress between grout and borehole wall or grout and bolt, MPa
ω	downwards vector
ω_1, ω_2, ω_3	eigenvectors
ψ_{ab}	true dip of the line ab
ψ_{abt}, ψ_{act}, ψ_{bct}	apparent dip of the traces ab, ac and bc respectively
ψ_{abt}', ψ_{bct}'	dips of the lines of intersection on the walls of an opening
ψ_i, ψ_j	angle between planes i and j and a vertical plane
ψ_{ij}	angle between P_i and P_j
ξ_1, ξ_2, ξ_3	dispersion parameters

DEFINITION OF GEOLOGICAL TERMS

The following definitions (Piteau, 1970, Goodman, 1976, ISRM, 1978) have been employed in the text:

Rock mass: Rock mass is defined as an aggregate of blocks of solid rock material containing systems of structural features, such as joints, bedding planes and faults. These features constitute mechanical discontinuities. The rock mass refers to any in-situ rock containing all inherent geomechanical anisotropies.

Rock material: Rock material or intact rock refers to the consolidated and cemented assemblage of mineral particles which form the intact blocks between discontinuities in the rock mass.

Structural discontinuities: These include all geological features that separate the solid blocks of the rock mass. The term 'discontinuity' is generally used to define the structural weakness plane upon which movement can take place, such as faults, dykes, bedding planes, tension joints, shear joints, fault zones and shear zones.

Major discontinuities: These structures which are sufficiently developed and have enough continuity that shear failure along them will not involve shearing of any intact rock materials.

Discontinuity sets: These are systems of discontinuities which have approximately the same inclination and orientation. As a result of the processes

involved in their formation, most discontinuities occur in families which have preferred directions.

Major discontinuity sets or dominant discontinuity sets: These discontinuity sets have significant bearing on the stability of structures and openings i.e. they dominate the behaviour of the rock mass surrounding a structure.

Infilling material or gauge: Infilling is the material between two faces of a discontinuity plane such as a fault. This material may be the debris resulting from the sliding of one surface upon another or it may be material which has been precipitated from solution or caused by weathering. The presence of infilling material in a discontinuity will have a significant influence on the shear strength of the discontinuity.

Roughness: Asperities of discontinuities which are considered to be sufficiently small that they are likely to be sheared off during movement along the discontinuity plane.

Waviness: A major or first order scale of roughness is regarded as waviness of the mean discontinuity surfaces. These are considered to be of such dimensions that they are unlikely to be sheared and for practical purposes appear as undulations of the planes.

The waviness and roughness used to be two fuzzy concepts. No quantitative data were available to separate them. In 1975 an extension was made in order to separate waviness from roughness in a quantitative manner. "Irregularities on the joint surfaces which occur with a base length of 250 mm or less are considered as

roughness" (Steffen et al, 1975). If the base length exceeds 250 mm the irregularity is described as waviness.

Spacing: Spacing is the term used to express the length between two discontinuity planes within a set of discontinuities. It can be defined as $ds=l\sin\phi_p/N_a$, where d_s is spacing, l is the length of a scanline, ϕ_p is an acute angle between the discontinuity plane and the observation line, N_a is the number of discontinuities observed on a scanline.

Continuity: Continuity (or persistence) is one of the most important rock mass parameters. However, it is also one of the most difficult to quantify. It is used to describe the size of a discontinuity within a plane and has a significant influence on the strength of the rock mass (Brady & Brown, 1985). A number of researchers(Cruden 1977, Priest & Hudson, 1981, and Pahl, 1981) have attempted to put a value on persistence and it is generally accepted that the trace length, as measured from a scanline survey, be used for classification (ISRM, 1978).

Ground water: Ground water has a significant influence on the stability of structures in a jointed rock mass when compared with any other parameter concerning the mechanical properties of the discontinuities.

CHAPTER 1

STABILITY PROBLEMS IN UNDERGROUND EXCAVATIONS

1.1 INTRODUCTION

Due to the large number of orebodies occurring at considerable depths below the surface, underground mining is extensively used to exploit these deposits to obtain valuable minerals. This may involve formation of different types of opening, such as shafts, inclines, adits or declines to reach the deposit. Most of these excavations in underground mining were, and indeed still are, of a temporary nature. An optimum design should therefore provide safe access for miners within the life span of the structures at minimum cost.

In order to be competitive in the world market mining companies are making every effort to develop mechanisation in underground operations, with the purpose of dramatically increasing the productivity coupled with a substantial reduction in

manpower. Larger sized entries and stopes, larger service stations and other underground chambers with longer service lives may be required to provide effective access and sufficient space for larger capacity mining equipment. This may create some stability problems and therefore adequate support should be installed to secure excavations against rock falls and other types of rock failure.

In civil engineering however the excavations, including tunnels, underground power stations, caverns for the storage of oil or gas and nuclear waste and underground military facilities, are required to have longer service lives than those in mining engineering, say tens or hundreds of years. Permanent reinforcement will therefore be needed to keep the excavations stable.

In the case of a rock mass of good quality, an underground excavation can remain stable for many years without any support. However this may not always be possible and there is sometimes no other option but placement of an excavation in very bad geological conditions. Some rock masses are heavily jointed and the instability of an excavation in such rock masses may be inevitable after the rock is exposed. It is very dangerous to work under such a roof without support. Data from current operations show that roof collapse is one of the major causes of mining accidents and interruption to operations.

In mining and civil engineering, a number of factors affect the stability of an underground excavation. Five of the most important sources of instability in jointed rock masses are summarised as follows:

- Instability tends to occur due to unfavourable geological features. Roof falls in the form of blocks are considered as the most likely failure mode as

several sets of discontinuities are frequently intersected. The failure can be minimised or prevented by relocation or reorientation of the excavations.

- Instability due to excessively high stress may occur when mining at great depth and when very large excavations are created at relatively shallow depths. The gravitational and tectonic stresses are the most important influences on the stability of an excavation. The determination of both the magnitude and direction of the in-situ stress field plays a key role in the design of an excavation, particularly the geometry and location of an excavation with respect to the applied stress field. An optimised design of an excavation should be carried out so that high stress concentrations can be avoided.

- Instability due to incorrect sequences of mining or interaction of various excavations on surrounding rocks may occur when the mining openings or excavations are constructed at several levels and intersect vertically and horizontally. Mining activity in the rock mass causes a redistribution of the stress, resulting in stress increases in one area and decreases in another.

- Instability due to poor physical properties of rocks may occur when the rock is heavily weathered or jointed. The physical properties of rock can be determined from measurements carried out on the specimen in either the laboratory or field. However the in-situ strength of a rock mass is significantly lower than that obtained from laboratory specimens due to the presence of structural features (Vutukuri and Hassaini, 1991, 1992).

- Instability due to excessive ground water pressure or inflow can occur in almost any rock mass and may create serious problems when associated

with one of the other forms of instability already listed. When there is no option for locating mine excavations away from a water bearing rock mass, the control of water inflow must be carried out using techniques such as grouting and pre-drainage.

In order to effectively control a potentially unstable rock zone, the rock mass may be supported using a variety of methods. Design of the support system is carried out prior to excavation. To date there are a number of methods available for rock support design, but due to the complexity of the systems, design is still carried out on a site-specific basis with reference to empirical data. Failure still occurs due to inappropriate rock support design. Although successful applications of rock bolting design have been reported in the literature, problems still remain due to limited application of a design method to a specific field condition. It is possible that a particular design method may succeed in one place and fail in another. Hence further research work is required to develop a versatile design approach for rock bolting systems.

1.2 RESEARCH OBJECTIVES

The research described in this thesis was undertaken to develop a computer aided method for stability assessment and the design of a rock bolting system for underground openings in a jointed rock mass. This will help on-site engineers assess the stability condition of structures in a jointed rock mass and carry out the design of rock bolting systems.

To achieve this goal the first objective was to develop an enhanced system for classifying major discontinuity sets based on their frequency, persistence and

various mechanical properties. Once the major discontinuity sets were defined, the stability condition of the rock mass will then be found out based on the assessment of the quality of a rock mass using a modified rock mass classification system. Initial design of a rock bolting system can then be carried out.

The second objective was to develop a computer aided stereographic projection technique for determination of the geometry of tetrahedral and polyhedral wedges defined by the major discontinuity sets mentioned above. The failure mode of these rock wedges can then be identified and the number of bolts required to stabilise those wedges can be determined. Therefore the final decision on the rock bolting system required in underground structures was made based on the initial design and support requirement of the unstable wedges.

1.3 THESIS LAYOUT

This thesis is presented in eight chapters. The flow diagram of the arrangement of this thesis is shown in Figure 1.1.

- Chapter 1 gives a brief introduction to the research and the arrangement of the thesis.

- Chapter 2 is concerned with a brief review of design approaches for various rock bolting systems, including optimisation of the parameters of rock bolting.

- Chapter 3 proposes a new method for determination of major discontinuity sets in a geological area. Three main aspects included are: (1) data acquisition from a scanline survey; (2) data processing using clustering

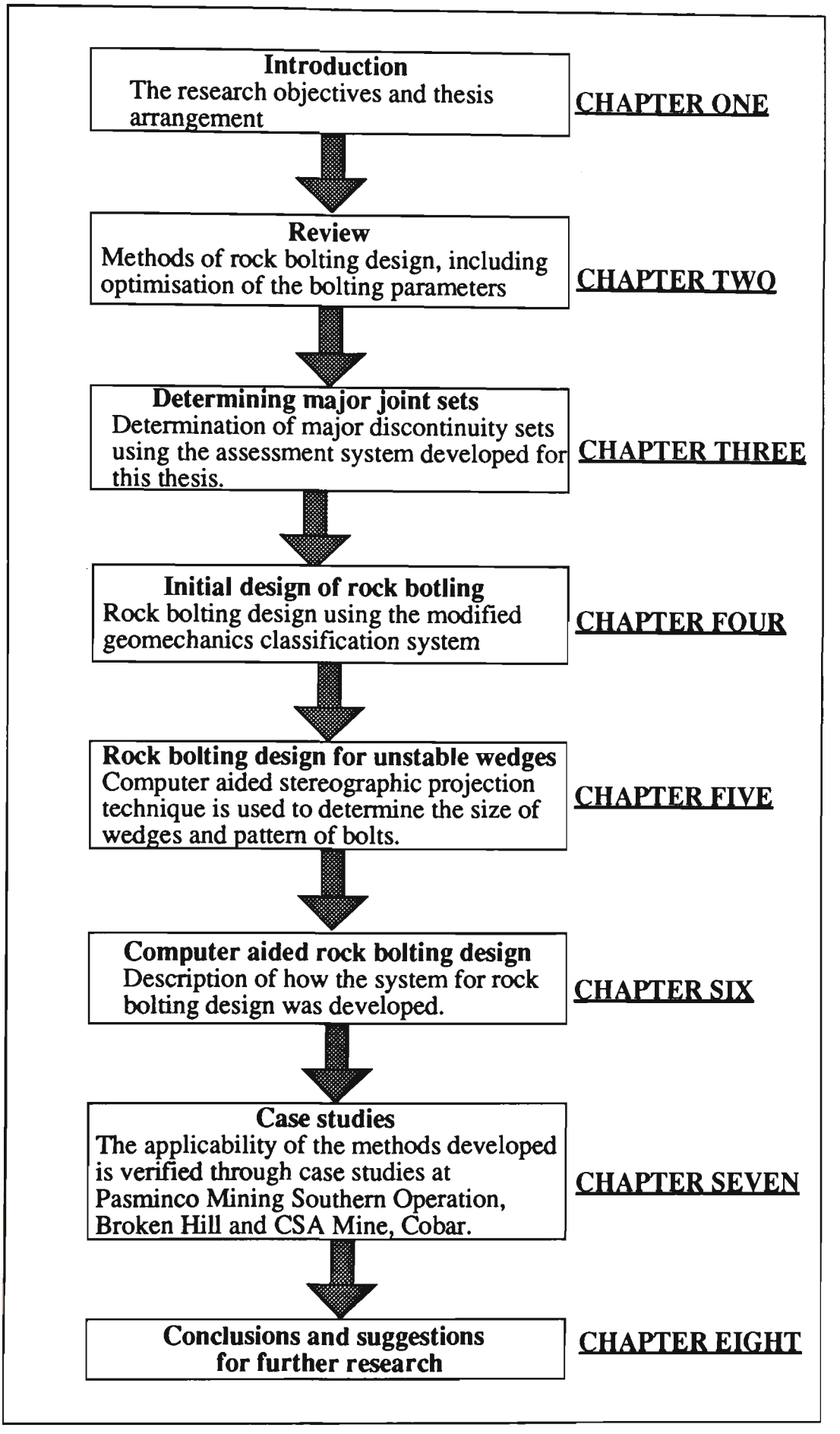

Figure 1.1. Flow diagram of the thesis

analysis and the stereographic projection technique; and (3) determination of major discontinuity sets using a new rating system based on an assessment of the importance of the frequency of discontinuity occurrence, physical characteristics and mechanical properties.

- Chapter 4 deals with the initial design of a rock bolting system using a modified geomechanics classification system. The classification system is the bases of a computer program and the output of which is the initial design.

- Chapter 5 is concerned with rock bolting design for unstable wedges, and incorporates stereographic projection techniques to identify potentially unstable wedges and to carry out rock bolting system design.

- Chapter 6 describes the computerisation of the rock bolting design system for unstable wedges. The flowcharts of the programs are given and the necessary input data and control variables are presented.

- Chapter 7 illustrates the applicability of the newly developed programs using case studies conducted at Pasminco Mining Southern Operation, Broken Hill and CSA Mine, Cobar.

- Chapter 8 summarises the results and principal conclusions of the research work presented in this thesis and presents suggestions for further research.

- Finally, an appendix is given in which original data collected from the mine sites are presented.

CHAPTER 2

REVIEW OF ROCK BOLTING DESIGN

2.1 INTRODUCTION

Since its introduction into engineering technology at the end of the 19th century (Stillborg, 1986), rock bolting has played an important role as a primary means of support in rock engineering. This technique has been widely used in coal and hard rock mining, underground hydro-electric schemes, tunnelling, and other rock structures in civil and military engineering. In the past decades major developments in the areas of rock bolting have been in the field of anchor devices, bolting and anchoring materials and the technique of rock bolting design. Significant developments have taken place in the following areas:

- Development from point-anchor bolts to fully grouted resin or cement dowels;

- Development of point anchored cable to fully grouted cable dowelling techniques;
- Pretensioned cables and anchors;
- Techniques of rock bolt placement; and
- Rock bolting design methods.

With the development of various analytical theories, new techniques such as finite element, boundary element, distinct element, probabilistical and statistical methods have been developed and used in rock bolting design. The design methods used in practice change from place to place and from time to time due to variation in geological conditions and underground structures. They are becoming increasingly complicated because of the adoption of a combination of several concepts in rock bolting design. A successful operation of rock bolting system depends on:

- accuracy of basic data, from both the laboratory and the field;
- correct selection of failure criteria and rock bolting material; and
- appropriate selection of design approach.

Generally, the approaches used in the design of rock bolting can be broadly divided into three categories: empirical approach, analytical approach, and a combined approach.

2.2 EMPIRICAL APPROACH

The design of rock bolting was largely empirical before the theory of elasticity was shown to be acceptable for the determination of stress around openings in hard rocks and analytical and numerical techniques were developed. Prior to this an

entirely empirical approach, based upon the premise that the support methods that were previously successful will also continue to be adequate, was used.

Gradually, the experience from past practice was formulated into a systematic approach, a rock classification system, derived from observation and by correlating the stability of a tunnel with one or more prominent parameters which control rock mass behaviour. On many occasions, the classification approaches served as the only practical basis for the design of complex underground structures (Bieniawski, 1984). Terzaghi was a pioneer of this approach and introduced rock load classification over 48 years ago.

2.2.1 Terzaghi's Rock Load Classification

Based upon his experience in steel-supported railroad tunnels in the Alps, Terzaghi (1946) established a rock classification system which was the first systematic method of evaluating rock loads. This approach considered the width and height of tunnel excavations as very important parameters and suggested that the whole range of rock types be divided into nine classes. This simple rock classification system was used to estimate the load to be supported by steel arches in tunnels.

Since then rock mass classification systems have improved greatly. The best-known rock mass classifications are those proposed by Lauffer (1958), Deere (1964), Wickham, Tiedeman and Skinner (1972), Bieniawski (1973), Barton, Lien and Lunde (1974), and Laubscher and Taylor (1976).

2.2.2 Lauffer-Pacher's Classification

Lauffer established rock mass classification on the basis of earlier work on tunnel geology by Stini (1950). Stini stressed the importance of structural defects in a rock mass. Lauffer proposed that the stand-up time for any active unsupported rock span is related to the rock mass characteristics. An active unsupported span is the width of the tunnel or the distance from the face to the support if this is less than the tunnel width.

Lauffer's original classification was modified by Pacher. The modified Lauffer-Pacher classification states that an increase in tunnel span leads to a major reduction in the stand-up time. This classification introduced the stand-up time and the span as relevant parameters in determining the type and amount of tunnel support, and it has influenced the development of more recent rock mass classification systems.

2.2.3 Rock Quality Designation (RQD)

In 1964 Deere recognised a particular rock parameter based on core recovery by diamond drilling, rock quality designation (RQD), and correlated it with rock load and support requirements taking into account the influence of construction type on support design. This rock quality designation has come to be widely used and has been shown to be particularly useful in classifying rock masses for the selection of support systems.

RQD is defined as the percentage of core recovered in intact pieces of 100 mm or more in length in the total length of a borehole. It is expressed by

$$\text{RQD (\%)} = 100 \times \frac{\text{Length of core in pieces} > 100\text{mm}}{\text{Length of borehole}} \qquad (2.1)$$

According to the value of the RQD obtained, the rock mass is divided into five classes: excellent, good, fair, poor, and very poor. Cording, Hendron and Deere (1972) modified Terzaghi's rock load factor and related this modified value to the RQD. An attempt to extend the range of application of the RQD for estimating tunnel support requirements was made by Merritt (1972), and his proposals are summarised in Figure 2.1.

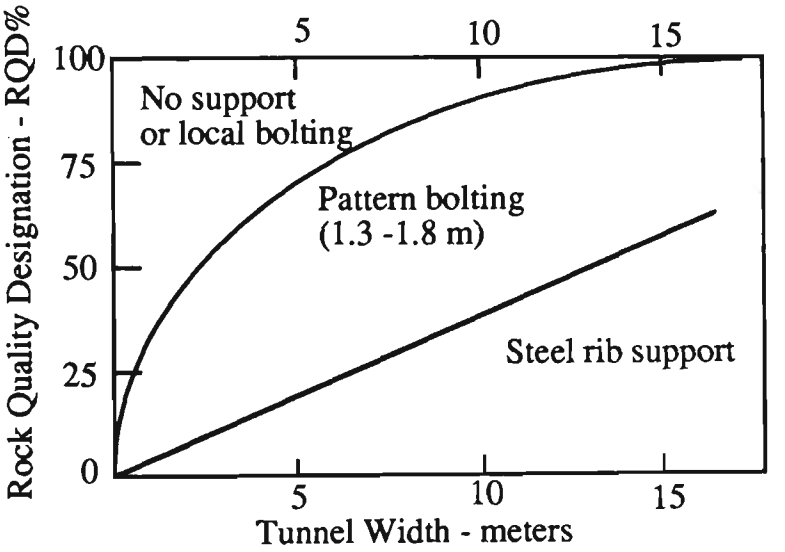

Figure 2.1. Proposed use of RQD for choice of rock support system (after Merritt, 1972)

2.2.4 Rock Structure Rating (RSR) System

The RSR was developed in the United States in 1972 by Wickham et al. The system represented a quantitative method for describing the quality of a rock mass and for the selection of appropriate ground support. This technique is the first

attempt at recognising a rock mass rating system and it is considered to be the first complete rock mass classification system (Bieniawski, 1984).

Wickham et al. suggested a support rating system based on three main parameters, which in themselves were evaluations of the relative effect of various geological factors on the support requirements. The three parameters are as follows:

- Parameter A: The effect of rock structure including rock type origin, rock hardness and geological structure.
- Parameter B: The effect of joint pattern with respect to the direction of the tunnel drive including joint spacing, joint orientation and direction of tunnel drive.
- Parameter C: The effect of joint condition and ground water.

The RSR value of any underground excavation is obtained by summing the weighted numerical values determined for each parameter. It reflects the quality of the rock mass with respect to its need for support. Based on the rating obtained a support method can be proposed as illustrated in Figure 2.2.

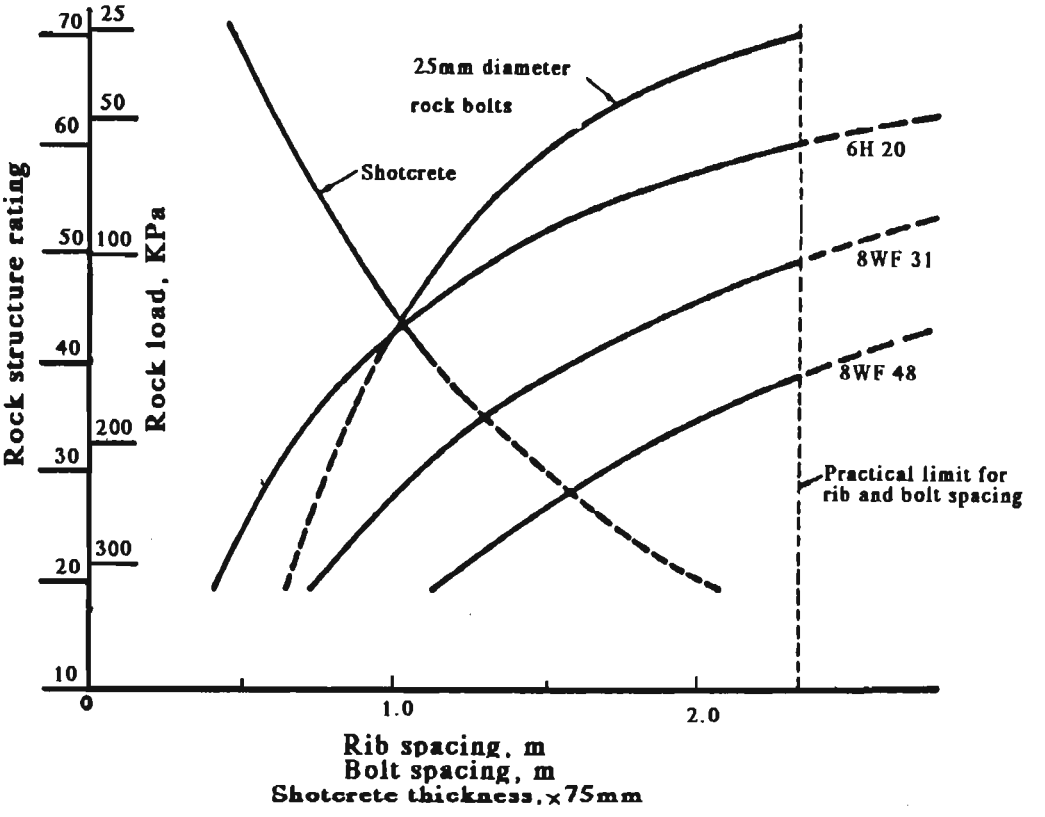

Figure 2.2. Support chart based on RSR (after Wickham et al, 1972)

2.2.5 Geomechanics Classification System

The geomechanics classification system was developed by Bieniawski (1973), and was based on the following characteristics:

- Best aspects of previously used classification systems were incorporated;
- It was based on the properties of rock materials and rock masses;
- It was functional (it can be applied to solutions of practical engineering problems);
- Standard terms were used;

- A rating system was provided to weigh the relative importance of various classification parameters.

At its early stage, six parameters were considered and they were: rock quality designation (RQD), weathering, intact rock strength, spacing of joints, continuity of joints and ground water. In addition, the strike and dip orientation of discontinuities were used to adjust the total rating. The stiffness of a discontinuity plane was not taken into consideration at that time. Since then much attention has been paid to the discontinuity in the field of rock mechanics. A lot of work was done on the influence of discontinuities on the shear strength of a rock mass (Barton, 1973, Bjurstrom, 1974, Barton & Choubey, 1977) and discontinuities were considered as the main reason for failure of a rock mass structure. Having recognised the importance of discontinuities in the assessment of a rock mass, Bieniawski (1976) then modified his geomechanics classification system and five parameters were taken into consideration; strength of intact rock, RQD, spacing of joints, condition of joints and ground water. As before the total rating was adjusted to take account of joint orientation. The term "condition of joints" is in fact the stiffness of joints, which includes roughness, waviness, aperture, continuity and joint wall condition. However, this system was only used in civil tunnelling before 1976, after which it was modified to be used in mining engineering (Laubscher and Taylor, 1976).

This classification system has now been widely used to determine support requirements in tunnelling (Bieniawski, 1974, 1979), mining (Laubscher & Taylor, 1976, Kendorski et al, 1983, Singh & Eksi, 1987 and Laubscher, 1990) and hydro-electric power works (Bieniawski, 1976). Recently an attempt was made to utilise this system for the initial design of roof bolting for coal mine roadways in the U. K. (Daws, 1992). In this application the rock mass rating was adjusted by

introducing a reduction factor related to the direction of the maximum principal stress. The final rock bolting design would be performed after monitoring the initial design in the field and installing, if necessary, secondary support. As shown in Figure 2.3 it is evident that application of the geomechanics classification system

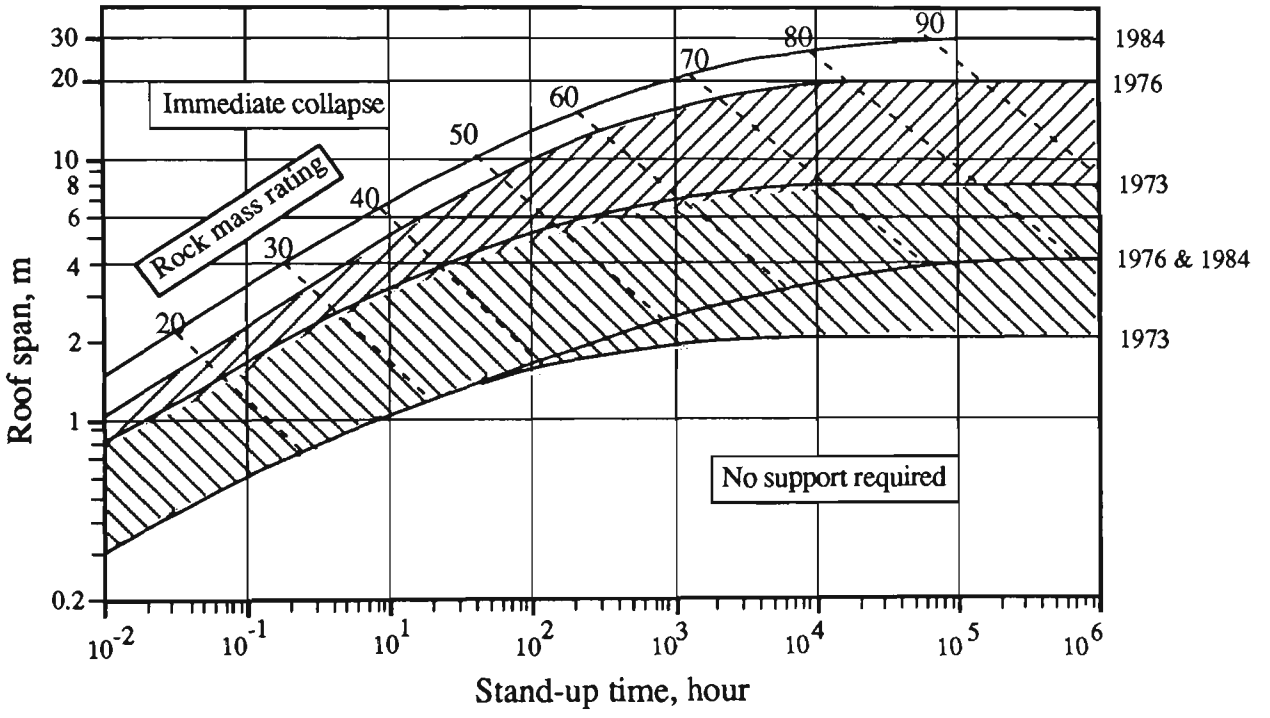

Figure 2.3. Development of the RMR system

has broadened. Also the suggestions for rock mass support were considerably conservative and general at the early stage of the development of the system.

1. Parameters Used for Rating a Rock Mass

The geomechanics classification system currently used in rock engineering includes a rating on the following parameters:

- Uniaxial compressive strength of intact rock material;
- Rock quality designation (RQD);
- Spacing of joints;
- Condition of joints;
- Ground water condition;
- Orientation of discontinuities.

The value of all parameters, with the exception of uniaxial compressive strength of intact rock material (which may be determined from laboratory tests), can be obtained from a field investigation such as a scanline survey; as discussed previously. A rating is assigned to each individual parameter listed above and the sum of the rating of every parameter concerned can be made. The geomechanics classification system is presented in Table 2.1.

Table 2.1. The geomechanics classification rating system (after Bieniawski, 1984)

	PARAMETER		RANGE OF VALUES						
1	Strength of intact rock material	Point-load strength index	>10 MPa	4 - 10 MPa	2 - 4 MPa	1 - 2 MPa	For this low range uniaxial compressive test is preferred		
		Nuiaxial compressive strength	>250 MPa	100 - 250 MPa	50 - 100 MPa	25 - 50 MPa	5 - 25 MPa	1 - 5 MPa	<1 MPa
	Rating		15	12	7	4	2	1	0
2	Drill core quality		90% - 100%	75% - 90%	50% - 75%	25% - 50%	<25%		
	Rating		20	17	13	8	3		
3	Spacing of discontinuity		>2 m	0.6 - 2 m	200 - 600 mm	60 - 200 mm	<60 mm		
	Rating		20	15	10	8	5		
4	Condition of discontinuities		Very rough surface Not continuous No seperation Unweathered wall rock	Slightly rough surface Seperation < 1 mm Slightly weathered walls	Slightly rough surface Seperation < 1 mm Highly weathered walls	Slickensided surfaces or Gauge < 5 mm thick or Seperation 1 - 5 mm Continuous	Slickened surfaces or Gauge <5 mm thick o Seperation 1-5mm Continuous		
	Rating		30	25	20	10	0		
5	Ground water	Inflow per 10 m tunnel length	None	>10 litres/min	10 - 25 litres/min	25 -125 litres/min	>125		
		Ratio Joint water pressure / major principal stress	0	0.0 - 0.1	0.1 - 0.2	0.2 - 0.5	>0.5		
		General condition	Completely dry	Damp	Wet	Dripping	Flowing		
	Rating		15	10	7	4	0		

The first five parameters are grouped into five ranges of values. Since the parameters are not equally important for the overall classification of a rock mass, the range of values for each parameter is not equal. It is considered that the orientation of discontinuities has some influence on the stability of a rock mass. The rating of the rock mass is therefore adjusted to account for orientation as shown in Table 2.2.

Table 2.2. Rock mass rating adjustment for discontinuity orientation (Bieniawski, 1984)

Strike & dip of joints		Very favourable	favourable	fair	unfavourable	Very unfavourable
Ratings	Tunnels	0	-2	-5	-10	-12
	Foundations	0	-2	-7	-15	-25
	Slopes	0	-5	-25	-50	-60

Having adjusted the rating for discontinuity orientation, the rock mass is classified according to Table 2.3. All five classes of rock mass have a range of twenty rating points. The practical meaning of an individual rock mass class is then deduced by relating it to specific engineering problems.

Table 2.3. Rock mass class determined from total rating (Bieniawski, 1984)

Rating	100 - 81	80 -61	60 - 41	40 - 21	<20
Class No.	I	II	III	IV	V
Description	Very good rock	Good rock	Fair rock	Poor rock	Very poor rock

2. Outcome from the Geomechanics Classification System

In addition to the rock mass rating, other useful information, which is used to characterise the mechanical properties of a rock mass, can be obtained from the

geomechanics classification system. The most relevant outputs from a rock bolting design stand point are internal angle of friction and cohesion, unsupported stand-up time, maximum unsupported span and rock load height. It has also been found that the uniaxial compressive strength of a rock material has a relationship with the rock mass rating (Krauland et al, 1989).

(1) Friction angle and cohesion

Table 2.4 shows the friction angle, cohesion and average stand-up time for each of the five classes of rock mass. Table 2.4 shows that a good rock mass has a high friction angle and cohesion, whilst a poor rock mass has a low friction angle and cohesion.

Table 2.4. Meaning of rock mass classes (Bieniawski, 1984)

Class No.	I	II	III	IV	V
Average stand-up time	10 years for 15m span	6 months for 8m span	1 week for 5m span	10 hours for 2.5m span	30 minutes for 1m span
Cohesion of the rock mass	>400 KPa	300 - 400 KPa	200 - 300 KPa	100 - 200 KPa	<100 KPa
Friction angle of the rock mass	>45°	35° - 45°	25° - 35°	15° - 25°	<15°

(2) Unsupported stand-up time

As mentioned previously, the unsupported stand-up time and maximum unsupported span were used by Lauffer (1958). Bieniawski (1973) however, related the unsupported stand-up time to his geomechanics classification system and a relationship between rock mass rating and the unsupported stand-up time was proposed as shown in Figure 2.4.

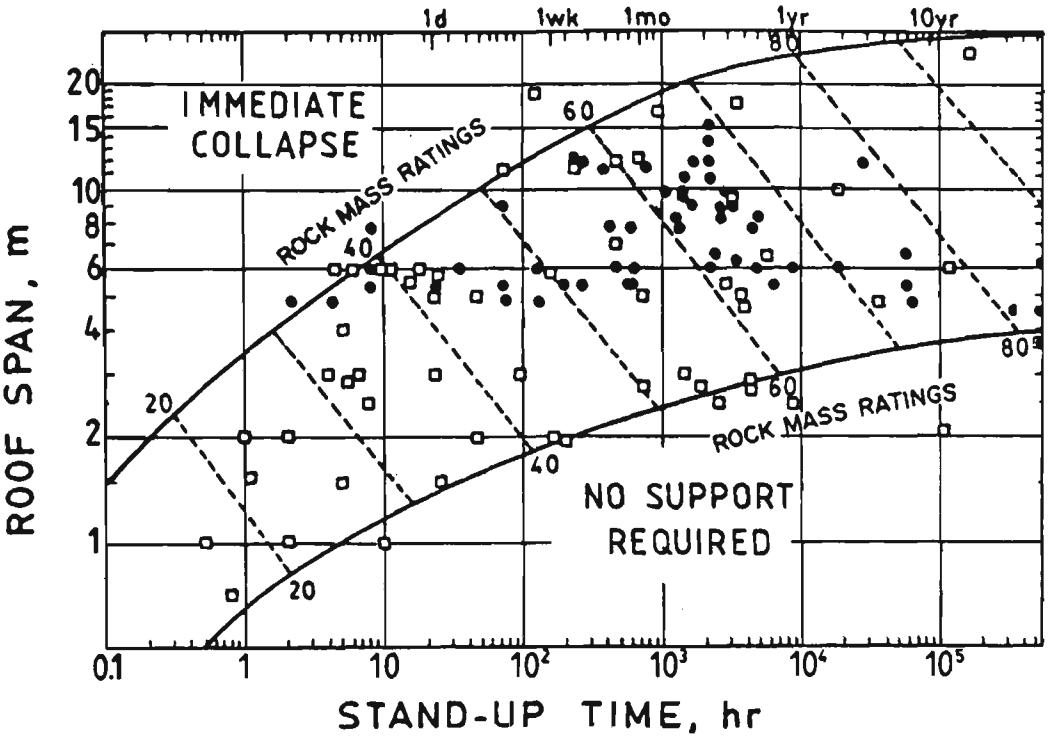

Figure 2.4. Relationship between stand-up time and unsupported span (after Bieniawski, 1973)

From Table 2.4 and Figure 2.4 it is evident that for a given rock mass rating, a particular roof span has a corresponding stand-up time.

(3) Rock load height

The concept of rock load height, H_t, was first proposed by Terzaghi (1946). The rock load height (the height of rock which should be supported) can be related to the rock mass rating using Equation (2.2) (Unal, 1983):

$$H_t = (100 - RMR) \times (2W)/100 \qquad (2.2)$$

Where; H_t is the rock load height, m;

$2W$ is the width of the excavation span, m; and

RMR is the rock mass rating.

Once rock load height has been determined the rock load, P_r, can be found using Equation (2.3).

$$P_r = \gamma_r H_t \qquad (2.3)$$

Where; P_r is the rock load per unit length of opening, kN/m; and

γ_r is the unit weight of rock material, kN/m^3.

Substituting Equation (2.2) into Equation (2.3), produces:

$$P_r = (100 - RMR) \times (2W) \times \gamma_r / 100 \qquad (2.4)$$

The variation of rock load with roof span for the various rock classes is shown in Figure 2.5.

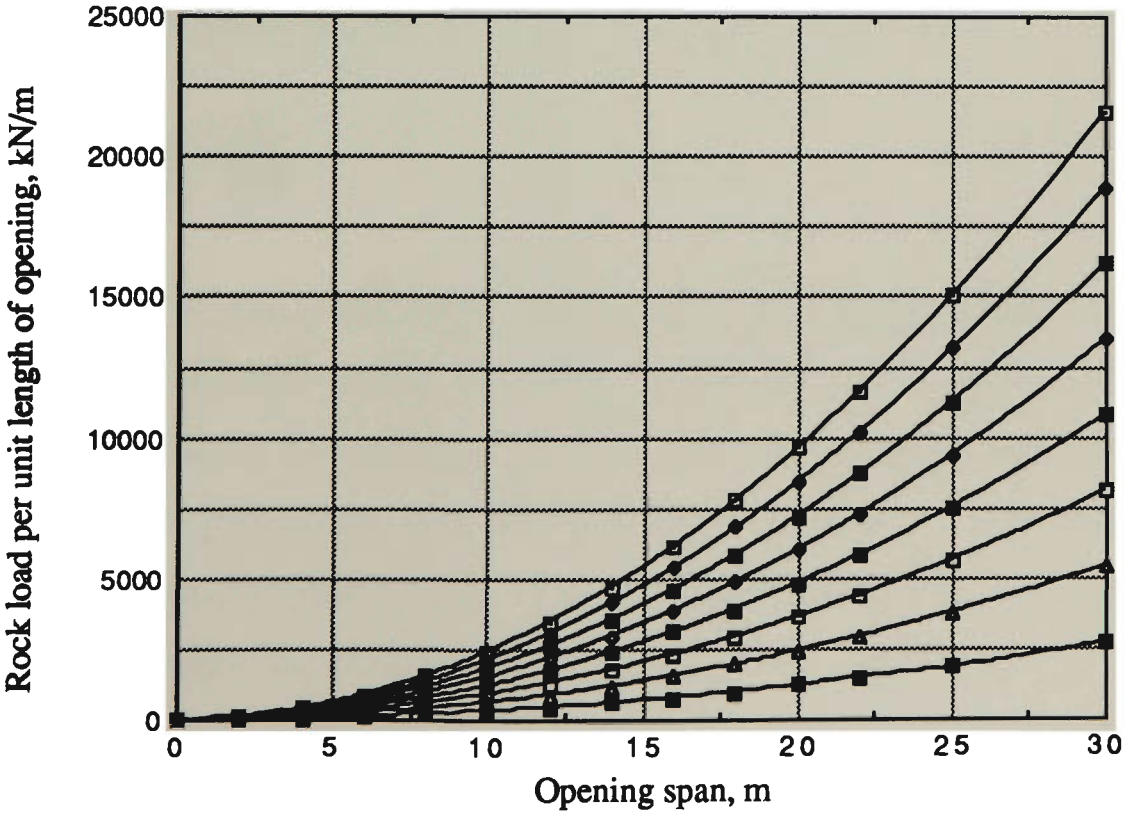

Figure 2.5. Rock load vs roof span in various rock classes (after Unal, 1983)

(4) Chart for rock bolting design

Table 2.5 presents Bieniawski's (1984) guide for the design of support in rock tunnels. It is evident that the guide-line is very general. In the guide-line shotcrete is used as a temporary support; is not normally used in Australian mines. Instead of shotcrete, W straps are used to assist the rock bolts to maintain a coherent rock mass in the roof. Therefore, in using this design guide-line, an adjustment should be made to incorporate the use of W-straps rather than shotcrete.

2.2.6 The Q System

Another concept widely used for rock mass classification is the Q system (Barton et al, 1974). Six factors are considered; RQD, joint set number (JN), joint roughness number (JR), joint alteration number (JA), joint water (JW), and stress reduction factor (SRF). From the six parameters the Q value for the rock mass can be determined from Equation (2.5):

$$Q = \frac{RQD}{JN} \times \frac{JR}{JA} \times \frac{JW}{SRF} \qquad (2.5)$$

Based on the Q values and equivalent dimensions (the excavation span, diameter or height / the excavation support ratio ESR), 38 types of support systems were suggested as shown in Figure 2.6. The ESR is related to the type of opening in mining and it ranges from 1.6 for permanent openings to between 3 and 5 for temporary openings (Barton, 1976). Interested readers can refer to the relevant references to find out the detail of these support systems (Barton et al, 1974, Barton, 1976, Hoek and Brown, 1980). Operational experience indicates that the Q

Table 2.5. The geomechanics classification guide for excavation and support in rock tunnels (Bieniawski, 1984)

Rock mass class	Excavation	Support		
		Rockbolts (20 mm dia., fully bonded)	Shotcrete	Steel sets
1. Very good rock RMR: 81-100	Full face: 3m advance	Generally no support required except for occasional spot bolting		
2. Good rock RMR: 61-80	Full face: 1.0-1.5 m advance; Complete support 20 m from face	Locally bolts in crown 3 m long, spaced 2.5 m with occasional wire mesh	50 mm in crown where required	None
3. Fair rock RMR: 41-60	Top heading and beach: 1.5-3 m advance in top heading; Commence support after each blast; Complete support 10 m from face	Systematic bolts 4 m long, spaced 1.5-2.0 m in crown and walls with wire mesh in crown	50-100 mm in crown and 30 mm insides	None
4. Poor rock RMR: 21-40	Top heading and beach: 1.0-1.5 m advance in top heading; install support concurrently with excavation - 10 m from face	Systematic bolts 4-5 m long, spaced 1-1.5 m in crown and walls with wire mesh	100-150 mm in crown and 100 in sides	Light ribs spaced 1.5 m where required
5. Very poor rock RMR: <20	Multiple drifts: 0.5-1.5 m advance in top heading; Install support concurrently with excavation; shotcrete as soon as possible after blasting	Systematic bolts 5-6 m long, spaced 1-1.5 m in crown and walls with wire mesh	150-200 mm in crown 150 mm insides and 50 mm on face	Medium to heavy ribs spaced 0.75 m with steel lagging and forepoling if required. Close invert

Application conditions: 1) tunnel shape: horseshoe; 2) width: 10 m; 3) vertical stress: below 25 MPa; 4) construction: drilling and blasting.

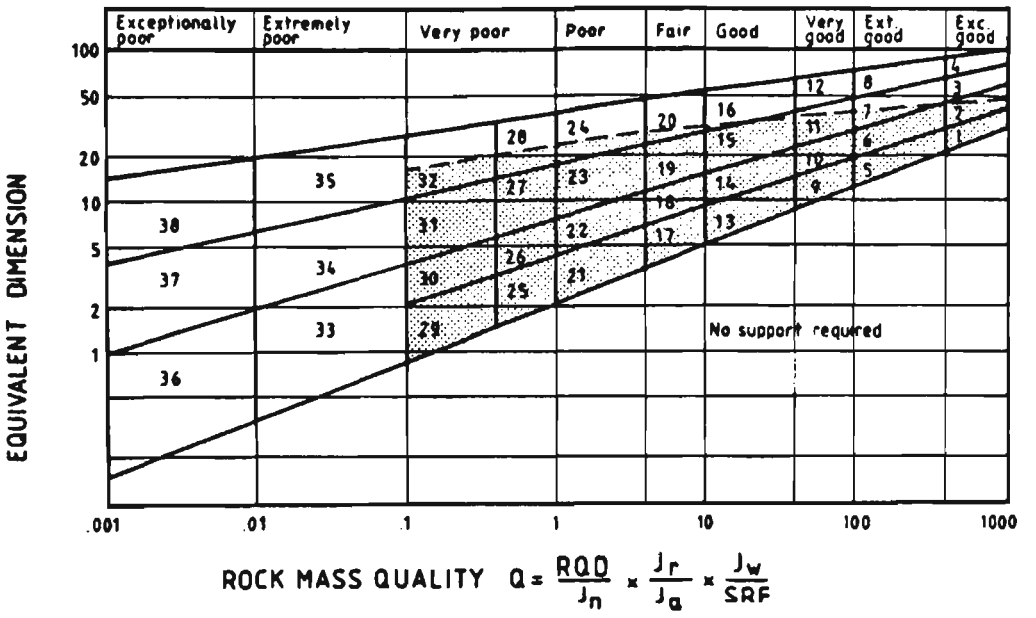

Figure 2.6. Relationship between rock mass quality, equivalent dimension and support required (after Barton et al, 1974)

system is an innovative and practical method of systematic mapping of the complicated geomechanical and technical material involved in rock mass support practice (Bergman & Bjurstrom, 1983). It has given designers a realistic method for the solving of a variety of rock mass support problems.

Bieniawski (1976) found that there is a relationship between RMR and the Q system. It can be expressed as

$$RMR = 9\ln Q + 44 \qquad (2.6)$$

2.2.7 Mining Rock Mass Rating (MRMR)

The RMR and Q systems were developed for civil tunnelling. In order to use the RMR system in mining, Laubscher and Taylor (1976) and Laubscher (1990) developed a system based on the use of RMR, called mining rock mass rating (MRMR). The same parameters as used in the RMR system are taken into account in this system, but it combines the ground water and joint condition factors and results in four parameters: design rock mass strength, RQD, joint spacing and joint condition.

In this approach the rock mass should be assigned an in-situ value regardless of its position in space provided the stress environment does not exceed 30 MPa. In deciding how the rock mass will behave and the support required, the value of rock mass rating must be adjusted depending on weathering, field and induced stress, changes of stress due to mining, the orientation and type of excavation with respect to geological structures and the effect of blasting.

Three important concepts which must be introduced first are:

1. In-situ Rock Mass Strength (IRMS)

Assuming that large specimens have an intact rock strength (IRS) value equal to 80% of that of the standard core sample, the IRMS can be found through the following steps:

- the rating for IRS, B, is subtracted from the total rock mass rating, A, and therefore the balance (RQD, joint spacing and joint condition) will be a function of the remaining possible rating of 80;

- o the IRS rating represents the strength of intact rock specimens, C, which must be reduced to 80% of its value;
- o the corrected IRS value is multiplied by the reduction factor to give the IRMS:

$$IRMS = \frac{(A - B)}{80} \times C \times \frac{80}{100} \qquad (2.7)$$

Where; A is the total rating;

B is intact rock strength (IRS) rating; and

C is IRS of intact rock specimen.

2. Design Rock Mass Strength (DRMS)

This is the strength after an adjustment to take account of weathering, joint orientation and blasting. It is noted that the influence of strong and weak bands of intact rock within the rock mass should be considered. Therefore, an average value of rock mass strength is introduced.

3. Mining Stress Environment

Mining-induced stresses are the redistributed field stresses caused by the geometry and orientation of mining excavations. The redistributed stresses of interest are the maximum stress, stress difference and minimum stress.

In addition, weathering will have significant influence on the behaviour of a rock mass. A reduction factor should therefore be considered if weathering has taken place in the rock mass. The size, shape and orientation of the excavation will affect the behaviour of the rock mass surrounding an opening. If the size, shape and

orientation of the excavation will lead to an unstable situation in the excavation, the rating of the rock mass should be adjusted.

After calculation of the mining stress environment, support systems can be determined. In addition to rock reinforcement, the effect of rigid lining, yielding lining, filling, spalling control and rock replacement should be considered to meet the different requirements of mining in a given rock mass.

2.2.8 Miscellaneous Classification Techniques

The advent of computers and numerical modelling techniques has resulted in new rock mass classifications, based on the numerical methods, being introduced. The Monte Carlo simulation technique and the transformation technique were the main approaches used in probabilistic analysis in rock engineering (Herget, 1982). Generally probabilistic analysis is used for the determination of stability of rock mass; however, until now no proposal for a support system based on probabilistic analysis exists.

In the 1980's an alternative classification approach was developed in which statistical analysis was used. With this technique rock masses in a geological area could be classified by computer calculations based on the input data. Although the classification and main parameters of the rock mass can be provided, indications of support requirements have not resulted (Lin et al, 1985 and Lin, 1988). Nguyen and Ashworth (1986) proposed a rock mass classification by means of "fuzzy" sets. Again the method was not related to support requirements.

2.3 ANALYTICAL METHODS

When the theory of elasticity was considered, designers of rock bolting systems found that the redistribution of stress around excavations in hard rock followed closely to the dictates of the laws of elasticity. The subsequent development of analogue and numerical analysis techniques has made it possible to determine the stress field surrounding any excavation. Traditional manual calculation is gradually being replaced by computers. At present, it is difficult to divide analytical approaches into several types because of their interdependence. Usually, this kind of approach can be described as incorporating theoretical calculation, physical modelling and numerical modelling.

2.3.1 Theoretical Approach

The mechanism of rock bolting has been studied for years, but it has not been understood fully because there are so many properties of bolts and rocks which need to be clearly realised. In order to explain some of the important bearing capacity mechanisms of rock bolting, four cases were studied by Habenicht (1983). They are summarised as the suspending effect, nailing effect, beam building effect and arch building effect as shown in Figure 2.7. The rock bolting system is designed to meet certain requirements on the basis of at least one of the above four effects. Sometimes the design is to be applied to a complex condition in which more than one effect is considered.

1. Suspension Effect

Design based on suspension, as shown in Figure 2.7(a), is considered as the simplest approach to rock bolting design. The effect of bolting is to suspend the

dead weight of the unstable block. The bolt should be sufficiently long to reach the strong strata in order to be effective.

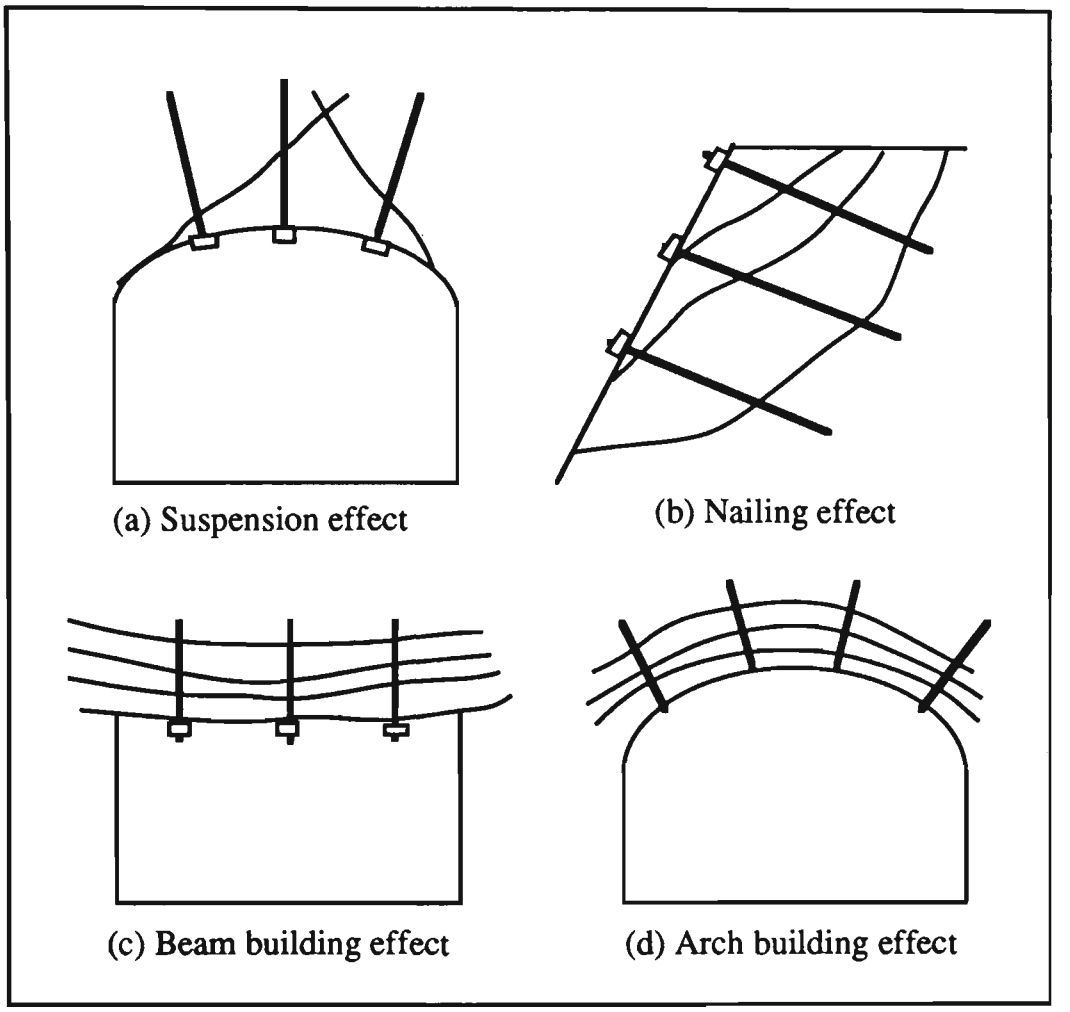

Figure 2.7. Bolting principles (after Larsson, 1984)

2. Nailing Effect

The nailing effect, as shown in Figure 2.7b, is usually applied to the design of slopes or underground structures with high-walls. Its main support objective is to increase the shear resistance along the failure planes. The increase in shear resistance is accomplished by increasing the components of shear force in the bolts

and the normal forces on the failure planes due to the tensile forces in the bolts. Its success or failure is related to several factors such as the properties of rock materials, mechanical parameters of discontinuities and the presence of ground water (specially in the case of slope engineering).

3. Beam Building Effect

In bedded strata, beam building, as shown in Figure 2.7(c), is considered to be the most efficient approach to bolting. The bearing capacity of the composite beam is greatly increased. There are many factors which influence the effectiveness of beam building, such as rock properties, material properties and geometry of the bolt hole. Bolt length and spacing are important in the overall design of rock bolting. In the case of beam building, the length of the bolt should be such that the thickness of the beam so generated can bear the load applied to it, i.e. the displacement in the beam can be controlled to some extent. This method also limits shear and is a type of 'nailing'.

4. Arch Building Effect

(1) Arch action

Arch building as shown in Figure 2.7(d) is a widely discussed topic in the field of rock bolting. Consideration of a rock self-support ring gives a satisfactory interpretation of this mechanism. However, differing opinions remain. The controversy focuses on whether the arch can bear load by itself. With respect to stress field conditions, it is certain that arch building is the result of the application of compression to improve resistance to shear and tension in the zone above an underground opening.

(2) Reinforced arch

Bischoff and Smart (1975) introduced the concept of the reinforced arch based on the concept of the "compression zone" proposed by Lang (1961), in which bolts can be used in the place of other support methods. They established the equivalence between patterns of fully grouted bolts and internal support, such as steel sets. The support system consists of internal supports equally spaced along an underground excavation. The relationship between the rock bolt spacing and the unit thrust capacity of the support system is shown in Figure 2.8. It is evident that a system of rock reinforcement is structurally equivalent to the support provided by steel sets.

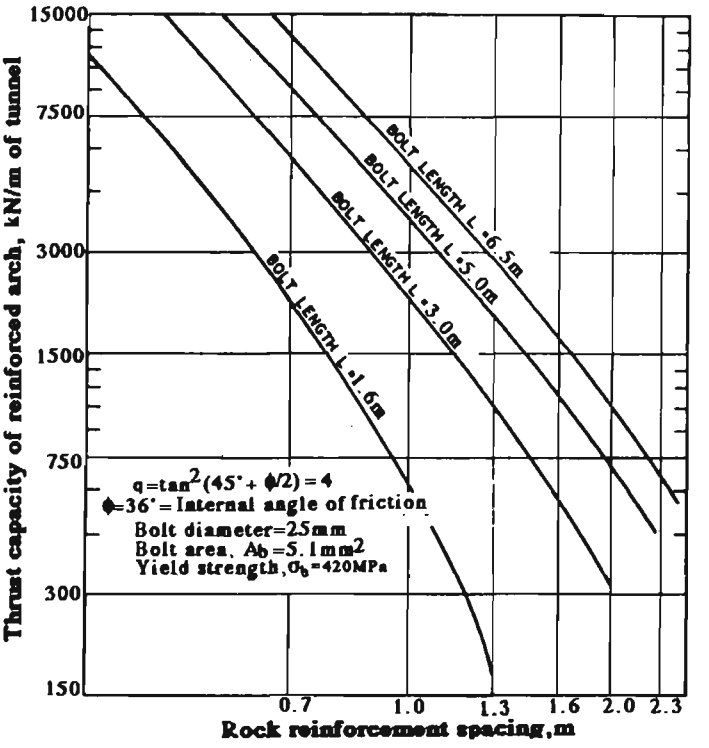

Figure 2.8. Thrust capacity of reinforced arch for various rock reinforcement patterns (after Bischoff and Smart, 1975)

2.3.2 Physical Modelling

Beginning in late 1950's, model studies were carried out in Essen, Germany by Everling and Jacobi (Everling, 1964). These large expensive models were an attempt to simulate the effects of various parameters on the stability of gate entries in longwall coal mining operations. Nearly every conceivable aspect of the actual situation was modelled.

In Great Britain, physical modelling was carried out by Hobbs (1968), beginning in the mid-1960's, to study entry stability. During the 1960's and 1970's, physical modelling which simulated fractures in tunnels and coal mines was carried out in Canada and South Africa for testing large scale models of tunnels (Barron & Larocque, 1962), simulation of fractures around coal and hard rock tunnels (Hoek, 1963, Bieniawski & Tonder, 1969) and determination of stress and displacement in the strata surrounding an excavation (Cook & Schumann, 1965, Salamon & Oravecz, 1970).

In the United States, the major thrust was directed to the development and use of the 'base friction' modelling technique (Bray and Goodman, 1981) and recently to the design and construction of a full scale model mine tunnel for roof support research at the Spokane Research Centre. A classic series of physical model tests of roof bolting in bedded rock were performed by Panek (1962). Panek investigated the reinforcement mechanism of friction and suspension with tensioned roof bolts. He then applied dimensional analysis to the results of the model tests and derived quantitative formulae for the design of rock bolting patterns. The base friction modelling technique can also be used to model highly discontinuous coal mine roof conditions (Mark, 1982)

In China the rock bolting mechanisms have been studied by Zhu and Wang (1986). C and ϕ were increased greatly in the model modelling reinforcement using bolts. Photo-elastic modelling and physical modelling were conducted in the Xiangxi Gold Mine research program, in the west of Hunan Province. The results showed that the stope studied would be unstable during extraction and the hangingwall of the stope should be reinforced by a combination of short bolts, steel mesh and long cables. Analysis from monitoring of the convergence and displacement in the stope confirmed that the results obtained from modelling tests were correct (Bao and Yang, 1986).

In addition, materials used in modelling have been greatly improved and as such can be used to simulate all kinds of rock materials and joint conditions. In modern test equipment and monitoring instruments, high stiffness and synchronous loading characteristics have led to increased accuracy of test results obtained from physical modelling.

2.3.3 Numerical Modelling

Numerical modelling aims at the determination of stress and displacement in complex underground structures. Two approaches can be identified, both recognising geological structures as being discontinuous due to joints, faults and bedding planes. A continuum approach treats the rock mass as a continuum intersected by a number of discontinuities while a discontinuum approach views the rock mass as an assemblage of independent blocks or particles.

2.3.3.1 Continuum approach

For mining and tunnelling purposes a wide range of two and three dimensional models are available using computer codes developed for various material behaviour. This includes the following constitutive behaviour types: linear-elastic, non-linear elastic, linear visco-elastic, elasto-plastic and elasto-viscoplastic. However, much more detailed model application and verification are required before any of those material models can be applied for practical design purposes in mining and tunnelling (Brady and St. John, 1982, Beer and Watson, 1989).

The finite element method is currently by far the most popular and useful technique for application as an analytical design tool. It was said by Zienkiewicz (1977), the finite element method is uniquely capable of handling complex geometries and inhomogeneties. The joint element (Goodman et al, 1968) has been introduced into the finite element method, which makes it possible to model discontinuities in rock mass (Goodman and St. John, 1977). The boundary element method was developed in the 1970's and the procedures involved are most appropriate for modelling linear-elastic systems, although certain forms of non-linearity may be treated. It also provides an economical means of two and three dimensional analysis of rock masses. They are particularly suitable for use when conditions at the boundary are of most concern (St. John et al, 1979, Beer and Watson, 1989).

2.3.3.2 Discontinuum approach

The discontinuum approach involves study of the rock mass intersected by discontinuities such as joints, faults and bedding planes. Generally it is called a jointed rock mass, which is a tightly-fitted three-dimensional mosaic of polyhedral

rock blocks created by intersecting discontinuities. In the late 1970's, the distinct element method was introduced in rock engineering for stability analysis and rock bolting design (Cundall & Strack, 1979). It is considered as most suitable to model highly jointed rock masses (Cundall, 1980, 1988, Cundall & Hart, 1989, and ITASCO Consulting Group INC., 1993). Two and three dimensional analysis of underground excavations have been conducted and have shown the great influence of discontinuities on support capacity and failure modes (Chio, 1989, Chio & Couthard, 1990, Chio & Yang, 1991). The discontinuous media is represented as an assemblage of discrete blocks and the discontinuities are treated as boundary conditions between blocks. The excavation of surface or underground openings, by cutting new planes through this mosaic, allows certain blocks to move. Judgement of the effect of removable rock blocks and design in jointed rock masses can also be performed using the rock mass classification techniques mentioned before and also the stereographic projection technique. Goodman (1976) described in detail the procedure of its application and Singh (et al, 1982) presented practical application of this technique for roof support design.

After the development of the rigid block method for the design of rock bolting systems (Croney et al, 1978), Goodman and Shi (1985) proposed the key block method to aid the design of rock bolting systems. In addition, Warburton (1981, 1983, 1985, 1987) developed a block theory entirely based on the application of vector theory. A polyhedral block with any free face can be determined. It is considered that Warburton's method can be used to handle block geometries as complex as those handled by Goodman and Shi's key block theory. Furthermore a keystone in the rock block system can also be identified. A detailed application of the discontinuum approach in rock bolt design is presented in the next section.

2.4 ROCK BOLTING DESIGN USING THE DISCONTINUUM METHOD

Within the various discontinuum methods stated above the stereographic projection technique is widely used. It is used for stability analysis and the determination of the shape and size of potentially unstable rock blocks (Goodman, 1976, Hoek and Brown, 1980, Sun and Gu, 1982, Singh et al, 1982, Goodman and Shi, 1985 and Priest, 1985). This method can be described as follows.

2.4.1 Representation of Geological Data

There are several types of spherical projection which can be used for the representation of orientation data collected from field investigations. The equal area and equal angle projection techniques are the most commonly used projection methods for the interpretation of the orientation data. There is no significant advantage in either method, and equal area projection is used throughout this work except where equal angle projection is used and notified.

Using equal area projection, the traces of the planes on the surface of a reference sphere are used to define the dip and dip direction of the planes. The great circle which is traced out by the intersection of the plane and the sphere will define uniquely the inclination and orientation of the plane in space, as shown in Figure 2.9. Since the same information is included in both upper and lower parts of the sphere, only one of them need be used and the lower hemisphere is used throughout this section.

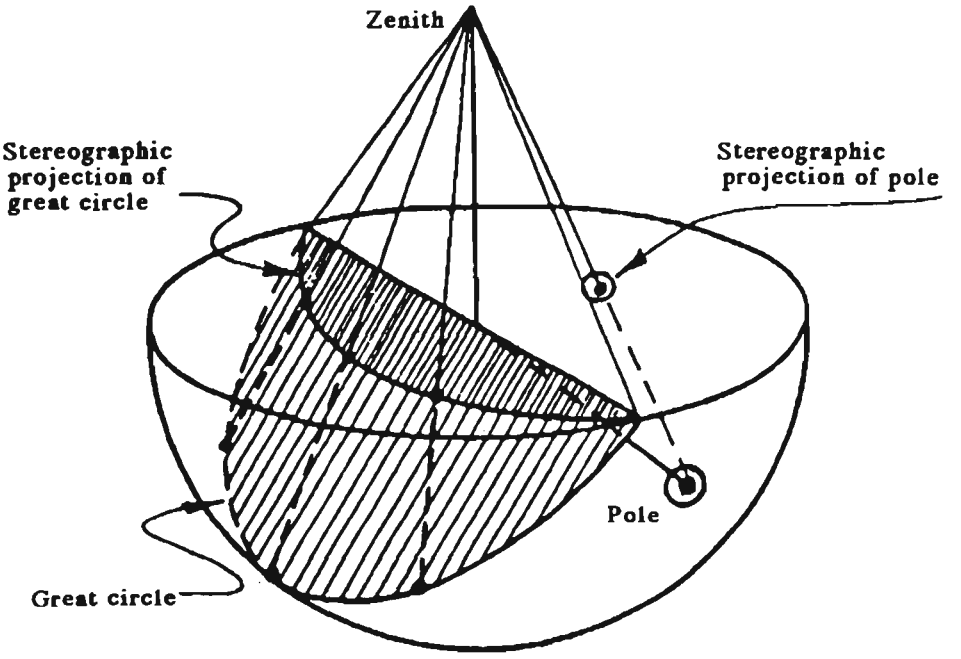

Figure 2.9. Representation of a discontinuity plane in hemispherical projection (after Hoek and Brown, 1980)

In addition to the great circle, the inclination and orientation of the plane can also be defined by the pole of the plane. The pole is the point at which the surface of the sphere is pierced by the radial line which is normal to the plane, as shown in Figure 2.9.

To communicate the information given by the great circle and the position of pole on the surface of the reference hemisphere, a two dimensional representation is obtained by projecting this information onto the horizontal or equatorial reference plane. The method of projection is illustrated in Figure 2.10. A point 'A' on the surface of the sphere is projected to point B by swinging it in an arc which is

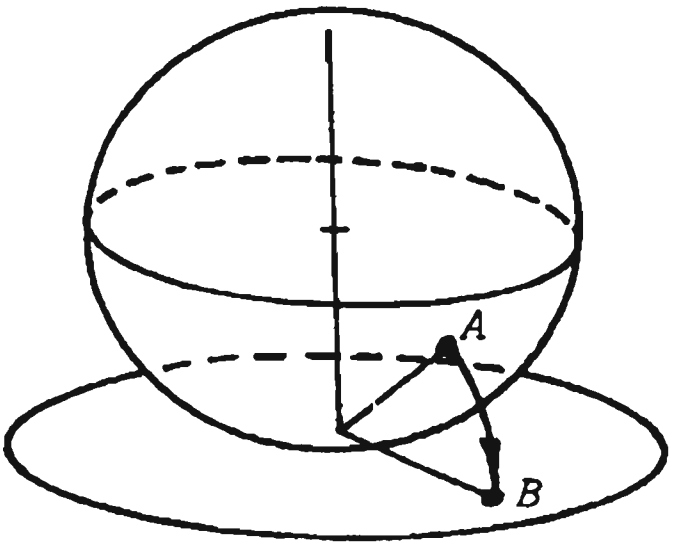

Figure 2.10. Method of construction of an equal-area projection
(after Hoek and Brown, 1980)

centred at the point of contact of the sphere and a horizontal surface upon which stands. If this process is repeated for a number of points, defined by the intersection of equally spaced longitude and latitude circles on the surface of the sphere, an equal area net will be obtained. The stereonets used in rock engineering are shown in Figures 2.11 and 2.12.

To present orientation data in a stereonet, it is convenient to work with poles rather than great circles since the poles can be plotted directly on a polar stereonet as shown in Figure 2.13. After all the orientation data have been plotted on the stereonet the pole density is determined by using a counting cell to count the number of the poles that fall in the cell. The points with the same pole density are connected to form a contouring diagram, Figure 2.14.

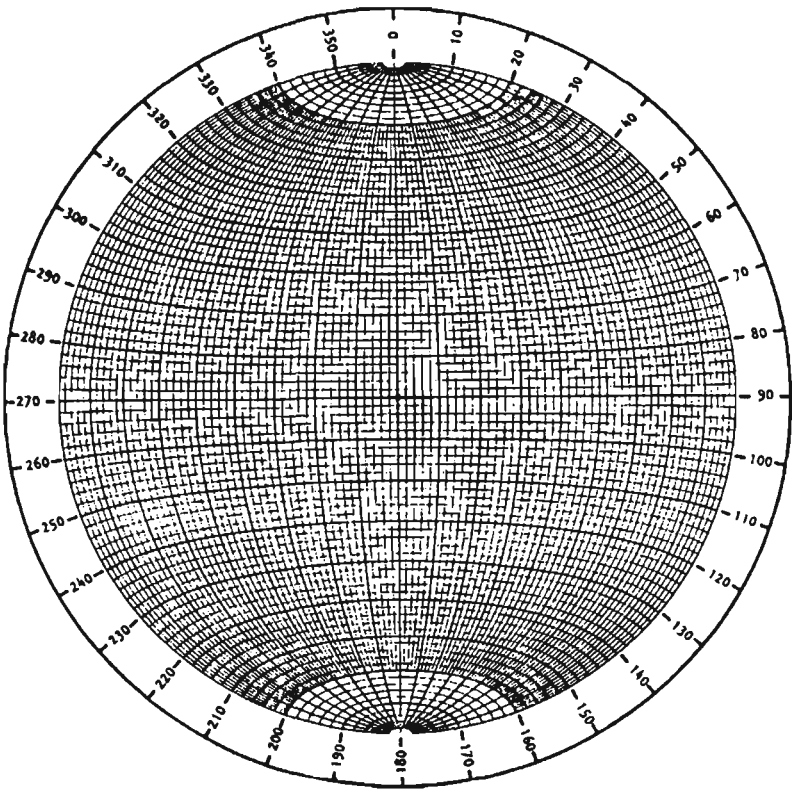

Figure 2.11. Equatorial equal-area stereonet (after Hoek and Brown, 1980)

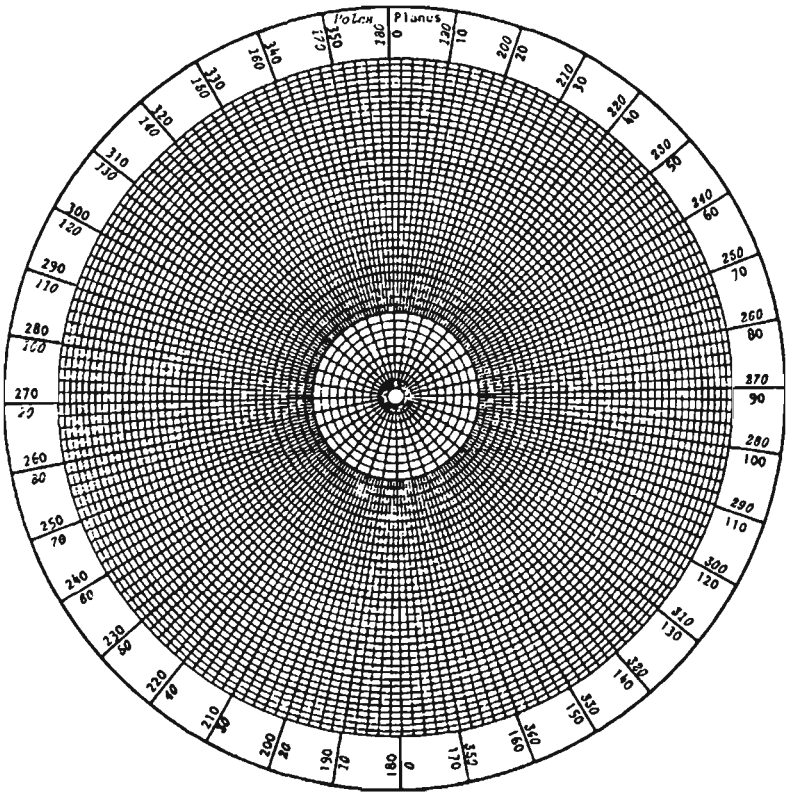

Figure 2.12. Polar equal-area stereonet (after Hoek and Brown, 1980)

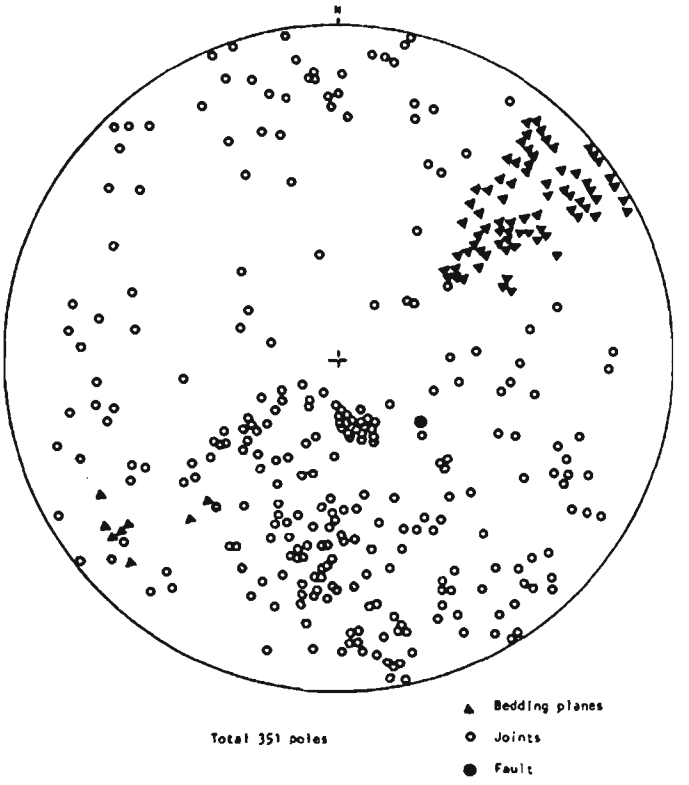

Figure 2.13. Pole distribution (after Hoek and Brown, 1980)

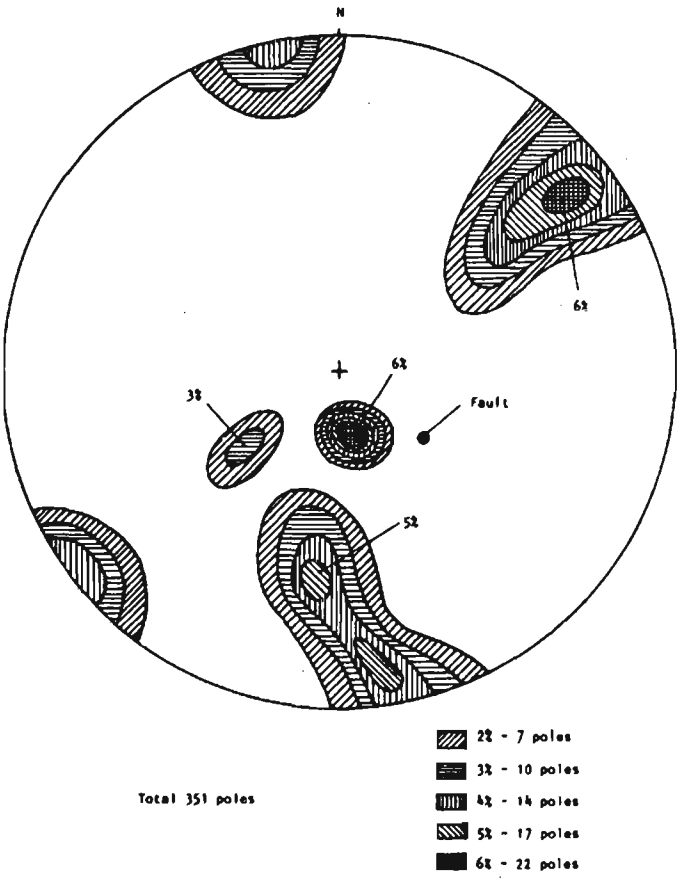

Figure 2.14. Pole contouring (after Hoek and Brown, 1980)

From Figures 2.13 and 2.14, statistically significant trends of the discontinuity can be clearly seen and therefore, the major geological structures in an area of interest can be determined. However, this technique is considered to be time consuming and tedious because of the large amount of work involved in the processing by manual and graphical techniques and as a result the accuracy of the results may sometimes be limited.

Once the major discontinuity sets in a geological area are determined, the discontinuity plane representing the planes defining a wedge can be plotted on a stereonet. Figure 2.15 shows the stereoplot of the discontinuity sets defining a wedge falling from the roof and Figure 2.16 shows a wedge sliding along discontinuity planes.

For a wedge to fall from the roof without sliding occurring on any of the wedge faces, a vertical line through the apex of the wedge must fall in the base of the wedge. It can be seen in Figure 2.15 that the great circles representing the bounding planes of the wedge enclose the centre of the net, i.e. the apex of the wedge. If three discontinuities intersect to form a wedge but the vertical line through the apex of the wedge does not pass through the base of the wedge, then failure may occur by sliding along one of the bounding planes. This can be seen in Figure 2.16 in which the three great circles representing the three discontinuity planes form a closed figure which does not enclose the centre of the net.

The condition for sliding to occur will depend on the angle of friction of the surfaces defined by the potential sliding planes. This condition is expressed on the stereographic plot by drawing the friction angle ϕ, which will be a circle, centred at the origin and then noting whether the figure formed by the bounding planes has any part of it within this circle. If the figure is completely outside this circle then the

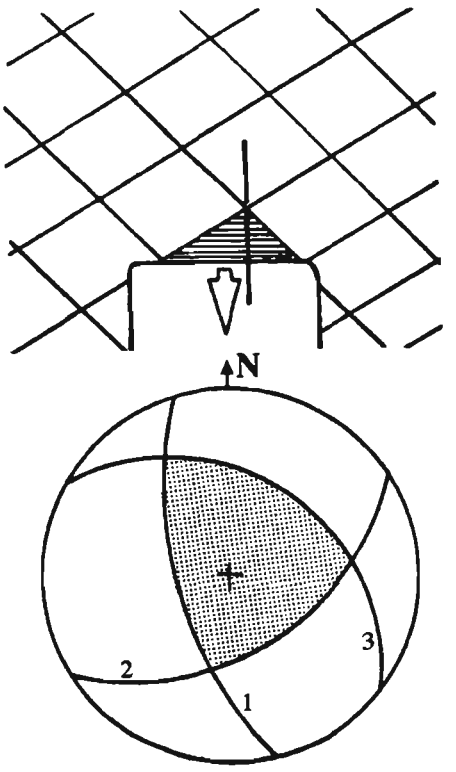

Figure 2.15. Rock wedge falling from the roof of an opening

(after Hoek and Brown, 1980)

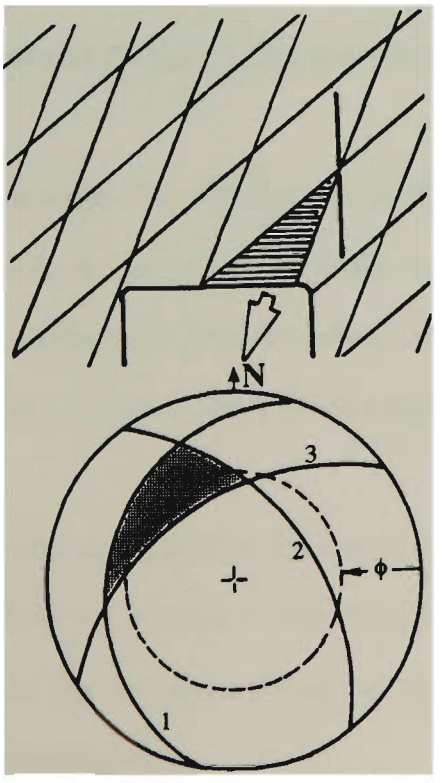

Figure 2.16. Rock wedge sliding along discontinuity planes

(after Hoek and Brown, 1980)

potential sliding plane is at a smaller angle than the angle of friction of the surfaces, and the wedge is stable. Figure 2.16 shows the unstable situation where the circle scribed by radius ϕ passes through the closed figure formed by the planes.

2.4.2 Determination of Size and Shape of a Wedge

The stereographic plot can also be used for a detailed estimation of the size and shape of a potentially unstable wedge in both the roof and sidewalls of an opening.

1. Roof Failure Analysis

Three planes determined by the maximum pole concentrations of discontinuity planes are represented by the three circles marked A, B, C (see Figure 2.17). The strike lines of these planes are marked a, b, c and the traces of vertical planes through the centre of the net and the great circle intersections are marked ab, ac, bc.

Considering a development width $2W$, the directions of the strike lines correspond to the traces of the planes A, B, and C on the back, assuming a horizontal back. These strike lines can be combined to give the maximum size of the triangle which can be accommodated within the space of the development.

In plan, the apex of the wedge is defined by finding the point of intersection of the lines ab, ac, bc projected from the corners of the triangular wedge base as shown in Figure 2.17. The height of the wedge is found by taking a section through the wedge apex normal to the development.

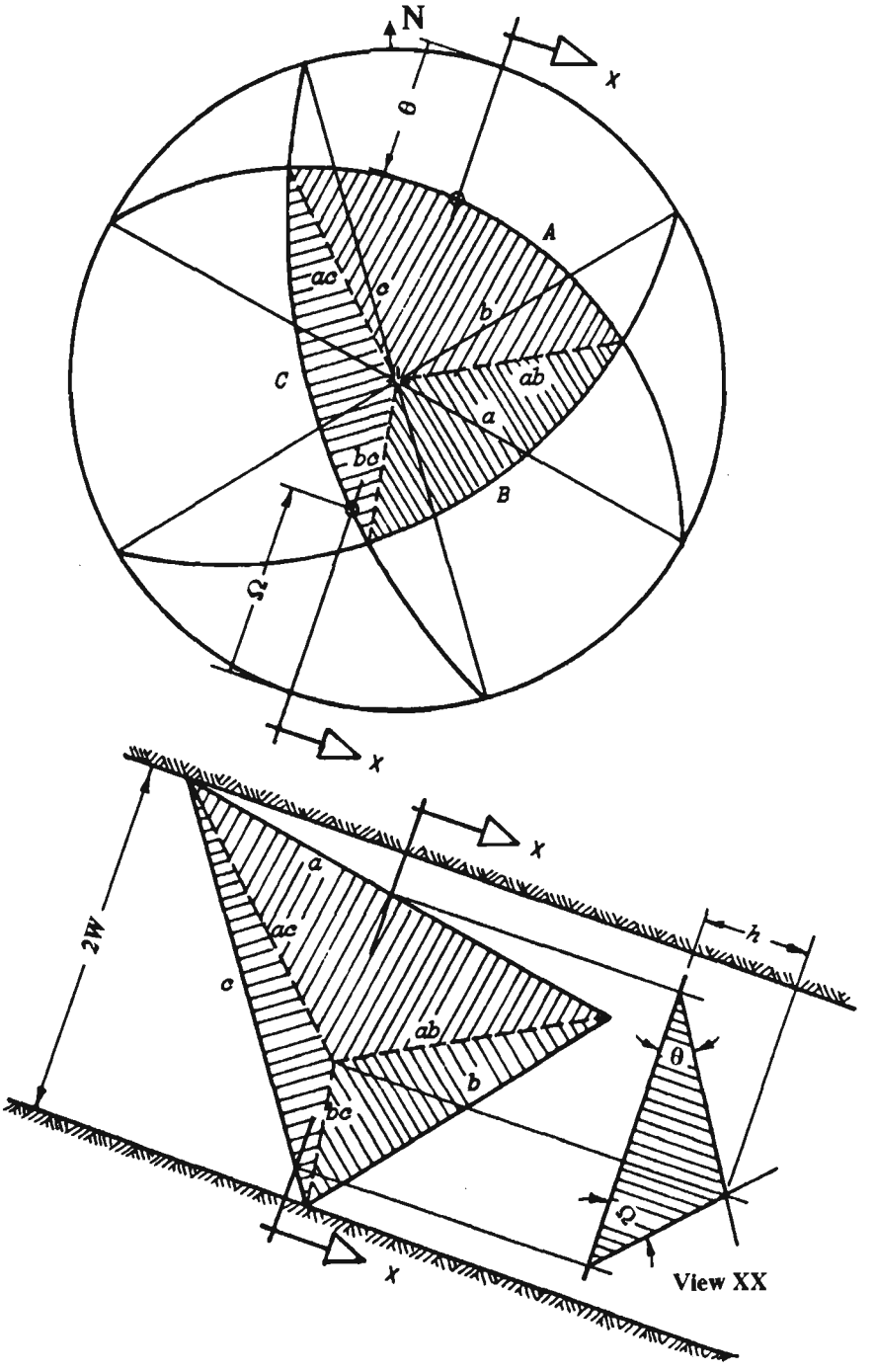

Figure 2.17. Stereoplot of three discontinuity sets defining a wedge falling from the roof (after Hoek and Brown, 1980)

The apparent dips of the planes A and C are given by the angles θ and Ω which are measured on the stereographic projections along the line X-X through the centre of the net. Having found the shape of the base of the wedge, its area can be obtained. The volume of the wedge is given by 1/3 base area $\times$ height, thus the weight of the wedge can easily be calculated.

In the case of sliding failure conditions, the principles used to construct the true plan view and height of the wedge are similar to that shown in Figure 2.18. In determining the height of the wedge the view X-X must be taken at right angles to the line ab which passes through the centre of the net and the intersection of the great circles representing the planes A and B. The angle Ω is the true dip of the line of intersection of these two planes.

2. Sidewall Failure Analysis

In order to determine the shape of a wedge which may fail in the sidewall of an excavation it is necessary to construct the intersection figure in the vertical plane, as shown Figure 2.19.

This intersection is obtained by rotating the great circle intersections through 90° about the excavation axis. Construction of the true view and height of the sidewall wedge is done in the same way as for the wedge in the back.

Sidewall failure can also be analysed by determining the apparent dips α, β and ξ of planes A, B and C in a vertical plane parallel with the excavation axis.

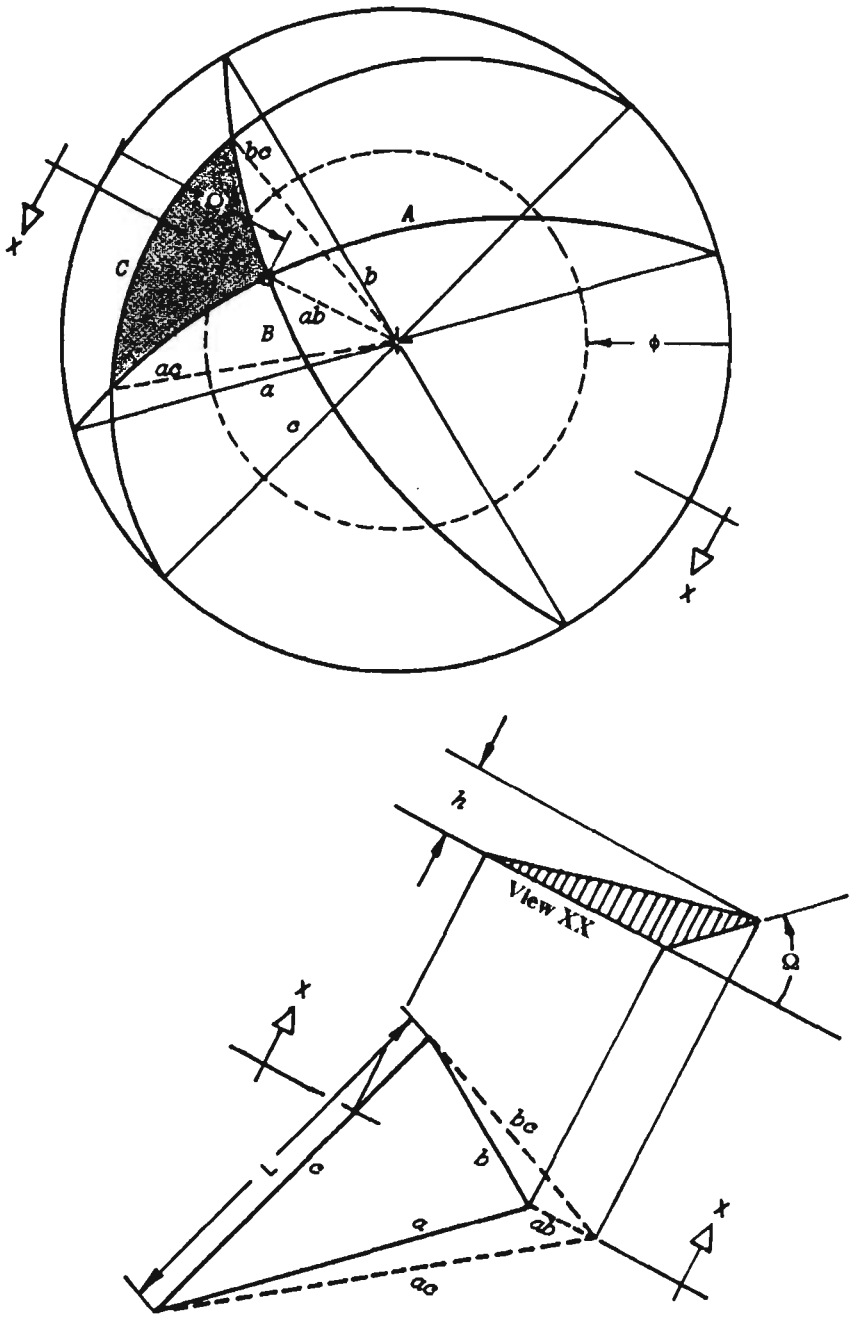

Figure 2.18. The determination of the shape and volume of a wedge sliding along the line of intersection of two planes, using stereographic projection, (after Hoek and Brown, 1980)

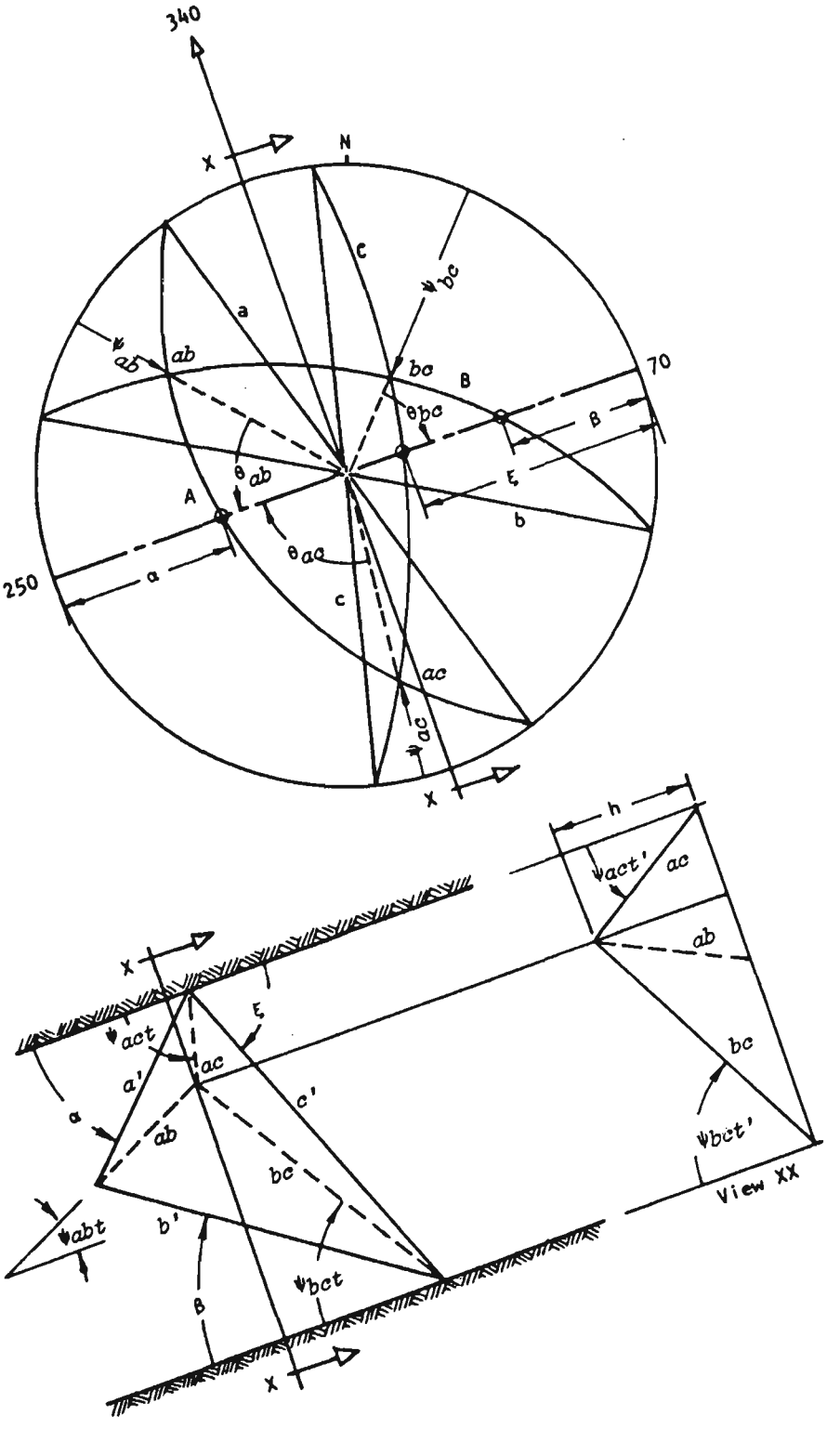

Figure 2.19. Construction of the true view of a wedge in the sidewall of an opening (after Hoek and Brown, 1980)

The apparent dips of the traces ab, ac and bc in the sidewall are established by finding the dips ψ_{abt}, ψ_{act} and ψ_{bct} of the projections of these lines of intersection onto the sidewall, assuming vertical sidewalls. The angle ψ_{abt} is given by:

$$\tan\psi_{abt} = \tan\psi_{ab}/\cos\theta_{ab} \qquad (2.8)$$

where; ψ_{ab} and θ_{ab} are the true dip and the angle between the development and the projection of the line of intersection ab respectively.

Similarly angles ψ_{act} and ψ_{bct} are found.

The height of the wedge is found by determining the angles $\psi_{bct'}$ and $\psi_{abt'}$ which represent the dips of the lines of intersection as seen in the vertical plane running normal to the excavation axis. $\psi_{bct'}$ is given by $\tan\psi_{bct'} = \tan\psi_{bc}/\sin\theta_{bc}$. Other angles are determined in a similar way.

Once the size and geometry of potentially unstable wedges of rock have been determined it is possible to design a bolting pattern to retain all such wedges.

2.4.3 Key Block Theory

The words "key block" indicate the objective of the theory. The theory is based on a rock block concept and the objective is achieved by combining basic concepts of geology, rock mechanics, vector geometry and topology (Warburton, 1981, 1982, 1985, 1987 and Goodman & Shi, 1985). According to the theory, the sliding of a rock mass is induced by a key block, as shown in Figure 2.20, which always slides first and leads to the sliding of other blocks. The numbers shown in Figure 2.20 represent the order of collapsing blocks, and here block 1 will collapse first, this

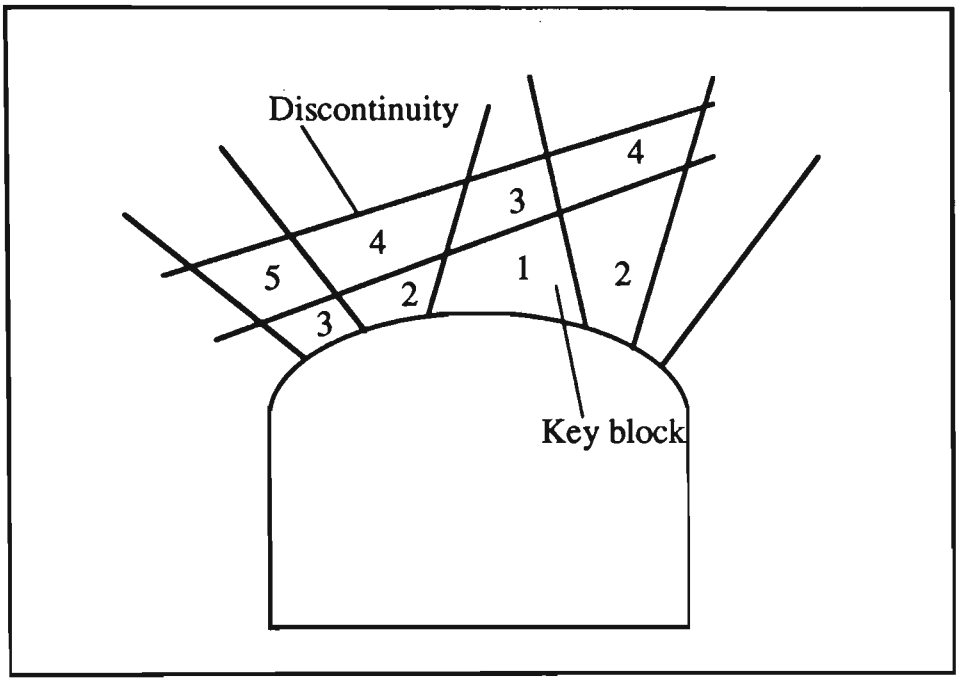

Figure 2.20. Key block in a rock mass

leads to the collapse of block 2, then 3 and so on. Therefore block number 1 is referred as to the key block. It is evident that a key block is potentially critical to the stability of an excavation because by definition it is finite, removable, and potentially unstable. Several concepts are introduced before any further discussion can be conducted. The joint pyramid, JP, is defined as the joint-plane subset of the half spaces determining a block pyramid. The excavation pyramid, EP, is the set of shifted excavation half spaces. The block pyramid, BP, is then defined as the intersection of the joint pyramid and the excavation pyramid for a particular block, i.e. BP = JP $\cap$ EP. The space pyramid, SP, is the set of directions that is complementary to EP, i.e. SP =~ EP.

In the analysis of the block system, graphical constructions and accompanying vector analysis enable the blocks to be classified according to their removability. A removable block should be finite and an infinite block, as shown in Figure 2.21 (a),

is not removable. However, a finite block is uncertainly removable. Five types of rock blocks can be identified as Table 2.6. An infinite block, as Figure 2.21 (a), is

Table 2.6. Five types of blocks and their removability

Type of block		Removability	Comments
I	Infinite	Unremovable	
II	Finite	Unremovable	Tapered
III	Finite	Stable even without friction	
IV	Finite	Stable with sufficient friction	Potential key block
V	Finite	Unstable without support	Key block

safe to an excavation. The finite blocks are divided into two groups, removable and unremovable. A block with a tapered shape is unremovable, as represented in Figure 2.21(b). Nontapered blocks are removable, but they may be removed under certain circumstances of loading. A type III block, as in Figure 2.21(c), has a favourable orientation with respect to the resultant force so that it tends to remain stable even without friction on its faces. However sufficient water pressure may lead to a unique failure type, which is lifting. A type IV block is shown in Figure 2.21(d); it is considered to be a potentially unstable block and will move towards the free face unless the friction on the potentially sliding face is sufficiently high. A true key block (V) is shown in Figure 2.21(e), which is not only removable but orientated in an unsafe manner and support must be installed to stabilise it. Mathematically a block is finite if and only if:

$$JP \cap EP = 0 \qquad (2.9)$$

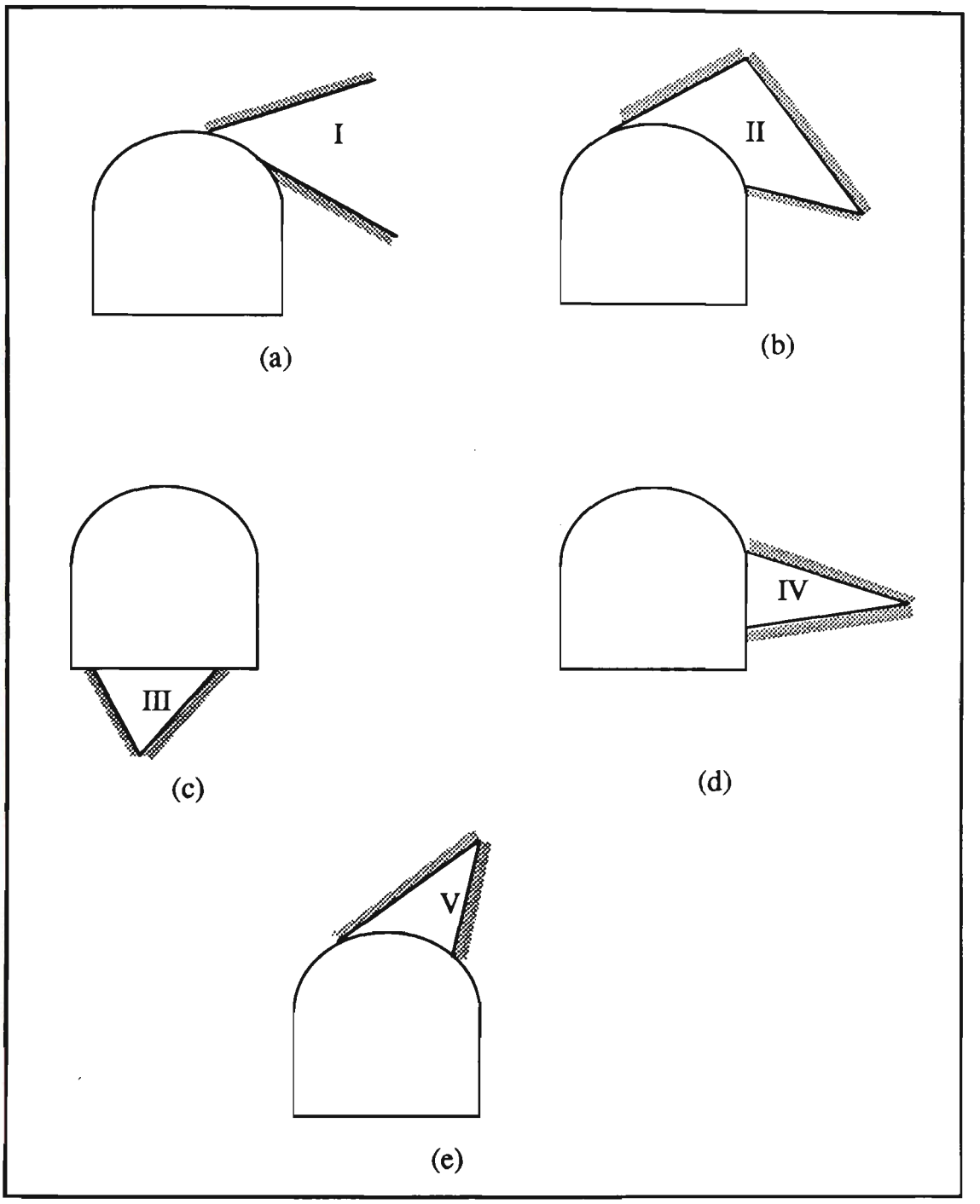

Figure 2.21. Different types of blocks (after Goodman and Shi, 1985)

i.e. the system of inequalities describing JP ∩ EP has an ordinary solution. It can also be stated in an equivalent manner that a block is finite if and only if its JP is entirely contained in the SP, that is, if and only if:

$$JP \subset SP \tag{2.10}$$

Therefore, the removability of a finite block can be judged: a finite block is removable if its BP is empty, $BP = JP \cap EP = 0$, and its JP is not empty, $JP = \bigcap_{i=1}^{h} JP(A_i) \neq 0$, where A_1, A_2, ...A_h are points on the block, and a finite block is not removable (tapered) if its BP is empty and its JP is also empty, $JP = \bigcap_{i=1}^{h} JP(A_i) = 0$.

After the determination of the key blocks the shape and size of the blocks can be found. Subsequently the direction of sliding can be determined from the direction of resultant force. To design parameters of rock bolting the limit equilibrium equation of a sliding block is established as;

$$\vec{r} - \sum_{ij} N_{ij}\hat{P}_{ij} - T\hat{S} = 0 \tag{2.11}$$

Where; $N_{ij}\hat{P}_{ij}$ is the normal reaction to the planes;

$T\hat{S}$ is the tangent force consisting of friction on the sliding joint planes; and

$\vec{r}$ is the active resultant.

Four types of movement can be identified: uplifting, sliding on a single sliding face, sliding on two sliding faces and falling from the roof. Obviously, no matter what kind of failure occurs, $T\hat{S}$ is the force that should be applied to the block to stabilise

it and in the situation where a block will fall directly the weight of the unstable rock block is the force required to be supplied by the rock bolts.

Recently, a probabilistic model was established to predict the required support on the basis of the key block theory (Tyler et al., 1991). One of the difficulties with its use was choosing the critical value of the probability of forming a block, based on which a judgement can be made on the existence of a 'real' block.

2.5 COMBINED APPROACH

If in-situ measurement is closely combined with engineering geology and mechanical analysis, which reveals the behaviour of underground structures and support elements, an understanding can be reached about the effectiveness of support. As a result, different forms of combined approach, including the New Austrian Tunnelling Method (NATM) (Rabcewicz, 1964, 1965), an information-feedback-based design in China (Sun, 1983), a field measurement aided design technique (FADT) by Sakurai (1983) and an in-situ measurement approach by Bawden and Milne (1987) have been developed. Although there are various kinds of combined methods used by designers in which the main procedure consists mainly of the following aspects: initial design, in-situ measurement and information feedback (of which feedback is the most important). The procedure is described in the diagram shown in Figure 2.22.

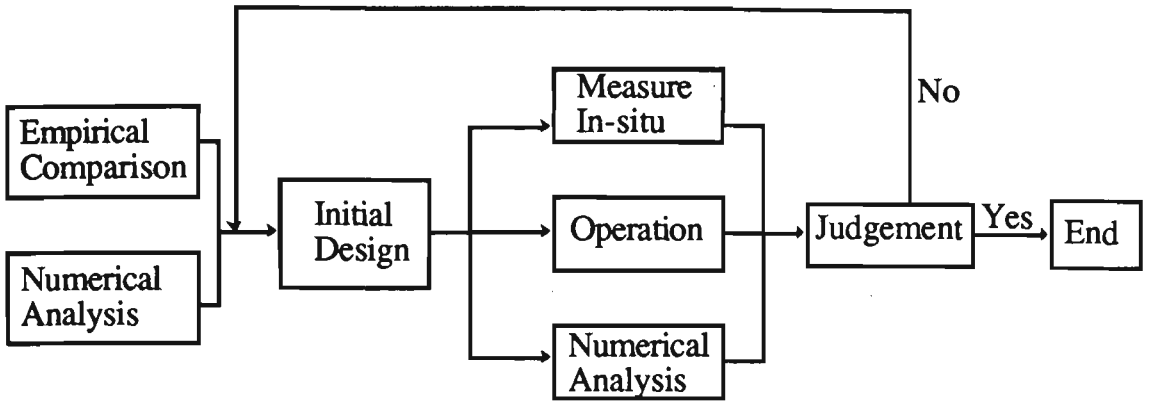

Figure 2.22. Main procedures of the combined approach

2.5.1 The New Austrian Tunnelling Method (NATM)

Since it was developed in late 1950's and early 1960's, the NATM has been applied all over the world for all kinds of underground works with differing success. The beginning of the NATM in its practical form took place just after the Second World War when there was a need to overcome tunnelling problems in very difficult geotechnical situations using an almost entirely empirical approach. This led to a very successful combination of theory with practical experience, giving a scientific-empirical design approach. After excavation of a tunnel the primary stress state of a rock mass is transformed through several intermediate steps of stress redistribution into a new, stable and secondary stress state. The concept of the NATM is to activate the ground surrounding the excavation such that it will maintain a loadbearing capacity and thus influence the time-dependent stress rearrangement process in such a way that a new secondary state of equilibrium can be reached with minimum support requirement. As its definition, Professor Rabcewicz (1964) said quite unequivocally '... a new tunnelling method - particularly adopted for unstable ground - has been developed which uses surface stabilisation by a thin auxiliary

shotcrete lining, suitably reinforced by rock bolting and closed as soon as possible by an invert. ... The method has been called The New Austrian Tunnelling Method.'

For the application of the NATM certain principles are to be followed which were described by Rabcewicz (1964, 1965) and Rabcewicz and Golser (1973 and 1974). These were summarised later by others to yield a series of rules (Brown, 1981). The main principle is that a tunnel is to be seen as a composite structure consisting of the surrounding ground, support, and ground strengthening elements. During the excavation of a tunnel analysis and observation are necessary. Only after analysing and observing failure and deformation phenomena can an understanding of the behaviour of a rock mass be gained and thus improve the design and construction methods (Golser, 1981).

Essentially the NATM is a scientific-empirical approach and has evolved from practical experience and what Rabcewicz called 'empirical dimensioning'. However it has a theoretical basis involving the relationship between the stresses and deformations around tunnels (better known as the ground support reaction curve).

2.5.2 Ground Support Reaction Curve

The gradually increasing deformation of an excavated rock mass is the basis of the NATM, in which support is provided by a thin shotcrete ring together with a systematic pattern of rock bolts. In soft ground at shallow depths, the shotcrete ring and rock bolts are installed as early as possible to prevent detrimental loosening. In deeper and more competent ground however, the time of installation is delayed and

the support stiffness chosen with a view to allowing the optimum mobilisation of the inherent strength of the rock mass. When the support is excessively stiff and /or is placed too early, points C and B in Figure 2.23, it will constrain deformation to a magnitude below the optimum point, thereby attracting excessive loads. In contrast, when the support is too soft and/or is placed too late, as shown at points G and H, the rock mass is likely to soften and weaken. Obviously the optimum support is set as points E and F, i.e. when the rock mass has deformed to some extent.

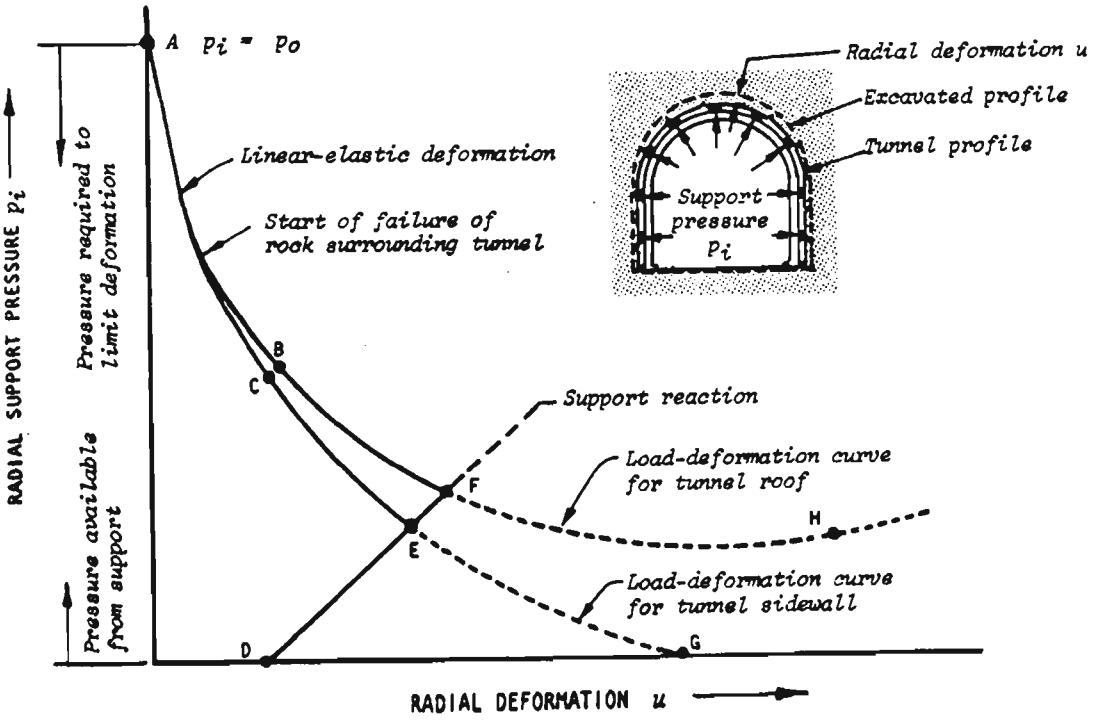

Figure 2.23. Ground support reaction curve (after Hoek and Brown, 1980)

2.5.3 Field Measurement Aided Design Technique

An analytical approach called the back analysis method (Sakurai, 1981, 1983) uses an inverse approach based on the finite element formulation. With this technique the data measured in-situ and from laboratory experiments are input into a computer, and as a result the initial stress field and constants of the rock materials can be determined. It can be closely combined with operational practices.

2.6 OPTIMISATION OF THE PARAMETERS

The design of rock bolting systems is very important in rock engineering. Any carelessness may lead to failure of an underground excavation. On the other hand, a conservative design will also cost much more than it should. Although some design methods are considered to be conservative, use of a safety factor is still necessary in design. To some extent, choosing a safety factor remains one of the main difficulties in design. In many mines, bolts are placed in a certain pattern and at a certain angle. Optimisation of rock bolting is rarely done. Whether the parameters chosen are reliable is not take into consideration until an underground excavation fails, which means that designers are often over-confident in their design. On the other hand, some mines are over-cautious regarding the stability of the rocks to be supported and little is done to seek a set of more reasonable parameters to reduce the cost of bolting and the time used for installation of the rock bolts. To design a satisfactory rock bolting system, the following points should be taken into consideration:

2.6.1 Bolting Angle

The angle of bolts placed in a rock mass is related directly to bearing capacity. Bolts should be so placed that the maximum bearing capacity can be reached. In cases of rock block sliding, bolts are often regarded as working mainly in shear and therefore it is recommended to design bolts on the basis of shear strength. It was considered that the most effective bolts are those fixed at an angle β_{opt} to the joint (Gaziev and Lapin, 1983).

$$\beta_{opt} = i_o(1-\frac{\sigma_{cjs}}{\sigma_{cjw}})^{10} + \phi_o \qquad (2.12)$$

Where; β_{opt} is the optimum bolting angle;

i_o is the original angle of the joint asperities rising in the direction of shear;

σ_{cjs} is the integral normal compressive stress on the joint surface;

σ_{cjw} is the compressive strength of the joint wall; and

ϕ_o is the angle of residual friction on the smooth joint surfaces obtained from laboratory or field tests.

In the case of bedded strata the bolts should form the largest possible angle with the bedding planes in order to spread the load to the maximum number of beds. A rock mass usually has two or more systems of discontinuity planes, which means that if the bolts are unfavourably placed there will be a further reduction in the effectiveness of the reinforcement. A series of tests were done, (Ludvig, 1983), which showed the influence of inclination of rock bolts on the shear strength of a rock mass. The shear strength of a rock mass bolted at an inclination of 45° was larger than that obtained when the inclination was 90°.

2.6.2 Bolt Length

Mining engineers usually consider that the length of bolts should be so chosen that the anchors of point-bolts or a part of the length of fully bonded bolts can be placed in competent rock. Some even consider the longer the bolt the better the bolting effect. In fact the length of bolts has a significant bearing on the formation of stabilised structures.

The natural arch is an old-fashioned concept but this is supported by the results of some new experiments. The study done by Hibino and Motojinia (1983), from 12 Japanese underground caverns with spans ranging from 14.6 to 28 m, showed massive evidence for the existence of natural arch action. Based on in-situ measurements, it was found that in the case of jointed rock masses, dilation or joint opening causes almost all roof subsidence to occur in a very limited part of the rock mass; from 0 to 5 m above the roof surface.

Some work on rock arches has been done in Greece, and this showed that the formation of a natural arch would be accompanied by high stress concentrations. The rocks in the failure zone under the natural arch required stabilisation (Habenicht, 1983). This means that the set of bolts should reach into the natural arch. The bolted arch combined with the natural arch is commonly used to resist the load.

In contrast, it is considered that long bolts, especially tensioned bolts, which reach far above the natural arch zone, do not seem to be a technically desirable support measure to control dilatancy in a stabilising way because their use destroys the ability for coherent downwards deformation necessary for arch action (Bergman and Bjurstrom, 1983). The reason for this difference is the situation in which the

bolts are applied. With a solid natural arch the bolts may be preferably placed into solid strata. In jointed rock masses the bolts should be placed so that a bearing ring can be formed.

There are several representative formulae which are available to calculate the length of bolts. The length of bolts is recommended:

- by the Norway Institute for Rock Blasting Technique (IFF) from hard rock practice in Scandinavia (Schach et al, 1979): $B_l = 1.40 + 0.36W$, Where B_l is the length of bolts, W is the half span of an opening (both in m).
- by Pender et al (1963) from experience on the Snowy Mountains project): $B_l = 1.80 + 0.013 \times (2W)^2$.
- by Rabcewicz (1955) from experience with the New Austrian Tunnelling Method: $B_l = 0.3 \times 2W$.
- by Singh et al (1982) from experience in Mount Isa Mines: $B_l = 0.5 \times 2W$.
- by Thompson and Windsor (1992) from experience on bolting of rock wedges: $B_l = H_{mw} + 2.0$, where H_{mw} is the maximum height of the wedge.

2.6.3 Bolt Spacing

The spacing of bolts should be designed such that the active zone of individual bolts intersects, otherwise arch building is impossible. It is considered that in the case of non-prestressed grouted rock bolts a reduction of bolt spacing produces a higher system strength than an increase in bolt diameter (Wullschlager and Natau, 1983). But if bolt spacing is reduced below a minimum the system strength may decrease due to the interference between the bolting forces. Generally, the bolt spacing, B_s, is designed as $B_s \leq 3 \times S_p$ (S_p = joint spacing) in a jointed rock mass and half the bolt length in other rock conditions (Stillborg, 1986). It is evident that when the

rock mass is heavily jointed, i.e. the joint spacing is very small, the bolt spacing may be large than $3 \times S_p$.

2.6.4 Bolting and Economy

When rock bolting, stability considerations are usually taken as the most important aspect. However, the cost of materials should be also taken into account. An optimum rock support system should be chosen from both a stability and economic viewpoints. The cost includes the sum of the cost for rock support and for operation disturbance (Krauland, 1983). The support effect of a bolting pattern can be determined from the following parameters: support principle, rock bolt length, bolt spacing, distance between rows and orientation of rock bolts. Therefore, in order to obtain the optimum support effect and support cost, the parameters above should be optimised.

2.7 CONCLUSIONS

Generally the methods for rock bolting system design can be divided into three categories: empirical methods, numerical methods and observational methods. The problem with the observational method is that the design done in the initial stage is very general, and hence continual monitoring and observation are essential. If the system is under-designed, remedial action in the form of secondary support will be required to be implemented. However in cases where failure does not occur, the support system may be over-designed, hence the costs are higher.

The problem in applying numerical modelling is that the properties of a rock mass, particularly a jointed rock mass, are not fully understood and the constitutive

relationships still remain uncertain. Hence design by numerical modelling is still doubtful due to the inherent inaccuracy of the input data.

The empirical method was considered the most useful method in rock bolting design in the 70's and 80's, however, there are disadvantages in using this approach. The Q system and the geomechanics classification system used extensively for rock support design do not provide a satisfactory assessment of the jointing system, and as such the rock bolting design suggested by these systems may be unreasonable due to the dominant behaviour of the discontinuities in a jointed rock mass.

The key block theory is considered to be a useful tool in stability analysis and rock bolting design. However topology and set theory are outside common course content encountered by engineering students and generally beyond the knowledge of most engineers, thus the complexities of this method make it unlikely to be understood by the on-site engineer. In addition, determination of the probabilistic value of a potentially unstable block is significantly influenced by the judgement of the engineer.

Other methods used, although relatively 'accurate' from a geomechanical view point are not practical under operational conditions (e.g. systems which suggest bolting patterns which are impossible to achieve in an underground situation). Obviously engineers can apply practical remedies on-site, but again this is time consuming and often based on crisis management. Therefore there is a great deal of room for improvement, with the direction being towards a rational, user-friendly and practical system for rock bolting design.

The main features of a method for rock mechanics design are presented in Figure 2.24 and they can be adopted in rock bolting design. However, a comprehensive

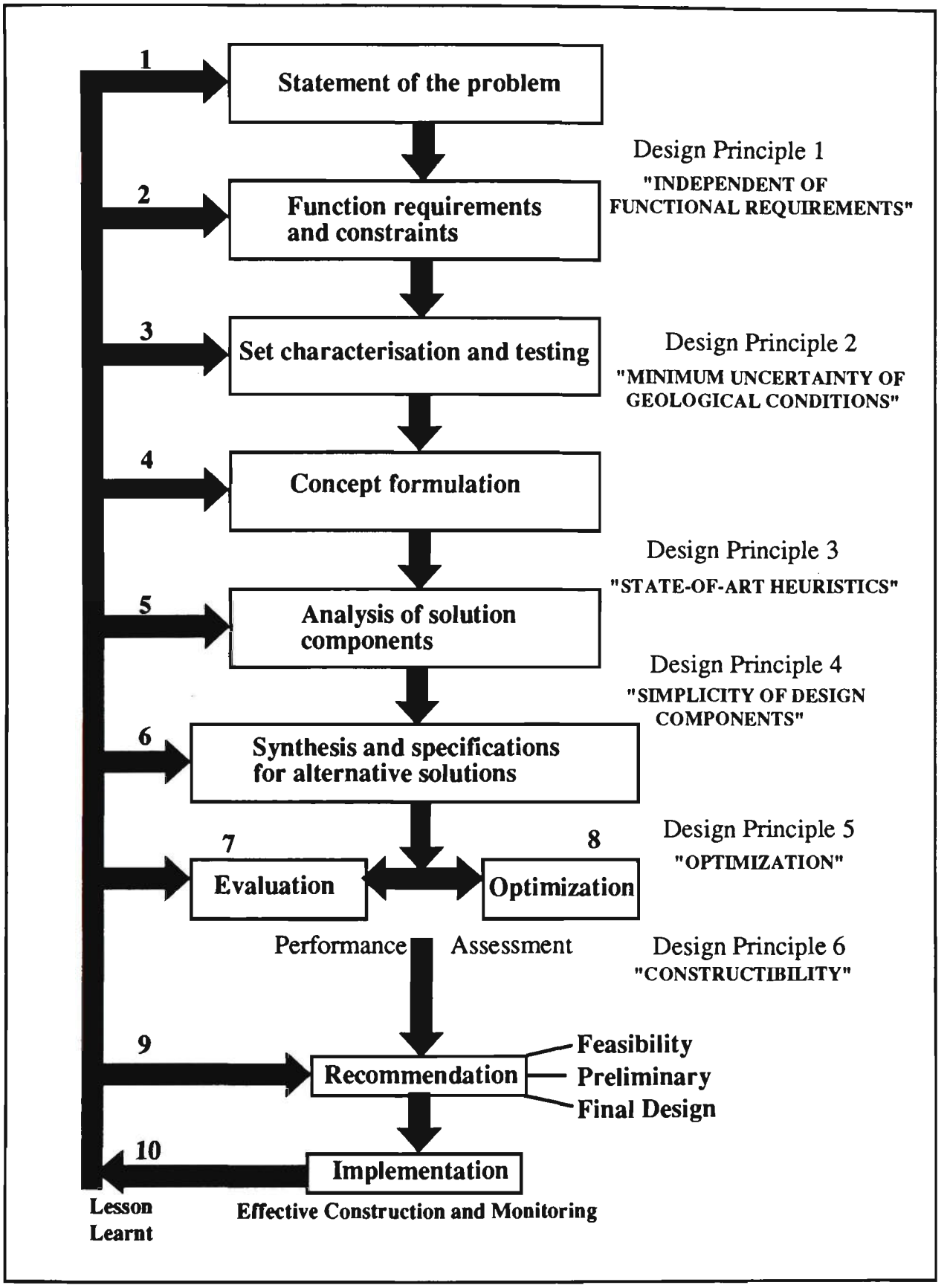

Figure 2.24. Methodology for rock mechanics design proposed by Bieniawski (1991)

design methodology is not just a flowchart for step-by-step design (Bieniawski, 1991). To be comprehensive, a method for rock bolting design must incorporate design principles which can be used to evaluate designs and to select the optimum which fulfils the perceived objectives. A design methodology must indeed recommend an order of design stages but these must be structured so as to assist in effective decision making and promote design innovation in accordance with the design principles.

CHAPTER 3

DETERMINATION OF MAJOR DISCONTINUITY SETS IN A GEOLOGICAL AREA

3.1 INTRODUCTION

In underground mining, excavations may not be self supporting, so support or reinforcement may be required to keep them in a stable condition. If the rock mass is jointed the task for design of such a support system will become more difficult, and it is first necessary to gain a thorough understanding of the jointing system and access the impact of the system on the stability of a structure in that rock mass. To achieve this goal a geological investigation should be carried out and the orientation data of the discontinuities collected. This may involve using a scanline survey.

In processing these data several techniques can be used as mentioned in the last chapter, the stereographic projection was favoured by many engineers and

geologists (Goodman, 1976, Hoek and Brown, 1980, Sun and Gu, 1982, Singh et al, 1982, 1991, Priest, 1985, Zhang and Tong, 1988). This technique allows interpretation of the statistically significant trends in the joint distribution and therefore tends to favour quantity and not quality, whilst other factors such as the grid density of the stereonet also have a significant influence on the outcome of the analyses.

In the determination of major discontinuity sets for stability analysis it is necessary to consider not only the joint concentration, but also the quality of the discontinuity. This takes into account other factors such as ground water influence, infilling material, spacing, roughness, waviness, aperture and continuity. If the quality of the discontinuity is not considered it may lead to discontinuity sets with a minor frequency and significant influence being inadvertently ignored.

3.2 DETERMINATION OF MAJOR DISCONTINUITY SETS

To overcome the limitation of the stereographic projection technique a method is presented where the geological data are processed by clustering analysis and stereographic projection, to classify the discontinuity sets according to their pole distribution, and then a rating system is applied to take account of groundwater and other parameters which characterise a discontinuity condition. Information received from the above analysis is used to determine an overall discontinuity rating, i.e. the effect the discontinuity has on the required support pattern and density. It should be noted that the rock mass is not being classified only the discontinuity.

Due to the varying use of the geological and geometrical terms in different text books, some terms most often used in this text are defined in page xvi.

Throughout this thesis, the geometrical characteristics of a discontinuity have been defined as dip and dip direction. Dip is the maximum acute angle the plane of a structural discontinuity makes with the horizontal; defined by the angle α, as shown in Figure 3.1. It ranges from 0 to 90°. Dip direction or dip azimuth is the direction of the horizontal trace of the line of dip, measured clockwise from north; as indicated by the angle β in Figure 3.1. Dip direction, β, ranges from 0 to 360°.

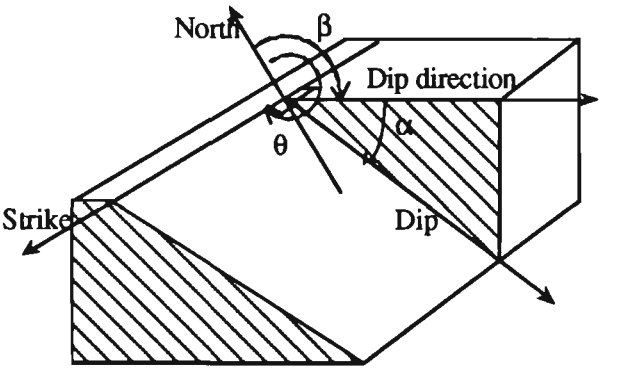

Figure 3.1. Dip and dip direction of a discontinuity plane

Strike is the trace of the intersection of an obliquely inclined plane with a horizontal reference plane and it is at right angles to the dip and dip direction of the oblique plane; defined by angle θ as shown in Figure 3.1. The range of strike is β - 90°.

Plunge is the dip of a line, such as the line of intersection of two planes or the axis of a borehole or a tunnel.

Trend is the direction of the horizontal projection of a line measured clockwise from north. Hence, it corresponds to the dip direction of a discontinuity plane.

3.3 COLLECTION OF GEOLOGICAL DATA

Data collection is the cornerstone of any practical rock mechanics analysis (Hoek, 1986). Before any stability analysis can be conducted on a scientific basis, a detailed survey must be conducted. It is very important to collect as much information as possible with respect to the salient features of each discontinuity. Various techniques are available; field mapping, core logging, borehole camera and scanline surveying, for collection of in-situ data. Recently an automatic mapping system has been developed, in which a video camera is used to record images produced from multiple scans of a rock exposure, with a thin laser beam (Ord et al, 1991). This technique is used to determine the orientation of discontinuities but other geological data such as ground water, infilling material, roughness and waviness cannot be obtained. Scanline surveying, whether on opening walls, bench faces or surface outcrops, can provide all discontinuity features of interest and is often used for gathering first hand in-situ data for the purpose of stability analysis.

To eliminate biases due to the favoured orientation a three dimensional scanline survey technique can be used. As shown in Figure 3.2a, the scanlines are arranged so that the scanning area will cover all three directions of an excavation. To undertake a scanline survey in one of the directions, as shown in Figure 3.2b, a measuring tape is fixed to the rock face at waist height by short lengths of wire attached to masonry nails hammered into the rock. The nails should be spaced at approximately 3 m intervals along the tape which must be kept as taut and as straight as possible. Where practicable, each scanline location should be photographed with the scanline number or location suitably identified. Once the scanline is established, the location (scanline number and place), date, rock type,

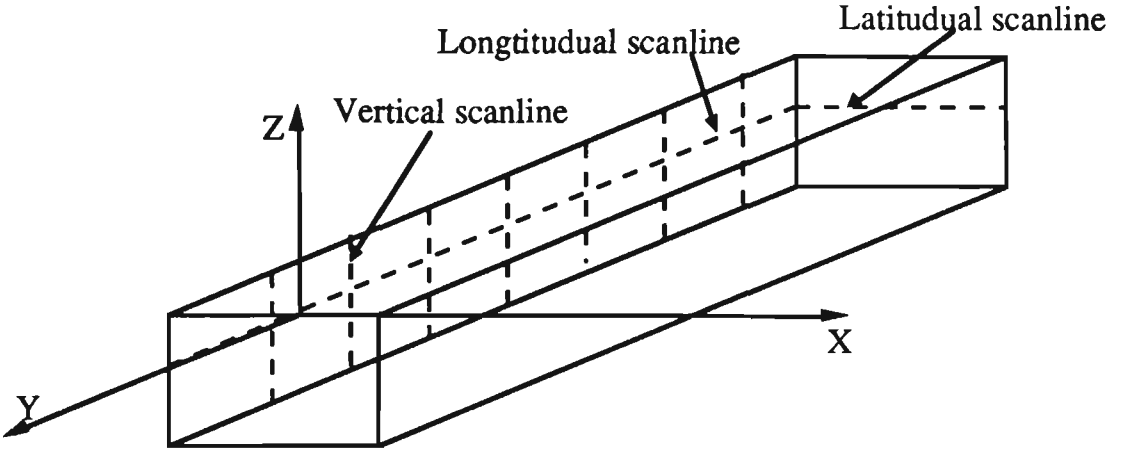

(a) Arrangement of a three-dimensional scanline survey

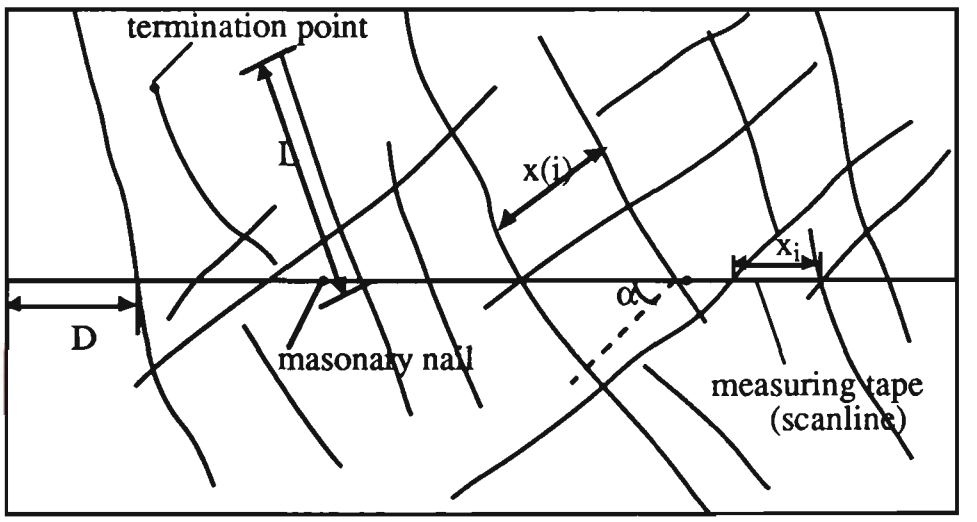

(b) Arrangement of a scanline in one of the three directions

Figure 3.2. Scanline surveying and arrangement

face orientation, scanline orientation and name of the surveyors are recorded on the record sheet. A clinometer is used to determine the orientation of the discontinuities intersected with the tape. The reading is taken by placing the folding lid against the plane to be measured and the body levelled with the target bubble. The orientation, dip and dip direction of all joints, faults and bedding planes crossing the scanline are recorded, together with distance D along the line. Type, continuity, infilling material and ground water are also recorded. All information gathered from the scanline is noted down on the scanline surveying record sheet as shown in Table 3.1.

Table 3.1. Scanline surveying record sheet

Location Face Orientation Scanline Orientation			Date	Rock type Observer Recorder		
D (m)	L (m)	NT	Orientation	CW	RN	Comments

D - distance along the scanline to the point at which the discontinuity intersects the scanline.

L - the length of the discontinuity measured above the scanline.

NT- nature of the termination point (A - terminated at another discontinuity; O - observed or extended beyond the extremity of exposure).

CW - curvature of waviness on a numerical scale, say one to five.

RN - roughness of small scale irregularities on a five-point scale.

Comments - particularly the nature of any infilling present, discontinuity aperture, water condition and type of discontinuity.

3.4 DATA PROCESSING

After the discontinuity data have been collected, data processing is conducted to obtain meaningful information. Processing of these data using the computer aided stereographic projection technique can be of great assistance, however this method does not help in the determination of the actual condition of each discontinuity set. The following section details the stereographic projection technique, clustering analysis and rating system used to determine the major discontinuity sets and their condition.

3.4.1 Computer Aided Presentation of Orientation Data

On the basis of the principle of stereographic projection, as shown in Figures 3.3 and 3.4, the distance from pole G to the centre O of the reference circle can be found using Equation (3.1).

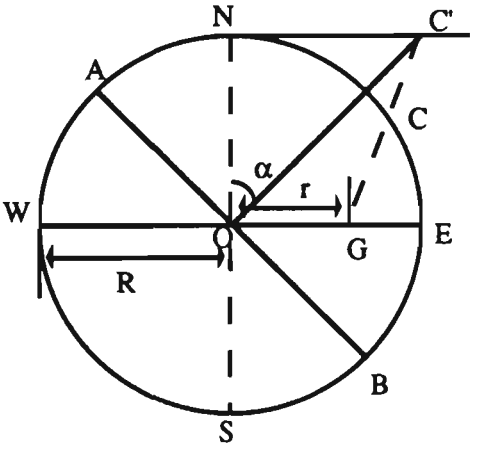

Figure 3.3. The distance from a pole G to the centre of the reference circle

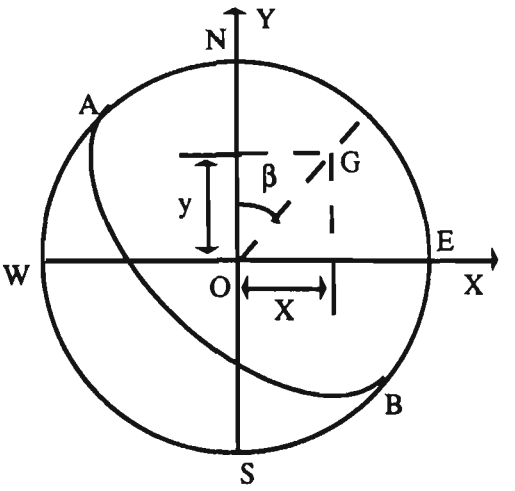

Figure 3.4. Coordinates of a pole

$$r = \sqrt{2}\, R \sin(\alpha/2) \tag{3.1}$$

Where; r is the distance from a pole G to the centre O of the reference circle;

R is the radius of the reference circle; and

α is the dip angle of the discontinuity plane.

In the coordinate system shown in Figure 3.4, the coordinate of any pole in the reference circle is given by Equation (3.2).

$$X_i = r \cos(90^\circ - \beta)$$
$$Y_i = r \sin(90^\circ - \beta) \tag{3.2}$$

Where; β is the dip direction of the discontinuities.

Substituting Equation (3.1) into Equation (3.2), the coordinate of the pole representing any discontinuity in the reference circle is found using Equation (3.3).

$$X_i = \sqrt{2}\, R \sin(\alpha/2) \cos(90° - \beta)$$
$$Y_i = \sqrt{2}\, R \sin(\alpha/2) \sin(90° - \beta) \qquad (3.3)$$

Based on Equation (3.3), it can be clearly seen that any structure may be expressed by a pole within the reference circle.

A net and ruler, as shown in Figure 3.5, are used for pole counting. The net consists of vertical and horizontal lines spaced at an interval of 1/20 to 1/50 of the

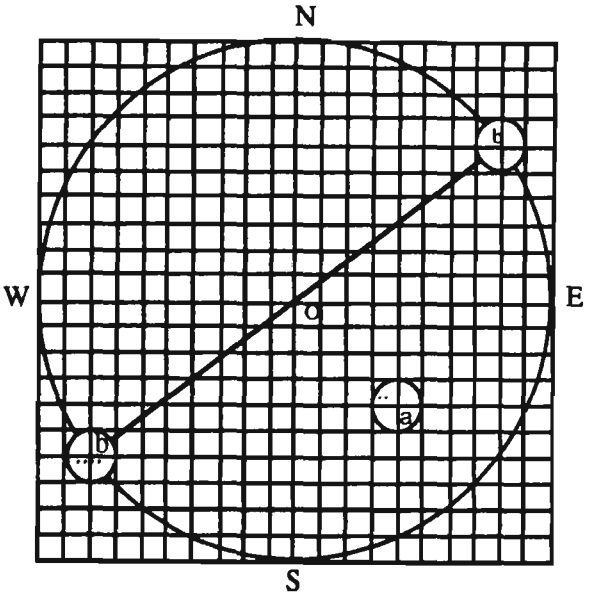

Figure 3.5. Net and ruler used in pole counting

radius, R, and the ruler, 1/10 to 1/40 of R, is a circle. As pole counting is performed, the ruler, a, is moved so that the centre of the small circle is located at the intersection of two lines in the counting net. The total number of poles within the circle is taken as the pole concentration at the intersection point of the lines. Ruler b is used at the fringe and the poles within the small circles at both ends are counted. The interval between the vertical lines or horizontal lines can be chosen freely. It is considered that the smaller the interval, the more accurate the results,

however more manual work is needed. This process can be automated using a micro-computer. The poles within each small circle are recorded at the intersection points of the lines and stored in a data file. Contours of pole concentrations are obtained by connecting the intersection points having the same pole count. The significant trends in the orientation data can be seen clearly from the stereoplot diagrams produced. Examples will be provided in the case studies in Chapter 7.

3.4.2 Clustering Analysis

Clustering analysis is a useful tool in rock engineering for classifying rocks and clustering orientation data (Shanley and Mahtab 1975, Lin 1985, and Xu et al, 1991). The various clustering analysis methods are based on three main techniques, hierarchical, dynamic and fuzzy clustering. The modified K-mean method, one of the dynamic clustering analysis techniques, is utilised to cluster the orientation data collected from the excavation site.

1. The Modified K-Mean Method for Clustering Orientation Data

As mentioned previously, any discontinuity plane can be expressed either by dip α and dip direction β, or by the dip and strike (an axis normal to the dip direction). This "strike axis" can form the basis of a three dimensional rectangular coordinate system, the origin of which is anywhere on the plane and which also acts as the origin of a spherical coordinate system. Any discontinuity plane can now be defined by the spherical coordinates (1, α, β), as shown in Figure 3.6.

Within a set of orientation data, Ω, where $\Omega=\{(\alpha_1, \beta_1), (\alpha_2, \beta_2), ..., (\alpha_n, \beta_n)\}$, there exists a partition, P, which is a collection of distinct nonempty subsets, Ω_i, of

Ω, such that each observation in Ω is contained in some Ω_i. Subset Ω_i, of partition P, is defined as a cluster of the orientation data.

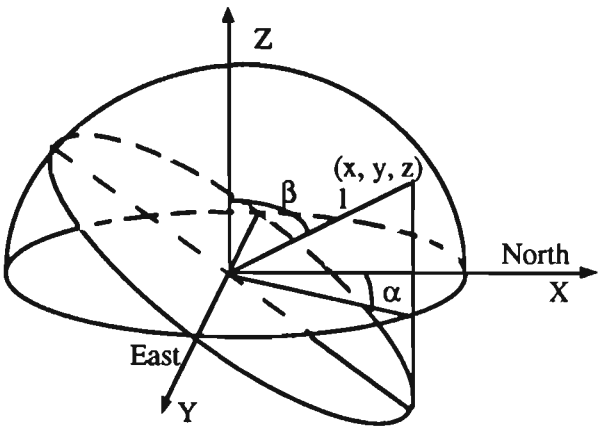

Figure 3.6. Representation of a discontinuity plane by point in a unit hemisphere

In the K-mean method the number of clusters is specified by the user and an initial reference point (coagulate point) is selected from the first sample. In using this method the problems are that the number of clusters is difficult to determine in advance and taking the first K sample as a coagulate point is not always reasonable if the two samples are very close. To modify this method, a 'dense point' is introduced to determine the cluster number and the coagulate points.

To find the density of any point, X_i, a sphere of arbitrary radius, R, is constructed around the point. A test is then performed to determine how many other points are contained within the sphere, i.e. a subset, Ω_i, is defined which has a provisional dense point, X_i. This test is performed for all points and the centre of these spheres which contain K or more observations are referred to as dense points. The number of points within a sphere is the density of the point, and the larger the number, the more qualified the point is to be a dense point.

Partitioning of the dense points can then be conducted from P_1 to P_k, in which every cluster contains only a single dense point. The initial test to find the dense points is repeated, so that if two dense points are within R of each other, a new partition, P_2, is defined. Subsequently appropriate points of the data set Ω are related to P_2 and a new partition P_3 is formed. This process is repeated until all points within the data set Ω belong to some cluster.

The problem in using thìs method is that the users have to select the elements of external control; R and K. Furthermore, some clusters may not contain any data points, depending on the sample and choice of R and K. The main reason for these difficulties is the randomness of the selection of R and K. Shanley and Mahtab (1975) modified the method by allowing the selection of R to remain arbitrary and setting K by means of a test for randomness derived from the Poisson distribution. The confidence degree is set at 95%. If two selected values of R are sufficiently different however, the two partitions defined by this technique will be different. Thus an objective function is introduced to characterise the variance of the set of orientation data. The best partition can be obtained from the minimum variance. The objective function can be expressed as Equation (3.4).

$$F(P)=\sum_{j=1}^{M}\sum_{i=1}^{N_j} d^2(X_j^i,\overline{X}_j) + \sum_{i=1}^{M-1}\sum_{j=i+1}^{M} d^2(\overline{X}_i,\overline{X}_j) \qquad (3.4)$$

Where; M is the number of clusters in partition P;

N_j is the number of points in cluster j of partition P;

X_j^i is the i-th element of cluster j;

$\overline{X}_i$, $\overline{X}_j$ are the centroids of clusters i and j respectively; and

$d(\overline{X}_i, \overline{X}_j)$ is the Euclidean distance between $\overline{X}_i$ and $\overline{X}_j$.

The centroid, $\overline{X}_c$, of a cluster i.e. a subset of orientation data, $\{(\beta_i, \alpha_i), i=1, 2, 3,...m\}$, is given by:

$$\overline{X}_c = \frac{1}{m}\sum_{i=1}^{m} X_i \qquad (3.5)$$

It is considered that the function F(P) is a good fit to circular symmetry about the mean. But the practical orientation data will not always follow a distribution of circular symmetry about their means. Other testing approaches should therefore be introduced.

2. Distribution and Testing of Orientation Data

For the majority of situations examined, the orientation of the data sets follows a distribution of elliptical symmetry about the mean; studied by Bingham (1964). This consideration is introduced in the following section.

(1) Bingham's distribution

Bingham's distribution (Bingham, 1964) can be expressed as:

$$\exp[\xi_1(\mu_1 x)^2 + \xi_2(\mu_2 x)^2 + \xi_3(\mu_3 x)^2]ds/[4\pi\, F(\tau; \eta; \xi)] \qquad (3.6)$$

Where; ξ_1, ξ_2, ξ_3 are dispersion parameters;

μ_3 is the best axis;

μ_1 is the axis of best zone;

μ_2 is the axis of a zone containing μ_1 and μ_3; and

$F(\tau; \eta; \xi)$ is a hypergeometric function of matrix argument; τ and η are constants.

Also

$$\xi = \begin{bmatrix} \xi_1 & 0 & 0 \\ 0 & \xi_2 & 0 \\ 0 & 0 & \xi_3 \end{bmatrix} \tag{3.7}$$

and the hypergeometric function can be expressed as:

$$F(\tau, \eta, \xi) = 1 + \frac{\Gamma(\eta)}{\Gamma(\tau)} \sum_{j=1}^{\infty} \frac{\Gamma(\tau+j)}{\Gamma(\eta+j)} \xi^j \tag{3.8}$$

While the Gamma function, $\Gamma(v)$, can be presented in its logarithmic form as Equation (3.9).

$$\ln\Gamma(v) = (v - \tfrac{1}{2})\ln v - v + \tfrac{1}{2}\ln(2\pi) - \int_0^{\infty} \left\{ \frac{1}{2} + \frac{1}{t} - \frac{1}{1 - e^{-t}} \right\} \frac{e^{-vt}}{t} dt \qquad (v > 0) \tag{3.9}$$

Where; v is an integer; and

t is a variable.

In Bingham's distribution $\tau = 1/2$; $\eta = 3/2$ and the constraint, $\xi_3=0$, is imposed. If the data are concentrated about a preferred orientation, both ξ_1 and ξ_2 will be negative. If $\xi_1 \neq \xi_2$, then $\xi_1 < \xi_2$ and the distribution of the data points in a cluster will be elliptical. The axes exist so that the axis μ_1 would be parallel to the minor axis of the ellipse, and the axis μ_2 parallel to the major axis of the ellipse. The axis μ_3, i.e. the best axis or the mean of the distribution, would be perpendicular to both μ_1 and μ_2.

Assuming a set of orientation data $\Omega=\{(\alpha_1, \beta_1), (\alpha_2, \beta_2), ..., (\alpha_n, \beta_n)\}$, the unit normal vector is given by

$$\mathbf{x}_i = \begin{bmatrix} \sin\beta_i \cos\alpha_i \\ \sin\beta_i \sin\alpha_i \\ \cos\beta_i \end{bmatrix} \tag{3.10}$$

The coordinates of the vector $\mathbf{x}_i$ are the rectangular coordinates of a point on the unit sphere whose spherical coordinates are (l, β, α). In addition, **X** can be defined as $[\mathbf{x}_1, \mathbf{x}_2, ..\mathbf{x}_n]$. Parameters ω_1, ω_2 and ω_3 ($\omega_1<\omega_2<\omega_3$) are the eigenvectors of following matrix:

$$\mathbf{X}\mathbf{X}^T = \begin{bmatrix} \Sigma x_i^2 & \Sigma x_i y_i & \Sigma x_i z_i \\ \Sigma x_i y_i & \Sigma y_i^2 & \Sigma y_i z_i \\ \Sigma x_i z_i & \Sigma y_i z_i & \Sigma z_i^2 \end{bmatrix} \tag{3.11}$$

Where; x_i, y_i and z_i are the coordinates of a point in the coordinate system in

Figure 3.6

As a result, the corresponding eigenvectors are the maximum likelihood estimates, $\hat{\mu}_1$, $\hat{\mu}_2$ and $\hat{\mu}_3$ of μ_1, μ_2 and μ_3. For ξ_1 and ξ_2 the estimation is made by interpolating from tables provided in the relevant text books.

E_{ij}^2 is utilised to express the variance of the rotation of $\hat{M}$ (a set of three axes in space) about the axis μ_k, where $i \neq k \neq j$. Here, $\hat{M} = [\hat{\mu}_1, \hat{\mu}_2, \hat{\mu}_3]$

$$E_{ij}^2 = 1/[2(E_i - E_j)(\omega_i - \omega_j)] \tag{3.12}$$

Where; E_{ij}^2 is the variance of the rotation of $\hat{M}$; and

E_i and E_j are the means.

After ξ, $\widehat{M}$ and E_{ij}^2 are known, the distribution of the orientation data in a unit hemisphere can be found using Equations (3.6), (3.7), (3.8) and (3.9). The test for distribution is then performed.

(2) The Chi-Square, χ^2, test

Assuming that $v_1, v_2, \ldots v_m$ are from a normal distribution $N(\mu, E_{ij}^2)$, in which E_{ij}^2 is not known, assumptions about E_{ij}^2 can be tested by the χ^2 distribution. Here, (β, α) denote the spherical coordinates of a unit vector computed with respect to $\widehat{\mu}_3$. The number n_k of points expected in a spherical quadrilateral $S = \{(\beta, \alpha) | \cos\alpha_2 \le \cos\alpha \le \cos\alpha_1, \beta_1 \le \beta \le \beta_2\}$ can be found from Equation (3.13) (Shanley and Mahtab, 1975).

$$n_k = \{n/[4\pi F(1/2, 3/2, \xi)]\} \int_{\beta_1}^{\beta_2} \int_{\alpha_1}^{\alpha_2} \exp[(\xi_1 \cos^2\beta + \xi_2 \sin^2\beta)\sin^2\beta] \sin\alpha d\alpha d\beta \quad (3.13)$$

Where; n is the total number of orientation data.

Before the χ^2 test can be applied to the set of orientation data, Ω, ξ and $\widehat{M}$ must be calculated. The poles of the data set Ω are then plotted onto the unit hemisphere by using a linear transformation which maps the three axes $\widehat{\mu}_1$, $\widehat{\mu}_2$ and $\widehat{\mu}_3$ onto the X, Y, Z axes, respectively. The image of C_1 is a set of points which are clustered about a point having (0, 0) as its spherical coordinates and (0, 0, 1) as its spherical rectangular coordinates. Next, the spherical coordinates of the points in the image of Ω are calculated.

Class intervals are structured so that each interval has an expected value greater than or equal to 5 percent of the total. The unit hemisphere is geometrically partitioned into a series of concentric circular bands, centred at $\widehat{\mu}_3$, each of which

is then divided into four class intervals. The expected number of points for each class interval is found using Equation (3.13). The χ^2 value obtained is then compared with the value in the table of the χ^2 distribution.

3.5 ASSESSMENT SYSTEM FOR DETERMINATION OF MAJOR DISCONTINUITY SETS

Clustering analysis and stereographic projection can only classify a set of orientation data into groups. A quantitative estimation cannot, however, be made using these techniques. In order to quantify the quality of the discontinuity sets for the purpose of stability analysis an assessment system should be introduced.

3.5.1 Assessment Parameters

There are so many factors that have an influence on the quality of a discontinuity set, it is difficult to take all of them into account. The factors considered in this system should characterise a discontinuity set as much as possible in respect of both quality and quantity. These parameters are:

- infilling material;
- roughness and waviness;
- aperture;
- trace length;
- ground water; and
- type and frequency of a discontinuity.

The definition of these parameters was given previously and here the quantitative description of these parameters will be presented.

1. Infilling Material

Based on its influence on the shear strength of a discontinuity plane, the infilling material can be classified as follows:

- Cemented: infilling material firmly cemented to the walls of a discontinuity.
- Noncohensive: soft infilling material between the walls of a discontinuity.
- Surface staining: stain on the surface of a discontinuity.
- Clean: no appearance of infilling material.

2. Roughness

In the preliminary stages of a field investigation, such as in scanline surveying, it is impossible to measure the roughness of every discontinuity using the standard method proposed by the International Society of Rock Mechanics (ISRM) (1976). Judgement is often made on the degree of roughness of the discontinuity based on the following:

- Very rough: very stepped discontinuity surface.
- Rough: stepped discontinuity surface.
- Mid rough: slightly stepped discontinuity surface.
- Slightly smooth: not stepped, but undalating.
- Smooth: smooth discontinuity surface.

3. Waviness

As applied to the definition of roughness there is a limitation on the time frame which prevents the surveyor measuring the waviness of every discontinuity. A judgement can be made on the basis of the following points.

- Very wavy: pronounced wavy profile.
- Wavy: wavy profile.
- Mid: irregular wavy profile.
- Slightly linear: apparently linear but slightly wavy profile.
- Linear: flat with no waves.

4. Aperture

Aperture is the perpendicular distance separating the adjacent rock walls of an open discontinuity. It can be recorded quantitatively as below:

- Wide: > 200mm.
- Mid wide: 60 - 200mm.
- Mid narrow: 20 - 60mm.
- Narrow: 6 - 20mm.
- Very narrow: 2 - 6mm.
- Extremely narrow: < 2mm.
- Tight: not obviously separated.

5. Water Conditions

The groundwater conditions are assessed based on the following considerations (Public Works Department, Hong Kong, 1981):

- Dry: no water.
- Seepage: damp discontinuity walls or filling materials.
- Slight inflow: visible but very small inflow.
- Mid flow: obviously visible inflow, 0.1 - 0.2 l/min.
- High flow: water flow > 1 l/min.

6. Type

The types of discontinuity considered here include fault zones, shear zones, faults, shears and joints. They are self explanatory.

7. Frequency

The number of discontinuities in a set, as determined from the clustering analysis of the field data (discussed previously in this chapter) can be expressed by the frequency of discontinuities. The frequency factor, F_F, is used to characterise this parameter and it can be calculated as:

$$F_F=\{[F_{max} - F(i)] / F_{max}\} \times 100\%$$

Where; F_{max} is the frequency of the discontinuities in the set with the maximum number of discontinuities; and

F(i) is the frequency of discontinuities in the i-th set.

8. Trace Length

This property of the persistence of a discontinuity set can be characterised by a quantitative factor, called the continuity factor, C_F. C_F can be found from:

$$C_F = \{[L_{max} - L(i)] / L_{max}\} \times 100\%$$

Where; L_{max} is the mean trace length of the discontinuities in the set with the maximum mean trace length; and

L(i) is the mean trace length of the discontinuities in the i-th set.

3.5.2 Rating System

A rating is assigned to each of the parameters by a mean value. The sum of the final ratings for every factor gives the final rating of the discontinuity set. The higher the rating value the lower the quality, and therefore in the determination of major discontinuity sets priority should be given to sets with higher rating values. The ratings for a single discontinuity set are given in Table 3.2.

From Table 3.2, it is evident that parameters 1-5 are used to assess the mechanical parameters of the discontinuity sets, parameter 6 is to indicate the differences in discontinuity types, parameter 7 is to assess the discontinuity sets in terms of their frequency, and finally parameter 8 is used to measure the continuity. Parameters 1 to 5 have been discussed in a previous section in this chapter. Parameter 6 is self explanatory. Whilst parameter 7, the frequency factor (F_F), characterizes the number of discontinuities in a discontinuity set (as determined from clustering analysis of the field data). Parameter 8, the continuity factor (C_F), is used to express the property of the persistence of a discontinuity set. The maximum total rating of the 8 parameters is 100.

Table 3.2. Rating system for the determination of major discontinuity sets

Par. / Cat. No.	1		2		3		4		5		6		7		8	
	water		infilling		waviness		roughness		aperture		type		frequency factor		continuity factor	
1	dry	0	clean	10	linear	10	smooth	10	wide >200mm	10	fault zone	20	100%	0	100%	0
2	seepage	3	surface staining	7	slightly linear	8	slightly smooth	8	mid wide 60-200mm	9	shear zone	20	80%	4	80%	2
3	slight flow	6	non-cohesive	4	mid.	6	mid.	6	mid. narrow 20-60mm	8	fault or shear	15	60%	8	60%	4
4	mid. flow 0.1-0.2l/min	8	cemented	0	wavy	3	rough	3	narrow 6-20mm	6	joint	5	40%	12	40%	6
5	high flow >1l / min	10	—		very wavy	0	very rough	0	very narrow 2-6mm	4	—		20%	16	20%	8
6	—		—		—		—		extr. narrow <2mm	2	—		0%	20	0%	10
7	—		—		—		—		tight	0	—		—		—	

3.6 CONCLUSIONS

Although they are useful tools for processing field data, the stereographic projection technique and clustering analysis may lead to a bias towards to the frequency of discontinuities. The rating system for the determination of major discontinuity sets will aid with rapid reduction of field data to useful information. It takes all important factors into consideration and characterises the discontinuity sets in a geological area in quantity and quality. The total rating of a discontinuity set indicates the quality of the discontinuity set and the higher the rating the worse the condition of a discontinuity set. Therefore, the use of this system should help avoid any bias that may arise when using the stereographic projection technique or clustering analysis alone. In addition, with the assistance of a microcomputer much of the tedious manual work can be eliminated when processing geological data.

CHAPTER 4

INITIAL DESIGN OF A ROCK BOLTING SYSTEM USING THE MODIFIED GEOMECHANICS CLASSIFICATION SYSTEM

4.1 INTRODUCTION

Rock bolting design is considered to be one of the most important steps in mining operations. However one of the difficulties faced by design engineers is to provide a set of reliable, rational and economical bolting parameters. To overcome these difficulties the geomechanics classification system is often used in designing rock bolting system. Practical use of this system showed that it was well suited to civil engineering and tunnelling. However this system was not suited to mining situations due to the complex mining environment. Modifications were made by Laubscher and Taylor (1976) and Laubscher (1990) to suit most mining conditions. Although the modified system is complex due to the incorporation of parameters

which account for weathering, blasting damage and the stress environment it is considered to be more suited to mining situation than other system. It is noted that shotcrete is still used for rock support in this modified system. This may cause difficulties when using this system as shotcrete is not normally used in Australian mines.

4.2 COMPARISON ON APPLICABILITY OF EXISTING CLASSIFICATION SYSTEMS

To date there are several rock mass classification systems available for the design of rock support. As mentioned in Chapter 2 there are still limitations in using these systems. In order to find the most suitable classification system for Canadian mines, a survey was conducted in Quebec to study the applicability of rock mass classification systems in the design of rock bolting support (Choquet and Charette, 1988). Ten underground mines in Quebec were involved in the survey and fifty-seven drift portions were classified according to four rock mass classification systems. These systems were:

- The geomechanics classification system (RMR) developed by Bieniawski (1974);
- The MRMR system by Laubscher (1976);
- The NGI (Q) system developed by Barton et. al. (1974);
- The simplified rock mass rating system (SRMR) developed by Brook and Dharmaratne (1985).

All the sites were stable, and the span of drifts varied between 2.8 m and 7.5 m, with the majority between 3.5 m and 5.5 m. The depth of drifts surveyed varied from 50 m to 1,000 m, with the majority between 100 m and 1,000 m.

The results from the survey showed that, a fair correlation between the ratings obtained from each system, the parameters included in the classifications are relevant to a mining environment and that they tend to give the same weight to similar types of information in the evaluation of the final rating. However, the RMR system is comparatively unsuitable for the mining environments surveyed.

4.3 MODIFICATION OF THE ROCK MASS RATING DUE TO THE STRESS FIELD

The reason for the inapplicability of the geomechanics classification system in the mining environment is that stress field was not considered in this system (Hoek and Brown, 1980). Practice shows that the stress field has a significant influence on the condition of joints by keeping the joints in compression, by increasing the possibility of a shear movement, or by allowing the joints to open. If the joints are kept in compression then the role of the field stress is taken as positive towards a stable state and correspondingly the rock mass rating will be retained or increased. If the role of the stress field is to open the joints the rock mass rating will be decreased. A series of models in appendix three of Underground Excavations in Rock written by Hoek and Brown (1980) indicates that the stress state in a rock mass varies as the ratio of horizontal to vertical stress changes. It is also related to the configuration of an opening. A favourable stress field will form a compressive zone around the opening and an unfavourable stress field will produce tensile stress

around some portion of the opening and excessive compressive stress around another portion of the opening.

The influence of the stress field on rock mass quality was summarised by Laubscher and Taylor (1976) and Laubscher (1990). The values set for modification of rock mass quality due to the stress environment range from 0.7 to 1.2 (Laubscher and Taylor, 1976). These values relate various stress field and opening configurations to obtain a stress modification coefficient, C_m. The correlation between the ratio of horizontal stress σ_h to vertical stress σ_v and the ratio of height H to width $2W$ of an opening is given in Figure 4.1.

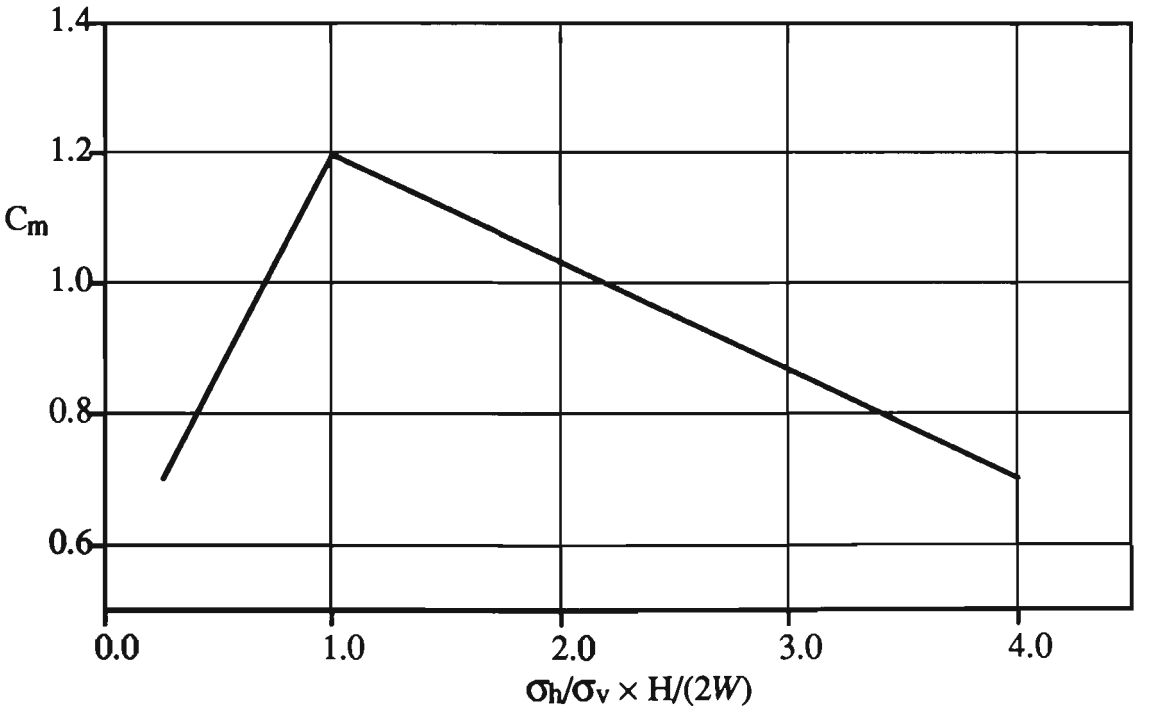

Figure 4.1. Modification of rock mass rating

For example, if σ_h = 20 MPa, σ_v = 10 MPa, H=4 m and $2W$ = 5 m, the value $\sigma_h / \sigma_v \times H/(2W)$ is 1.6. Therefore from Figure 4.1, the stress modification coefficient, C_m, is 1.1.

4.4 STRESS ANALYSIS AROUND AN UNDERGROUND OPENING

The rock mass near the surface of an unsupported excavation is in the unconfined state, and the stability of the excavation is dependent on the shear strength properties of the jointed rock mass, its unconfined compressive strength, and the state of stress in the rock after excavation. Failure of the unsupported excavation will result if the strength of the jointed rock mass is not enough to withstand the stress in the rock mass.

In order to reinforce the potentially unstable zone rock bolting may be utilised. Systematic rock bolting may tie the blocky or layered rock mass together and increase the shear strength of the rock mass by increasing the confining pressure in the rock adjacent to the opening. Rock bolting may increase confining pressure in two ways; by tensioning of rock bolts at the time of installation, thus actively confining the rock between the ends of the bolts, and by tensioning of unstressed bolts caused dilation of the rock mass after excavation.

Therefore in a systematic rock bolting situation the rock bolts increase the confining pressure of the rock in the reinforced roof beam and produce a triaxial stress state. This may be linked to triaxial testing and Mohr's failure criterion (Bischoff and Smart, 1975). The rock bolts effectively increase the allowable stress in the reinforced roof by $\Delta\sigma_1$. The relationship between $\Delta\sigma_1$ and the rock reinforcement confining pressure is a function of the rock mass friction angle, ϕ, as illustrated in Figure 4.2. If the thickness of the reinforced beam is t, then the load to be provided by bolting is given by following expression.

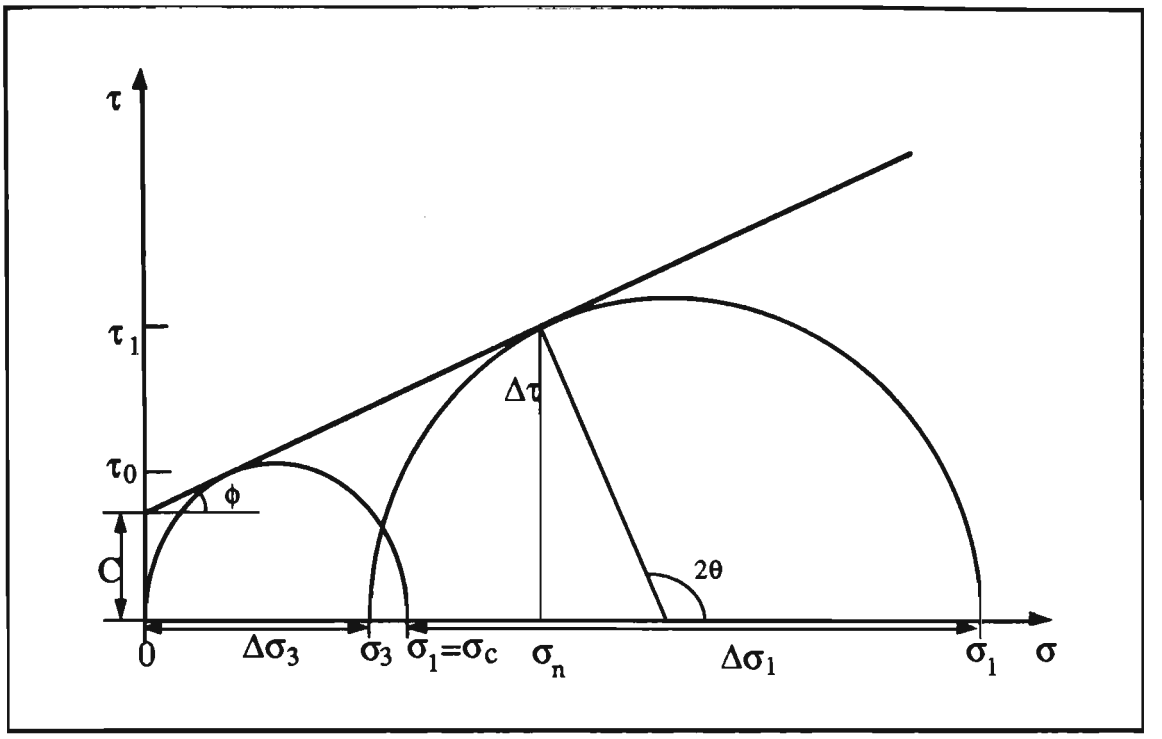

Figure 4.2. Mohr's stress circle

$$P_b = \Delta\sigma_1 t \qquad (4.1)$$

Where P_b is the load per unit length of excavation provided by the bolting system, kN/m;

$\Delta\sigma_1$ is the effective increase in the allowable stress of the rock mass in the reinforced zone, kN/m^2; and

t is the effective thickness of the reinforced rock, m.

If $\Delta\sigma_3$ represents the increase in confining pressure induced by the rock reinforcement in the rock mass at orientations perpendicular to the boundary of the excavation the corresponding effective increase in allowable rock stress $\Delta\sigma_1$ is given by Equation (4.2).

$$\Delta\sigma_1 = \Delta\sigma_3 \tan^2(45^\circ + \frac{\phi}{2}) \qquad (4.2)$$

Where $\Delta\sigma_3$ is the increase in rock mass confinement provided by the reinforcement;

ϕ is the friction angle of the rock mass.

4.5 INITIAL DESIGN OF A ROCK BOLTING SYSTEM

For a given thickness, t, of reinforced rock mass the load resistance per unit length of opening that should be provided by a rock bolting system is calculated by $\Delta\sigma_1 t$. The load capacity of the rock bolting system in a unit length of an opening can be obtained by substituting Equation (4.1) into Equation (4.2) as follows:

$$P_s = \Delta\sigma_3 t \tan^2(45^\circ + \frac{\phi}{2}) \qquad (4.3)$$

Where P_s is the load capacity provided by bolts in a unit length of an opening, kN/m.

It is clear that the increase in rock mass confinement, i.e. the minimum principal stress, $\Delta\sigma_3$, is the allowable strength of the rock bolting system used, i.e. $\Delta\sigma_3 = P_y / B_s^2$, where P_y is the yield load of the rock bolt and B_s is the bolting spacing. Therefore Equation (4.4) becomes:

$$P_s = P_y\, t \tan^2(45^\circ + \frac{\phi}{2})/B_s^2 \qquad (4.4)$$

For the stability of a rock mass the bolting force, P_s, required to support a potentially unstable zone must be larger than the rock load, P_r. A factor of safety, F_s, should be introduced, i.e.

$$P_s = F_s \times P_r \tag{4.5}$$

Since P_r can be calculated from Equation (2.3) as discussed in Chapter 2, substituting Equations (2.3) and (4.5) into Equation (4.4), the rock bolt spacing, B_s, required to provide sufficient support in the rock mass can be determined using Equation (4.6).

$$B_s = \sqrt{\frac{P_y\, t \tan^2(45^\circ + \frac{\phi}{2})}{F_s\, P_r}} \tag{4.6}$$

For various rock mass classes, the rock bolt spacing for a number of factors of safety can be found using the set of charts shown in Figures 4.3, 4.4, 4.5, 4.6 and 4.7.

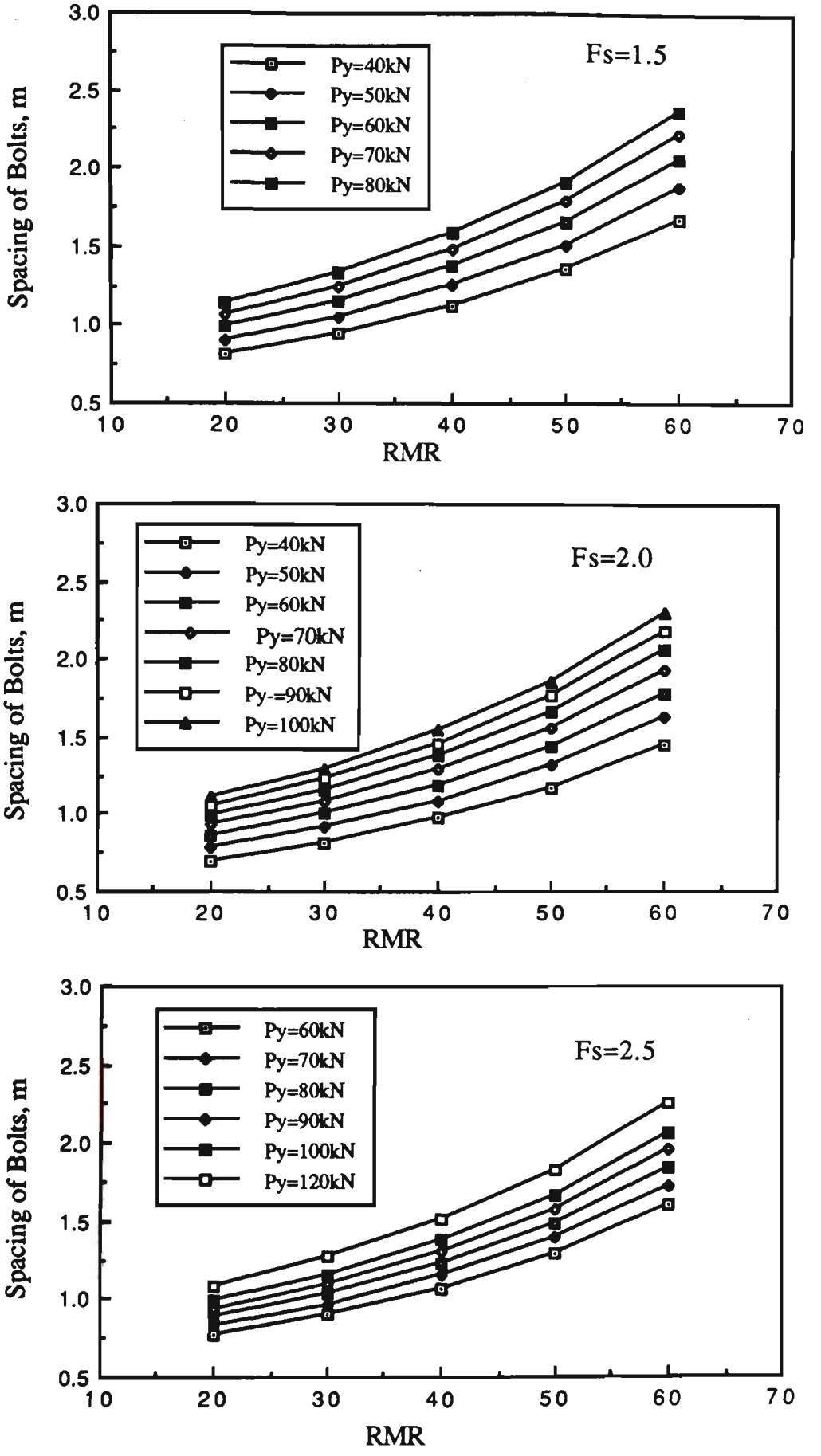

Figure 4.3. Relationship between bolt spacing and modified RMR when span =5m

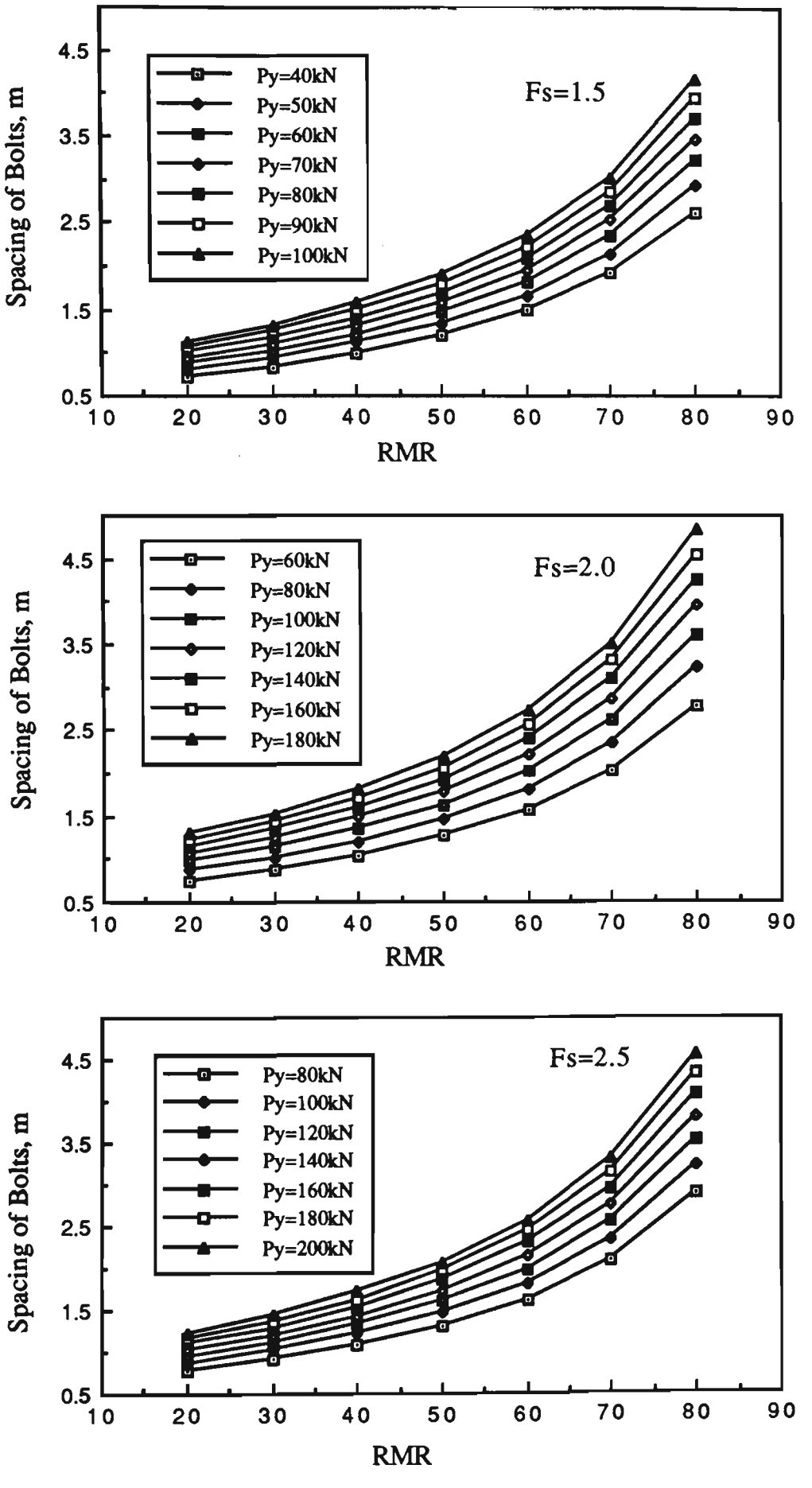

Figure 4.4. Relationship between bolt spacing and modified RMR when span=8m

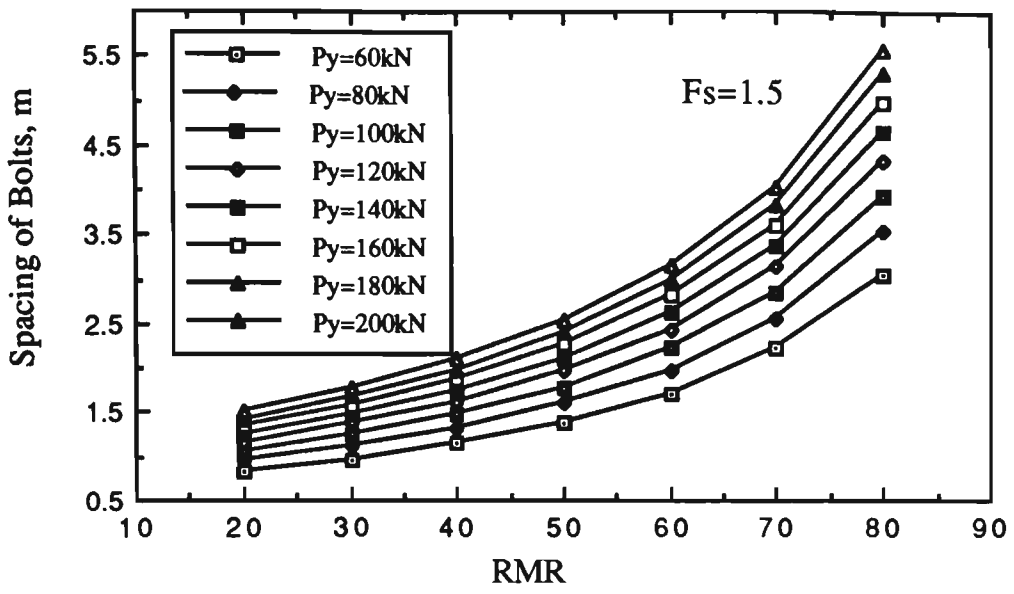

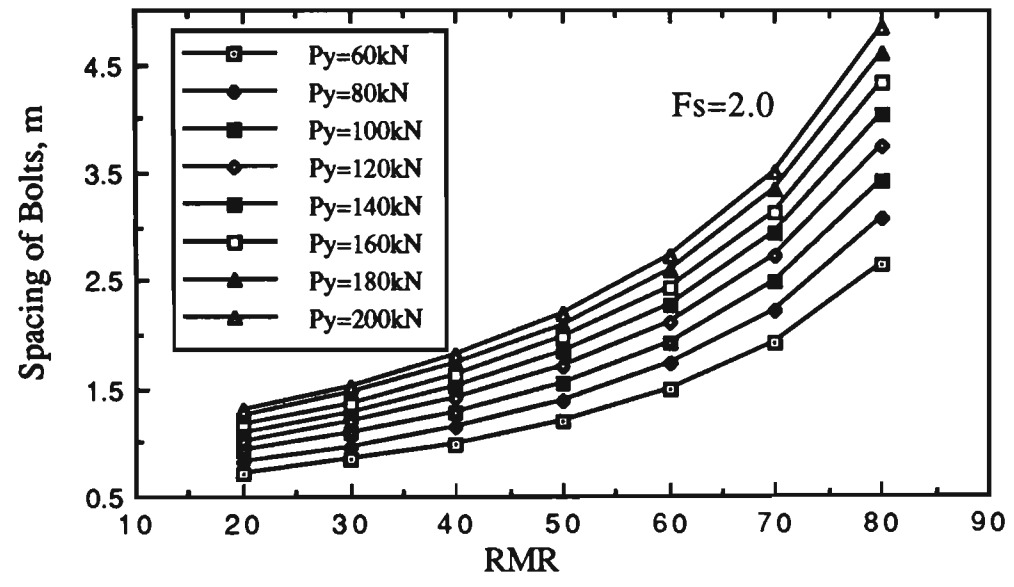

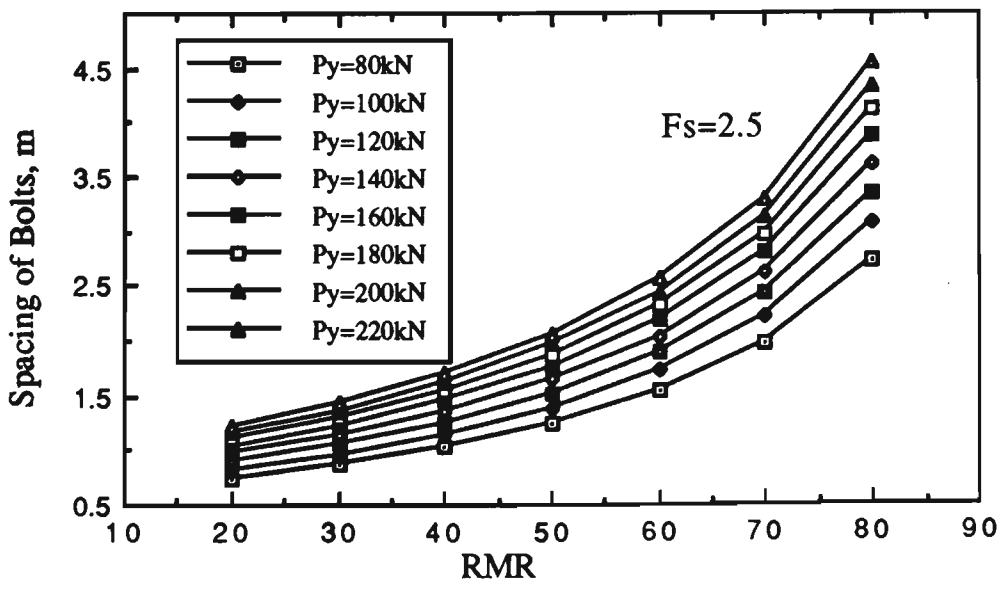

Figure 4.5. Relationship between bolt spacing and modified RMR when span=10m

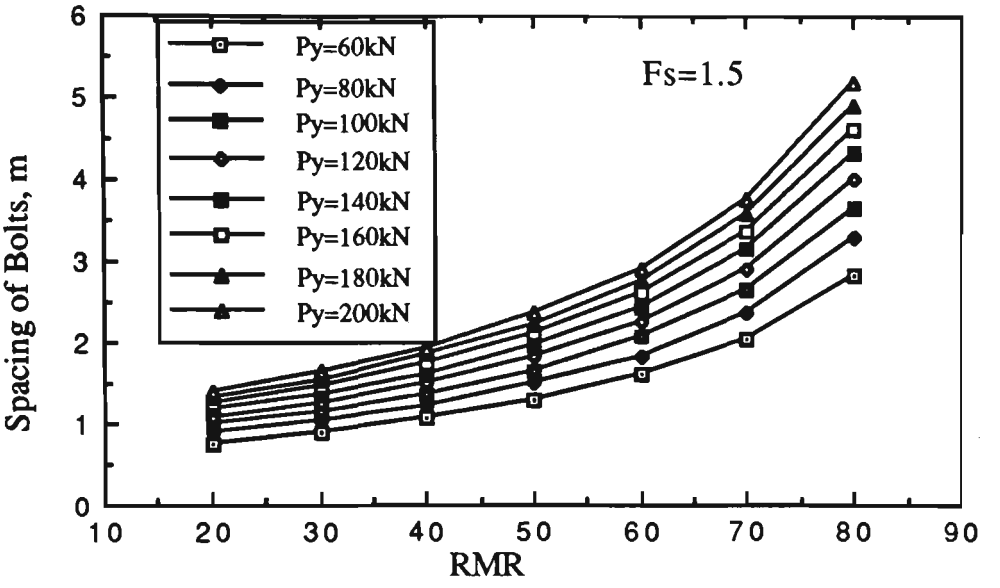

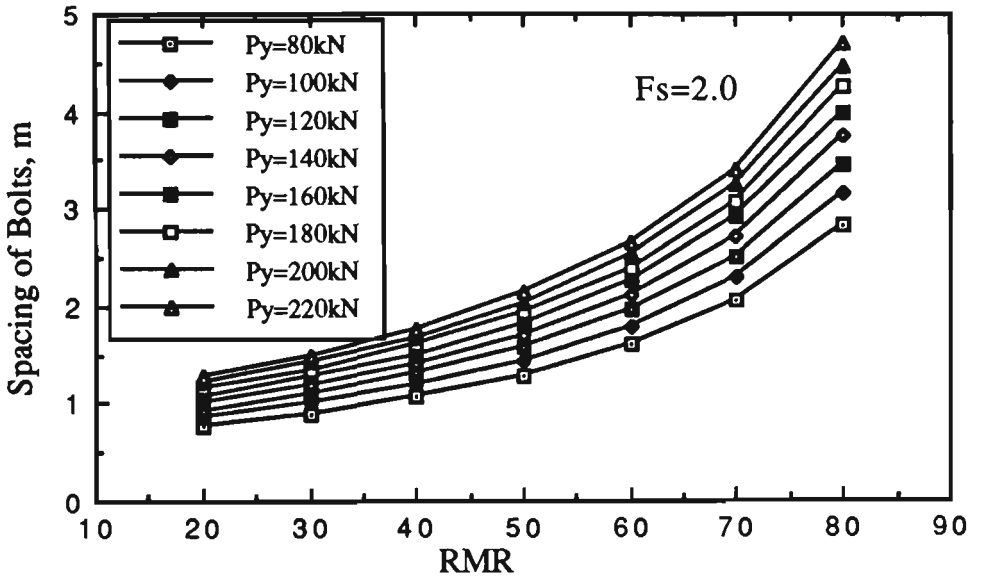

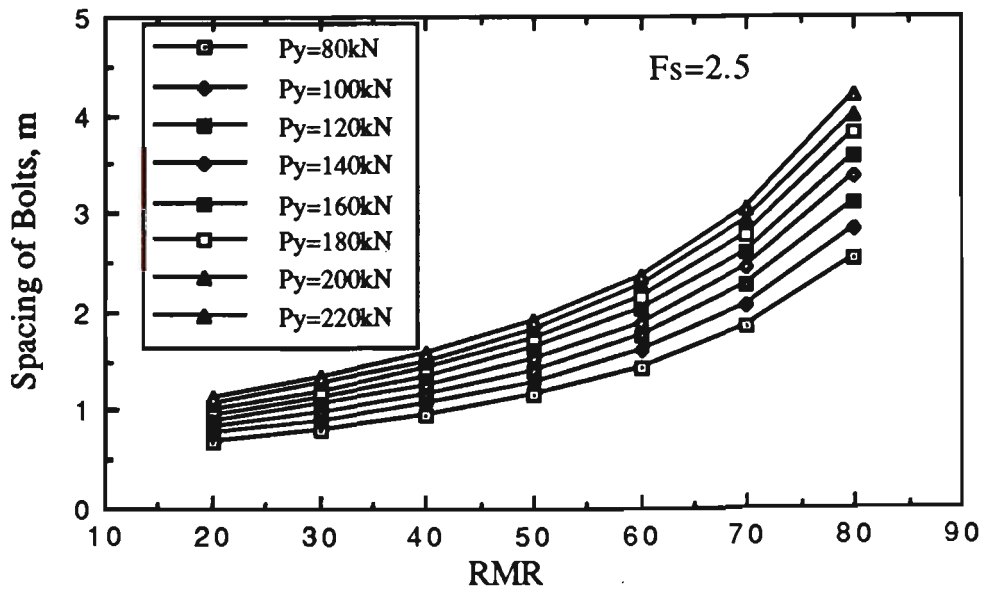

Figure 4.6. Relationship between bolt spacing and modified RMR when span=15m

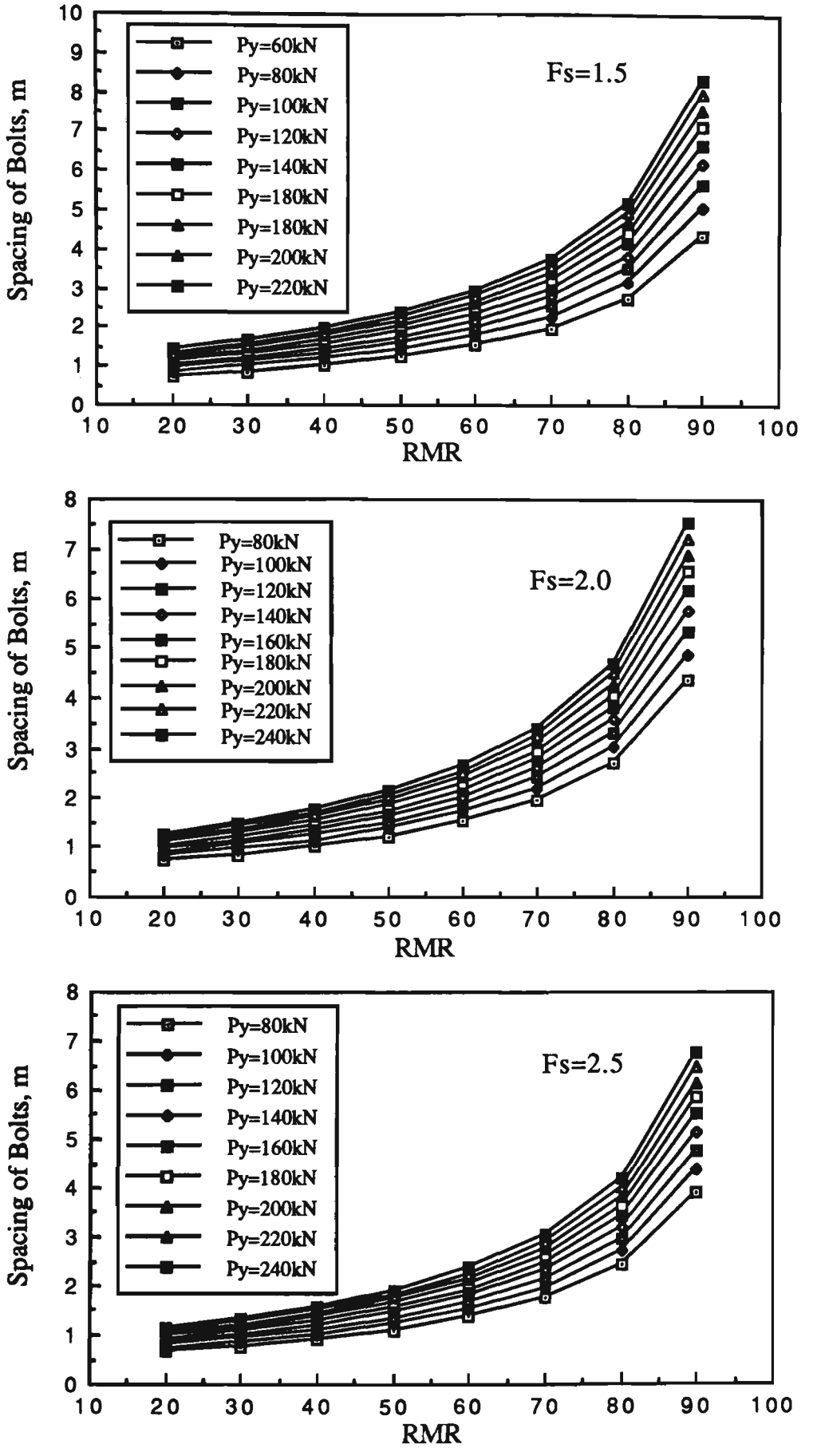

Figure 4.7. Relationship between bolt spacing and modified RMR when span=20m

It can be seen that the spacing of bolts may be less than 1 m, as shown in the above figures. This may be impractical in a mining operation. Therefore bolts with a larger diameter or with greater bolting force should be chosen to achieve a practical spacing. The maximum load provided by the bolt is dependent upon the diameter and the material of the bolts. Figure 4.8 presents the maximum load of typical bolts used in Australia mines.

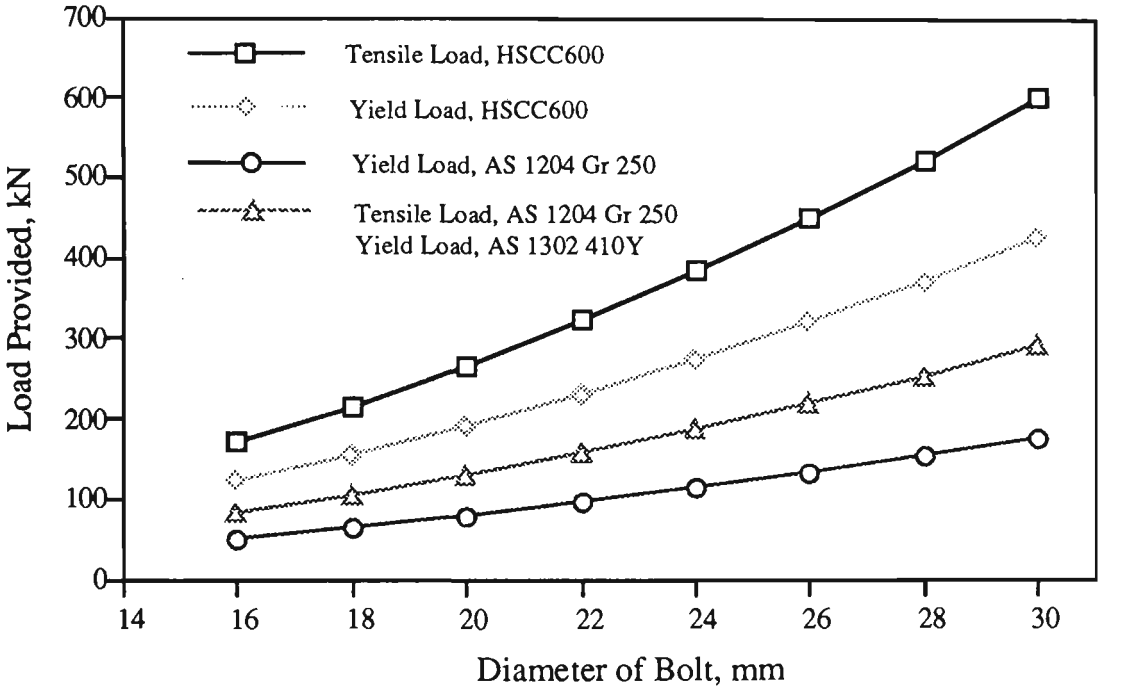

Figure 4.8. The maximum load provided by typical bolts used in Australia

4.6 CONCLUSIONS

The guide-lines for rock bolting design suggested by the geomechanics classification system are not always suitable due to variable geological conditions and engineering requirements. However, the practice of using this system indicates that it serves very well in the assessment of rock mass quality. After determination of the rock mass rating, the rating is multiplied by a modification coefficient to take

account of the local stress field and the geometry. Using Mohr's circles which relate shear stress, normal stress and the angle of internal friction, an estimate of bolt spacing, thickness of reinforced zone and bolt length can be determined. The final decision is always made by the site engineer and will take into account a factor of safety and other design considerations. A series of charts which show the relationship between rock bolt spacing and modified rock mass rating at different factors of safety and excavation span can be used to aid with the initial design.

CHAPTER 5

ROCK BOLTING DESIGN FOR UNSTABLE ROCK WEDGES

5.1 INTRODUCTION

In the previous chapter the application of the modified geomechanics classification system for the determination of the pattern and capacity of rock bolts used to reinforce the rock mass surrounding a roadway was discussed. However, this system may not be always suitable for all geological circumstances. In the case of a jointed hard rock, for example, the discontinuities may dominate the behaviour of the rock mass and a stable roadway structure cannot be achieved by installing only systematic short rock bolts. The possibility of rock failure depends heavily on the orientation of these discontinuity sets and the roadway drivage. If the orientation of these discontinuity sets against a roadway is unfavourable wedges having the potential to fall may be formed. The failure volume relates closely to the orientation and trace length of the

discontinuities. A set of unfavourably orientated discontinuities with long trace lengths may create a large wedge which may be beyond the control of a short rock bolt system. Alternative bolting measures, such as cable bolts must be used to stabilise these large wedges.

One of the difficulties in dealing with this situation is trying to locate potentially unstable wedges and identify their removability. The stereographic projection technique is usually employed to conduct a geometrical analysis of the wedges, but it is very tedious, time-consuming and sometimes inaccurate if it is carried out manually. With the assistance of a microcomputer, the problems listed above can be eliminated. After some simplifications and idealizations, the geometrical analysis of wedges can be performed and the shape and volume of the wedges and their removability can be determined. Rock bolting design can then be carried out.

5.2 ASSUMPTIONS

Generally the profile of a discontinuity surface is irregular and it is very difficult to characterise mathematically, and also the continuity of the discontinuity plane is limited. Therefore, some idealisations and simplifications must be made. These can be achieved by a set of assumptions. The main assumptions are presented as follows:

1. Profile

Discontinuity surfaces of interest are assumed to be planar. This assumption enables us to determine the shape of a wedge by using mathematical expressions to describe the discontinuity planes.

2. Continuity

Discontinuity planes extend through the wedge of interest. This means that all discontinuity planes will reach the outside boundary of a wedge and will not terminate within a wedge. No matter how large a wedge is, all discontinuity planes will have at least three appearances on the outside boundary of a wedge. These appearances can be in form of a curve profile or a straight line depending on the profile of the roof.

3. Spacing, Orientation and Mechanical Properties

Discontinuity planes within a set are evenly spaced in a rock mass. Spacing in different discontinuity sets can be different. In addition, all discontinuity planes in a set have the same orientation, i.e. dip and dip direction. The mechanical properties of a discontinuity set are also assumed to be the same.

4. Rigidity

Wedges created by the intersection of discontinuity planes are considered to be rigid. Since the movement of a wedge may occur along the discontinuity surfaces it is assumed that this movement will not cause deformation in adjacent wedges.

5.3 LOCATING A WEDGE

One of the difficulties of geometrical analysis using the stereographic projection technique is to find the coordinates of the intersection of discontinuity planes which define a wedge. Once these coordinates are known, further analysis can be

conducted; such as kinematic analysis and bolting design. Therefore this section will deal with the procedures used to find the coordinates of the intersection of the discontinuity planes on the basis of the stereographic projection technique. From the outcome the volume of a wedge can be obtained.

5.3.1 Coordinate System

Discontinuity planes can be presented in the form of a stereographic projection. Figure 5.1 shows the stereographic projection of three discontinuity planes, 1, 2

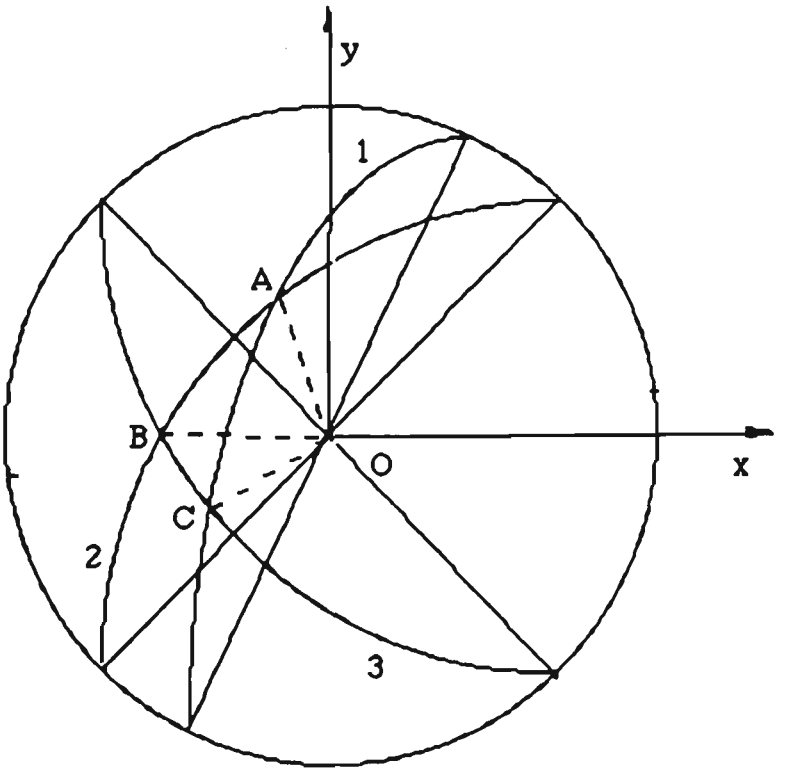

Figure 5.1. Intersection of stereographic projection of three joint planes

and 3, where A, B and C are the intersections of the three discontinuity planes. The lines AB, BC and CA are the three lines on the free face. This can be clearly seen in the coordinate system for an underground excavation as shown in Figure

5.2. Wedge oABC is created by the three intersecting discontinuity sets, oAC, oAB and oBC, in a rectangular roadway. The coordinate axes are orientated so that the X axis lies horizontally in the cross section of a roadway, the Y axis is in

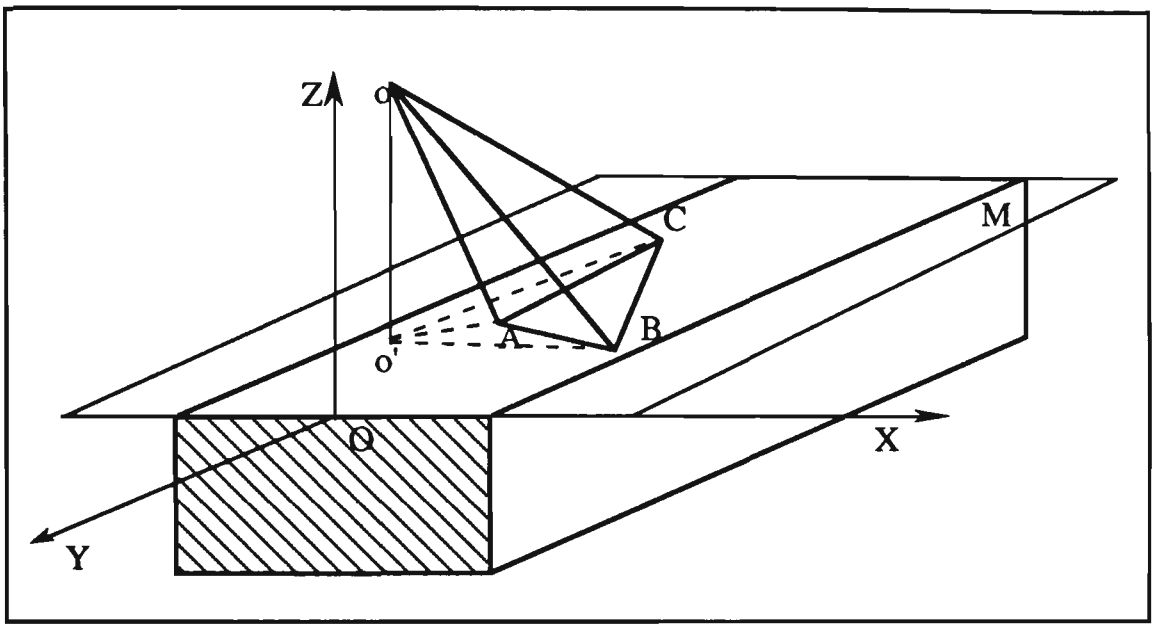

Figure 5.2. Intersection of planes and a flat free face

the drivage direction and the Z axis is upwards. Points A, B and C are the intersections of the three discontinuity planes, oAC, oAB and oBC, and connect to give free face ABC on the projection plane, M, as shown in Figure 5.2. For rectangular openings, the projection plane is set on the roof. For arched roofs M is set at the abutment of the roof and sidewalls as shown in Figure 5.3. Points A_1, B_1 and C_1 are the three intersection points on the curved free face.

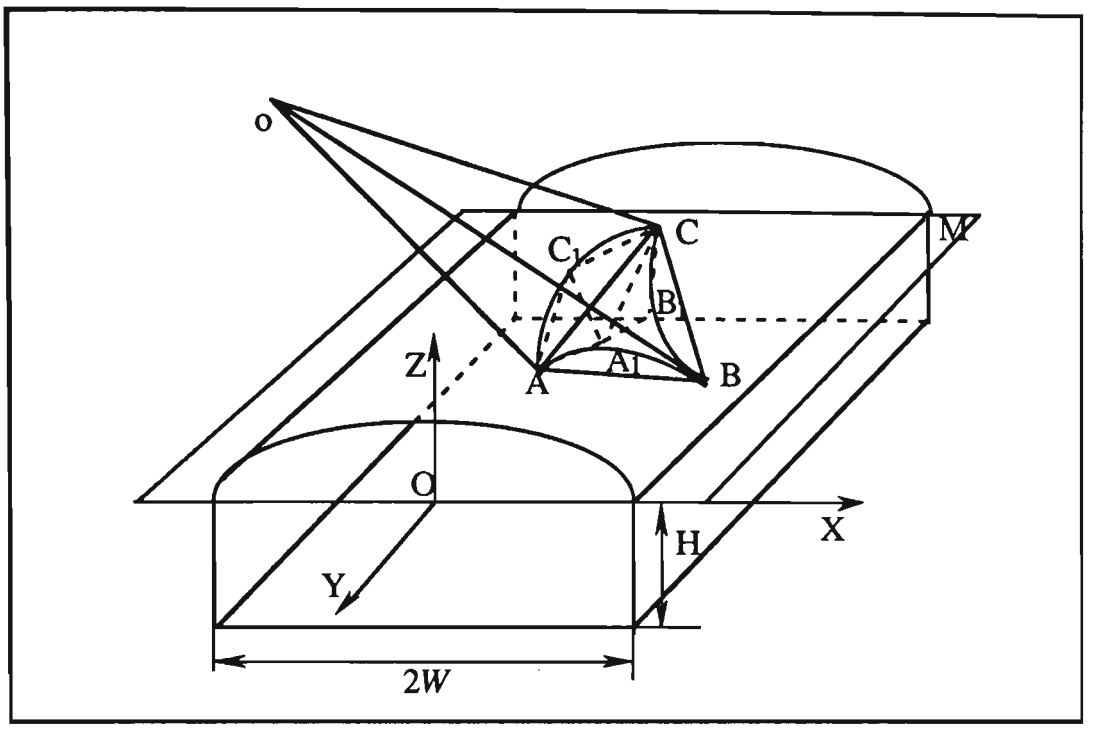

Figure 5.3. Intersection of planes and a curved free face

5.3.2 Some Definitions

Prior to discussing how to find a wedge, some concepts must first be defined. The concepts which are about to be defined are semi-space, corner, apex and face.

1. Semi-space

Any plane can divide space into two halves, i.e. two semi-spaces (Goodman and Shi, 1985). Assuming a plane, existing in space, **AX + BY + CZ = D**, as shown in Figure 5.4, the half space above the plane P is the upper semi-space, and the half space below P is the lower semi-space. As shown in Figure 5.4, t_1 (x_1, y_1, z_1) is in the lower semi-space and t_2 (x_2, y_2, z_2) is in the upper semi-space.

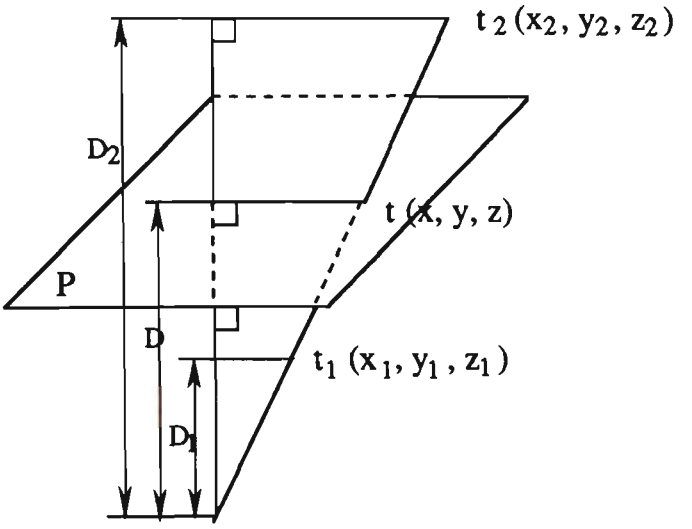

Figure 5.4. A plane divides space into two semi-spaces

2. Corner

A corner is a point, Ct_i (xt_i, yt_i, zt_i), that simultaneously belongs to three planes, as shown in Figure 5.5. Mathematically, Ct_i can simultaneously satisfy the equations of the three planes, i.e. (xt_i, yt_i, zt_i) are the solutions of the three equations, which intersect each other in space.

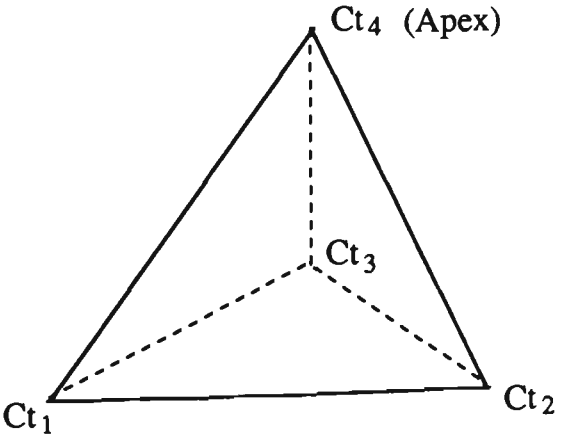

Figure 5.5. Corners of a wedge

3. Apex

Apex is a corner of a wedge without appearance on a free faces, i.e. an apex is a corner in the depth of a rock mass.

4. Face

A face consists of at least three corners or two corners and an apex. As shown in Figure 5.5, Ct_1, Ct_2 and Ct_4 define a face.

5.3.3 Coordinates of a Point on Any Plane

In the previous section, the spacing and orientation assumption was made to simplify the conditions, i.e. all discontinuity planes in the same set are assumed to be parallel to each other and evenly spaced in the rock mass. In the coordinate system the origin is set at the starting point of the area under consideration, at the projection level, and at the centre line of an opening, as shown in Figure 5.2. The coordinates, $(x_1(i), y_1(i), z_1(i))$, of a point on any discontinuity plane can be defined by Equation (5.1).

$$\left.\begin{aligned} x_1(i) &= n \cdot S_P \cdot \bar{l} \\ y_1(i) &= n \cdot S_P \cdot \bar{m} \\ z_1(i) &= n \cdot S_P \cdot \bar{n} \end{aligned}\right\} \qquad (5.1)$$

Where n is the order number of a discontinuity in a set;

S_P is the spacing of discontinuity planes in a set;

$\bar{l}$, $\bar{m}$ and $\bar{n}$ are the direction cosines of a discontinuity plane, they can be

expressed as: $\begin{pmatrix} \bar{l} \\ \bar{m} \\ \bar{n} \end{pmatrix} = \begin{pmatrix} \sin\beta\sin\alpha \\ \sin\beta\cos\alpha \\ \cos\alpha \end{pmatrix}$, where α and β are the dip and dip direction of a discontinuity plane respectively.

5.3.4 Equations of Strike Line of a Discontinuity Plane on the Projection Level

1. Coordinates of the Centre of a Great Circle

In the previous section the presentation of a discontinuity plane using stereographic projection was discussed. In this part it will be presented using mathematical equations based on the graphical form. The first step is to find the coordinates of the centre of a great circle representing a discontinuity plane on a stereographic projection. Figure 5.6 presents a discontinuity plane of dip α, which intersects the sphere at NBSA.

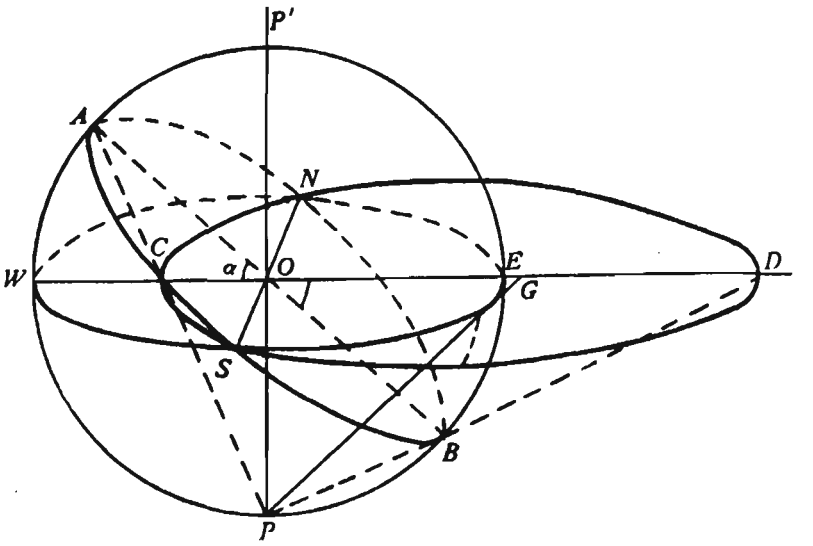

Figure 5.6. Stereographic projection of a discontinuity plane

It is evident that NDSC is the great circle of the stereographic projection of the discontinuity plane and CD is the diameter of the great circle. The centre of the great circle, G, is located by drawing a line, PG, normal to AB through P to intersect CD at G.

On the projection level, as shown in Figure 5.7, the centre of the great circle can be obtained by the following steps: (1) form line SC; (2) extend SC to intersect the reference circle at A'; (3) connect A'O and extend A'O to intersect the reference circle at B'; (4) draw SH normal to A'B' to intersect with line CD at G. It can be shown that $\angle$A'OC is the dip of the discontinuity plane.

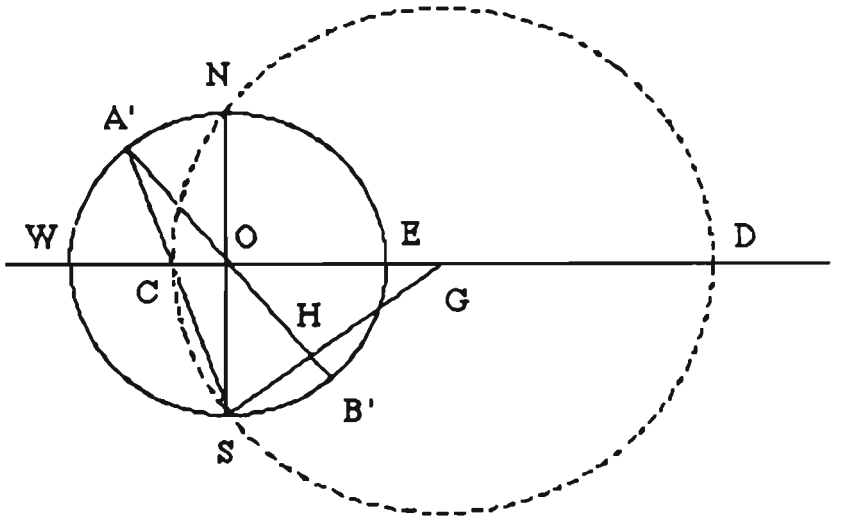

Figure 5.7. Dip of the discontinuity plane on the projection level

Thus the radius, R_i, of the great circle representing the i-th plane can be found from:

$$R_i = SG = R/\cos\alpha_i \qquad (5.2)$$

Where R is the radius of reference circle;

α_i is the dip of the i-th discontinuity plane.

Hence, the coordinates, (x_i, y_i), of the centre of the great circle can be calculated:

$$\begin{pmatrix} x_i \\ y_i \end{pmatrix} = R\begin{pmatrix} \tan\alpha_i \sin\beta_i' \\ \tan\alpha_i \cos\beta_i' \end{pmatrix} \qquad (5.3)$$

Where $\beta_i' = \beta_i - \beta_0$, as shown in Figure 5.8;

β_0 is the azimuth of the Y axis; and

β_i is the dip direction of the i-th discontinuity plane.

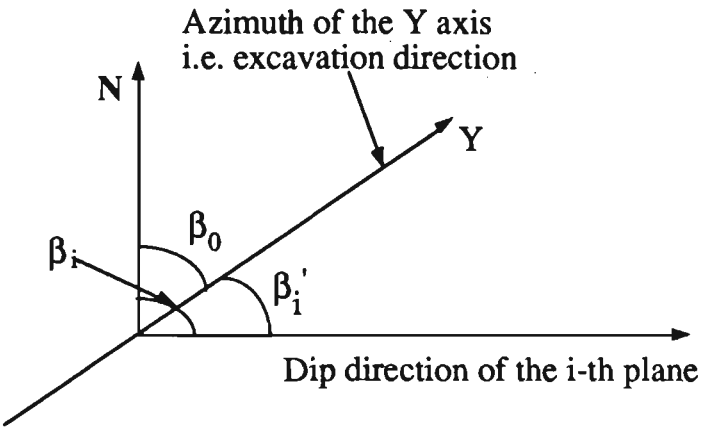

Figure 5.8. Angle between the dip direction of the i-th plane and the Y axis

2. Equation of a Great Circle

Since the coordinates of the centre of the great circle are known, the equation of the great circle representing a discontinuity plane can be written as:

$$(x - x_i)^2 + (y - y_i)^2 = R_i^2; \ (i=1 \text{ to } N) \qquad (5.4)$$

Where N is the total number of discontinuities in all sets;

x and y are the coordinates of a point on the circumference of the great circle.

3. Equations of Strike Lines

Having obtained the coordinates of a point on a strike line using Equation (5.1), the equation of the strike line of a discontinuity plane can then be expressed as Equation (5.5).

$$\mathbf{AX + BY = D} \tag{5.5}$$

Where

$$\mathbf{A} = \begin{pmatrix} K_1 \\ K_2 \\ \vdots \\ K_N \end{pmatrix} \tag{5.6}$$

B is column matrix (N×1), Where all elements are unity;

$$\mathbf{D} = \begin{pmatrix} D_1 \\ D_2 \\ \vdots \\ D_N \end{pmatrix} = \begin{pmatrix} y_1(1)-K_1x_1(1) \\ y_1(2)-K_2x_1(2) \\ \vdots \\ y_1(N)-K_Nx_1(N) \end{pmatrix} \tag{5.7}$$

and K_1 to K_N are the slopes of the strike lines. They can be calculated from Equation (5.8).

$$K_i = \tan(180^\circ - \beta_i') \quad (i = 1 \text{ to } N) \tag{5.8}$$

5.3.5 Coordinates of Intersections on the Projection Level

1. Coordinates of the Intersection of Two Great Circles

The coordinates of intersection of two great circles, i-th and j-th, can be found using Equation (5.9).

$$\left.\begin{aligned}(x - x_i)^2 + (y - y_i)^2 &= R_i^2 \\ (x - x_j)^2 + (y - y_j)^2 &= R_j^2\end{aligned}\right\} \tag{5.9}$$

Since (x_i, y_i) and (x_j, y_j) are known, Equation (5.9) can be solved and the coordinates of the intersection of two great circles can be found as follows.

$$\left.\begin{aligned}x_L(I) &= \frac{-B_1 + \sqrt{B_1^2 - A_1C_1}}{A_1} \\ y_L(I) &= -\frac{Ax_L(I) + C}{B}\end{aligned}\right\} \tag{5.10}$$

and

$$\left.\begin{aligned}x_L(I) &= \frac{-B_1 - \sqrt{B_1^2 - A_1C_1}}{A_1} \\ y_L(I) &= -\frac{Ax_L(I) + C}{B}\end{aligned}\right\} \tag{5.11}$$

Where $A = 2(x_j - x_i)$;

$B = 2(y_j - y_i)$;

$C = x_i^2 + y_i^2 - x_j^2 - y_j^2 - R_i^2 + R_j^2$;

$$A_1 = 1 + \frac{A^2}{B^2};$$

$$B_1 = \frac{AC}{B^2} + \frac{A}{B}y_i - x_i;$$

$$C_1 = x_i^2 + y_i^2 + 2\frac{C}{B}y_i + \frac{C^2}{B^2} - R_i^2.$$

It is noted that the coordinates obtained from Equations (5.10) and (5.11) must satisfy the equations of the reference circle, i.e. $x^2 + y^2 < R^2$. This means that the coordinates of intersection of the two great circles must be within the reference circle.

2. Coordinates of the Intersection of Discontinuity Planes

Assuming that the number of discontinuity planes forming a wedge is N_c, from set theory, the number, N_i, of possible intersection points of every two strike lines is $C_{N_c}^2$. If N_c=5, N_i = 5!/[(5-2)! × 2!]= 10; there are 10 possible intersections. However, only 5 out of the 10 will be critical. How to determine the critical intersections will be discussed later in this section but first the method of determining the coordinates of the intersection of any two strike lines will be described. It is evident that the intersection of two strike lines must simultaneously belong to these two strike lines and the coordinates, $(x_c(h), y_c(h), z_c(h)$, of these two strike lines must satisfy the corresponding equations. Therefore, the coordinates of the intersection of any two strike lines can be obtained by solving the following equations.

$$\left.\begin{aligned} K_i x + y &= y_i - K_i x_i \\ K_j x + y &= y_j - K_j x_j \end{aligned}\right\} \qquad (5.12)$$

The coordinates are:

$$\left.\begin{aligned} x_c(h) &= \frac{y_1(j) - y_1(i) + K_i(i)x_1(i) - K_j x_1(j)}{K_i - K_j} \\ y_c(h) &= K_j x_c(h) - x_1(j) + y_1(j) \end{aligned}\right\} \qquad (5.13)$$

Where h varies from 1 to N_c.

$(x_1(i), y_1(i))$, $(x_1(j), x_1(j))$ are the coordinates of two known points on planes i and j respectively.

It is noted that when strike line i is parallel to the Y axis, i.e. $K(i) \rightarrow \infty$, the coordinates are:

$$\left.\begin{aligned} x_c(h) &= x_1(i) \\ y_c(h) &= K_j(x_c(h) - x_1(j)) + y_1(j) \end{aligned}\right\} \qquad (5.14)$$

If $K(j) \rightarrow \infty$, the coordinates are:

$$\left.\begin{aligned} x_c(h) &= x_1(j) \\ y_c(h) &= K_i(x_c(h) - x_1(i)) + y_1(i) \end{aligned}\right\} \qquad (5.15)$$

When strike line i is parallel to strike line j, these two strike lines have no intersection points.

After the coordinates of all possible intersections are obtained, it is necessary to determine which of these intersections are critical with respect to the particular wedge under analysis. Because a plane will divide the space into two halves, upper and lower, a known wedge will be defined if a point on each plane of the wedge is known. Thus, the wedge is located above or below the plane, indicated

by P^u or P^l. Mathematically, if plane P_m is located in the upper semi-space, the number N_u of intersection points which satisfy the equation;

$$A_m x_c(h) + B_m y_c(h) \geq D_m \tag{5.16}$$

is larger than the number N_l of intersection points which satisfy;

$$A_m x_c(h) + B_m y_c(h) \leq D_m \tag{5.17}$$

Where m is the order number of the planes;

h is the order number of the intersections under consideration.

This can be illustrated by an example in two dimensions. Figure 5.9 presents the diagram of all strike lines. All planes are labelled P_1, P_2, ...P_5 and all possible

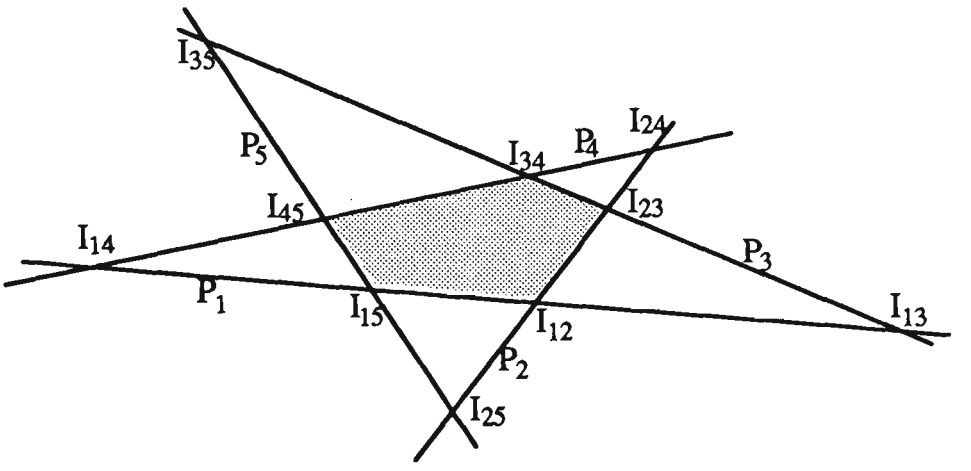

Figure 5.9. Determination of the critical intersections of discontinuity planes (after Goodman and Shi, 1985)

intersections are labelled I_{12}, I_{23}, I_{25}, ····. P_1^u means that the wedge is located above plane 1 and P_2^l means that the wedge is located below plane 2. Considering P_1^u, if the coordinates of an intersection, $(x_c(1), y_c(1))$, do not satisfy Equation

(5.16), it will be eliminated, here I_{25} is eliminated. Repeating this procedure, I_{13}, I_{24}, I_{35} and I_{14} are eliminated. The projection of the wedge on the projection level is defined by I_{12}, I_{23}, I_{34}, I_{25} and I_{45}.

Correspondingly, the subscripts of all variables, concerning the intersection points should be replaced by the new subscripts determined by the above method.

3. Slope of the Line of Intersection of Two Discontinuity Planes

Since the coordinates of the intersection of great circles are known, the slope, K_i^I, of line of the intersection of two planes , i and j, can be found:

$$K_i^I = y_c(i)/x_c(i) \tag{5.18}$$

5.3.6 Equations of the Intersection of Discontinuity Planes on the Project Level

From Equations (5.12) to (5.18) the coordinates of the intersection of the strike lines of two discontinuity planes and slope, K_i^I, of the line of intersection of the plane are known, and hence the equations of intersection of two planes are established as Equation (5.19).

$$\mathbf{A_k X + B_k Y = D_k} \tag{5.19}$$

Where

$$\mathbf{A_k} = \begin{pmatrix} K_1^I \\ K_2^I \\ \vdots \\ K_{N_c}^I \end{pmatrix} \tag{5.20a}$$

$$\mathbf{B_k}=1 \tag{5.20b}$$

$$\mathbf{D_k} = \begin{pmatrix} K_1^I(x_c(1)-y_c(1) \\ K_2^I x_c(2)-y_c(2) \\ \vdots \\ K_{N_c}^I x_c(N_c)-y_c(N_c) \end{pmatrix} \tag{5.20c}$$

It is evident that the solution from Equation (5.19) must satisfy the corresponding plane equations, i.e. the intersection of two planes must simultaneously be within two planes.

5.3.7 Coordinates of the Apex

1. Coordinates of the Apex on the Projection Level

From Figure 5.2 the projection of an apex, o, on the projection level is o'. Knowing the slope of the line of intersection of two planes, and the coordinates of the intersection of strikes of the planes, the coordinates of the apex on the projection level can be determined using Equation (5.21).

$$\left.\begin{aligned} K_i^I x - y &= K_i^I x_c(i) - y_c(i) \\ K_j^I x - y &= K_j^I x_c(j) - y_c(j) \end{aligned}\right\} \tag{5.21}$$

The coordinates, (x_t, y_t) of an apex on the projection level M are calculated as follows.

$$\left.\begin{aligned} x_A(t) &= \frac{y_c(j) - y_c(i) + K_i^I x_c(i) - K_j^I y_c(j)}{K_i^I - K_j^I} \\ y_A(t) &= K_i^I(x_A(t) - x_c(i)) + y_c(i) \end{aligned}\right\} \qquad (5.22)$$

If the intersection projection of any two planes, i and j , is parallel to the Y axis, i.e. $K_i^I \rightarrow \infty$ or $K_j^I \rightarrow \infty$. The coordinates of the intersection are:

$$\left.\begin{aligned} x_A(t) &= x_c(i) \\ y_A(t) &= K_j^I(x_A(t) - x_c(j)) + y_c(j) \end{aligned}\right\} \qquad (5.23)$$

or

$$\left.\begin{aligned} x_A(t) &= x_c(j) \\ y_A(t) &= K_i^I(x_A(t) - x_c(i)) + y_c(i) \end{aligned}\right\} \qquad (5.24)$$

respectively. If projections of two planes i and j are parallel, these two planes do not intersect and have no intersection point.

2. Dip of the Line of Intersection of Discontinuity Planes

Since the coordinates $(x_L(i), y_L(i))$ of the intersection of two great circles and the line of intersection of two planes i and j are known, as shown in Figure 5.10, the dip, α_i' , of the line of intersection of two planes is given as:

$$\alpha_i' = \frac{\pi}{2} - 2 \arctan\left(\sqrt{(x_L(i)^2 + y_L(i)^2)}/R\right) \qquad (5.25)$$

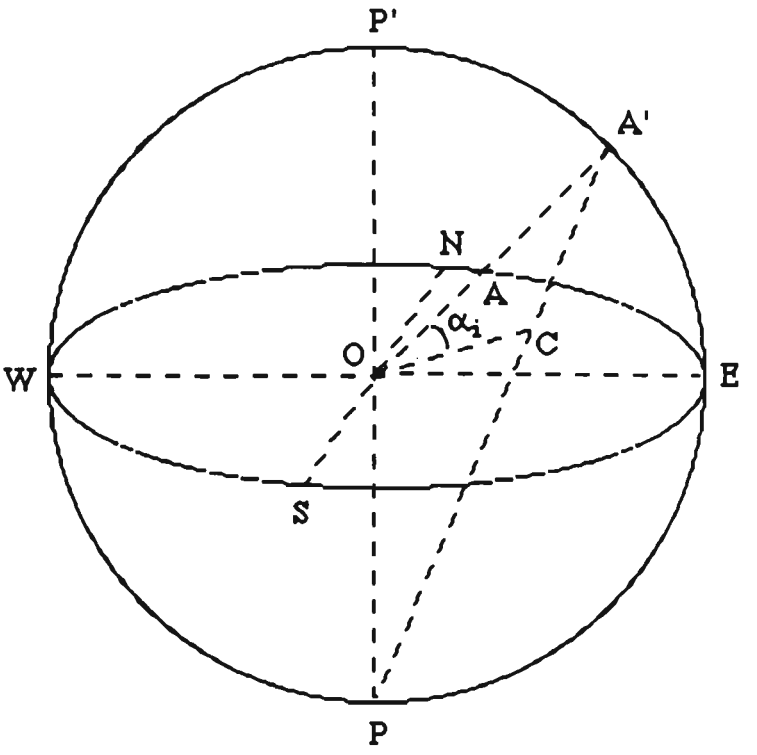

Figure 5.10. Determining the dip of the intersection of two planes

3. Coordinates of the Apex

Obviously, the X and Y coordinates of the apex are the same as that for two dimensions, i.e. $ox(t)=x_A(t)$ and $oy(t)=y_A(t)$. The Z coordinate of the apex can be computed from:

$$\mathbf{AX + BY + CZ = D} \qquad (5.26)$$

i.e. the Z coordinate of the apex defined by the i-th plane and others is:

$$oz(t) = (D_i - A_i x_A(t) + B_i y_A(t)) / C_i \qquad (5.27)$$

Assuming that a wedge is defined by N_c discontinuity sets, from set theory the number of possible corners is $C_{N_c}^3$. The coordinates of the corners should satisfy simultaneously the equations of the three planes. After obtaining all combinations of every equation, Equation (5.19) is solved to get the coordinates of all possible corners. On the basis of the method discussed above, the critical corners defining a wedge can be determined. The Z-coordinate of an apex, oz(t), must satisfy simultaneously the equations of the three planes.

5.3.8 Location of a Wedge on a Free Face

Since the coordinates of the apex of a wedge have been found, the next step is to calculate the location of the wedge on the free face. It is evident that if the projection level M is set at the roof of a rectangular opening, the coordinates of the corners of the wedge will be on the free face. Therefore the coordinates of a corner on the free face must satisfy Equation (5.28).

$$\left.\begin{aligned} K_i x - y &= K_i\, x_1(i) - y_1(i) \\ K_j x - y &= K_j\, x_1(j) - y_1(j) \\ z &= 0 \end{aligned}\right\} \qquad (5.28)$$

If the opening has a curved roof, the coordinates of intersection of the corner on the projection level are no longer the same as that on the flat free face. To find the coordinates of the corners of a wedge on a curved free face, the coordinates of the corner must first be computed at the projection level. This can be achieved by connecting the intersection of two strike lines to apex. If the roof of the opening is semi-circular, the coordinates of the corners of a wedge on the free face can be found using Equation (5.29).

$$\left.\begin{aligned} &\frac{x-x_c(i)}{ox(t)-x_c(i)} = \frac{y-y_c(i)}{oy(t)-y_c(i)} = \frac{z}{oz(t)} \\ &x^2-(z-C_o)^2 = R_0^2 \end{aligned}\right\} \qquad (5.29)$$

Where R_0 is the radius of the semi-circular arc;

C_o is the Z coordinate of the centre of the semi-circular arc, and if the centre of the semi-circular arc is set at the projection level, C_o=0; and

i ranges from 1 to n_1 (n_1 is the number of corners of the wedge, including apexes).

Solving Equation (5.29) the coordinates on the semi-circular free face are:

$$\left.\begin{aligned} xf(i) &= \frac{K_o(C_o + K_o\,ox(t) - oz(t)) + \sqrt{B}}{1+K_o^2} \\ yf(i) &= \frac{(oy(t)-y(i))(zf(i)-oz(t))}{oy(t)} + oz(t) \\ zf(i) &= K_o(xf(i)-ox(t)) + oz(t) \end{aligned}\right\} \qquad (5.30a)$$

or

$$\left.\begin{aligned} xf_{II}(i) &= \frac{K_o(C_o + K_o\,ox - oz) - \sqrt{B}}{1+K_o^2} \\ yf_{II}(i) &= \frac{(oy-y(i))(zf_{II}(i)-oz)}{oy} + oz \\ zf_{II}(i) &= K_o(xf_{II}(i)-ox) + oz \end{aligned}\right\} \qquad (5.30b)$$

Where $B= [K_o(oz(t) - C_o - K_o ox(t))]^2 - (1 + K_o^2)[(oz(t) - C_o - K_o ox(t))^2 - R_0^2)]$;

$K_o = oz(t)/(ox(t) - x_c(i))$.

If the free face is a wall of an opening, the equation of a roof plane in Equation (5.29) should be replaced with the equation of a wall plane. This is presented as:

$$\left.\begin{array}{l} \dfrac{x-x_c(i)}{ox(t)-x_c(i)} = \dfrac{y-y_c(i)}{oy(t)-y_c(i)} = \dfrac{z}{oz(t)} \\ x = W \end{array}\right\} \tag{5.31}$$

or

$$\left.\begin{array}{l} \dfrac{x-x_c(i)}{ox(t)-x_c(i)} = \dfrac{y-y_c(i)}{oy(t)-y_c(i)} = \dfrac{z}{oz(t)} \\ x = -W \end{array}\right\} \tag{5.32}$$

Where W is the half span of an opening.

Solving the above equations, the coordinates of a corner on a free face can be obtained:

$$\begin{pmatrix} xf(i) \\ yf(i) \\ zf(i) \end{pmatrix} = \begin{pmatrix} W \\ \dfrac{(oy(t)-y_c(i))(zf(i)-oz(t))}{oz(t)} + oy(t) \\ K_o(xf(i)-ox(t)) + oz(t) \end{pmatrix} \tag{5.33a}$$

or

$$\begin{pmatrix} xf(i) \\ yf(i) \\ zf(i) \end{pmatrix} = \begin{pmatrix} -W \\ \dfrac{(oy(t)-y_c(i))(zf(i)-oz(t))}{oz(t)} + oy(t) \\ K_o(xf(i)-ox(t)) + oz(t) \end{pmatrix} \tag{5.33b}$$

5.4 VOLUME OF A WEDGE AND AREA OF A FACE

In the previous section, the determination of wedge geometry was discussed. This section will deal with the volume of a wedge. Wedges can be generally divided into two categories, tetrahedral and polyhedral. A polyhedral wedge consists of multiple tetrahedral wedges. If the volumes of all tetrahedrons forming a polyhedron are known, the volume of the polyhedron can be easily obtained.

5.4.1 Volume of a Single Tetrahedral Wedge

In order to find the volume of a polyhedron, it is simply divided into a number of tetrahedrons. Once the coordinates of the four corners of a tetrahedron are known its volume can be determined. The remaining problem is to determine which four corners belong to which tetrahedron. Therefore, the four corners defining each tetrahedral wedge should first be identified.

Consider a wedge defined by five discontinuity planes and one planar free face, with one apex, as shown in Figure 5.11. The five corners are labelled t_1, t_2, t_3, t_4

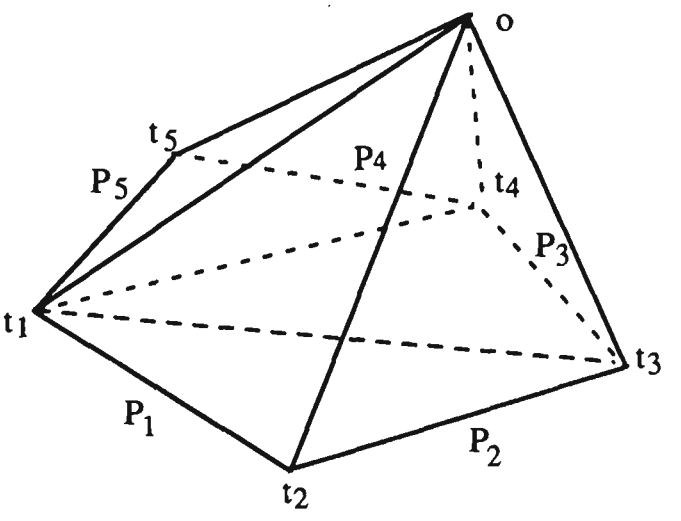

Figure 5.11. A polyhedral wedge

and t_5 and o is the apex. The order of planes is 1 - 2 - 3 - 4 - 5. The five equations of the five discontinuity planes can be expressed as Equation (5.34):

$$\begin{aligned} A_1x + B_1y + C_1z &= D_1 \\ A_2x + B_2y + C_2z &= D_2 \\ A_3x + B_3y + C_3z &= D_3 \\ A_4x + B_4y + C_4z &= D_4 \\ A_5x + B_5y + C_5z &= D_5 \end{aligned} \qquad (5.34)$$

Where A_1, $A_2...A_5$, B_1, $B_2...B_5$, C_1, $C_2...C_5$ and D_1, $D_2...D_5$ are the constants associated with orientation of the discontinuity planes.

The three tetrahedrons are defined by t_1-t_2-t_3-o, t_1-t_3-t_4-o, and t_1-t_4-t_5-o respectively. In order to identify the three planes which form a tetrahedron, one of the corners (in this case, o) is chosen as the vertex. Writing anti-clockwise from t_1 the equation for plane 1, passing through t_2, is:

$$A_1xf(2) + B_1yf(2) + C_1zf(2) = D_1 \qquad (5.35)$$

Where (xf(2), yf(2), zf(2)) are the coordinates of corners t_2 on the flat free face.

To identify the second plane a point must be found adjacent to t_2; in this case t_3. The equation for plane 2 is:

$$A_2xf(3) + B_2xf(3) + C_2xf(3) = D_2 \qquad (5.36)$$

Where (xf(3), yf(3), zf(3)) are the coordinates of corner t_3 on the flat free face.

Having identified t_1, t_2, t_3 and the vertex, o, as the corner points of tetrahedron 1, the other tetrahedrons t_1-t_3-t_4-o and t_1-t_4-t_5-o can also be determined. The corners of a plane and the coordinates of the corners are presented in Table 5.1.

After determining the corners of a tetrahedron, its volume can be computed since the coordinates of all the corners including the apex are already known. Using Equation (5.37) the volume of tetrahedron defined by t_1-t_3-t_5-o can be found:

$$V_{tetr}(g) = \begin{vmatrix} xf(i) - ox(g) & yf(i) - oy(g) & zf(i) - oz(g) \\ xf(j) - ox(g) & yf(j) - oy(g) & zf(j) - oz(g) \\ xf(k) - ox(g) & yf(k) - oy(g) & zf(k) - oz(g) \end{vmatrix} \qquad (5.37)$$

Where $V_{tetr}(g)$ is the volume of the tetrahedron;

g is the order number of the tetrahedral wedge;

(xf(i), yf(i), zf(i)), (xf(j), yf(j), zf(j)) and (xf(k), yf(k), zf(k)) are the coordinates of the corners of the wedge on the free face;

(ox(g), oy(g), oz(g)) are the coordinates of the apex of the tetrahedral wedge.

Table 5.1. The corners on related faces and their coordinates

Plane	1	2	3	4	5
Corner	o, t_1, t_2	o, t_2, t_3	o, t_3, t_4	o, t_4, t_5	o, t_5, t_1
Coordinates	ox(t), oy(t), oz(t)	ox(t), oy(t), oz(t)	ox(t), oy(t), oz(t)	ox(t), oy(t), oz(t)	ox(t), oy(t), oz(t)
	xf(1), yf(1), zf(1)	xf(2), yf(2), zf(2)	xf(3), yf(3), zf(3)	xf(4), yf(4), zf(4)	xf(5), yf(5), zf(5)
	xf(2), yf(2), zf(2)	xf(3), yf(3), zf(3)	xf(4), yf(4), zf(4)	xf(5), yf(5), zf(5)	xf(1), yf(1), zf(1)

Similarly the volumes of tetrahedrons t_1-t_5-t_4-o and t_1-t_4-t_2-o can be obtained.

However, the free faces are not always planar and horizontal (e.g. the flat roof of an excavation), but are sometimes curved and partly or completely vertical (e.g. a curved roof and the associated wall). Taking the situation where the free face is an arched roof, if the coordinates of the corners on the free face are known, the volume of the wedge, oABC, can be found by subtracting the part volume formed between the free face and the reference plane, as shown in Figure 5.3, i.e.

$$V_{tetr}(g)= V_{oABC} - (V_{ABCA_1} + V_{A_1BCB_1} + V_{A_1CC_1A}) \qquad (5.38)$$

To find the volume of these small tetrahedrons, the coordinate of points A_1, B_1 and C_1 should first be obtained. Looking at the simplified situation as shown in Figure 5.12a, assuming that Φ is the angle between oA_1 and the reference plane,

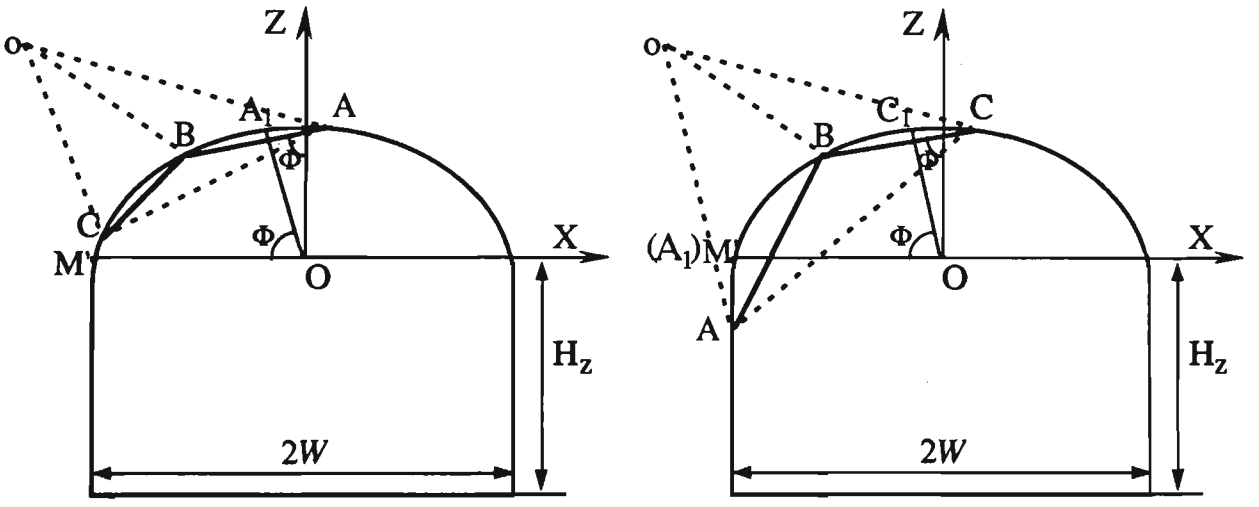

Figure 5.12. Calculation of the volume of a wedge with a curved free face

the coordinates of A_1 are computed from Equation (5.39) when $\Phi \geq \arctan [(H - H_Z - C_0)/W]]$, $x_A \neq x_B$ and $z_A \neq z_B$.

$$\left.\begin{aligned} x_{A_1} &= R_0 \cos\Phi \\ z_{A_1} &= R_0 \sin\Phi + C_o \end{aligned}\right\} \qquad (5.39)$$

Where H is the height of the wall, m;

H_z is the distance from the projection level M to the floor (if M is set at the abutment of the roof and sidewalls, $H_z = H$), m;

W is the half the width of the opening, m;

C_0 is the Z-coordinate of the centre of the semicircular roof, m;

R_0 is the radius of curvature of the arch roof, m; and

$\Phi = \arctan[-(x_A - x_B)/(z_A - z_B)$.

If $\Phi<0$, $\Phi = 180 + \arctan[-(x_A - x_B)/(z_A - z_B)]$. If $\Phi< \arctan[(H - H_z - C_0)/W]$ it is evident that the wedge is in a complex position, i.e. in both the roof and wall, as shown in Figure 5.12b, the point M', i.e. the abutment, is set as A_1. The coordinates of A_1 are:

$$\left.\begin{aligned} x_{A_1} &= SGN(ox(t))W \\ z_{A_1} &= H - Hz. \end{aligned}\right\} \qquad (5.40)$$

Obviously when $z_A = z_B$; $x_{A_1} = 0$, and $z_{A_1} = R_0$.

Therefore, the Y coordinate of point A_1 is

$$y_{A_1} = \frac{(x_A - ox(t))\begin{vmatrix} y_A - oy(t) & z_A - oz(t) \\ y_B - oy(t) & z_B - oz(t) \end{vmatrix} + (z_{A_1} - oz(t))\begin{vmatrix} x_A - ox(t) & y_A - oy(t) \\ x_B - ox(t) & y_B - oy(t) \end{vmatrix}}{\begin{vmatrix} x_A - ox(t) & z_A - oz(t) \\ x_B - ox(t) & z_B - oz(t) \end{vmatrix}} + oy(t) \qquad (5.41)$$

If $x_A = x_B$, the coordinates are

$$\left.\begin{aligned} x_{A_1} &= x_A \\ y_{A_1} &= (y_A + y_B)/2 \\ z_{A_1} &= (z_A + z_B)/2 \end{aligned}\right\} \qquad (5.42)$$

Similarly, the coordinates of B_1 and C_1 can be obtained.

Let

$$\mathbf{A_f} = \mathbf{Q_f} \tag{5.43}$$

Where

$$\mathbf{A_f} = \begin{pmatrix} x_{A_1} & y_{A_1} & z_{A_1} \\ x_{B_1} & y_{B_1} & z_{B_1} \\ x_{C_1} & y_{C_1} & z_{C_1} \end{pmatrix} \tag{5.44a}$$

and

$$\mathbf{Q_f} = \begin{pmatrix} xf(i) & yf(i) & zf(i) \\ xf(j) & yf(j) & zf(j) \\ xf(k) & yf(k) & zf(k) \end{pmatrix} \tag{5.44b}$$

Therefore the volume, V_{oABC}, of the tetrahedral wedge with a curved free face can be computed using Equations (5.43), (5.44a), (5.44b) and (5.37). Using the same principle, the volumes of other tetrahedrons, $ABCA_1$, A_1BCB_1 and A_1CC_1A, can be gained. Finally, the volume of the tetrahedron with a curved configuration can be determined using Equation (5.38).

5.4.2 Volume of a Polyhedral Wedge

After the volumes of all tetrahedrons are found, the volume, V_{poly}, of the polyhedral wedge can be obtained by simply summing the volumes of all tetrahedrons forming the polyhedron. Therefore

$$V_{poly} = \sum_{i=1}^{m} V_{tedr}(i) \tag{5.45}$$

Where m is the number of tetrahedral wedges in a polyhedral wedge; and

$V_{tedr}(i)$ is the volume of the i-th tetrahedral wedge.

5.4.3 Area of a Face

From the previous section, we know that the coordinates of the three points defined one of the triangular faces of the wedge, as shown in Table 5.1. The area of a face can be calculated as below.

$$A_r(q) = \frac{1}{2}\left\{\begin{vmatrix} xf(i) - ox(t) & yf(i) - oy(t) \\ xf(j) - ox(t) & yf(j) - oy(t) \end{vmatrix}^2 + \begin{vmatrix} yf(i) - oy(t) & zf(i) - oz(t) \\ yf(j) - oy(t) & zf(j) - oz(t) \end{vmatrix}^2 + \begin{vmatrix} zf(i) - oz(t) & xf(i) - ox(t) \\ zf(j) - oz(t) & xf(j) - ox(t) \end{vmatrix}^2\right\}^{\frac{1}{2}} \quad (5.46)$$

Where $A_r(q)$ is the area of the face;

subscript q is the order number of a face in a tedrahedral wedge.

Similarly the area of any polygon can be found.

5.5 KINEMATIC ANALYSIS

In the preceding section the size, i.e. volume, of a wedge was obtained. However the failure mode of a wedge still remains unknown. Based on the rigidity assumption, it is found that the wedge may move along one or two planes and no deformation occurs during the movement. Therefore, the sliding faces on which the wedge may slide should first be identified, so that judgment on the removability of the wedge can be made (Shi, 1977, 1982).

5.5.1 Modes of Wedge Failure

The failure mode of a wedge will define its direction of motion. Falling from the roof of a roadway, sliding on one plane or the intersection of two planes are the basic failure modes considered in this thesis. Other failure modes, such as toppling, are not analysed. In other words, the failure modes to be discussed are those where the movement of a wedge will follow a certain direction without any rotation.

1. Falling from Roof

It is considered that gravity and water pressure are considered to be the forces which will cause the wedge to fall from the roof as shown in Figure 5.13. In this case the direction of motion of a wedge coincides with the direction of the resultant force associated with the wedge.

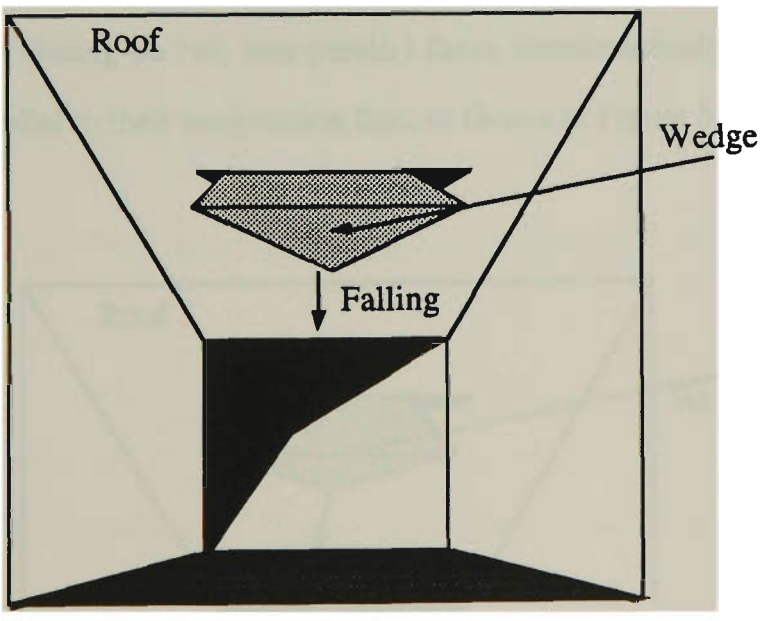

Figure 5.13. A wedge falling from the roof

2. Sliding on Single Face

A wedge may move on one of its faces, as shown in Figure 5.14. In this case the initial sliding direction is parallel to the discontinuity plane on which it slides.

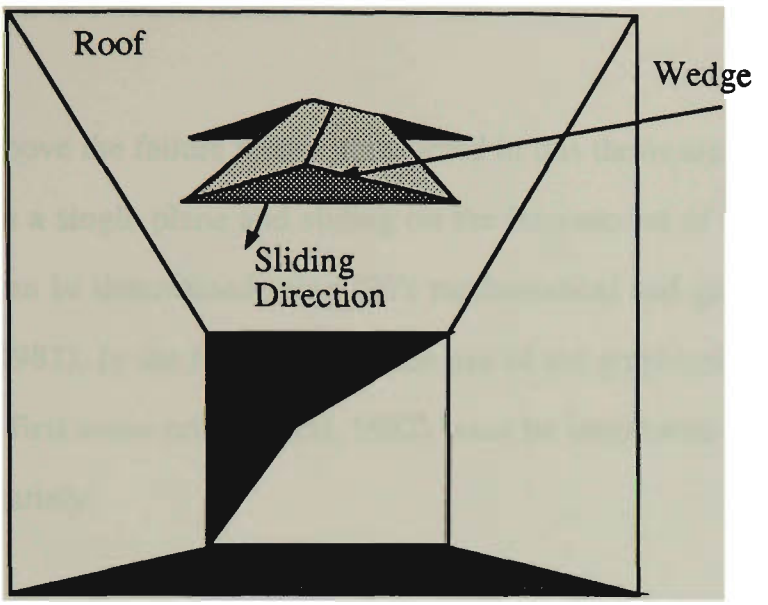

Figure 5.14. A wedge sliding on one plane

3. Sliding on Two Faces

If a wedge is sliding on two non-parallel faces simultaneously, the direction of motion is parallel to their intersection line, as shown in Figure 5.15.

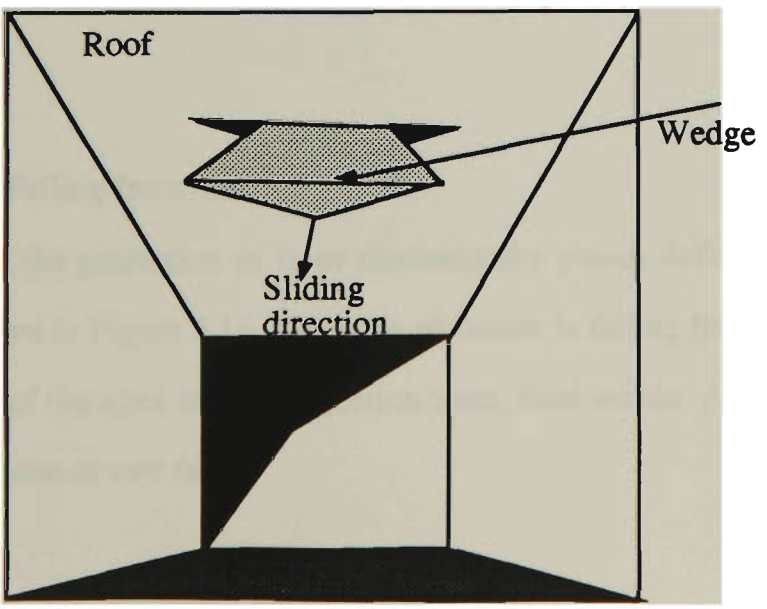

Figure 5.15. A wedge sliding along the intersection of two planes

5.5.2 Judgement of Failure Mode

As described above the failure modes considered in this thesis are falling from the roof, sliding on a single plane and sliding on the intersection of two planes. The failure mode can be determined using Shi's mathematical and graphical methods (Shi, 1977 & 1982). In the following section use of the graphical method will be described, but first some criteria (Shi, 1982) must be introduced. For a wedge to fail, it should satisfy:

- Boundary condition: Three or more discontinuity planes intersect each other, i.e. it is a real wedge;

- Compatibility condition: Compatibility condition tests whether or not the wedge is removable. To satisfy the compatibility condition all points in the wedge must move in a direction which allows them to pass through the free face.

If a wedge satisfies the above conditions, the failure mode can be determined as follows:

(1) Falling from roof

Assuming that the projection of three discontinuity planes defines a tetrahedral wedge, as shown in Figure 5.16, the mode of failure is falling from the roof if o', the projection of the apex on the projection level, falls within A'B'C'. Otherwise it will slide on one or two faces.

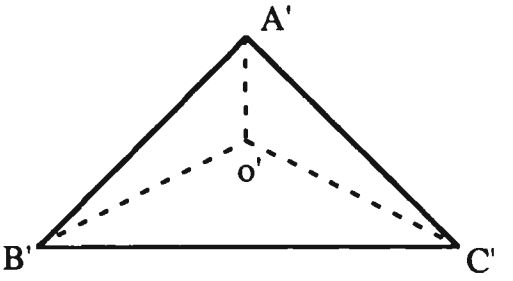

Figure 5.16. Wedge falls from the roof

(2) Sliding on one or two planes

To determine if a wedge will slide on a single plane or along the intersection of two planes it is necessary to construct the diagram shown in Figure 5.17. Lines are drawn perpendicular to A'B', B'C' and A'C', running through o' and intersecting at D', E' and F'. Three other lines, o'A', o'B' and o'C', are also constructed.

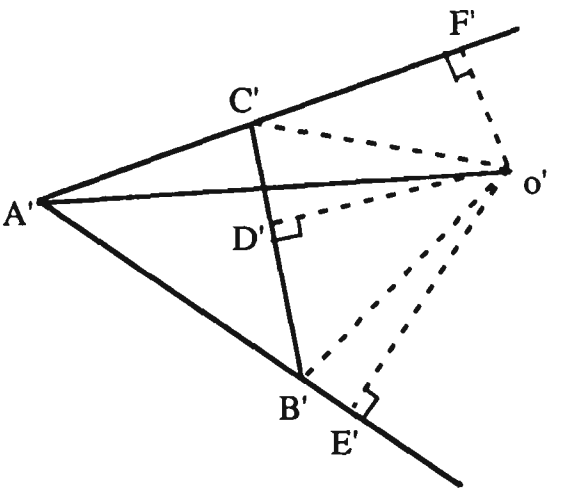

Figure 5.17. Judgment of sliding planes

To satisfy the compatibility condition one of o'D', o'E' or o'F' must intersect one of the lines A'B', B'C' and A'C'. In the case of Figure 5.17, o'D' splits line B'C'

into B'D' and D'C', therefore satisfying the compatibility condition. If one of the lines o'D', o'E' and o'F' is the shortest of the six constructed lines, the wedge will slide on a single plane. If the shortest line is o'A', o'B' or o'C' the wedge will slide on the intersection of two planes.

If the sliding direction is along o'D' or o'E' or o'F', the wedge oABC, as shown in Figure 5.3, will slide on a single face, oBC or oAB or oAC; if sliding direction is along o'A' or o'B' or o"C', the wedge oABC will slide on the intersection of two faces, oAC and oAB or oAB and oBC or oAC and oBC.

5.6 ANALYSIS OF FORCES ACTING ON A WEDGE

So far, the potential failure mode of a wedge has been determined. Next step is to determine its removability. To achieve this, an analysis of the forces acting on the wedge should be conducted.

5.6.1 Consideration of Forces Acting on a Wedge

Generally, the forces acting on a wedge are gravity cohesion and friction.

1. Gravity

The weight of a wedge is obtained by multiplying the volume of the wedge with the unit weight of the rock material of the wedge. It is clear that the gravity force, F_g, is the weight of the wedge:

$$F_g = V_w \gamma_r \tag{5.47}$$

Where γ_r is the unit weight of rocks, kN/m^3; and

V_w is the volume of a wedge, m^3.

2. Cohesive Force

Cohesion discussed here is the cohesive force, F_c, of the fill material between the walls of a discontinuity. Normally, it is assumed that cohesion is constant over a face and the cohesive force is the product of the known area of the face $A_r(i)$ and cohesion coefficient C_i of the i-th discontinuity plane, i.e.

$$F_c = C_i A_r(i) \tag{5.48}$$

3. Friction Force

Friction provides a resistance to oppose motion or potential motion. The friction force is expected to resist the sliding of a wedge, but it is not considered in the case of a wedge falling from the roof. If the sliding direction is **s**, the friction direction will be -**s**. Suppose that P_n^i, i=1, 2, ..., N_c, are the magnitudes of the normal reaction forces from each sliding plane, P_i, i=1, 2, ..., N_c. The resultant friction force, F_f, on plane i is:

$$F_f = - (P_n^i \tan (\phi_i))\mathbf{s} \tag{5.49}$$

Where ϕ_i is the friction angle for sliding in direction **s** on plane i.

5.6.2 Equilibrium of Forces on a Wedge

If a wedge is in a limit critical situation, the forces acting on it must be in equilibrium, i.e. the resultant force, F_t, on the wedge must be zero. This can be expressed by Equation (5.50)

$$F_t = \sum_{i=1}^{n_f} F(i) = 0 \qquad (5.50)$$

Where F(i) are the forces acting on a wedge, kN;

n_f is the number of forces acting on a wedge.

Suppose that F_t represents the total force to produce sliding of the wedge and F_w the total force to retain the wedge in stability. The difference F_d of these two forces can be expressed in Equation (5.51).

$$F_d = F_t - F_w \qquad (5.51)$$

If $F_d > 0$, the resultant force will drive the wedge to move; following one of the modes discussed in the previous section. If $F_d < 0$, the resultant force will prevent the wedge moving so that the wedge will remain stable and no failure will occur. Obviously, when $F_d > 0$, F_d is the force that should be provided by the rock bolting system. If $F_d = 0$, the wedge will be critical.

5.7 ROCK BOLTING DESIGN

According to the failure modes a wedge may have three potentials, to fall from the roof, slide on single wedge plane and slide along the intersection of two planes. The resultant force acting on a removable wedge will be towards the removal direction and not be zero. The term 'rock bolting' includes short bolt bolting and cable bolting. In a broad sense rock bolting can be divided into two categories: passive bolting and active bolting. The basis of design for passive and active bolting system will be discussed in the following sections.

5.7.1 Design Based on the Passive Bolting Concept

1. Resultant Force of a Falling Wedge

If a wedge has the potential to fall from the roof of an opening, as shown in Figure 5.13, the resultant force acting on the wedge is only its dead weight, i.e.

$$F_t = W \tag{5.52}$$

Where W is the weight of a wedge, kN.

The direction of the resultant force is vertically downwards and separation occurs on all faces. No frictional force or cohesion is considered in the computation of the resultant force.

2. Resultant Force on a Wedge with a Single Sliding Face

If a wedge has the potential to slide on a single face as shown previously in Figure 5.14. The forces acting on it are gravity and cohesion. Gravity has two components, normal compression and sliding, as shown in Figure 5.18. The resultant force can be obtained using Equation (5.53).

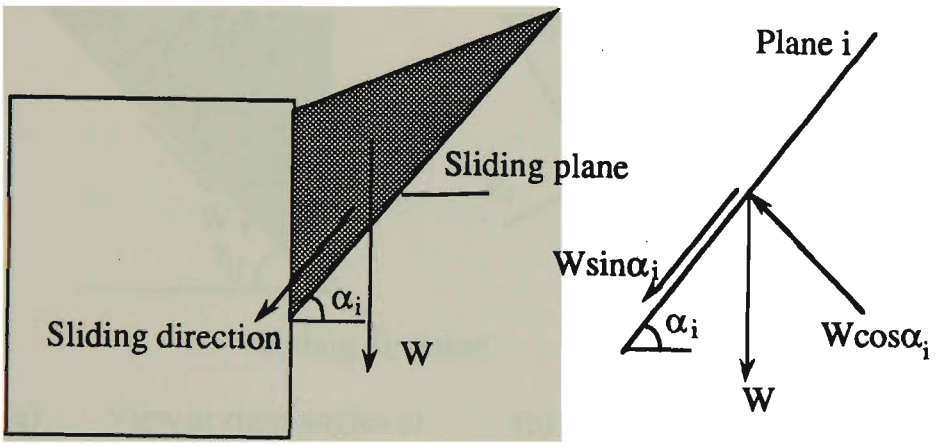

Figure 5.18. Forces acting on a wedge sliding on a single face

$$F_t = W(\sin\alpha_i - \cos\alpha_i \tan\phi_i) - C_i A_r(i) \qquad (5.53)$$

Where F_t is the resultant force in the sliding direction, kN;

W is the weight of the wedge, kN;

α_i is the dip of the i-th plane;

ϕ_i is the friction angle of the i-th plane; and

C_i and $A_r(i)$ are the cohesion coefficient and area of the i-th plane respectively.

3. Resultant Force on a Wedge Sliding on Two Planes

On some occasions, the wedge may slide along the intersection of two planes as shown in Figure 5.16. The acting direction of the resultant force is also along this intersection. The acting forces on the wedge are shown in Figure 5.19 (Hoek and Bray, 1979).

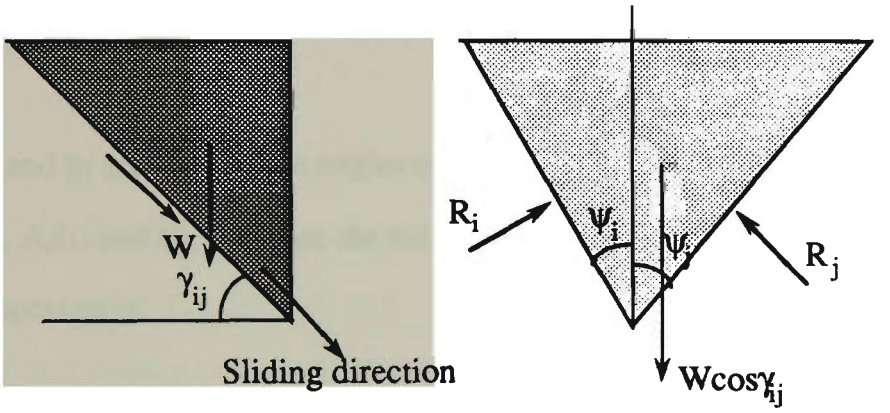

(a) View at right angles to the line of intersection

(b) View along the line of intersection

Figure 5.19. Forces acting on a wedge sliding on two faces, (after Hoek and Bray, 1979)

In order to find R_i and R_j, the equilibrium equation is established horizontally and vertically as Equation (5.54).

$$\left.\begin{aligned} R_i\cos\psi_i &= R_j\cos\psi_j \\ R_i\sin\psi_i + R_j\sin\psi_j &= W\cos\gamma_{ij} \end{aligned}\right\} \qquad (5.54)$$

Where R_i and R_j are the normal reactions provided by planes i and j;

ψ_i and ψ_j are the angle between planes i and j and the vertical plane passing through the intersection of planes i and j respectively; and

γ_{ij} is the dip angle of the intersection along which the wedge slides.

Solving Equation (5.54), let $\psi_{ij} = \psi_i + \psi_j$, we obtain

$$\left.\begin{aligned} R_i &= W\cos\gamma_{ij}\cos\psi_i/\sin\psi_{ij} \\ R_j &= W\cos\gamma_{ij}\cos\psi_j/\sin\psi_{ij} \end{aligned}\right\} \qquad (5.55)$$

Hence the resultant force, F_t, can be found using Equation (5.56).

$$F_t = W\sin\gamma_{ij} - [\frac{W\cos\gamma_{ij}}{\sin\psi_{ij}}(\cos\psi_i\tan\phi_i + \cos\psi_j\tan\phi_j) + C_iA_r(i) + C_jA_r(j)] \qquad (5.56)$$

Where ϕ_i and ϕ_j are the friction angles of planes i and j respectively;

C_i, $A_r(i)$ and C_j, $A_r(j)$ are the cohesion and area of planes i and j respectively.

4. Number of Bolts

After knowing the bolting force required to stabilize the unstable wedge the number of bolts, N_b, can be found using (5.57).

$$N_b = F_sF_t/\sigma A_b \qquad (5.57)$$

Where F_s is the factor of safety;

Ft is the resultant force, i.e. bolting force, provided by bolts, kN;

A_b is the cross-sectional area of a single bolt, m^2; and

σ is the strength of bolts.

If support is required to prevent a wedge falling directly from the roof, σ would be taken as the tensile strength of bolts. However, if support is required to prevent sliding from the roof or the walls on one or two joint planes, σ would be taken as the shear strength of bolts.

5. Length of Bolts

The length of the bolts or cables should be long enough to ensure that, within certain limits, the portions anchored inside the solid rock will be capable of holding the weight of the wedge. The length of anchor, L_1, can be obtained using Equation (5.58) (Hanna, 1982).

$$L_1 = \frac{P_A}{\pi d \tau_{bond}} \qquad (5.58)$$

Where P_A is the bolting load, kN;

τ_{bond} is the average working bond stress between grout and borehole wall or grout and bolt, kN/m^2; and

d is the diameter of the borehole if τ_{bond} is the average working bond stress between grout and borehole; or the diameter of bolt if τ_{bond} is the average working bond stress between grout and bolt, m.

The length of bolts is given by

$$B_l = L_1 + L_2 \qquad (5.59)$$

Where B_l is the length of bolts, m;

L_1 is the length of anchor, m; and

L_2 is the length in zone to be stabilised, m.

In the case of wedge failure L_2 is relevant to the shape of the wedge, particularly the height of the wedge. Normally the L_2 is chosen to be equal to the height, H_w, of the wedge, as shown in Figure 5.20.

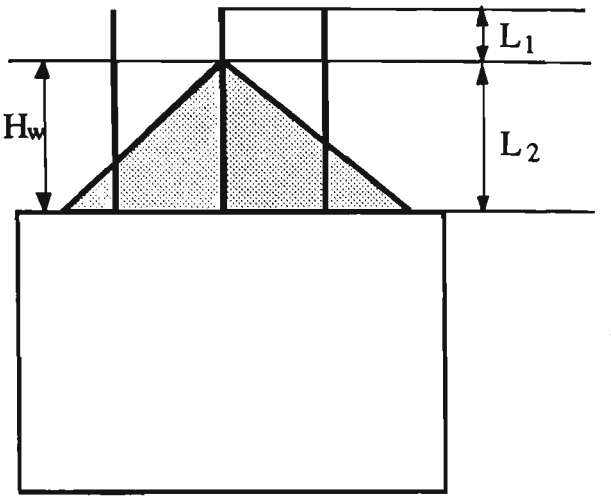

Figure 5.20. Design of the length of cables

5.7.2 Design Based on the Active Bolting Concept

In some circumstances special techniques should be adopted to obtain a better bolting effect. Prestressed bolts are used to achieve this goal. With this technique, the potentially unstable zone can be reinforced under prestressing and movement can be limited soon after the installation of the bolts. The prestressing not only provides a bolting force earlier than other types of bolting, but also improves the nature of the bolting force. Active bolting changes the initial force field and it may prevent the failure more effectively. In the case of a wedge falling from the roof, it may make no difference, but, if the wedge may slide along one or two planes, the prestressing will largely increase the anti-sliding force.

1. Resultant Force of a Wedge Sliding on One Plane

As a result of prestressing the bolts the frictional force on the sliding plane will be increased, which may make a contribution towards the stability of a potentially

unstable wedge. This may be illustrated by Figure 5.21. The resultant force on the wedge can be computed using Equation (5.60) (Hoek and Brown, 1980).

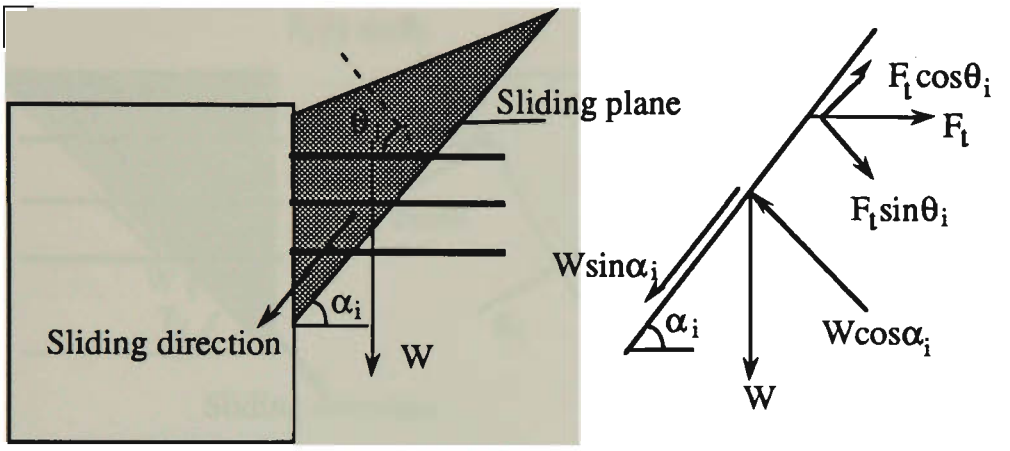

Figure 5.21. Prestressed bolts to reinforce a wedge sliding on a single plane

$$F_t = \frac{W(F_s\sin\alpha_i - \cos\alpha_i\tan\phi_i) - C_iA_r(i)}{\cos\theta_i\tan\phi_i + F_s\sin\theta_i} \qquad (5.60)$$

Where θ_i is the angle between the plunge of the bolt and the normal to the sliding face;

F_s is the factor of safety.

2. Resultant Force of a Wedge Sliding on Two Planes

If prestressed bolts are used to reinforce a wedge against sliding along the line of intersection of two planes as shown in Figure 5.22, the resultant on the wedge may be different from that without pre-tension. In Figure 5.22 θ_i and θ_j are the angles between the plunge of bolts and the normal to the sliding planes i and j

respectively. Assuming that the bolts are installed in planes i and j and the corresponding bolting forces on these two planes are $F_t(i)$ and $F_t(j)$ the normal

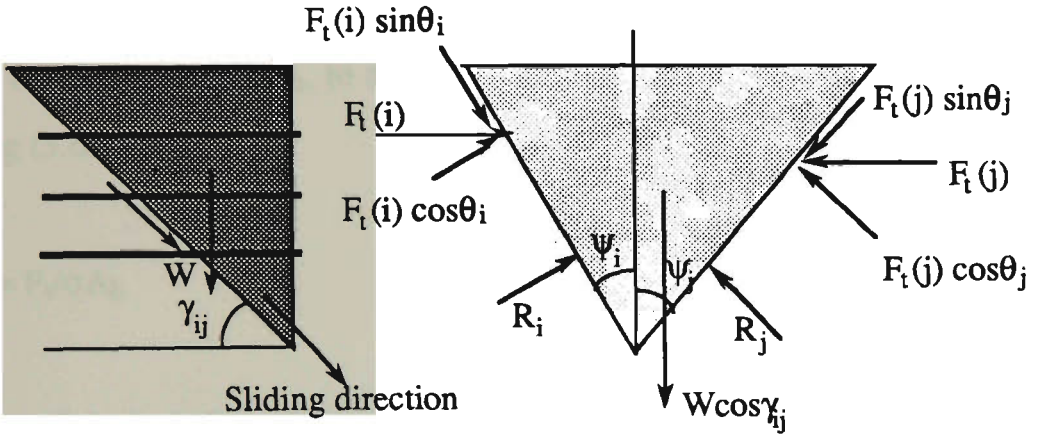

Figure 5.22. Bolts to reinforce a wedge sliding on the intersection of two planes

reactions on these planes are $F_t(i)\cos\theta_i$ and $F_t(j)\cos\theta_j$ and the frictional forces $F_t(i)\sin\theta_i$ and $F_t(j)\sin\theta_j$. Supposing that a certain number of bolts are installed over two sliding planes with certain areas, the number of bolts installed at each sliding plane may be proportional to its surface area. Therefore, the bolting force provided on each sliding face can be computed as Equation (5.61).

$$\left.\begin{aligned} F_t(i) &= \frac{F_i}{F_i + F_j} F_t \\ F_t(j) &= \frac{F_j}{F_i + F_j} F_t \end{aligned}\right\} \qquad (5.61)$$

Let $B_i = F_i/(F_i+F_j)$ and $B_j = F_j/(F_i+F_j)$. Hence the equilibrium equation can be established and the bolting force required can be determined using the equation below.

$$F_t = \frac{W[F_s \sin\gamma_{ij} - \frac{\cos\gamma_{ij}}{\sin\psi_{ij}}(\cos\psi_i \tan\phi_i + \cos\psi_j \tan\phi_j)] - C_i A_r(i) - C_j A_r(j)}{B_i(\cos\theta_i \tan\phi_i + F_s \sin\theta_i \sin\psi_{ij}) + B_j(\cos\theta_j \tan\phi_j + F_s \sin\theta_j \sin\psi_{ij})} \quad (5.62)$$

3. Number of Bolts Required

The number of bolts, N_b, to stabilise the potentially sliding wedge is computed using (5.63).

$$N_b = F_t/\sigma A_b \quad (5.63)$$

Where F_t is the bolting force required, kN;

σ is the strength of bolts, as defined as previous section, kN/m^2; and

A_b is the cross-sectional area of a bolt, m^2.

5.8 CONCLUSIONS

Due to the existence of the jointing system the behaviour of a rock mass may be greatly influenced by discontinuities. Identification of potentially unstable rock wedges is necessary and if the failure mode of these wedges can be identified the reinforcement requirements can be determined. The main procedures in analysing the stability of these rock wedges and carrying out rock bolting design can be summarised as follows:

- Locate the discontinuity planes, i.e. find out the coordinates of a point on the plane;
- Compute the coordinates of the wedge on the free face;
- Compute the coordinates of the apex;

- Calculate the volume of the wedge and the area of the faces;
- Judge the potential failure modes;
- Judge the removability of the wedge;
- If the wedge is unstable, determine the number of bolts can be determined.

CHAPTER 6

COMPUTER AIDED ROCK BOLTING DESIGN SYSTEM

6.1 INTRODUCTION

With the development of computer techniques the manual design of mine support is gradually being replaced by computer methods. There are many computer languages available for programming and BASIC, FORTRAN, PASCAL and C languages are most commonly used for the purpose of engineering computation. Due to the rapid development of the menu techniques most of the computer programs used in engineering design are user friendly. For the sake of pursuing a fine graphical display, most packages are designed for Workstations. However in small mines and companies only microcomputers are available and this may reduce the number of the packages available. From this it was decided that the computer package developed in this thesis be suitable for the in the MS DOS environment on microcomputers.

In this chapter, the programming techniques and flowcharts of the sub-programs which make up the package are presented in detail. Also the necessary input data are listed in tables and the arrangement of the programs are summarised. The programs are written in Quick Basic except CLUSTER. The main reason for choosing Quick Basic is that it does not need compiling and linking before running and this saves a considerable amount of time when the program is tested.

Under the main control program, there are five subprograms for different procedures in the design; CLUSTER, POLE, MAJORSET, INITIAL and ROCKWEDGE, together with a sub-program INPUT. The arrangement of the package is shown in Figure 6.1.

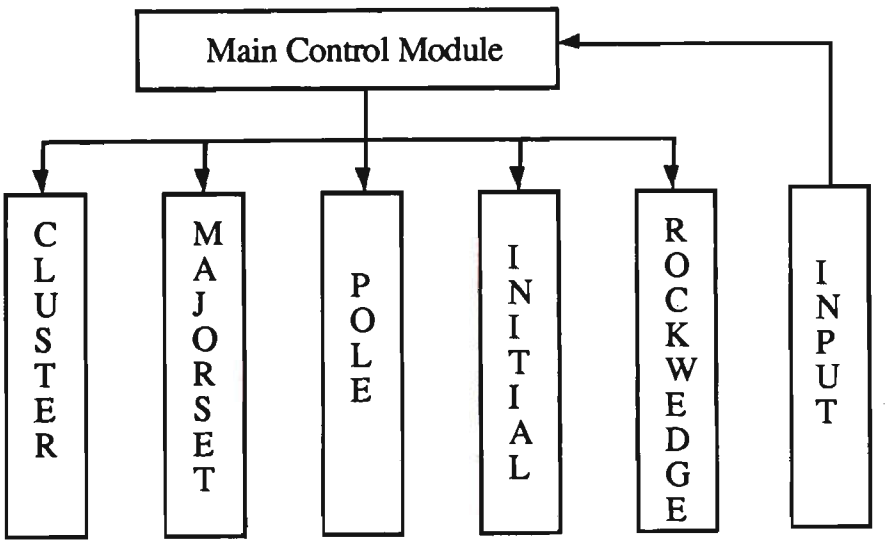

Figure 6.1. The arrangement of the package

6.2 SUB-PROGRAM FOR DATA INPUT

The sub-program INPUT is used to generate the data files for the sub-programs using the particular format and order required. A screen handling technique is used for a multi-viewing. A set of example data are generated when the system is started

and these data can be changed by inputting new data in the user's data set. The input data go to the corresponding data files and stored in the corresponding storage elements. The specified data required by the system are presented in Table 6.1.

Table 6.1. Input data required by the system

No.	Parameter	Data File	No.	Parameter	Data File
1	Total number of joints	Init.dat, Inp.dat	16	Height of project level	Inp.dat
2	Length of scanline	Init.dat, Inp.dat	17	Adjustment factor of joint orientation	Inp.dat
3	Orientation of scanline	Init.dat, Inp.dat	18	Type of bolt	Inp.dat
4	Dip of joint*	Init.dat	19	Type of cable	Inp.dat
5	Dip direction of joint*	Init.dat	20	Shear Strength of bolt	Inp.dat
6	Infilling*	Init.dat	21	Yield strength of bolt	Inp.dat
7	Water condition*	Init.dat	22	Diameter of bolt	Inp.dat
8	Roughness*	Init.dat	23	UCS of intact rock	Inp.dat
9	Waviness*	Init.dat	24	Cohesion	Inp.dat
10	Continuity*	Init.dat	25	Friction angle	Inp.dat
11	Type of discontinuity*	Init.dat	26	RQD**	Inp.dat
12	Radius of small circle	Init.dat, Inp.dat	27	F_s for bolts	Inp.dat
13	Azimuth of opening	Inp.dat	28	Unit weight of rocks	Inp.dat
14	Shape of opening	Inp.dat	29	K for clustering	Inp.dat
15	Width of opening	Inp.dat	30	R for clustering	Inp.dat

* Amount of datum is from 1 to N (total number of discontinuities).

** This can be input or calculated in the program.

It is clear that the data are recorded in two data files, INIT.dat and INP.dat, and these data files can be shared by all five sub-programs as shown in Figure 6.2.

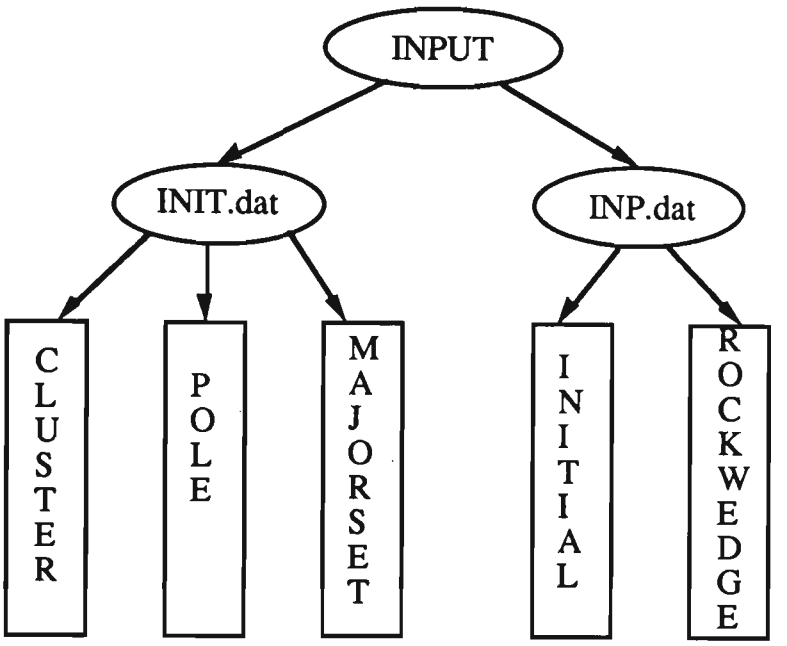

Figure 6.2. Data sources of the sub-programs

The data files can also be generated using Lotus 123, based on the format and order required.

6.3 SUB-PROGRAM FOR CLUSTERING ANALYSIS

The sub-program CLUSTER, modified from FRACTAN, is used to carry out the necessary computations for clustering analysis. The original program FRACTAN was developed by Shanley and Mahtab of the U.S. Bureau of Mines. FRACTAN was written for a 6400 Computer using Fortran IV and therefore the modification was made suitable for the DOS environment using Fortran 77L. The modified program was developed by dividing the half unit hemisphere into 400 equal area

cells. The data points in each cell are examined in increasing order of dip direction of the discontinuity plane to determine if they are dense, i.e. the centre of spheres of arbitrary R containing K (R and K were defined in Chapter 3) or more data points. Once a dense point is found in a cell all other points in the cell are allocated to it and no further points in the cell are examined. Then all the points are sorted into groups and distribution of the points in groups are tested by both the objective function and the χ Square test.

The input data for CLUSTER are presented in Table 6.2. The flowchart of the sub-program is shown in Figure 6.3.

Table 6.2. Input data for CLUSTER

No.	Parameter	No.	Parameter
1	Total number of points	4	Radius of small circle
2	Dip of discontinuity*	5	A positive integer, K
3	Dip direction of discontinuity*	6	Arbitrary radius of the sphere

* Total number of points is N.

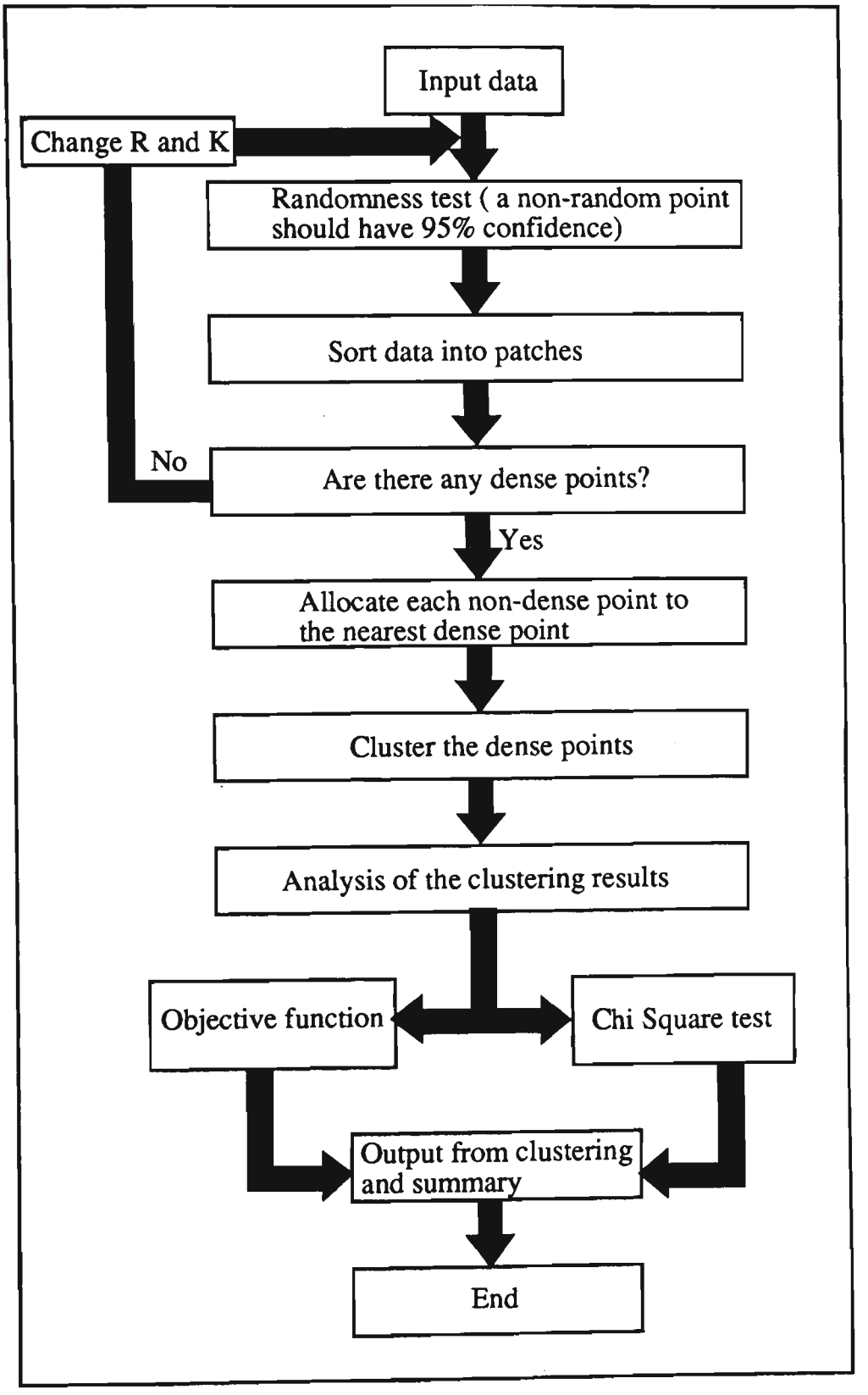

Figure 6.3. Flowchart of the sub-program CLUSTER

6.4 SUB-PROGRAM FOR PRESENTATION OF GEOLOGICAL DATA

POLE is a sub-program that can be used solely to present the geological data collected from the site investigation. It is based on the stereographic projection technique and determines pole distributions and pole concentrations. This program consists of two modules: one for pole distributions and one for pole concentrations. A 7475A plotter can be driven by the program and the results from running this program can be presented graphically.

The input data for the sub-program are in Table 6.3 and the flowchart of the sub-program is shown in Figure 6.4.

Table 6.3. Input data for POLE

No.	Parameter
1	Total number of points
2	Dip of discontinuity*
3	Dip direction of discontinuity*
4	Radius of small circle
5	Density of the projection meshes

* Total number of the points is N.

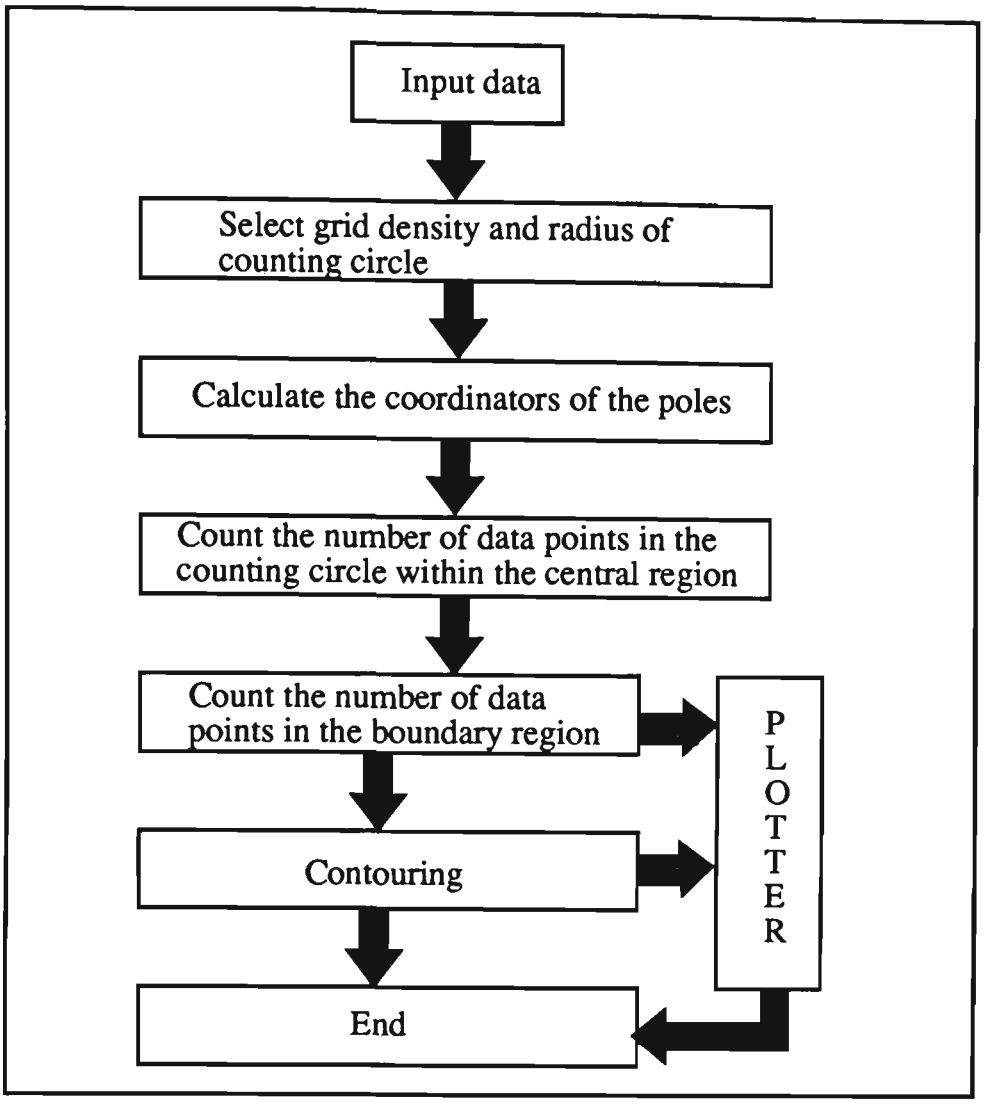

Figure 6.4. Flowchart of the sub-program POLE

6.5 SUB-PROGRAM FOR DETERMINING MAJOR DISCONTINUITY SETS

Running sub-program MAJORSET will result in the determination of the major discontinuity sets in an area of interest. This involves a quantitative analysis of various parameters such as groundwater condition, roughness, waviness, continuity and type of discontinuity. The rating system and the weighted average method was used for determination of the rating of each parameter was discussed previously. Table 6.4 shows the input data for MAJORSET and Figure 6.5 presents the flowchart of the sub-program MAJORSET.

Table 6.4. Input data for MAJORSET

No.	Parameter	No.	Parameter
1	Number of clusters	7	Ground water condition
2	Number of points in I-th cluster*	8	Roughness
3	Dip of i-th point in I-th cluster	9	Waviness
4	Dip direction of i-th point in I-th cluster	10	Continuity
5	Length of scanline	11	Type of discontinuity
6	Orientation of scanline		

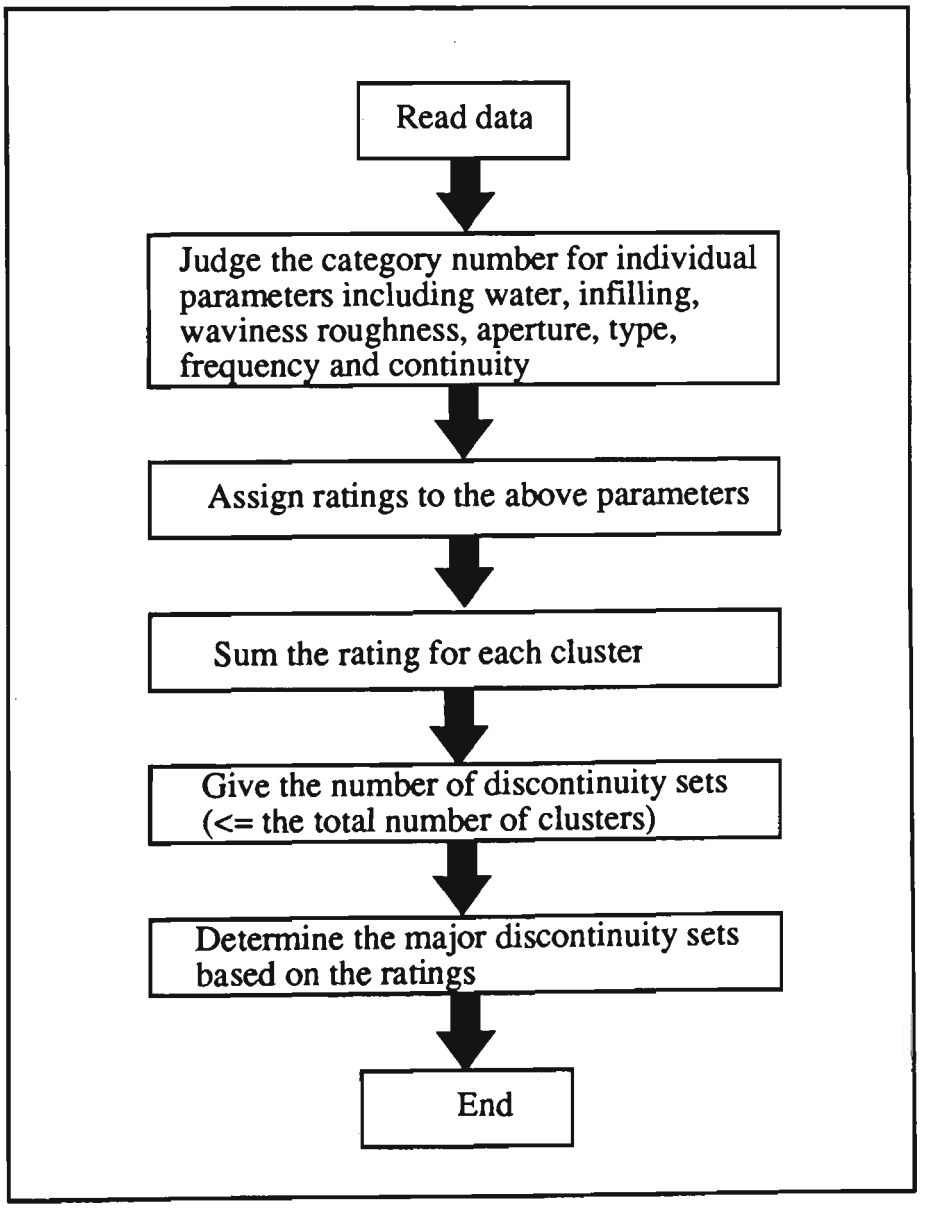

Figure 6.5. Flowchart of the sub-program MAJORSET

6.6 SUB-PROGRAM FOR THE INITIAL DESIGN OF A ROCK BOLTING SYSTEM

The sub-program INITIAL was written for the initial design of rock bolting system. Based on the procedures described in the previous chapter, the outcome of the sub-program is to give a suggestion on the pattern of rock bolting system. This sub-program involves two modules: one for computing and one for graphical viewing. In the computing module the necessary calculations related to individual parameter used to evaluate the quality of a rock mass are carried out. In the multi-viewing module the pattern of the rock bolting system suggested from the design are presented graphically.

The necessary data are presented in Table 6.5 and the flowchart of the sub-program is shown in Figure 6.5.

Table 6.5. Input data for INITIAL

No.	Parameter	No.	Parameter
1	Length of scanline	8	Shear strength of bolts
2	orientation of scanline	9	Yield strength of bolts
3	Total number of discontinuities	10	UCS of intact rock
4	Height of opening	11	Max. principal stress
5	Width of opening	12	Min. principal stress
6	Type of bolt	13	Unit weight of rocks
7	Diameter of bolt		

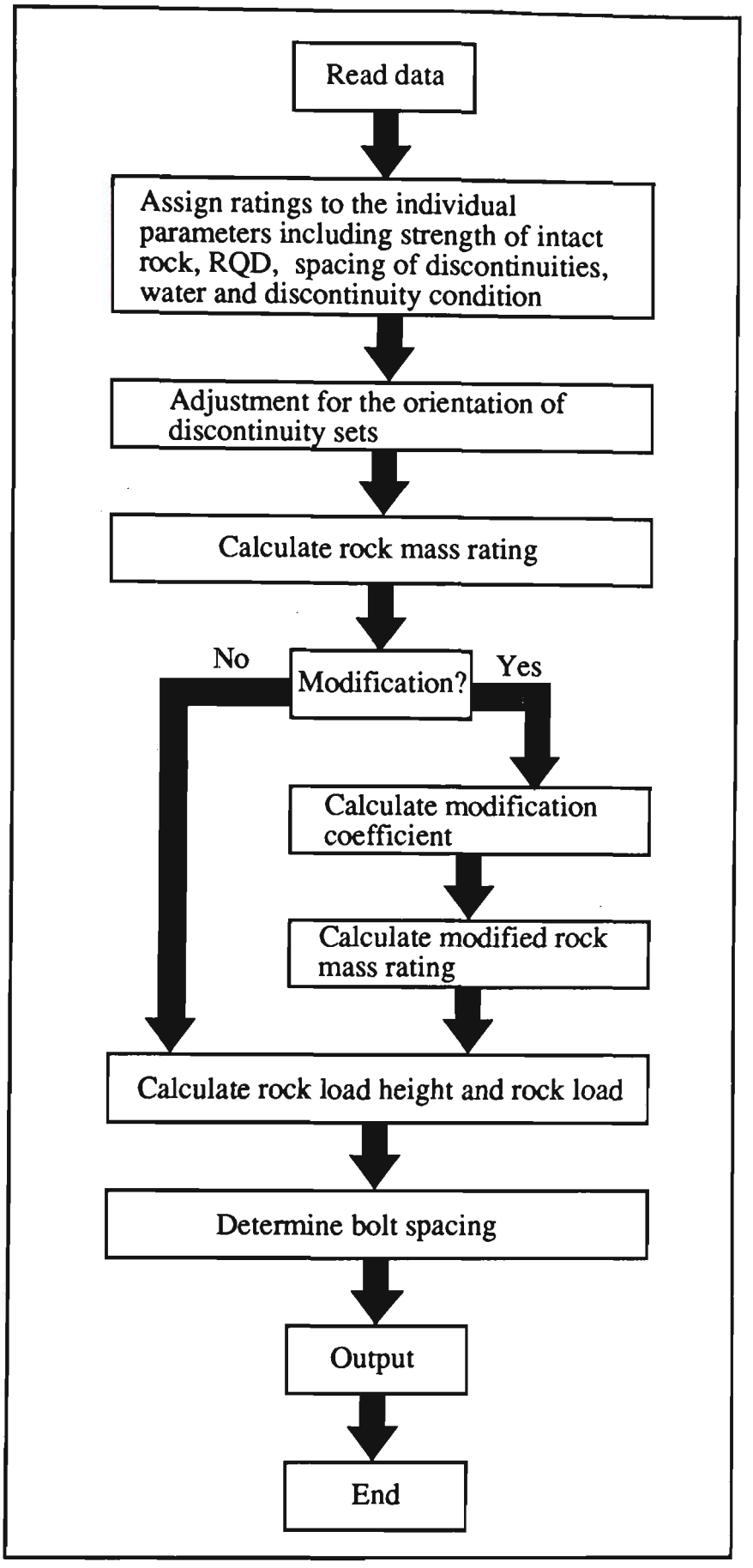

Figure 6.6. Flowchart of the sub-program INITIAL

6.7 SUB-PROGRAM FOR ROCK BOLTING DESIGN OF UNSTABLE WEDGES

The sub-program ROCKWEDGE is one of the most important parts of the whole system. All procedures dealing with the identification of unstable wedges, judgement of the failure mode and the removability of the wedges and suggestions on the final design of a rock bolting system are integrated in this sub-program. The maximum number of discontinuity sets handled by this sub-program is 11. The input data for the sub-program are presented in Table 6.6 and the flowchart of the sub-program is given in Figure 6.7.

Table 6.6. Input data for ROCKWEDGE

No.	Parameter	No.	Parameter
1	Number of discontinuity set	11	Radius of small circle
2	Dips of discontinuity sets	12	Cohesion
3	Dip directions of discontinuity sets	13	Angle of internal friction
4	Length of scanline	14	Unit weight of rocks
5	Orientation of scanline	15	Type of bolts
6	Orientation of opening	16	Radius of bolt
7	Shape of opening	17	Shear strength of bolts
8	Height of opening	18	Yield strength of bolts
9	Width of opening	19	Factor of safety
10	Height of projection level	20	Control variables

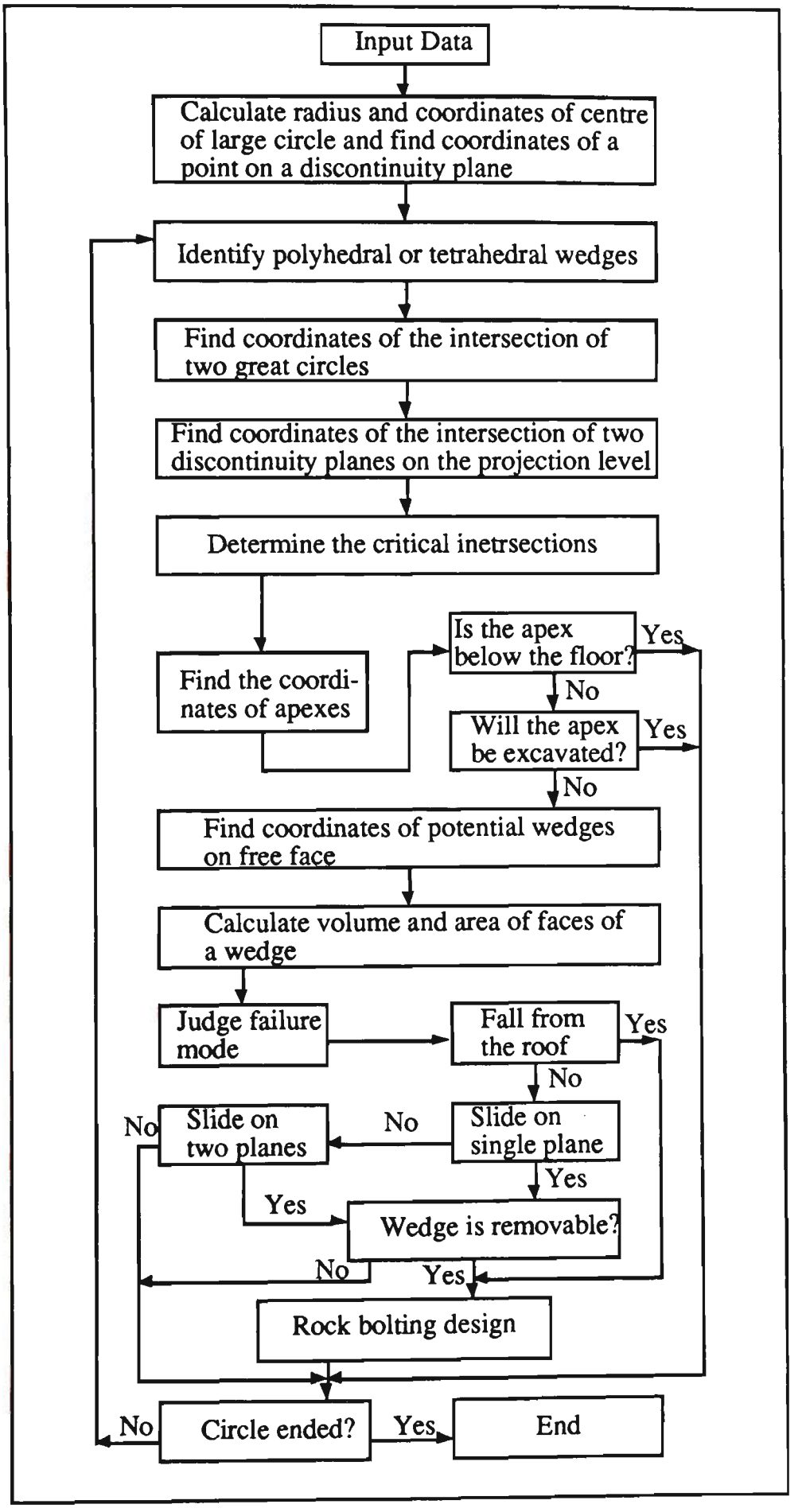

Figure 6.7. Flowchart of the sub-program ROCKWEDGE

In this program N' discontinuity sets are taken out from the total N discontinuity sets and the polyhedral wedges are identified first. This is followed by a search for tetrahedral wedges. If the apex of a wedge is not removed by excavating or is not located below the floor of the excavation the size of the wedge is determined from the coordinates of the apex and the intersection on the free face. The failure mode of the wedge is identified and removability of the wedge is determined. The possible failure modes considered in the program are falling from the roof and sliding on one or two discontinuity planes. If the wedge is removable, design of a rock bolting system, number of bolts to stabilise the wedge, is then proposed. After all possible combinations of all discontinuities in the area of interest are identified the computation is complete.

6.8 CONCLUSIONS

It is evident that the programs developed can be used for data processing, determination of major discontinuity sets, initial design of the rock bolting system and rock bolting design for unstable wedges. A large number of data collected from a geotechnical survey can be sorted into useful information. Due to computerisation of all procedures, the objective bias from personnel can be eliminated and errors caused by manual computation and graphing minimised. It can also save on-site engineers a considerable amount of time in the design of a reliable rock bolting system.

CHAPTER 7

APPLICATION OF THE ROCK BOLTING DESIGN SYSTEM - CASE STUDIES

7.1 INTRODUCTION

As mentioned in the previous chapters, the method developed for the design of a rock bolting system will suggest the number and pattern of bolts required to secure the stability of an underground opening in a jointed rock mass and provide a safe working environment for miners. In order to test the applicability of this method, field investigations were conducted in two mines: Broken Hill Southern Operation, owned by Pasminco Mining (NBHC Mine), and the CSA Mine, Cobar, owned by CRA Limited. The geological data were collected from scanline surveys and processed by a statistical manner. A series of analyses were then carried out, including determination of the major discontinuity sets, assessment of rock quality, initial design of the rock bolting system and searching for unstable wedges. This

led to a final presentation of the design of a rock bolting system for the area of interest in these two mines.

7.2 DESIGN OF ROCK BOLTING FOR THE NBHC MINE

NBHC Mine produces predominantly lead and zinc concentrates. Up to the beginning of 1993, a total of 82.2 million tonnes at a combined lead plus zinc grade of 20 per cent was mined from the southern portion of the lode since Zinc Cooperation began underground mining operations in 1912. Current ore reserves are quoted at 30.8 million tonnes at 10 per cent zinc, 6 grams per tonne silver and 7 per cent lead (Smith & Spreadborough, 1993).

7.2.1 Geological Environment

The Broken Hill ore body consists of several discrete stratiform lodes or lenses which contain economic quantities of lead and zinc sulphides accompanied by silver minerals and traces of copper. The deposit lies in a thick sequence of highly metamorphosed and deformed Proterozoic sedimentary and volcanic rocks. The sequence is called the Willyama Supergroup and was laid down under shallow marine and continental conditions between 1,700 and 2,000 million years ago, as shown in Figure 7.1(Pasminco Mining Broken Hill Operation, 1990).

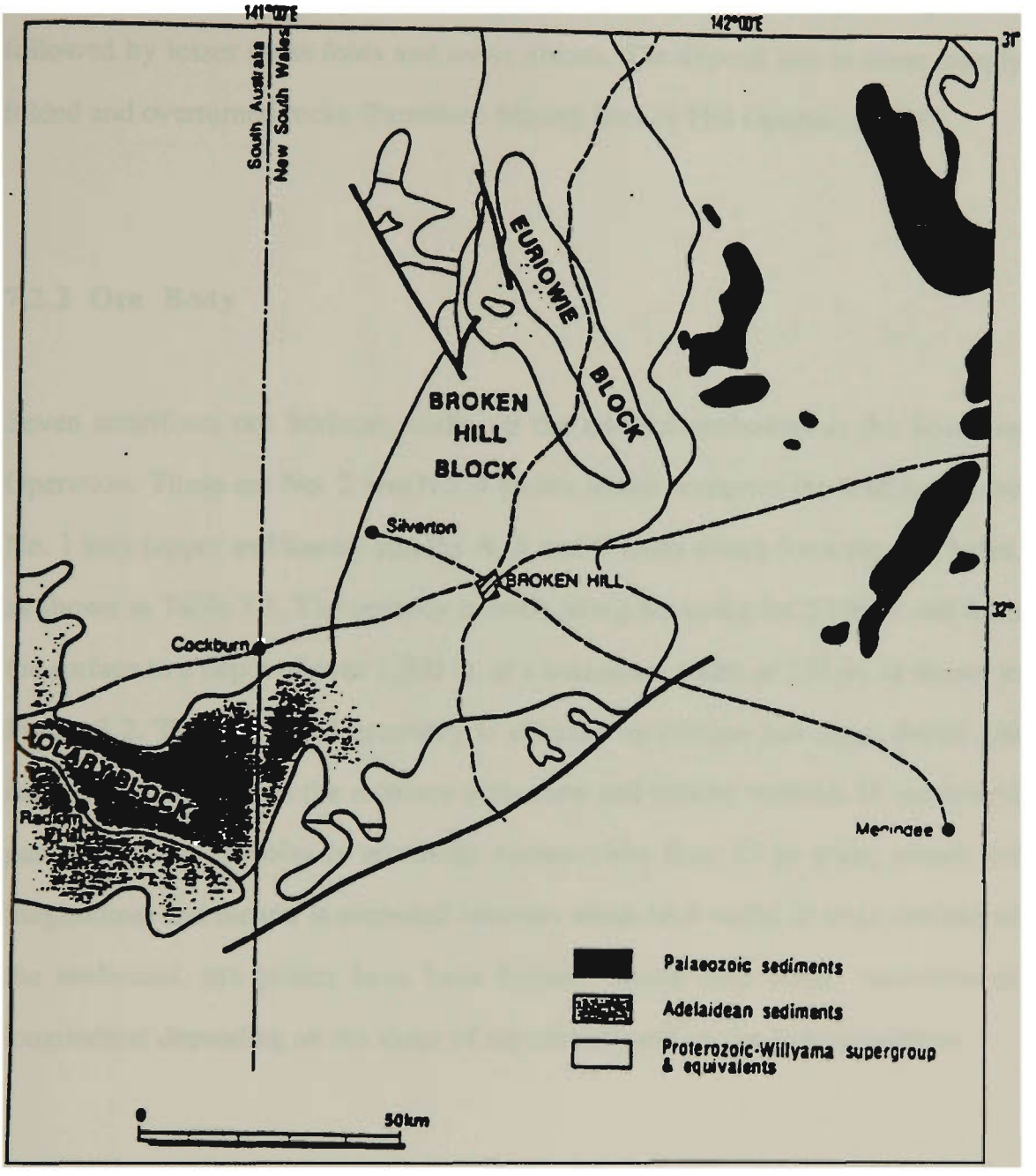

Figure 7.1. Regional geology in NBHC

(Pasminco Mining Broken Hill Operation, 1990)

Following deposition of the sediments and the ore, the sequence was intensely folded and sheared in several episodes during and after the main granulite facies metamorphic event. An early fold overturned the sequence in much of the district

including Broken Hill and on this was later superimposed steep, sharp folds, followed by lesser cross folds and many shears. The deposit lies in these steeply folded and overturned rocks (Pasminco Mining Broken Hill Operation, 1990).

7.2.2 Ore Body

Seven stratiform ore horizons make up the mineral orebodies at the Southern Operation. These are No. 2 and No. 3 lenses which comprise the lead lodes, the No. 1 lens (upper and lower) and the A, B and C lodes which form the zinc lodes, as shown in Table 7.1. The orebody extends along the strike for 2,100 m and from the surface to a depth of over 1,200 m, at a maximum width of 250 m, as shown in Figure 7.2. The basic fold geometry is affected by various late stage shears and faults which impact on the resource utilisation and mining method. In the central part where the oreboby is relatively narrow, less than 15 m wide, stopes are longitudinal and the ore is extracted between waste rock walls, in wide sections of the orebodies, ore pillars have been formed. These may either transverse or longitudinal depending on the shape of the orebody and on the local conditions.

Table 7.1. Seven stratiform ore horizons present in Broken Hill (Pasminco Mining Broken Hill Operation, 1990)

Zinc Lodes	A Lode B Lode C Lode No. 1 Lens - Upper - Lower
Lead Lodes	No. 2 Lens No. 3 Lens

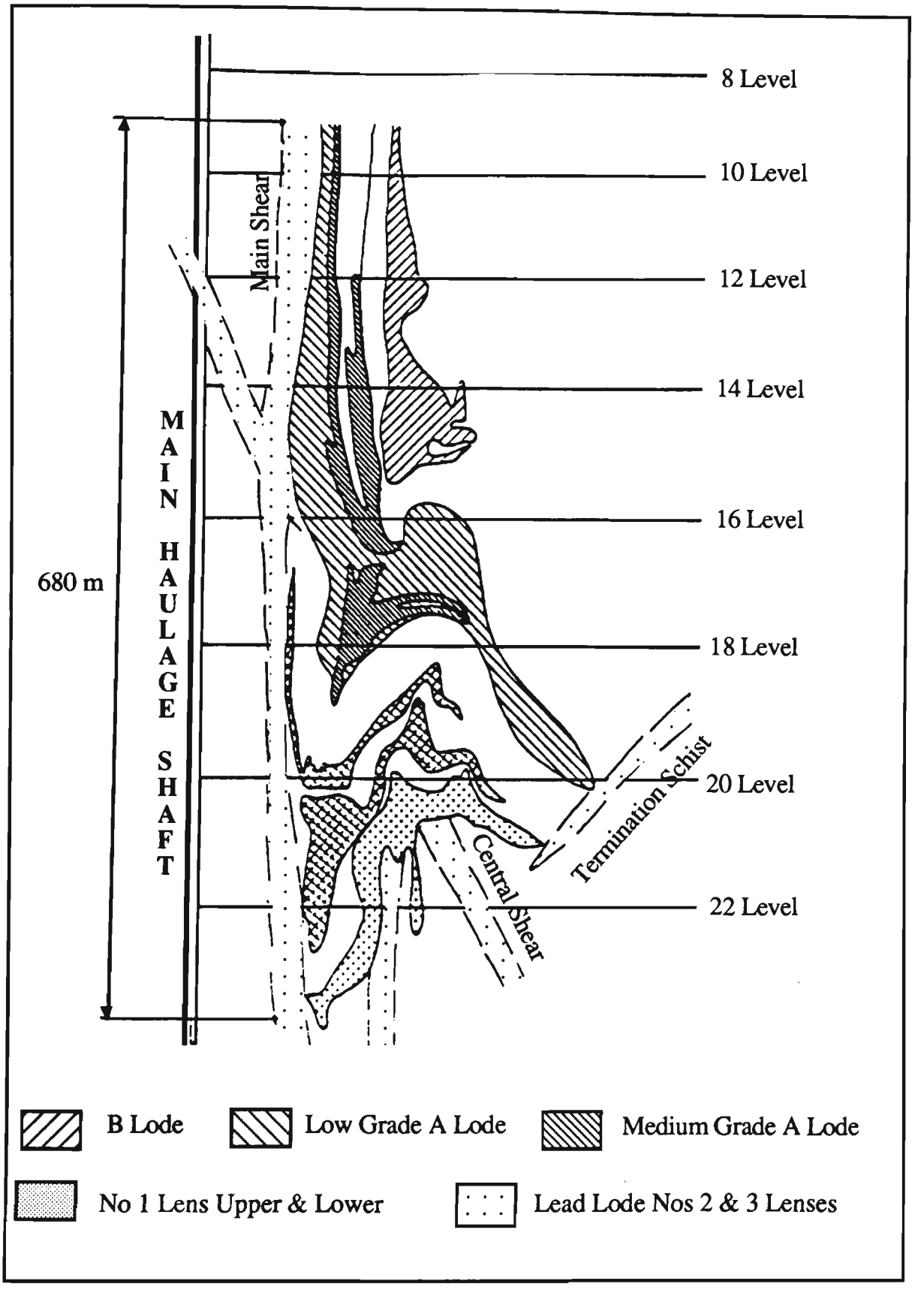

Figure 7.2. Mine geology in NBHC

(Pasminco Mining Broken Hill Operation, 1990)

7.2.3 Mining Methods Used in the NBHC Mine

Due to the complexity of the lode configurations and past experience in controlling poor ground, a variety of mining methods have been used to maximize ore recovery. The mining methods currently used are as follows:

- o Longhole-open stoping (LHOS) including vertical crater retreat (VCR);
- o Loader cut and fill mining (LCAF);
- o Timber methods including square-set stoping and undercut and fill (UCAF);
- o Open stoping; and
- o Mechanised undercut and fill (MUCAF).

The contribution of each method to ore production for each year since 1980 is presented in Figure 7.3 together with the ore produced by development activities.

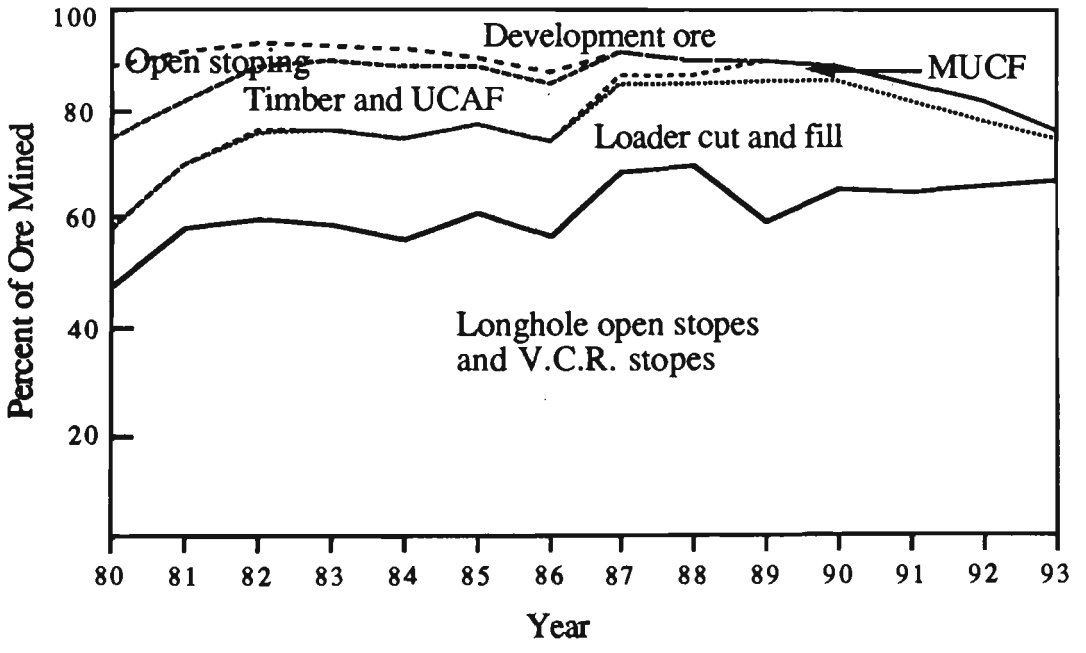

Figure 7.3. Ore production by mining methods in the NBHC Mine

The mining method adopted in 9 pillar upper stope is longhole open stoping. A longitudinal section and plan of the area of interest are presented in Figures 7.4a and 7.4b respectively.

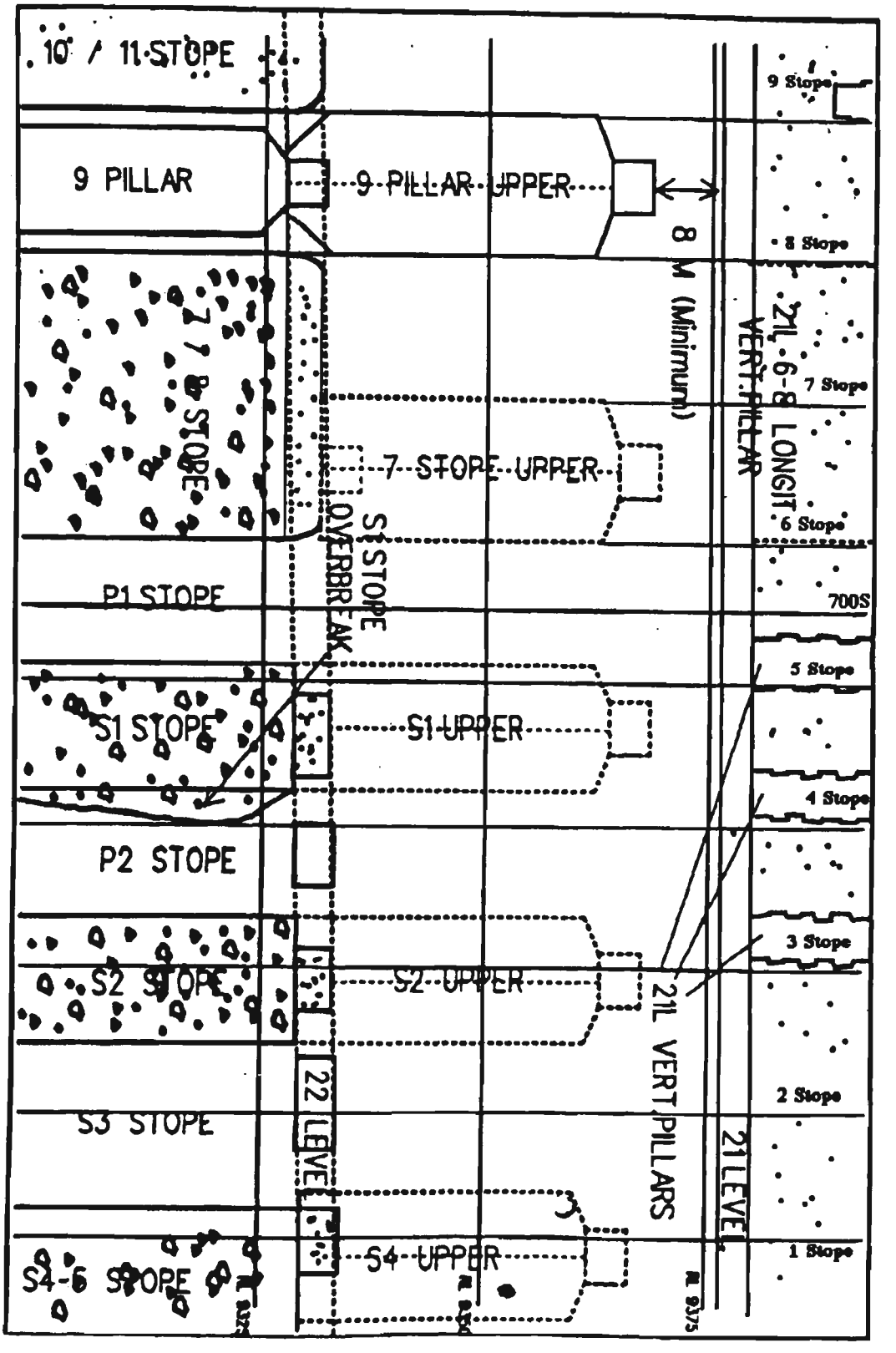

Figure 7.4a. Longitudinal section of stoping area at the 22 level

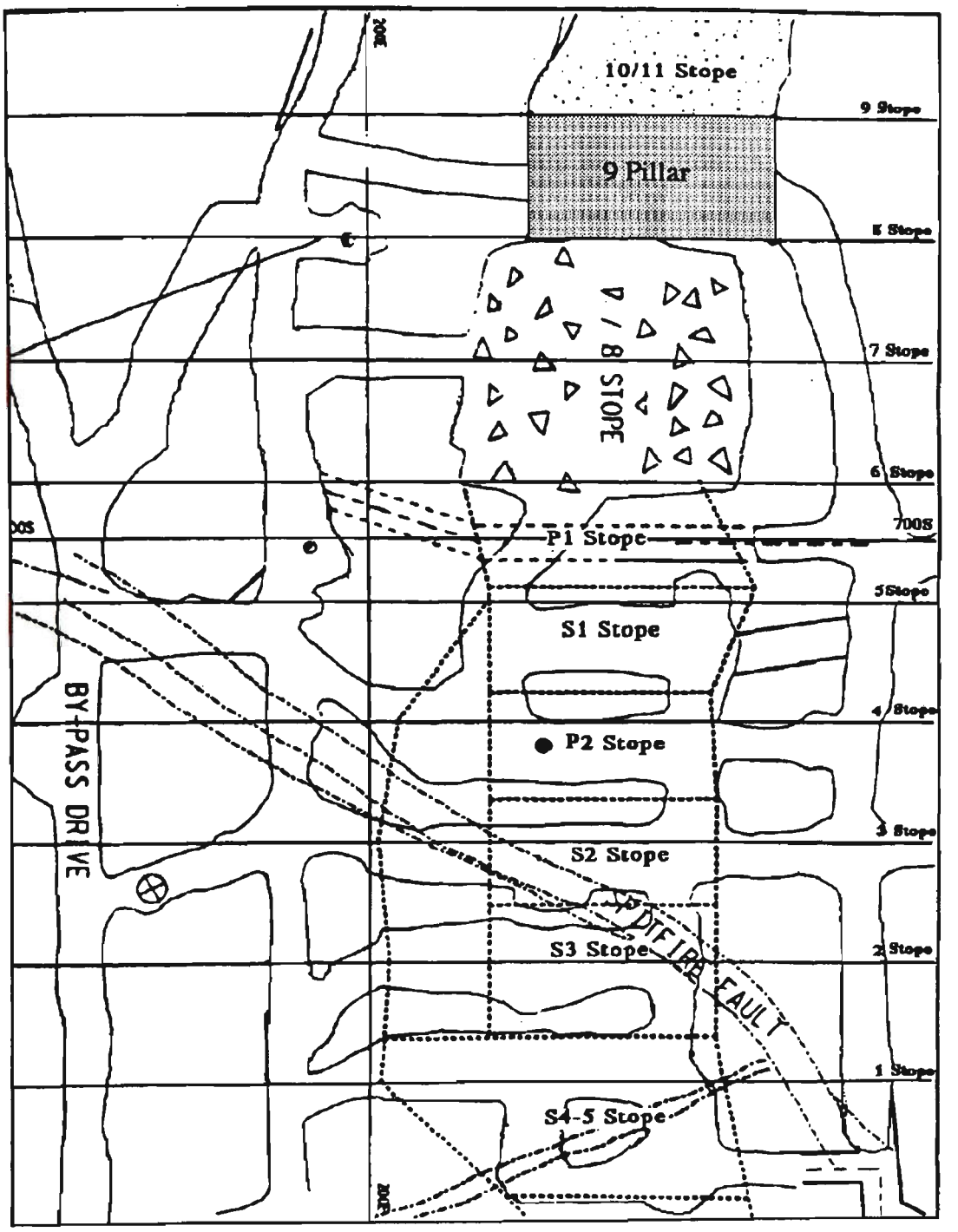

Figure 7.4b. Plan of stoping area at the 22 level

One of the problems arisen in the management of mining production in Southern Operation is the safety of employees. Clearly evident by Figure 7.5 is that the Southern Operations had a historical trend towards a lost time incident frequency rate of about 105/annual. On a number of occasions production interruptions were

caused by instability of the rock mass. To reinforce the stope excavation rock bolting has been introduced in NBHC on the basis of empirical design. To seek for an optimum bolting reinforcement and find stress distribution in 9 pillar upper stope, a research project is being conducted cooperating with CSIRO. Our research team of three carried out our field work in the same stoping area for stability analysis and rock bolting design for mining excavations.

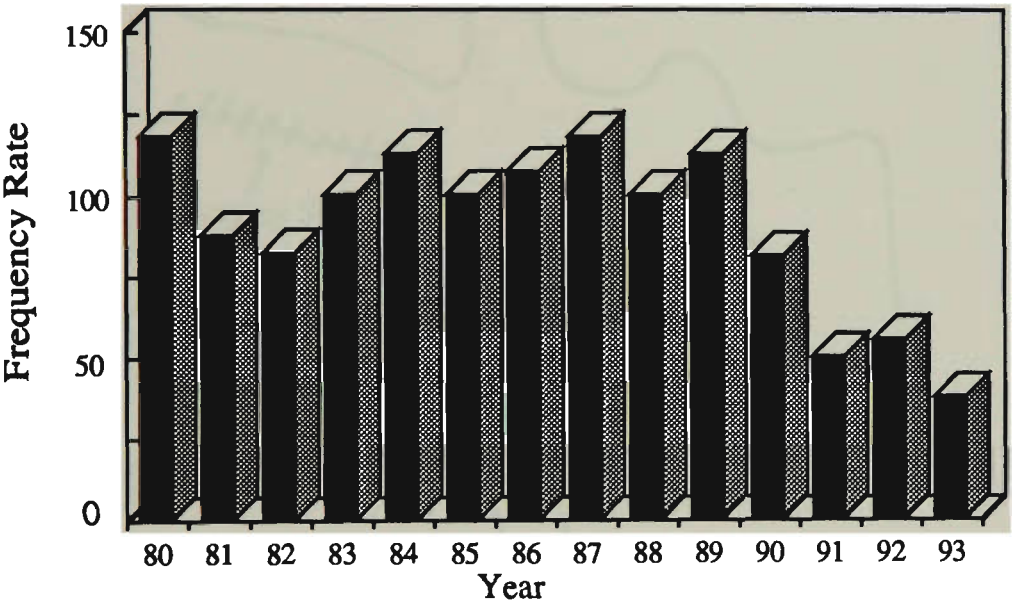

Figure 7.5. Lost time incident frequency in the Pasminco Southern Operations (after Smith and Spreadborough, 1993)

7.2.4 Collection and Processing of Geological Data

In order to collect structural geological data from 9 pillar upper stope, a scanline survey was conducted in this area. To avoid bias towards discontinuities running in a particular direction, three mutually perpendicular scanline directions were chosen. This involved setting up one 'main' horizontal scanline, two 'auxiliary' scanlines (horizontal and normal to the main scanline) and a number of short vertical scanlines along the 'main' and 'auxiliary' scanlines. This arrangement is shown in

Figure 7.6. 193 discontinuities were observed on the scanlines and 1,400 readings were taken.

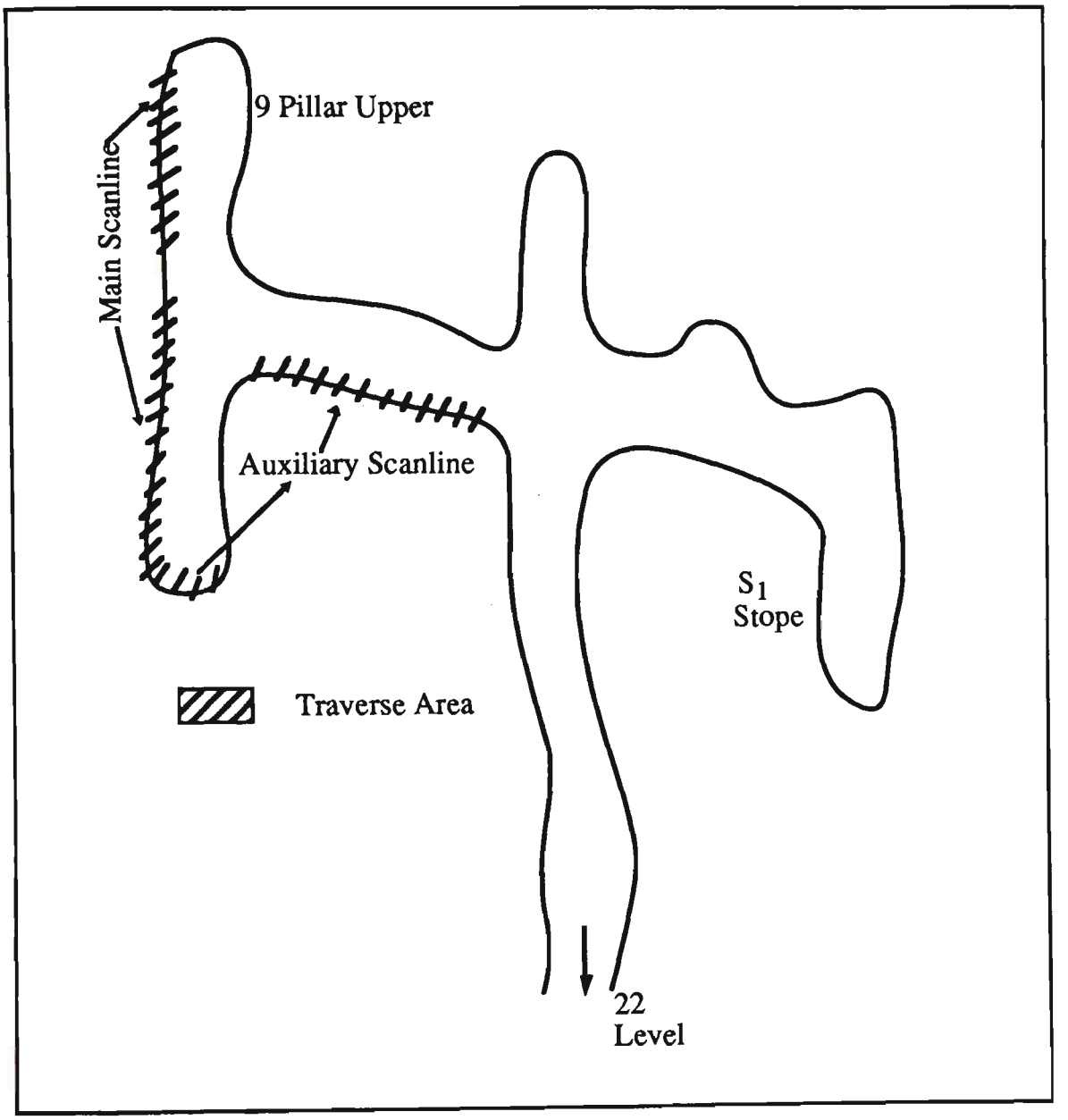

Figure 7.6. Location of scanline survey in 9 pillar upper stope, Broken Hill

The orientation data were clustered into 4 classes by using clustering analysis, with the results shown in Table 7.2. The clustering analysis indicated that four discontinuity sets were evident, and these were subsequently plotted and contoured to get the pole distribution and pole concentration of each, as shown in Figures 7.7 and 7.8.

Table 7.2. Discontinuity orientations of four clusters in 9 pillar upper stope

Cluster No. 1							
355/85	358/86	009/80	018/82	330/83	340/84	010/75	011/75
340/75	342/75	350/77	330/74	338/72	350/74	032/70	335/67
340/66	014/65	024/63	026/65	030/62	340/62	022/60	359/56
Cluster No. 2							
137/85	145/85	302/88	315/90	120/81	133/84	136/84	140/80
140/80	141/80	146/82	164/80	298/82	304/80	310/81	118/78
141/76	150/75	150/75	150/75	160/75	200/75	136/70	140/70
144/68	166/70	138/62	185/65	105/60	178/60	172/55	108/50
126/50	108/42	136/45	140/45	167/45	167/45		
Cluster No. 3							
046/88	085/85	214/89	266/87	278/85	048/80	048/80	082/80
258/82	262/82	268/82	272/80	275/80	256/75	259/75	262/77
262/79	262/75	264/75	265/75	265/75	268/75	268/75	275/75
280/75	293/75	045/72	072/73	048/67	205/69	236/70	242/70
255/67	260/70	264/70	270/70	270/70	277/68	298/70	057/63
058/65	090/65	238/62	245/65	252/65	264/65	270/65	270/65
283/63	044/60	050/60	055/60	266/58	270/60	276/58	220/55
235/55	268/50						
Cluster No. 4							
217/56	192/53	224/47	216/45	213/40	242/38	248/40	256/40
270/38	282/40	028/35	083/31	190/34	190/35	300/35	040/28
045/30	206/30	226/30	235/28	240/28	264/30	265/30	030/25
055/20	232/20	232/20	235/25	272/22	289/25	294/25	300/25
300/25	300/25	302/25	322/24	334/18	024/10	215/11	220/10
230/15	230/11	250/15	261/15	278/14	285/15	286/14	294/15
305/10	316/15	316/15	325/15	330/15	018/05	020/05	080/05
150/05	160/08	160/08	160/08	160/08	160/08	190/05	270/05
294/08	302/08	305/07	350/08	90/00	135/00	135/00	336/00

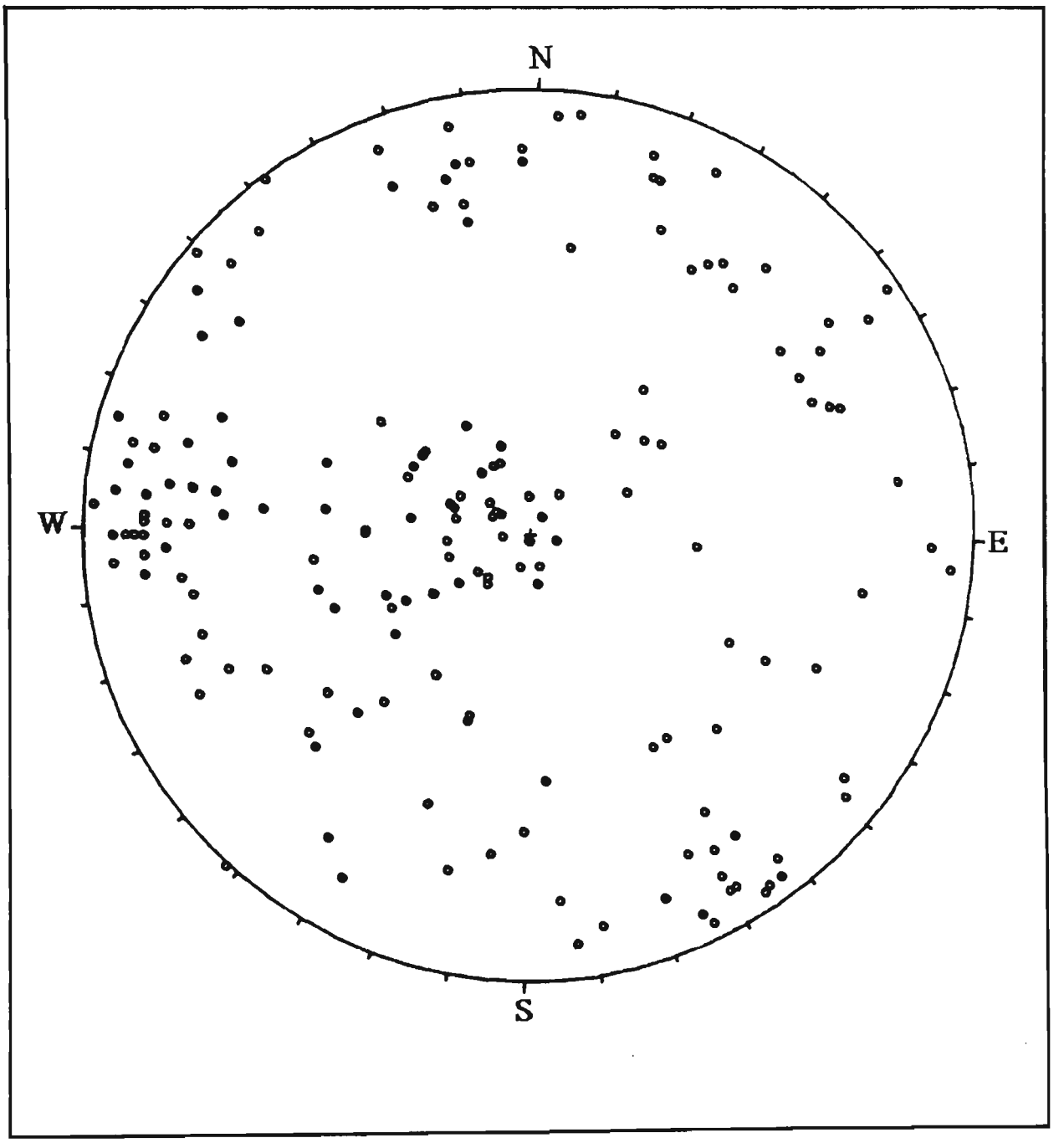

Figure 7.7. Pole distribution in 9 pillar upper stope

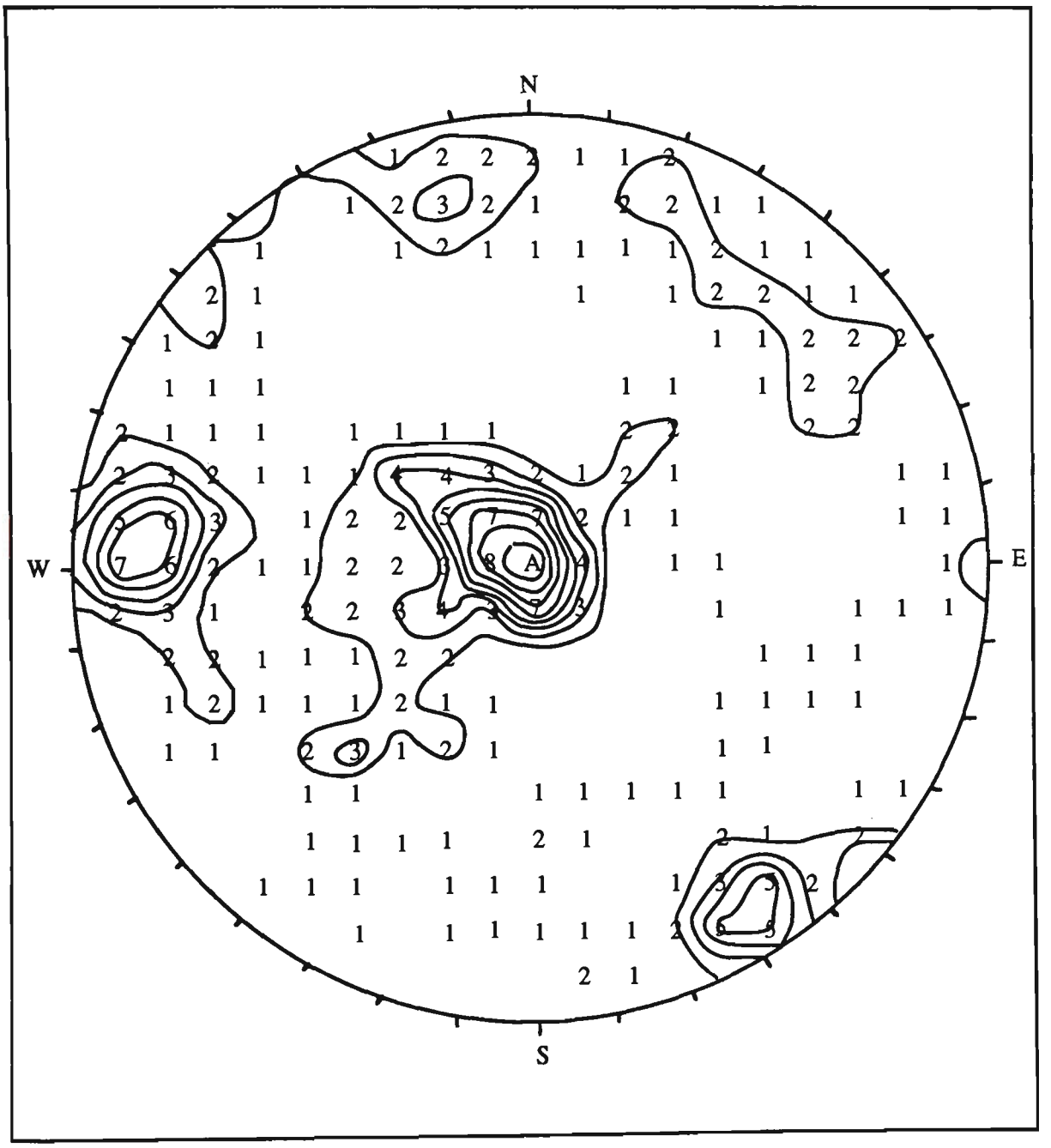

Figure 7.8. Pole concentration in 9 pillar upper stope

The maximum likelihood estimates of parameters associated with Bingham's distribution, and computed from the data points belonging to the four clusters are given in Table 7.3.

Table 7.3. Maximum likelihood estimates of parameters for data of Table 7.2

Cluster No.	1	2	3	4
μ_1	-.322, -.175, .930	.549, .272, .790	-.638, -.743, 0.201	-.652, .748, .125
μ_2	-.022, .984, .178	.382, .759, -.527	.290, .011, .957	-.757, -.636, -.147
μ_3	.947, -.036, .320	.743, -.591, -.313	.713, -.669, -.209	.031, .190, -.981
ϕ_1 / θ_1	21.5/208.6	37.8/26.4	44.5/155.6	82.8/131.1
ϕ_2 / θ_2	79.8/91.3	121.8/63.3	132.0/179.2	98.4/220.0
ϕ_3 / θ_3	71.3/357.8	108.2/321.5	102.0/78.1	168.9/80.9
ω_1	.48	2.44	3.39	3.03
ω_2	2.42	4.03	7.52	6.35
ω_3	21.10	32.54	47.09	62.61
σ_1	*	18.22	9.23	9.01
σ_2	*	2.49	2.01	1.48
σ_3	*	3.18	2.98	2.12
ξ_1	*	-8.79	9.32	12.57
ξ_2	*	-5.68	-4.66	-6.48
0.00	0	0	0	0

* - Values out of test.

The objective function F(P) is 0.78×10^2, which is the least error in the analysis.

Discontinuity set 1 (Table 7.2) had a data set of only 24 points after clustering, significantly less than sets 3 and 4. This may suggest that this set has a lesser importance in the rock mass make up. But after using the rating system for determination of the major discontinuity sets, described in Chapter 3, the importance of this set is nearly equivalent to the other three. The rating of each set for every parameter is presented in Table 7.4.

Table 7.4. Rating of four major discontinuity sets in 9 pillar upper stope

	Item	1	2	3	4
1	Water	1.0	0	0.4	0.4
2	Infilling	8.0	8.5	9.0	9.0
3	Waviness	7.5	7.5	7.0	7.0
4	Roughness	6.0	6.0	6.5	6.5
5	Aperture	2.0	1.7	1.0	1.0
6	Type of discontinuity	5.0	5.0	5.0	5.0
7	Frequency factor	7.0	11	16	20
8	Continuity factor	10	9.0	7.0	7.0
9	Total rating	46.5	48.7	51.9	55.9

From Table 7.4, it is evident that the number of discontinuities in one set has a significant influence on the final rating. Other parameters however, such as infilling, waviness, roughness, aperture and continuity, are also important in the assessment of major discontinuity sets. The major discontinuity sets in 9 pillar upper stope area are therefore identified in order of their total rating value; as Table 7.5.

Table 7.5. The major discontinuity sets in 9 pillar upper stope

Set No.	1	2	3	4
Frequency of discontinuity	72	57	39	25
Magnetic north (°)*	12/260	78/256	72/141	71/357
Mine north (°)	12/220	78/216	72/101	71/317

* - Magnetic declination at the time of survey was - 40°.

7.2.5 Design of Rock Bolting System for NBHC

As mentioned in the previous chapters, the design of a rock bolting system in a jointed rock mass is conducted in two steps. The geomechanics classification system is used for initial design and the method described in Chapter 5 is used for the design related to unstable wedges. The design of rock bolting here includes both rock bolts and cables bolts. Generally, the rock bolts act as a common support elements which are placed soon after excavation, and cables act as reinforcement for large potentially unstable wedges created by an unfavourable combination of discontinuities. Cable bolts are also suitable for controlling large areas of unstable rock at a greater depth. In NBHC both types of reinforcement method have been adopted.

1. Design Based on the Geomechanics Classification System

The following design is based on the work discussed in Chapter 4. Firstly, the quality of rock mass in 9 pillar upper stope is evaluated using the geomechanics classification system and secondly, the rock bolting design is conducted using Mohr's failure criteria.

(1) Calculation of rock quality designation (RQD)

The value of RQD is found from:

$$RQD\ (\%) = 110.4 - 3.68 \times \lambda$$

Where $\lambda = 3.3/m$.

Therefore, RQD = 97.4%.

(2) Rock mass rating (RMR)

RMR can be obtained by using Table 2.1 to assign a value to each parameter. The RMR for 9 pillar upper stope is presented in Table 7.6.

Table 7.6. RMR for 9 pillar upper stope

1	Strength of intact rock	117 MPa	7.9
2	RQD	97.4%	20.0
3	Spacing of discontinuities	0.3 m	13.9
4	Discontinuity conditions	Class 4	10.0
5	Ground water condition	Class 2	10.0
6	Excavation orientation	Fair	-5.0
7	Total		56.8

(3) Cohesion C and friction angle ϕ

Having determined the rock mass rating in 9 pillar upper stope, C and ϕ of the rock mass in this area can also be determined from Table 7.4. It is evident that the rock mass in this area belongs to class III, with C = 0.30 MPa and $\phi = 31°$. However in this research the cohesion of discontinuities is considered to be zero due to the soft infilling materials between the discontinuity walls in most conditions.

(4) Stand-up time

From Figure 7.2 the stand-up time for an unsupported excavation span can be determined. The stand-up time for various excavation are shown in Table 7.7.

Table 7.7. Stand-up time for excavations in 9 pillar upper stope

No.	Name of excavation	Span (m)	Stand-up time
1	Drill drive	5.0	1 month
2	Crown pillar	15.0	approx. 1 week
3	Draw drive	5.0	1 month

(5) Modification of RMR

As mentioned in Chapter 4, the RMR may be affected by adverse stress conditions. To measure the principal stresses in 9 pillar upper stope two overcoring tests were carried out (CSIRO, 1992). One test was undertaken in country rock and the other in ore, as shown in Figures 7.9a and 7.9b. The test results are presented in Tables 7.8 and 7.9.

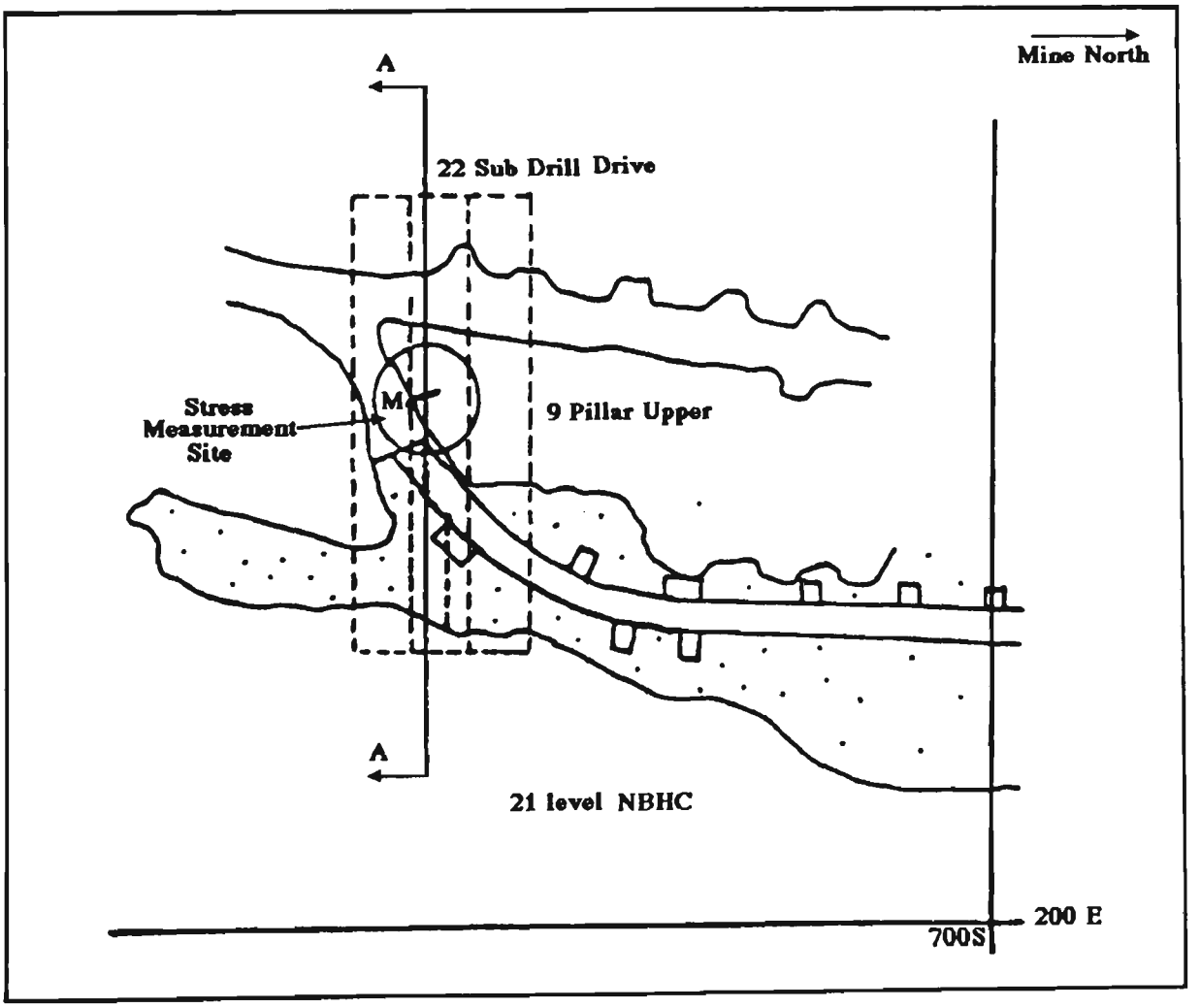

Figure 7.9a. Plan view of the stress measurement site in 9 pillar upper stope

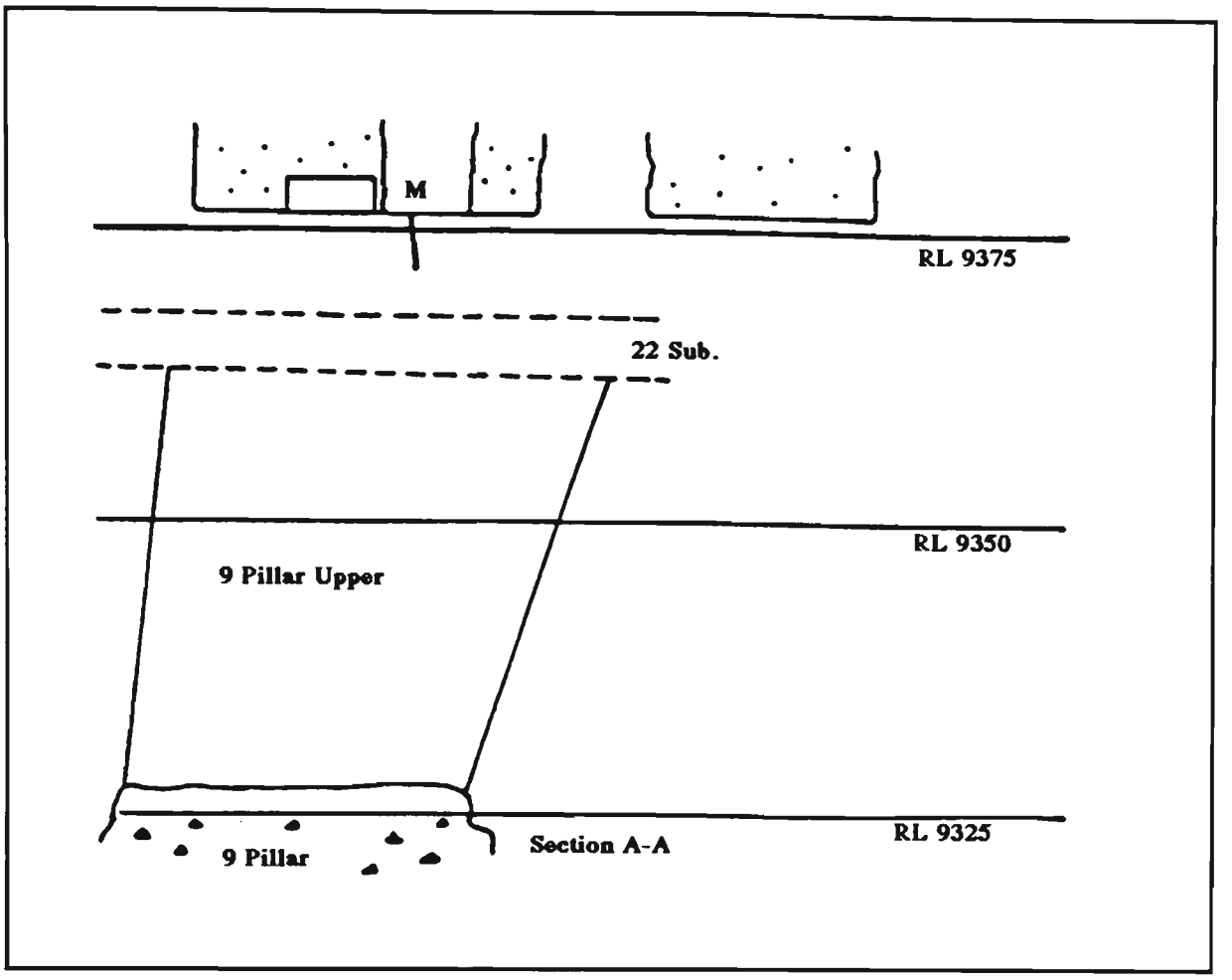

Figure 7.9b. Longitudinal section of stress measurement site in 9 pillar upper stope

Table 7.8. Stress components (MPa) in 9 pillar upper stope

Test No.	E (GPa)/υ	σ_{NS}	σ_{EW}	σ_V	τ_{NE}	τ_{EV}	τ_{VN}
1	79.5/0.212	20.6	37.7	39.9	-13.2	-0.7	-6.2
2	62.3/0.186	35.1	61.1	57.8	-2.2	-7.8	-12.8

Table 7.9. Principal stresses (MPa) in 9 pillar upper stope

No.	σ_1	Brg. 1	Dip1	σ_2	Brg. 2	Dip 2	σ_3	Brg. 3	Dip 3
1	46.0	123°	25°	40.0	275°	62°	12.2	28°	12°
2	70.4	246°	44°	54.3	112°	35°	29.3	3°	25°

Brg. - Bearing, east of grid north,

Dip - Positive downwards.

The results from test 2 were chosen for design due to the test sites proximately close to the area of interest. A ratio of σ_h/σ_v of 1.06 is obtained. The height and width of the drilling drive in the stope is 4m and 5m respectively. The ratio of H/(2*W*) of 0.8. Therefore, $(\sigma_h/\sigma_v)\times(2W/H)$ is 0.85 and the modification coefficient for the RMR can be found from Figure 4.3, here the modification coefficient is 1.15.

As a result, the rock mass rating after modification is

$$RMR' = 56.8 \times 1.15 = 65.3$$

A similar modification to the RMR for the crown pillar and draw drive can be made. The result are presented in Table 7.10.

Table 7.10. Modification of rock mass rating in 9 pillar upper stope

No.	Name of excavation	Modification factor	RMR after modification
1	Drill drive	1.15	65.3
2	Crown pillar	0.95	54.0
3	Draw drive	1.1	62.5

(6) Rock load height H_t and rock load P_r

The rock load height H_t and rock load P_r were obtained and the results are presented in Table 7.11.

Table 7.11. Rock load height and rock load in 9 pillar upper stope

No.	Name	H_t (m)	P_r (kN/m)
1	Drill drive	1.75	122.5
2	Crown pillar	6.90	483.0
3	Draw drive	1.87	128.6

(7) Spacing of rock bolts, B_S

To support the openings in 9 pillar upper stope, the spacing of rock bolts was determined using Equation (4.22). Using a factor of safety of 2.0, a friction angle of 31° and a rock load P_r as Table 7.11, the spacings of rock bolts can be found. The results are presented in Table 7.12. It is evident that rock bolts will be used in the drill drive and draw drive and cable bolts in the crown pillar. The bolt patterns designed for this area are typical in Australian underground mines.

Table 7.12. Spacings of rock bolt for openings in 9 pillar upper stope

No.	Name of opening	Design spacing	Yield load of bolts	Length of bolts
1	Drill drive	1.5×1.5 m	60kN	2.3 m
2	Crown pillar*	2.0×2.0 m	160kN	9.0 m
3	Draw drive	1.8×1.8 m	60kN	2.3 m

* Cable bolts used.

2. Design of Cable Bolting for Unstable Wedges

Having designed the pattern of rock bolts used to reinforce the rock mass surrounding the openings, a search for unstable wedges in 9 pillar upper stope was conducted. Further design should be done to obtain a reliable rock bolting system to reinforce potentially unstable wedges. A computer program has been developed to identify these wedges and the procedures and the results are presented below.

The stereographic projection of four major discontinuity sets determined in 9 pillar upper stope can be presented as Figure 7.10. The origin of the coordinate system

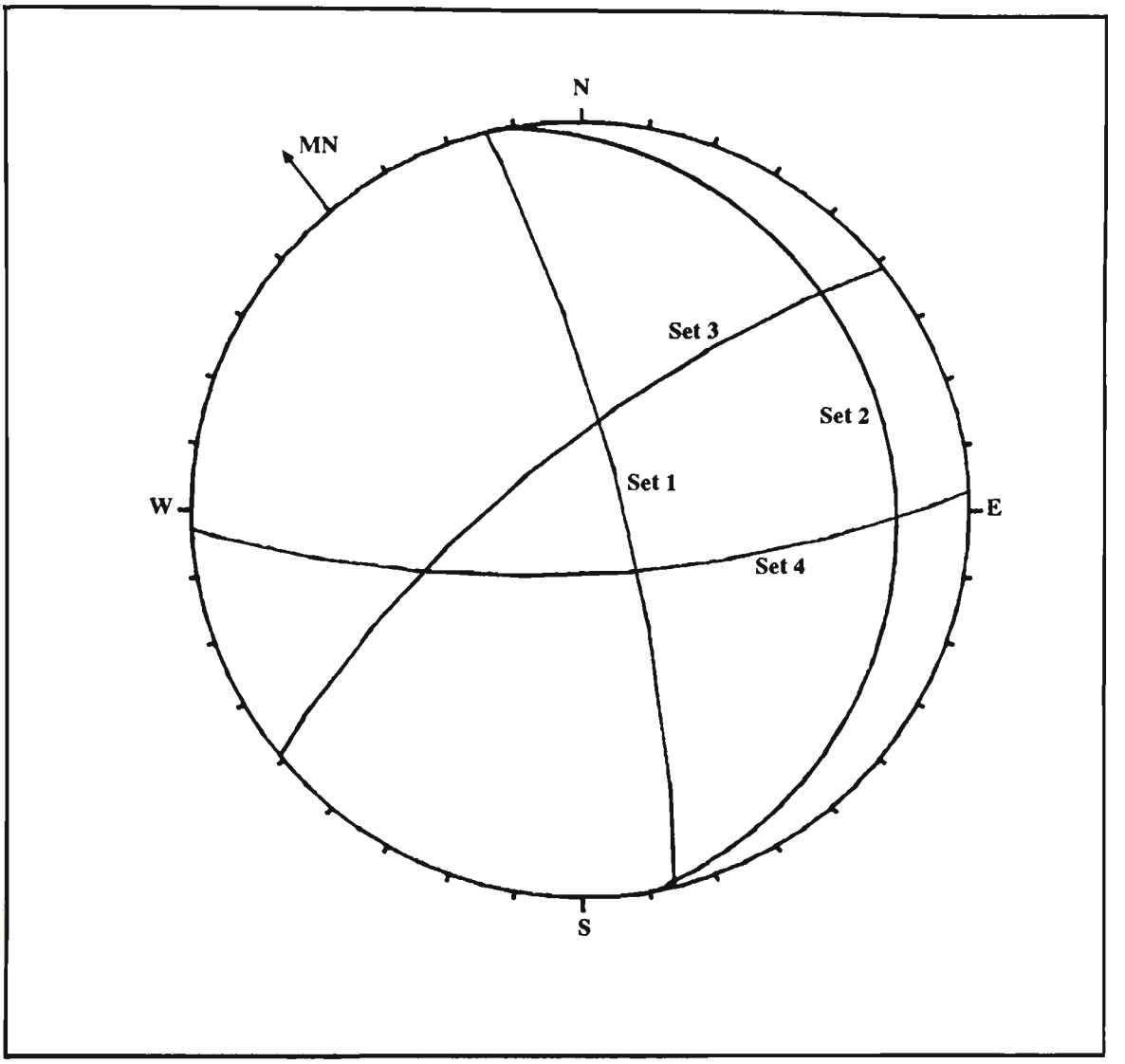

Figure 7.10. Stereoplot of four major discontinuity sets in 9 pillar upper stope

is placed at one end of the opening under consideration; as discussed in Chapter 5. First, a search for polyhedral wedges was conducted followed by a search for tetrahedral wedges. Finally, potentially unstable wedges, both tetrahedral and polyhedral, were identified. The input data for the design of the rock bolting system in 9 pillar upper stope are presented in Table 7.13.

Table 7.13. Input data for rock bolting design in 9 pillar upper stope

No.	Parameter	Value	Comments
1	Total length of scanline	80 m	
2	Radius of small circle	50 mm	
3	Azimuth of opening	*140°, #56°	
4	Shape of opening	rectangular	
5	Height of opening	4 m	
6	Width of opening	*15 m, #5 m	
7	Height of projection level	4 m	
8	Declination of opening	0°	
9	Adjustment of orientation	fair	
10	Bolt type number	1	1=passive; 2=active
11	Tensile strength of bolt	512 MPa	
12	Yield load of bolt	160 kN	
13	Shear strength of bolt	312 MPa	
14	Diameter of bolt	25 mm	
15	Strength of intact rock	116 MPa	
16	Cohesion of rock mass	30 kPa	
17	Friction angle	31°	
18	RQD	97.4%	
19	Spacing of discontinuities	@	
20	Factor of safety for bolt	2.0	
21	Factor of safety for cable	1.5	
22	Unit weight of rocks (kN/m^3)	3.5 (ore) 2.9 (rock)	

* crown pillar; # draw drive and drill drive; @ calculated from scanline data.

The results show that there are polyhedral and tetrahedral wedges formed in the crown pillar. The polyhedral wedges defined by all four discontinuity sets are presented in Table 7.14 and the tetrahedral wedges defined by any three of the four sets in Table 7.15.

Table 7.14. Polyhedral wedges (>10m^3) formed in 9 pillar upper stope

No.	Discontinuity No.	Volume (m^3)	Apex Coordinates	Slide Face
1	1, 48, 70, 86	24.85	-3.20, 9.82, 1.52	48
2	3, 49, 69, 85	17.31	-4.97, 7.84, 1.37	49
3	6, 53, 72, 86	33.84	-5.80, 11.89, 1.60	53
4	10, 53, 72, 87	20.54	-4.54, 14.06, 1.16	53
5	12, 52, 74, 89	13.80	-1.15, 18.21, .85	52
6	13, 57, 74, 88	36.60	-5.36, 18.10, 1.37	57
7	14, 64, 78, 90	140.62	-6.49, 26.05, 2.24	64
8	15, 58, 73, 87	27.34	-7.13, 16.13, 1.25	58
9	16, 54, 79, 93	17.08	2.45, 28.43, 0.77	54
10	17, 59, 79, 92	48.78	-1.39, 28.32, 1.29	59
11	18, 64, 79, 91	97.60	-5.24, 28.22, 1.81	64
12	20, 63, 81, 93	75.44	-2.21, 32.37,1.50	63
13	22, 62, 76, 89	24.70	-6.70, 22.35, 1.01	62
14	23, 58, 82, 95	10.36	2.89, 34.65, 0.54	58
15	24, 61, 78, 91	13.82	-3.67, 26.50, 0.71	61
16	24, 63, 82, 94	40.26	-0.96, 34.54, 1.06	63
17	26, 60, 73, 87	38.40	-7.50, 16.48, 0.23	60

Table 7.15. Tetrahedral wedges (>10 m^3) formed in 9 pillar upper stope

No.	Discontinuity No.	Vol. (m^3)	Apex Coordinates	Slide Face
1	1, 69, 85	17.50	-4.80, 7.76, 1.58	69
2	1, 71, 86	39.03	-5.32, 11.73, 2.06	71
3	3, 72, 87	26.50	-3.90, 13.84, 1.81	72
4	6, 73, 88	17.00	-2.56, 15.98, 1.47	73
5	7, 74, 88	31.76	-4.78, 17.92, 1.93	74
6	9, 75, 89	20.98	-3.36, 20.03, 1.68	75
7	10, 76, 90	15.59	-1.84, 22.10, 1.52	76
8	12, 77, 90	29.62	-4.17, 24.08, 1.88	77
9	14, 78, 91	19.32	-2.74, 26.18, 1.63	78
10	18, 80, 92	23.61	-3.63, 30.27, 1.74	80
11	20, 81, 93	14.85	-2.20, 32.37, 1.49	81
12	22, 82, 93	28.49	-4.53, 34.35, 1.86	82
13	23, 83, 94	21.86	-3.00, 36.42, 1.70	83
16	40, 72, 87	88.2	2.15, 11.76, 7.88	40
17	40, 73, 88	74.54	3.41, 13.92, 7.45	40
18	41, 69, 85	30.54	-0.85, 6.42, 5.53	41
19	42, 75, 89	117.39	3.61, 17.63, 8.67	42
20	44, 74, 88	169.74	3.07, 15.22, 9.81	44
21	46, 77, 90	125.10	2.80, 21.68, 8.86	46
22	48, 79, 91	184.14	3.00, 25.39, 10.0	48
23	49, 80, 92	137.22	3.74, 27.73, 9.14	49
24	51, 81, 93	81.49	3.97, 30.25, 7.68	51
25	52, 82, 93	171.36	3.43, 31.35, 9.84	52
26	60, 73, 87	38.63	-7.5, 16.48, 0.23	60

From Table 7.14 it is evident that the volume of the maximum polyhedral wedge is 140.62 m^3, defined by discontinuities 14, 64, 78 and 90. The coordinates of the apex of this wedge are (-6.49, 26.05, 2.24). If the wedge is reinforced by cables, 14 cables may be required to resist shear failure. Because Z coordinate of the apex is 2.24 m, the wedge can be reinforced by installing a system of short bolts only. The flat dipping discontinuities in set 1 produce a more flattened wedge shape.

The maximum tetrahedral wedge is defined by sets 2, 3 and 4, and has a volume of 184.14 m^3, in which the coordinates of the wedge apex are (3.00, 25.39, 10.0). Obviously this wedge will be unstable if only a systematic rock bolt is installed and it is therefore necessary to place long cables to secure the stability of this potentially unstable wedge. 19 cables are required at a factor of safety of 1.5 to prevent wedge failure.

Although all polyhedral wedges formed in the crown pillar are flat shaped and can be reinforced by systematic bolting, cables must be placed to stabilise the potentially unstable tetrahedral wedges. The tetrahedral wedges numbered 16 to 25 in Table 7.13 will slide into the stope and cables are required to stabilise them. A total volume of 1179 m^3 should be reinforced by 121 cables. The spacing of cable bolts for the crown pillar are 2.2 m. From Tables 7.12 and 7.13 it is obvious that the cables will work to prevent sliding failure.

The probabilistic distributions of the geometry of the wedges in 9 pillar upper stope are shown in Figures 7.11, 7.12 and 7.13. The width of the wedge in the X axis direction follows approximately a normal distribution and the length in the Y axis direction and the height follow a negative exponential distribution. Figure 7.14 presents the distribution of the size of rock wedges and it also follows a negative

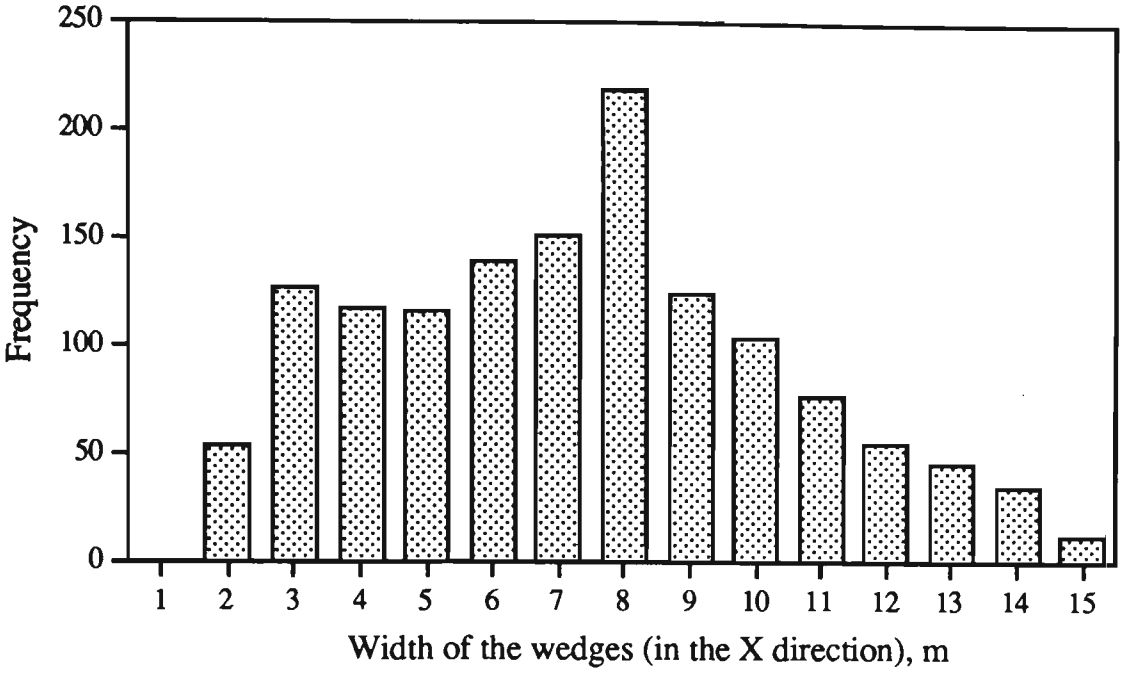

Figure 7.11. Distribution of wedge width in the X direction, 9 pillar upper stope

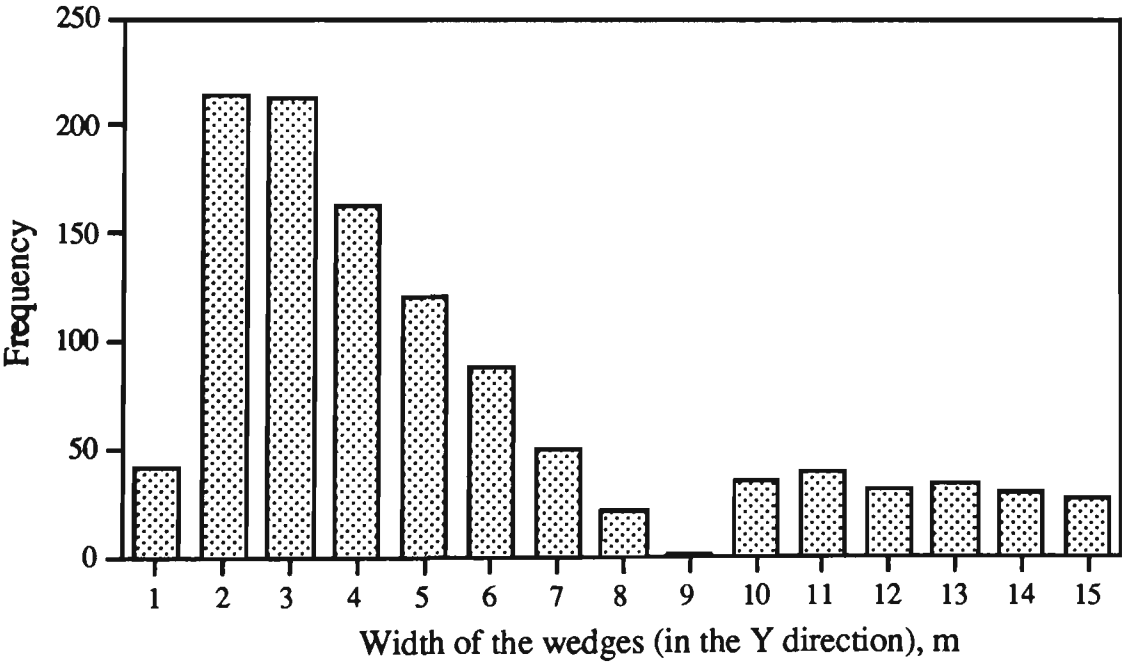

Figure 7.12. Distribution of wedge width in the Y direction, 9 pillar upper stope

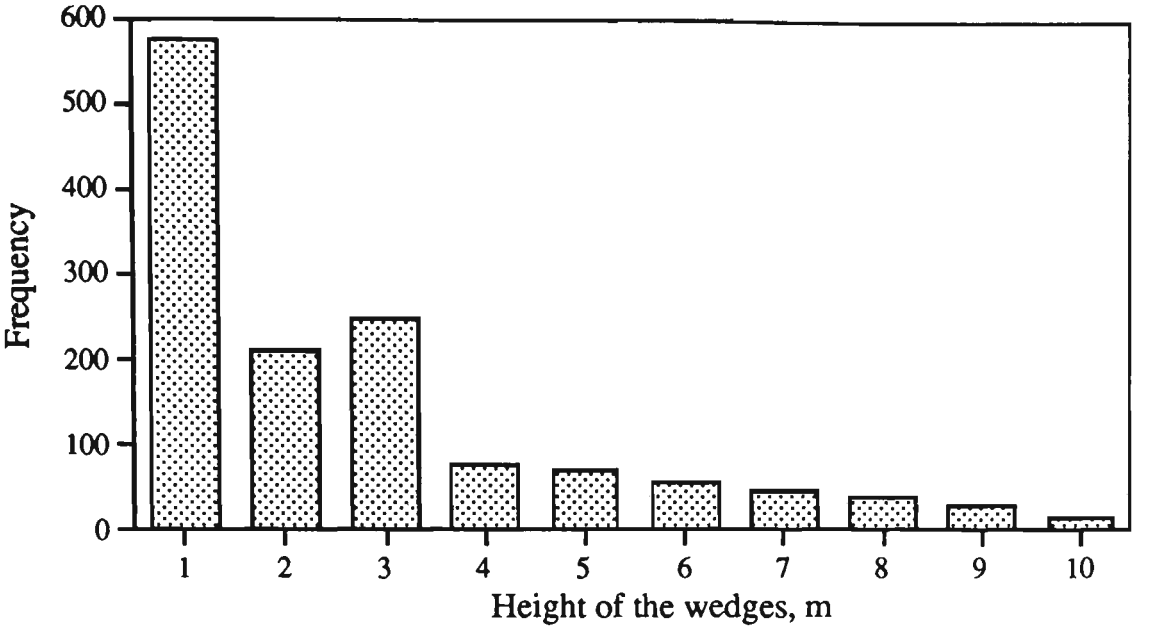

Figure 7.13. Distribution of wedge height in 9 pillar upper stope

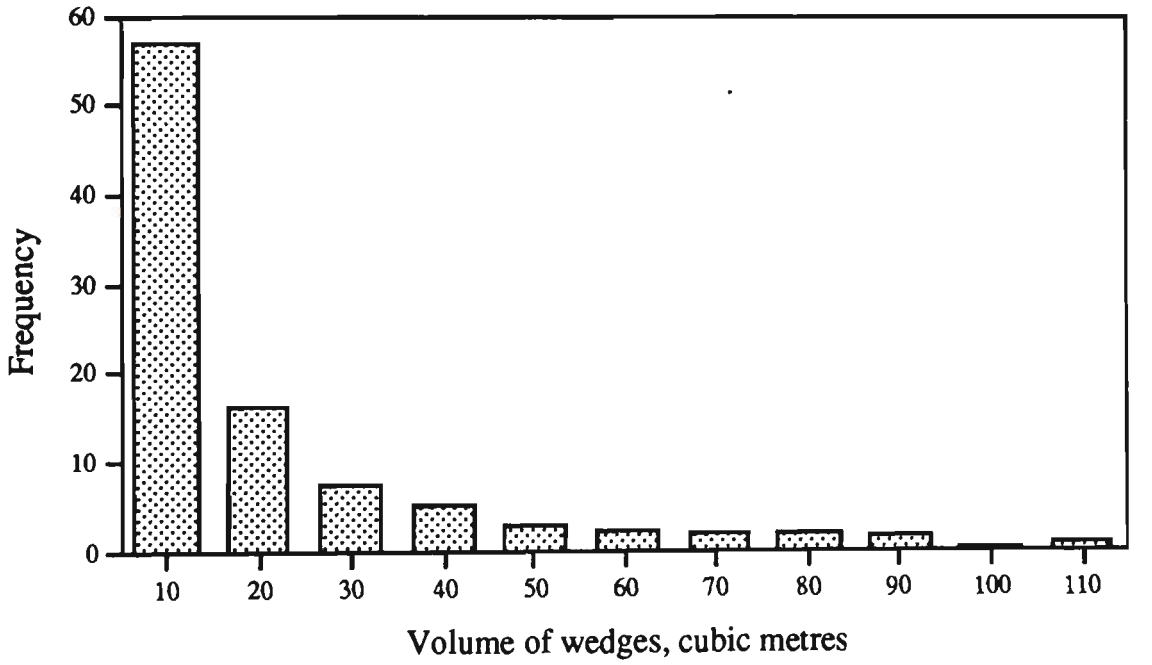

Figure 7.14. Distribution of wedge volumes

distribution. It is evident that the volume of most wedges is less than 20 m^3. Hence if design is based on the mean wedge in the distribution there likely to be a large number of much smaller wedges. This will have some influence on the choice of support elements. Together with consideration of supporting large wedges, smaller wedges which cause most fatal accidents (Vervoort, 1990) should be stabilised as

well. This may involve the use of meshes and W straps. However, this would not be practical in the crown pillar of 9 pillar upper stope.

In the drill drive the volume of the maximum wedge is 7.7 m^3 as shown in Table 7.16, which is significantly smaller than the maximum wedge formed in the crown

Table 7.16. Wedges formed in the drill drive of 9 pillar upper stope

No.	Discontinuity No.	Vol. (m^3)	Apex Coordinate	Slid. Face
1	16,52,75,90	3.62	-.26, 20.38, .41	52
2	28,61,79,92	2.16	-2.4, 28.67, 0.27	61
3	2, 38, 69	2.07	2.5, 8.10, 0.11	38
4	3, 39, 70	2.14	2.5, 10.14, 0.14	39
5	2, 38, 87	2.07	2.5, 7.51, 0.10	38
6	37, 67, 85	2.05	1.23, 3.34, 2.25	37
7	37, 72, 90	7.70	2.5, 14.18,0.12	37
8	41, 69, 86	2.60	.42, 7.40, 2.44	41
9	44, 69, 86	3.27	.61, 7.34, 2.63	44
10	47, 74, 89	7.17	1.05, 17.33, 3.42	47
11	52, 77, 91	3.40	0.98, 23.73, 2.66	52
12	56, 80, 93	2.56	1.41, 29.95, 2.42	56
13	59, 82, 94	5.49	1.10, 33.83, 3.12	59

pillar. This is because the width of the drill drive is one third of the crown pillar. With same orientation, the narrower opening will create smaller wedges, hence, only a systematic rock bolt pattern (no cable bolts) will be required in this opening. In the draw drive, the largest wedge is 11.18 m^3 over an area of 24 m^2, which is defined by sets 2, 3, and 4, as shown in Table 7.17. It is evident that this wedge can be entirely controlled by a systematic rock bolts pattern designed on the basis of

the modified geomechanics classification system. As with the drill drive cable bolts will not be required.

Table 7.17. Wedges formed in the draw drive of 9 pillar upper stope

No.	Discontinuity No.	Vol. (m^3)	Apex Coordinate	Slid. Face
1	4, 63, 90, 94	3.38	-1.5, 11.45, 1.56	63
2	16, 70, 90, 95	2.26	-1.77, 16.31, 1.06	70
3	24, 69, 91	2.65	2.5, 11.71, 0.11	69
4	32, 76, 91	5.64	2.5, 15.62, 0.11	76
5	41, 84, 91	11.18	2.5, 20.08, 0.12	84
6	42, 85, 91	8.43	2.5, 20.64, 0.14	85
7	43, 86, 91	5.69	2.5, 21.20, 0.16	86
8	49, 90, 92	3.10	0.99, 1.69, 2.58	49

7.2.7 DISCUSSIONS

From the modified geomechanics classification system, it is known that the rock mass in 9 pillar upper stope is categorized as fair rock. Also, the results from the wedge analysis indicated that there was a significant risk of wedge failure. To reduce the risk of instability it is necessary to identify the size, shape and location of the wedges, based on the information obtained from the wedge analysis sub-program, and recommend an appropriate cable bolt pattern.

In this situation a systematic pattern of short bolts will not be adequate due to the existence of large potentially unstable wedges. It is proposed that the final design utilise 150 cable arranged as 10 rows with 8 cables in each row and 10 rows with 7 cables in each row at an interval of 2.0 m. The suggested reinforcement for the crown pillar is presented in Figure 7.15. The cables are fully grouted. Systematic

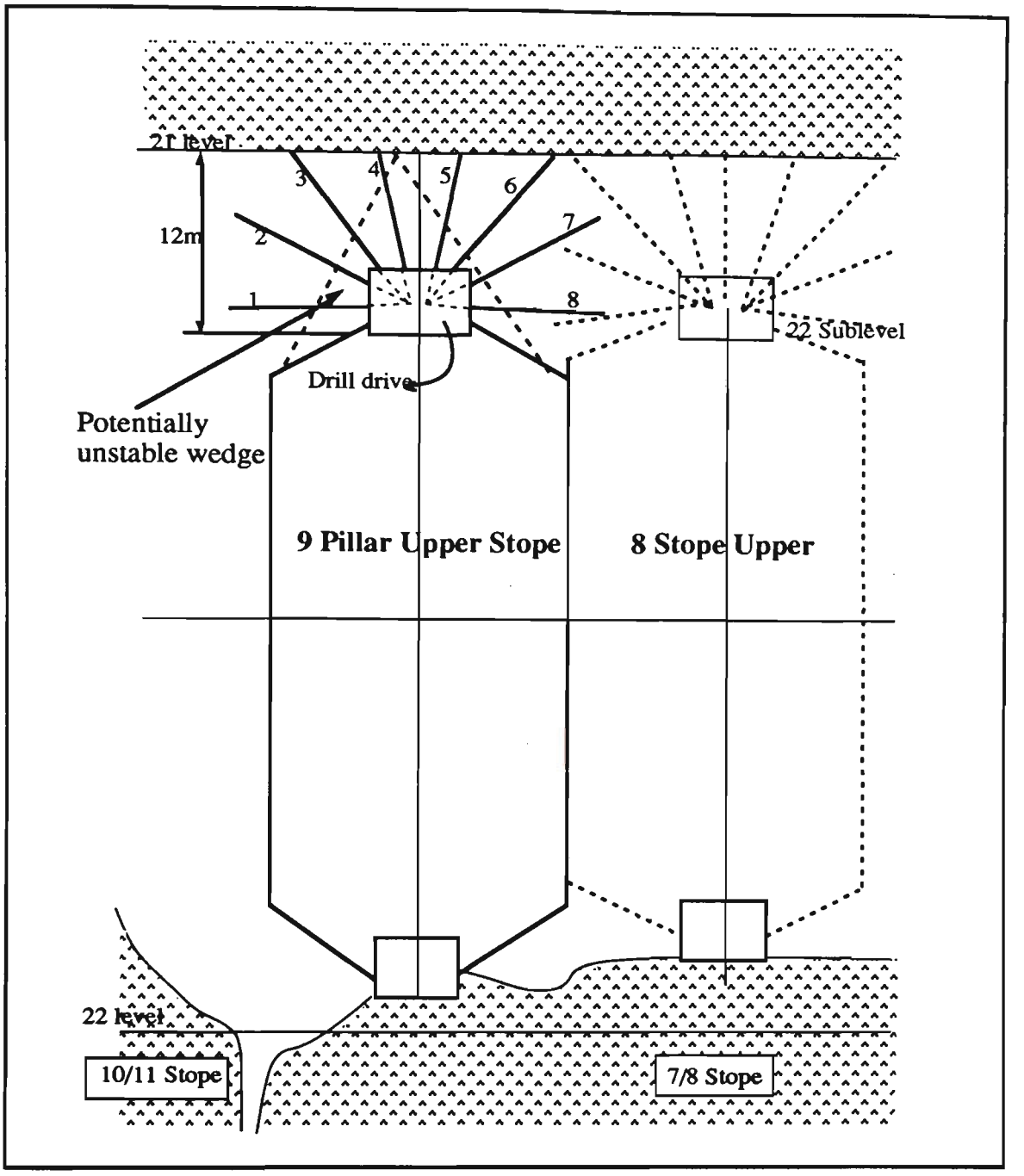

1	2	3	4	5	6	7	8
-5°	20°	55°	80°	80°	55°	25°	-5°
7.5 m	8.0 m	10 m	7.5 m	7.5 m	8.0 m	10 m	7.5 m

Figure 7.15. Design of rock bolting for the crown pillar in 9 pillar upper stope

rock bolt support, with a spacing of 1.5 x 1.5 m, is suggested for the drill drive. However, in draw drive a rock bolt spacing of 1.8 x 1.8 m is proposed. No cables will be needed in either the drill drive or the draw drive.

7.3 DESIGN OF ROCK BOLTING FOR THE CSA MINE, COBAR

The CSA Mine, Cobar, produces copper, lead and zinc concentrates for sale to smelters in Australia and overseas. Mining commenced in the early 1900's in oxidised ore to approximately 180 m below the surface. Both open and cut and fill methods were used. Mining ceased around 1920 and recommenced in 1965 as a mechanised cut and fill operation with inclined ramp access. Due to economic reasons, the mining method changed to open stoping in the 1970's (Price & Fuller, 1979).

7.3.1 Regional Geological Setting

The Cobar mining field located in western N.S.W. (Figure 7.16) contains a number of copper, gold and lead-zinc orebodies in a mineralised belt 80 km long and up to 4 km wide.

The CSA copper-lead-zinc orebodies occurs within the steeply dipping north-south trending shear zones which cut across the sedimentary rocks of the Upper Silurian-Lower Devonian Cobar Group. The CSA Mine lies on a major mineralised tectonic lineament which extends along the western limb of a south plunging anticline. The general dip of the strata is steeply to the west. Country rock within the mine area is overwhelmingly composed of chlorotic and quartzitic siltstone to salty claystone. Sedimentary rocks are altered to a green schist metamorphic grade (Barton, 1977).

The sedimentary country rocks are known as the CSA beds and occupy a position, at the top of the Cobar Group Sequence, between the underlying Cobar slate and the overlying Lower Devonian Amphitheatre Group.

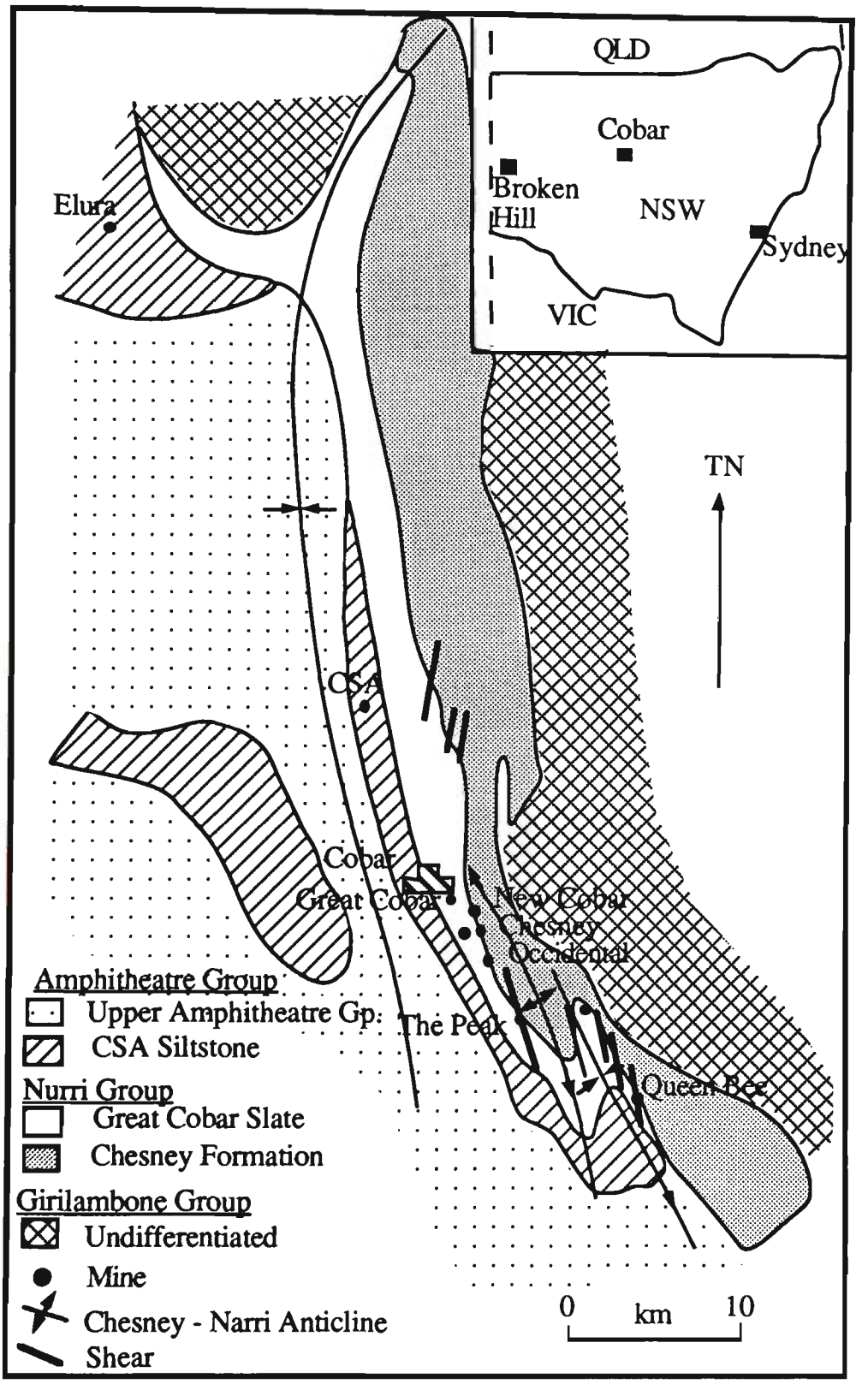

Figure 7.16. Regional geology of the CSA Mine, Cobar

7.3.2 Mine Geology

In general aspect the structure in the mine area is remarkably simple. Bedding generally strikes at 345° N and dips steeply at approximate 80° to the west, as shown in Figure 7.17. Occasional steepening of dip and overturning is evident. In the south-east of the mine the bedding strike generally swings to approximately 330° N. Cylindrical style folds are present in the plat areas of the extreme south east of the mine. The fold axes generally plunge at 70° in a direction of 150° - 160° N, with the axial surface coincident with the cleavage (Barton, 1977). The main cleavage, in common with most shears and ore shoots, trends approximately north-south and dips at 75 -85° E. Mineralisation occurs in a number of vein complexes or sub-massive to massive orebodies, all of which are locally called lenses. There are five main ore systems which all strike roughly north-south and dip steeply to the east, grossly sub parallel to cleavage orientation. Most ore lenses at CSA Mine have a relatively short strike length (rarely exceeding 80 m) and are narrow (6 - 20 m). The vertical dimension is the most continuous (several 100's of meters).

A broad halo of pervasive chlorite alteration surrounds individual lens for up to 50 m laterally (The CSA Mine, 1990). In many cases this is accompanied by a pervasive silicification. The chlorite alteration is predominantly green in colour (Fe - rich) and may only occur as a coating on cleavage surfaces in the outermost part of the halo. A magnesium-rich black chlorite is more intimately associated with certain ore types; as is talc. Later shears containing black chlorite and occasionally talc are common in all mineralised systems, and in some cases form a sharp boundary to the ore lenses. Generally, ore bodies are located within quartz-rich shear zones which strike approximately north-south, dip at 75-85 east and pitch steeply to the north. The separate lenses or shoots are generally lenticular and occur within a 300 - 400 m wide tubular mineralised envelope. Ore 'shoots' are 60 - 120 m long and 12 m wide on average (Barton, 1977).

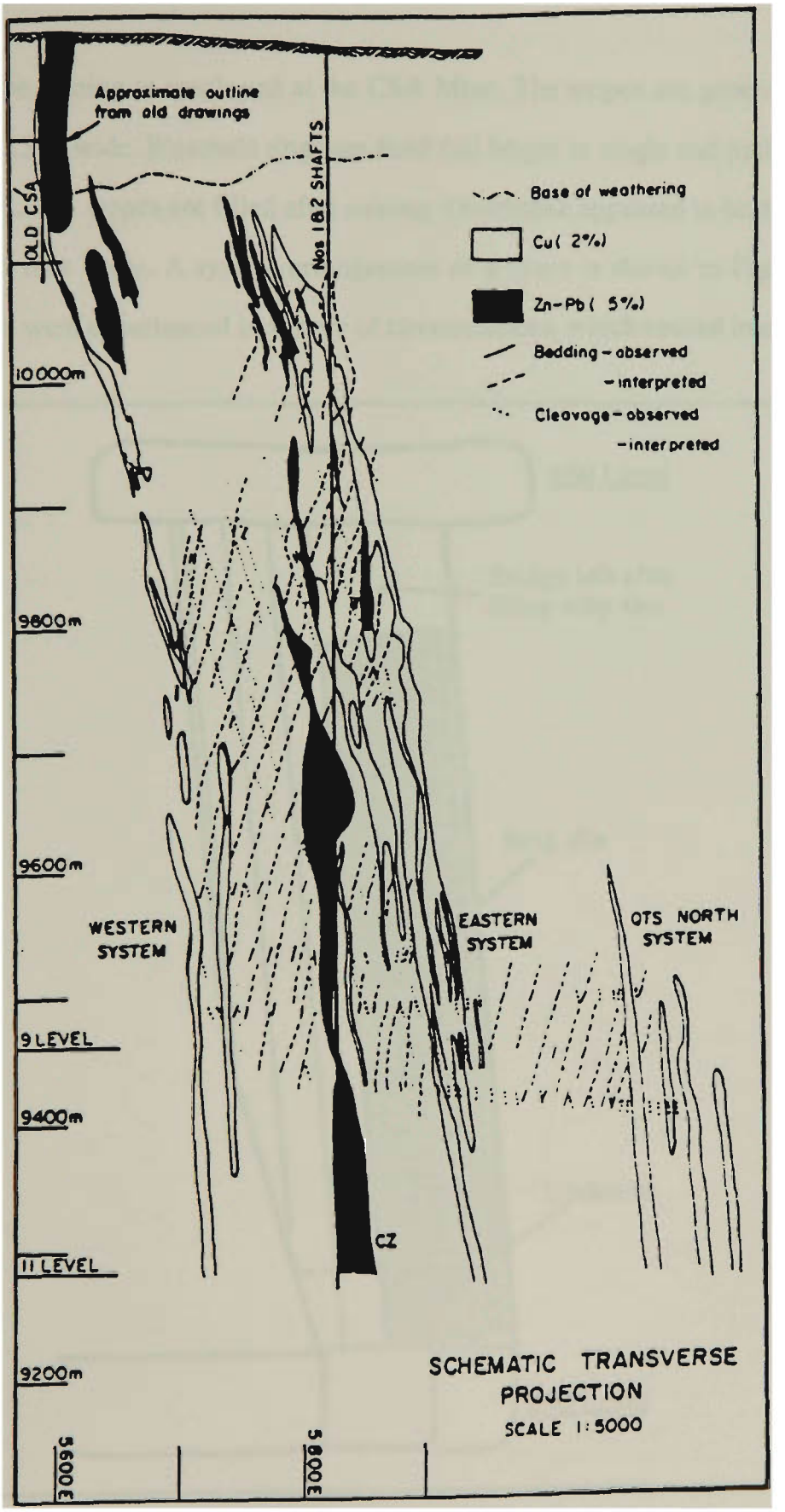

Figure 7.17. Mine geology in the CSA Mine

7.3.3 Mining Method

Open stope mining is employed at the CSA Mine. The stopes are generally 40 m high and 15 m wide. Blasthole rings are fired full height in single and multiple ring sequences. The stopes are filled after mining. Overbreak appeared in both hanging walls and foot walls. A typical arrangement of a stope is shown in Figure 7.18. Rock falls were experienced in variety of circumstances, which caused interruption

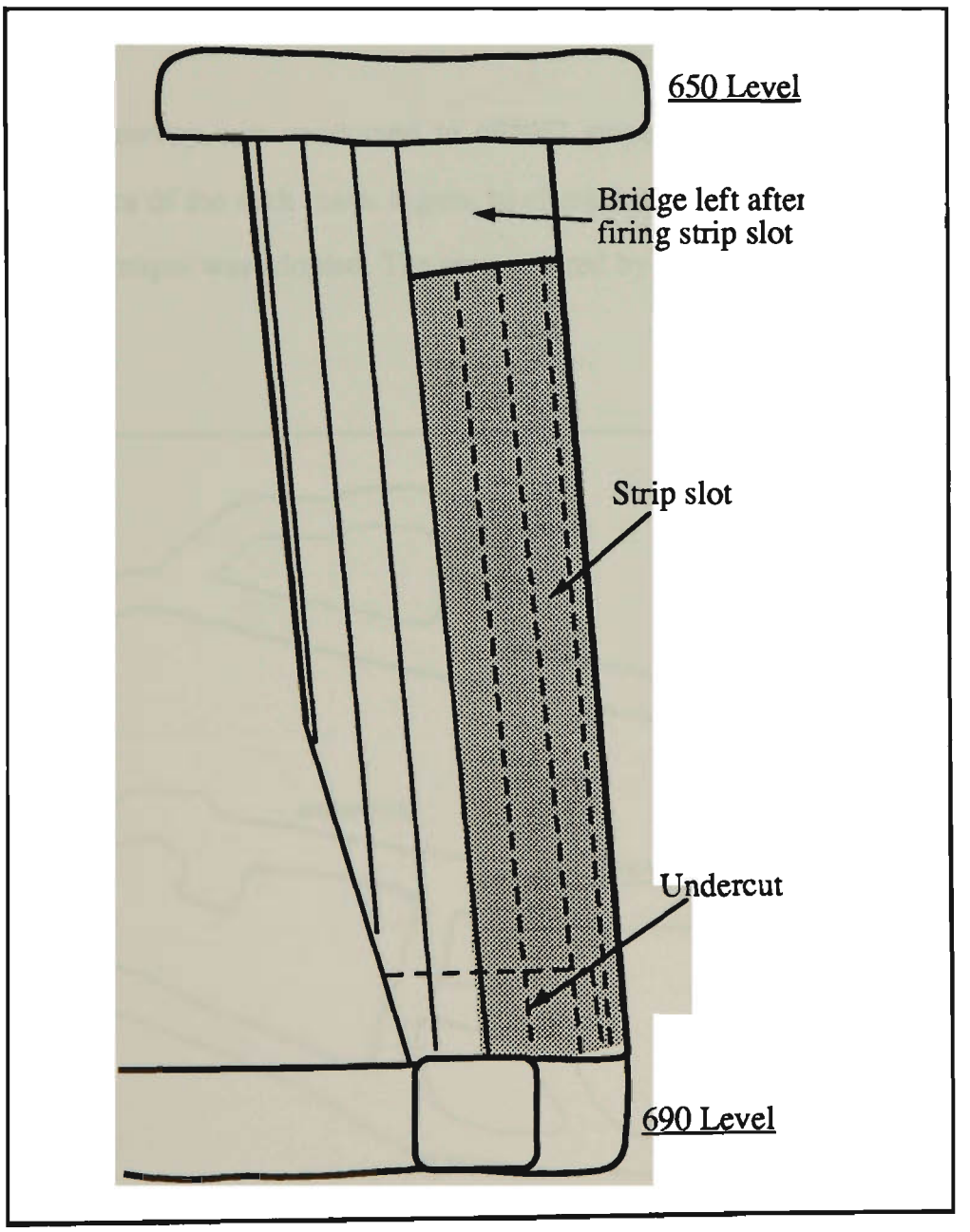

Figure 7.18. Open stop mining in the CSA Mine

of normal operations. This led to a number of of rock mechanics studies to investigate the behaviour of the rock mass surrounding the stopes (Barton, 1977, Price and Fuller, 1979, Worotnicki, 1979, Maconochie et al, 1981, Tavakoli, 1994)). The studies were used to examine the performance of the support elements, determine local conditions and help in the design of an appropriate support system.

7.3.4 Collection and Processing of Geological Data

A scanline survey was conducted in 69NE2 stope to determine the structural characteristics of the rock mass. Again, to eliminate the bias, a three dimensional scanline technique was adopted. The area covered by the survey is shown in Figure 7.19.

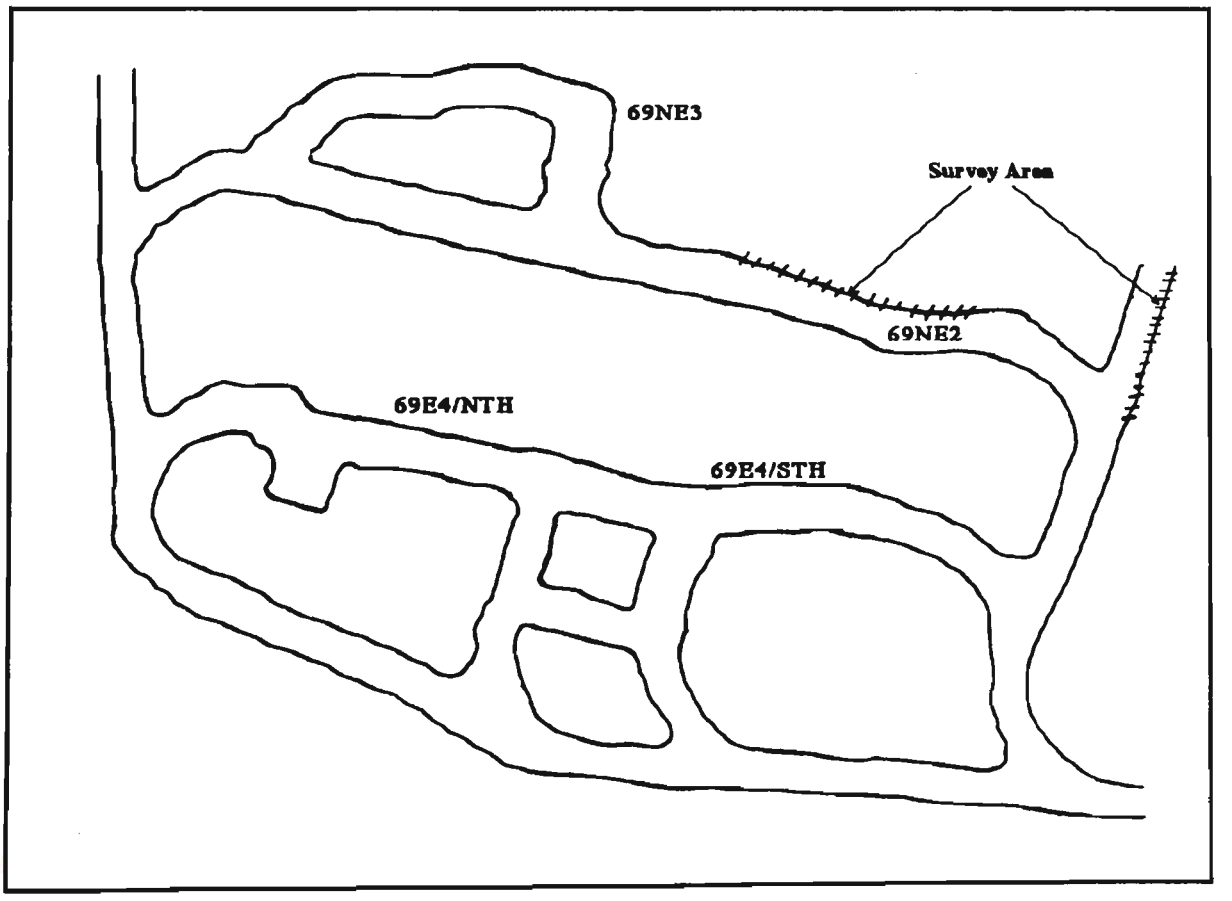

Figure 7.19. Arrangement of scanlines in 69NE2 stope

Structural details for 69NE2 stope were grouped using clustering analysis. The results are presented in Table 7.18.

Table 7.18. Results from clustering analysis in 69NE2 stope

Cluster No. 1							
118/86	125/90	130/85	285/85	286/89	290/86	296/90	332/86
114/80	114/80	115/84	116/80	122/84	138/82	288/84	320/84
118/75	120/79	120/75	132/75	275/75	275/75	288/76	296/76
118/74	141/73	116/67	120/68	122/68	130/68	132/67	145/66
346/68	298/65						
Cluster No. 2							
008/87	066/90	068/89	070/90	073/90	074/86	076/86	078/88
078/90	080/90	082/90	082/86	084/86	089/88	090/87	090/88
090/85	091/90	094/89	094/90	094/87	100/85	100/89	102/85
102/88	104/86	106/89	110/89	230/89	242/85	247/85	248/90
250/85	252/86	258/88	258/86	260/89	260/89	266/88	270/85
270/85	274/90	068/84	068/84	068/84	071/80	074/80	078/83
079/84	083/80	090/82	090/83	092/80	094/82	094/80	096/80
097/84	098/80	098/84	100/80	100/80	102/80	102/82	102/80
106/84	108/82	110/82	242/82	244/80	246/83	250/80	057/76
069/78	072/75	078/76	080/78	084/75	090/79	090/76	090/75
092/78	095/75	098/78	098/76	098/75	100/76	102/78	102/78
102/75	108/77	240/75	242/76	245/75	248/75	248/75	253/75
256/75	259/75	090/72	102/73	104/73	104/71	112/73	112/73
231/72	246/72	250/74	086/70	088/68	088/66	088/66	098/70
100/68	100/68	214/68	216/69	235/66	244/66	210/62	226/63
022/60	062/60	068/60	257/56	230/55			
Cluster No. 3							
260/32	261/32	262/32	262/34	2621/32	264/31	246/29	260/30
260/29	260/30	265/30	265/30	184/20	278/25	032/10	120/12
293/05							

The structures in this area are clustered into three sets. Set 3, which is flatter dipping, is considered to be less important than set 2 in the rock mass make up. However field investigations showed that the flat dipping discontinuities have significant influence on the stability of the rock mass in this mine. Hence this set is taken to be as important as the other two. The ratings for all three discontinuity sets are shown in Table 7.19.

Table 7.19. Rating of three discontinuity sets in 69NE2 stope

No.	Items	1	2	3
1	Water	0.0	0.0	0.0
2	Infilling	9.6	8.4	8.4
3	Waviness	7.5	6.0	6.0
4	Roughness	9.5	9.3	9.3
5	Aperture	0.2	1.0	0.7
6	Type of discontinuity	5.0	5.0	5.0
7	Frequency factor	5.0	20	2.5
8	Continuity factor	10	4.0	4.0
9	Total rating	47.3	53.7	35.7

* Magnetic declination during the field work was -10°.

The major discontinuity sets in 69NE2 stope were determined as Table 7.20.

Table 7.20. The major discontinuity sets in 69NE2 stope

Set No.	1	2	3
Frequency of discontinuity	34	125	17
Dip/Dip direction	86°/084°	85°/121°	24°/260°

The pole distributions and concentrations from the data collected from this area are presented in Figures 7.20 and 7.21.

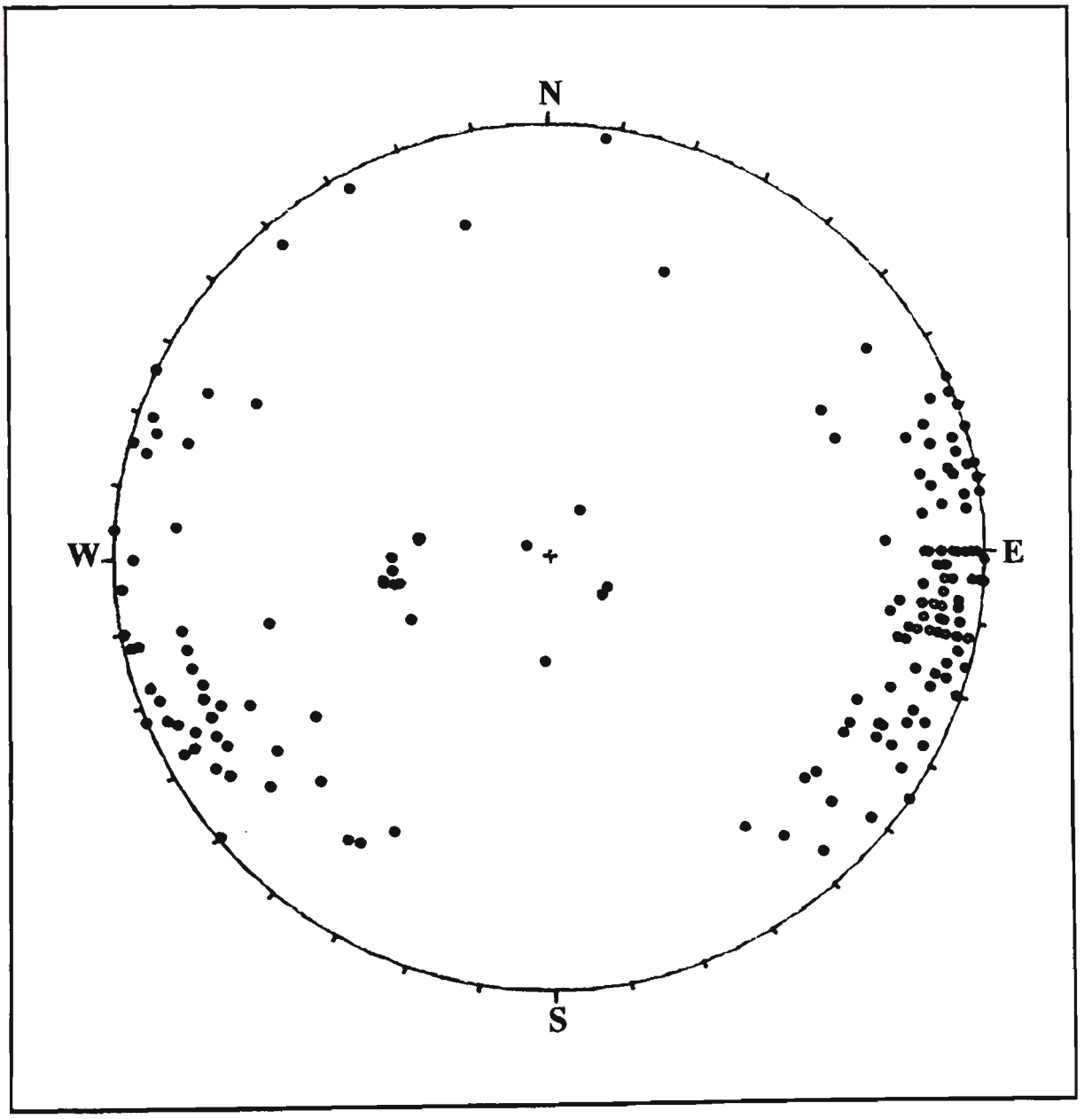

Figure 7.20. Pole distributions at 69NE2 stope

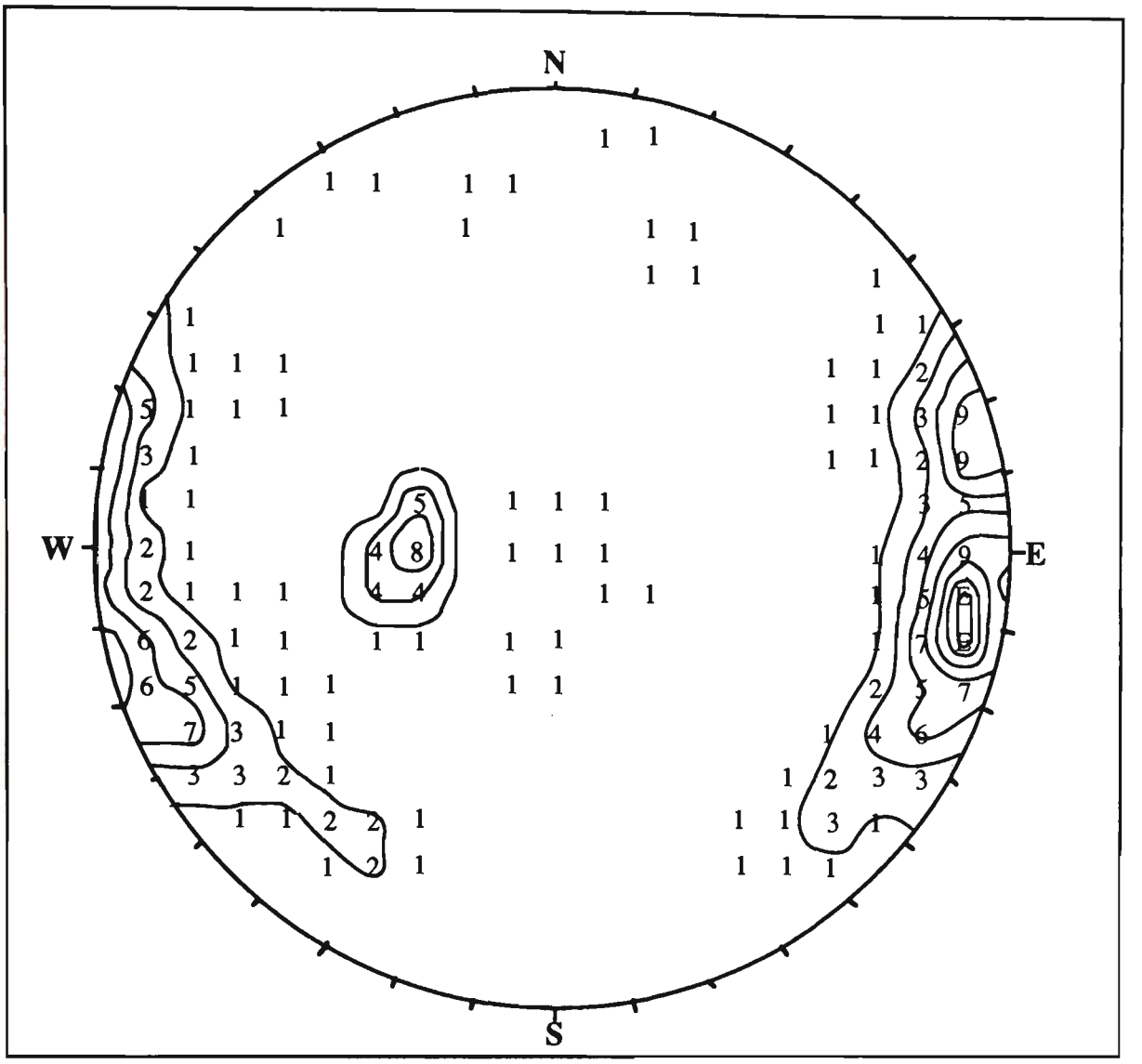

Figure 7.21. Pole concentrations at 69NE2 stope

7.3.5 Design of Rock Bolting System

1. Design Based on the Modified Geomechanics Classification

As for the case study at NBHC Mine, rock bolting design using the modified geomechanics classification system is performed to select a suitable bolting pattern. The procedures used in this section are the same as that used in section 7.2.5. The rock quality designation (RQD) is 90%. The ratings of the rock mass for each parameter are presented in Table 7.21. A total rating of 66.4 is obtained by summing the rating of each parameter.

Table 7.21. Ratings using geomechanics classification in 69NE2 stope

No.	Parameter	Measurement	Rating
1	Strength of intact rock	117 MPa	8.0
2	RQD	90%	20
3	Spacing of discontinuities	.27m	9.2
4	Discontinuity conditions	Class III	20
5	Ground water	Class I	15
6	Adjustment by orientation	IV	-10
7	Total Rating		62.2

A number of stress measurements were made over the depth interval from 250 m to 630 m below surface. The vertical, east-west, and north-south stress components were obtained against depth below surface. The results of the stress studies by Worotnicki and Denham (1976), Worotnicki (1979) and Maconochie et al (1981) are presented in Figures 7.22a, b and c respectively. For the area covered by the

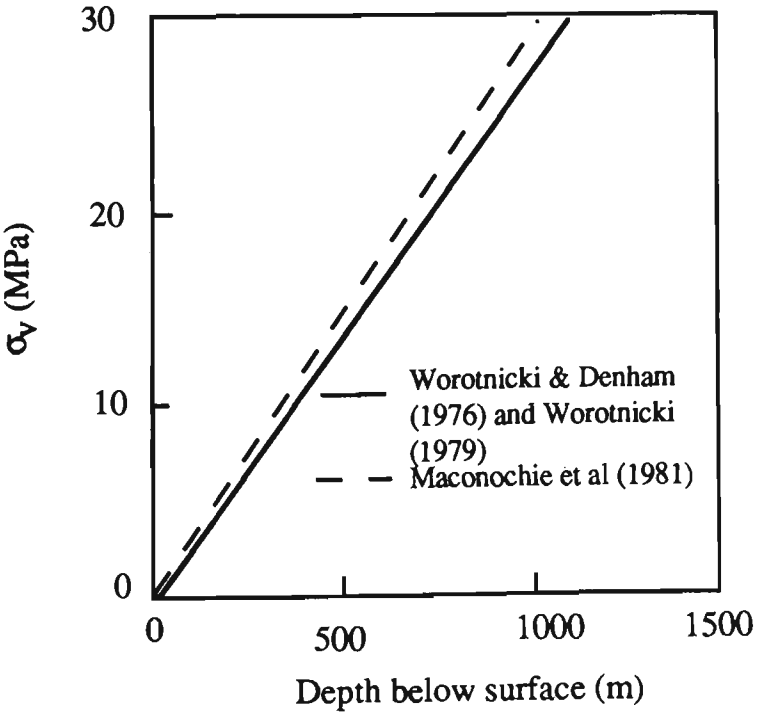

Figure 7.22a. Vertical stress in 69NE2 stope

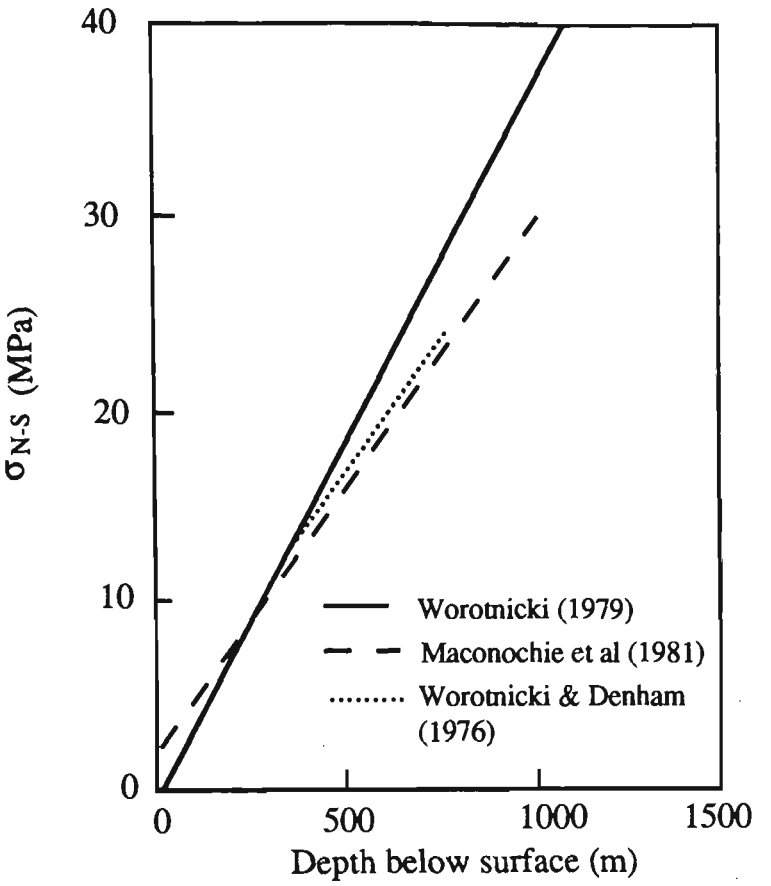

Figure 7.22b. North-South stress in 69NE2 stope

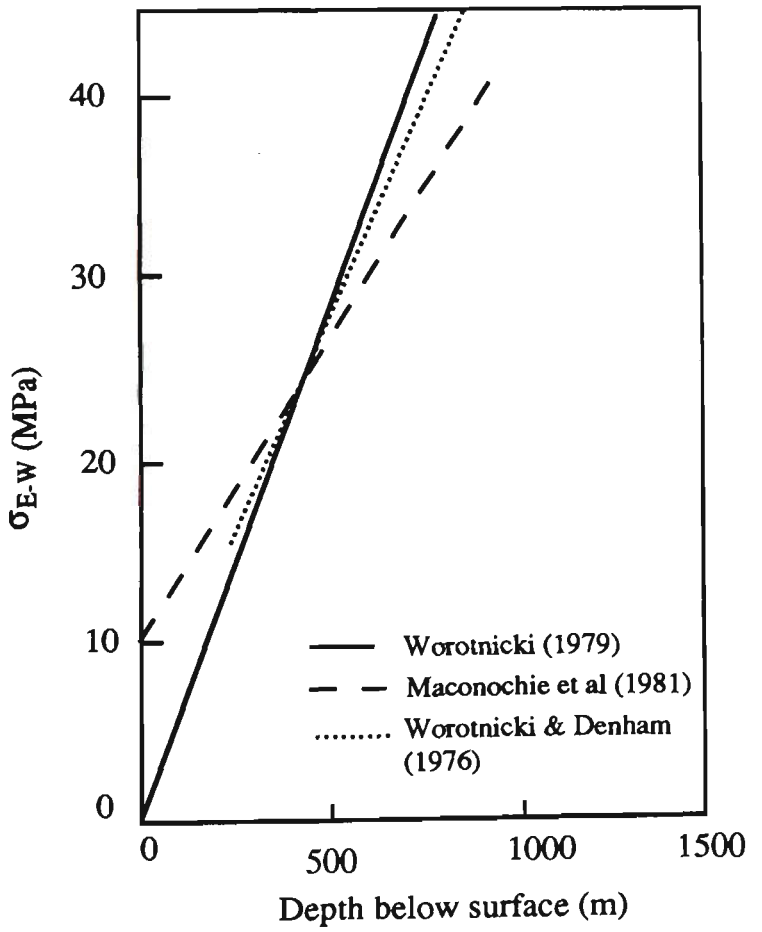

Figure 7.22c. East-West stress in 69NE2 stope

scanline survey, it is reasonable to assume that the in-situ stresses are as presented in Table 7.22.

Table 7.22. In-situ stresses in 69NE2 stope

Vertical Stress	East - West Stress	North - South Stress
17 MPa	36 MPa	22 MPa

In the drill drive the ratio of horizontal stress σ_h to vertical stress σ_v is taken as 2.0. The height (H) and width (2*W*) of the drill drive are 4 m and 5 m respectively, which produces a ratio of H/2*W* of 0.8. Therefore, $(\sigma_h/\sigma_v)\times(H/2W)$ is 1.6. From Figure 4.1 a modification coefficient of 1.15 can be determined, and hence the rock mass rating after modification is $62.1 \times 1.12 = 70.0$.

Similarly the modified rock mass rating of the crown pillar and draw drive can be calculated. The results are present in Table 7.23.

Table 7.23. Modification of rock mass rating in 69NE2 stope

No.	Name of excavation	Modification factor	RMR after modification
1	Drill drive	1.12	70.0
2	Crown pillar	0.70	43.5
3	Draw drive	1.05	65.2

From the value for the modified rock mass rating, other parameters which are used for the design of rock bolting can be found using the equations or diagrams described in Chapter 4. The stand-up time, rock load height H_t and rock load P_r are presented in Table 7.24.

Table 7.24. Stand-up time, H_t and P_r of openings in 69NE2 stope

No.	Term	Excavation		
		Crown Pillar	Drill drive	Draw drive
1	Stand-up time	1 months	12 months	12 months
2	H_t (m)	8.5	1.37	1.73
3	P_r (kN/m)	481.0	77.0	98.9

Therefore, in order to reinforce the openings in 69NE2 a primary system of rock bolts is utilised. The spacing of rock bolts required for the openings in this stope is shown in Table 7.25. To determine if secondary support or modification of the primary support pattern is required wedge analysis must be conducted.

Table 7.25. Design of rock bolts for 69NE2 stope

Excavation	Crown pillar	Drill drive	Draw drive
Design spacing (m)	2.0 × 2.0	Spot bolting	1.8 × 1.8
Yield load of bolts (kN)	200*	60**	60**
Length of bolts (m)	10	2.0	2.3

* cables and ** split sets.

2. Wedge Analysis

A search for tetrahedral rock wedges defined by the three discontinuity sets shown in Figure 7.23 can be carried out using program "ROCKWEDGE". The size of the wedges may be calculated and the cable bolt requirements determined.

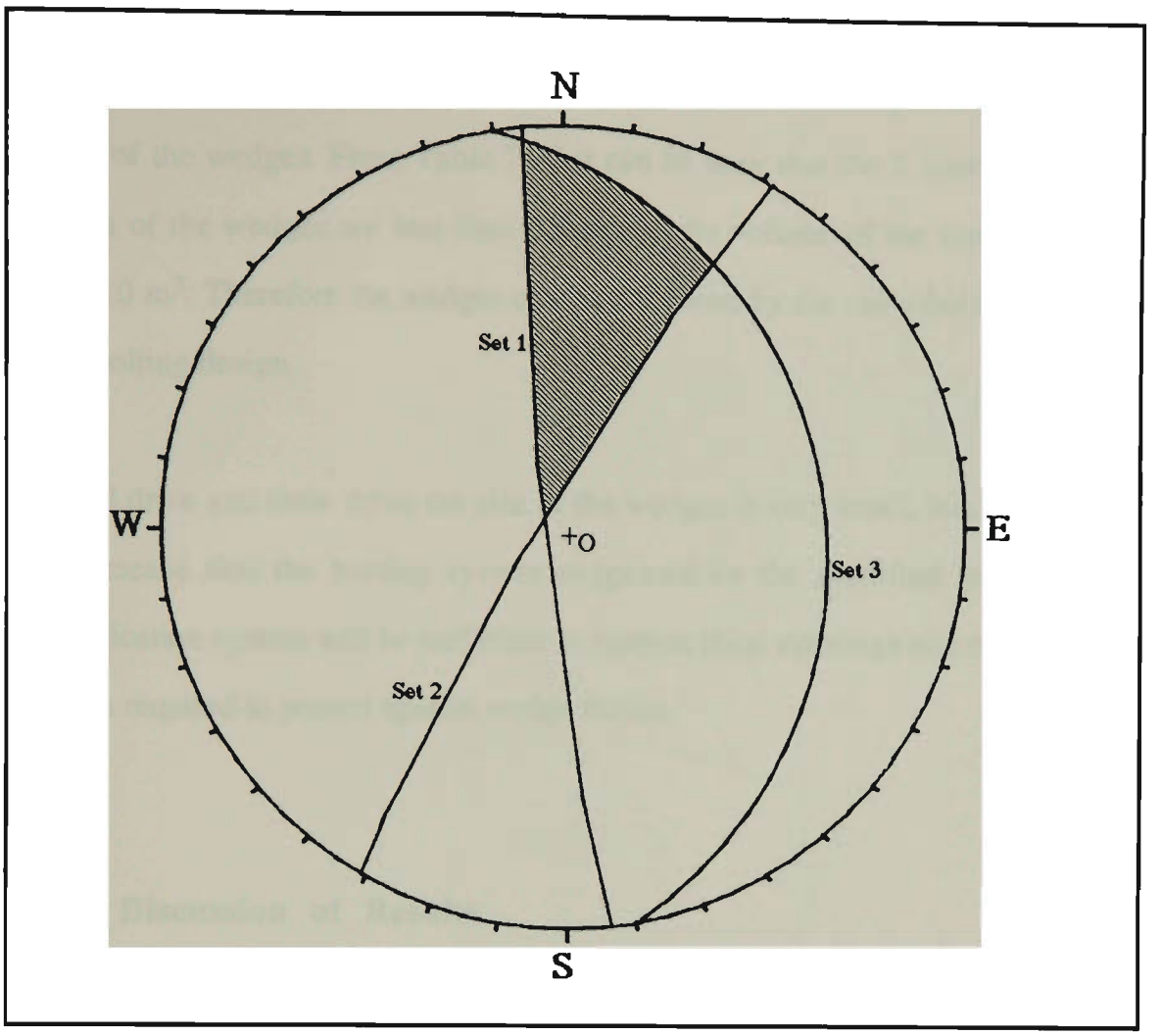

Figure 7.23. Stereoplot of the three major discontinuity sets in 69NE2 stope

The wedges that may be formed in the area of 69NE2 stope are shown in Table 7.26.

Table 7.26. Wedges (>1 m^3) formed in the crown pillar of 69NE2 stope

No.	Discontinuity No.	Vol. (m^3)	Apex Coordinates	Sliding Faces
1	6, 79, 80	1.40	-1.79, 4.63, 0.49	3, 74
2	13, 79, 81	1.08	-1.56, 6.47, 0.45	13, 81
3	14, 79, 81	1.71	-1.53, 6.77, 0.527	14, 81
4	21, 79, 82	1.34	-1.30, 8.58, 0.49	21, 83
5	28, 79, 83	1.03	-1.07, 10.43, 0.44	28, 83
6	36, 79, 84	1.29	-0.81, 12.54, 0.47	36, 84

It is evident that the existence of the flat dipping discontinuity set leads to a flat shape of the wedges. From Table 7.22 it can be seen that the Z coordinate of the apexes of the wedges are less than 0.6 m and the volume of the wedges are less than 2.0 m^3. Therefore the wedges can be stabilised by the cable bolts from initial rock bolting design.

In drill drive and draw drive the size of the wedges is very small, less than 1.0 m^3. This means that the bolting system suggested by the modified geomechanics classification system will be sufficient to support these openings and no cable bolts will be required to protect against wedge failure.

7.3.6 Discussion of Results

As can be seen from Figure 7.19 there are four stopes in close proximity to one another at the 645 NE level. The extraction sequence was scheduled as follows:

- 69NE3;
- 69E4/NTH;
- 69E4/STH; and
- 69NE2.

This scheduling may create stability problem for the extraction of 69NE2 stope. In addition, the existence of three major discontinuity sets lead to a very jointed rock mass in this area. A support system is necessary. The suggested bolting system for the crown pillar of 69NE2 stope is presented in Figure 7.24. The bolting pattern designed for the draw drive is a systematic pattern with a bolt spacing of 1.8 m. No long cables will be required, and however W straps may be necessary to control

small wedges. In the drill drive, spot bolting will be installed in places of potential instability.

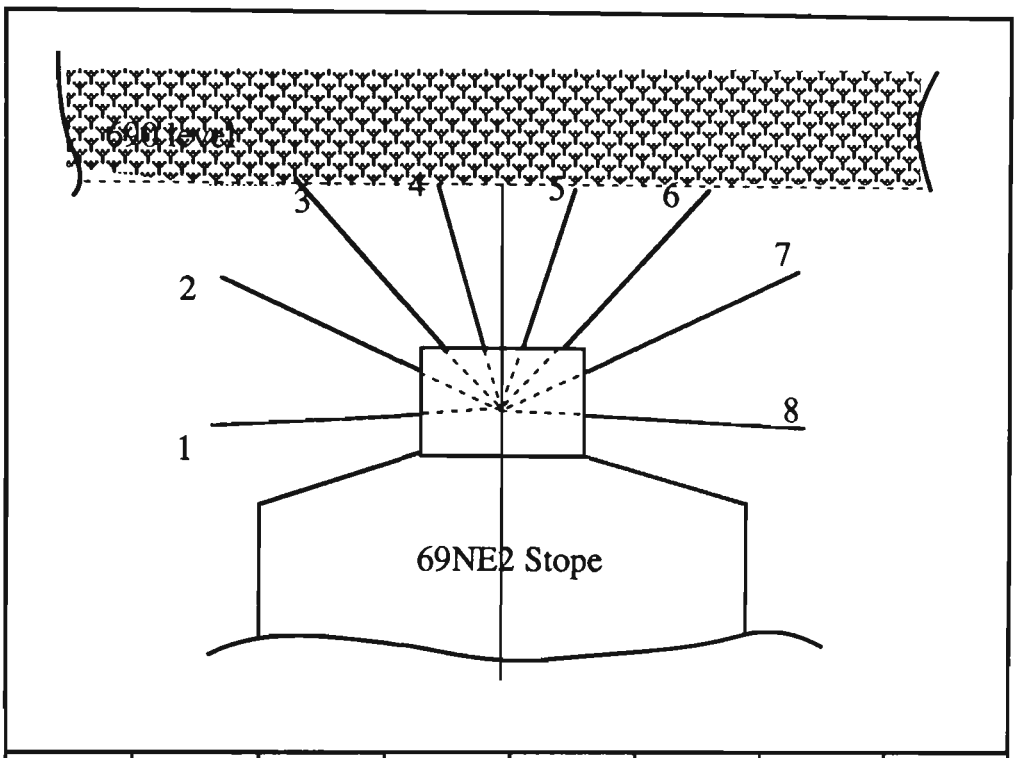

1	2	3	4	5	6	7	8
-5°	30°	45°	75°	75°	45°	30°	-5°
7.5 m	8.0 m	8.0 m	6.5 m	6.5 m	8.0 m	8.0 m	7.5 m

Figure 7.24. Suggested cable bolt pattern for the crown pillar of 69NE2 stope

7.4 CONCLUSIONS

The case studies conducted in the Pasminco Mining Southern Operation, Broken Hill and the CSA Mine, Cobar showed that the proposed method is applicable to rock bolting design in heavily jointed rock masses. The processing of data collected from these two mining sites resulted in the determination of the major discontinuity

sets in these two areas. Four major discontinuity sets were found in 9 pillar upper stope of the NBHC Mine and three in 69NE2 stope of the CSA Mine.

In both these operations it was necessary to identify potentially unstable wedges which may have significant influence on the stability of an underground structure. The size and shape of the wedges are dependent upon the orientation of discontinuities. Discontinuities with a steep dip angle can create large wedges. In contrast, flat dipping discontinuities will create smaller wedges. In addition, the strike direction of the discontinuities also has influence on the size and shape of the wedges. For example in the case of 69NE2 stope in the CSA Mine, as the intersection of the strike lines of two discontinuity sets is a small acute angle small tetrahedral wedges ware formed. It is evident that the wedges in 69NE2 stope are flat-shaped and have a large base area. These wedges are comparatively easy to stabilise and a rock bolting pattern suggested by the modified geomechanics classification system may be sufficient to reinforce the structures. However, it is still important to identify these wedges to ensure that systematic bolting will be adequate.

In the case of 9 pillar upper stope, the NBHC Mine, the size of wedges is comparatively larger. The identification of wedges in this area indicated that the rock bolting system suggested by the modified geomechanics classification system was inadequate and that long cables should be installed to reinforce these wedges.

CHAPTER 8

CONCLUSIONS AND SUGGESTIONS FOR FUTURE RESEARCH

8.1 GENERAL CONCLUSIONS

The computer aided method developed in this study is applicable in dealing with the stability analysis and carrying out rock bolting design for underground structures in jointed rock masses. This method can expediently determine major discontinuity sets in an area of interest, evaluate rock mass quality and carry out rock bolting design. Hence, the stability of an underground structure can be evaluated and accidents caused by roof failure can be minimised. By using this system site engineers can also save a large amount of time when processing vast quantities of geological data.

8.1.1 Applicability in Assessment of Major Discontinuity Sets

This study has shown that geological structures dominate the behaviour of a jointed rock mass. Hence, a detailed geological survey is necessary for complete

design of a rock bolting system. The results from processing the geological data collected from a scanline survey are also essential to assess the quality of a rock mass and to identify potentially unstable wedges.

The field investigations conducted in the Pasminco Mining Southern Operation, Broken Hill, NSW and the CSA Mine, Cobar, NSW show that the geological information obtained from a particular mining area plays an important role in rock bolting design. A three-dimensional scanline technique was used in these studies and it is considered that this technique can eliminate the biases towards certain discontinuity directions which is inherent in a single scanline. The information collected from the above mining areas can be used for assessing the dominant geological structures and the quality of the rock mass. The studies also indicate that clustering analysis is a useful tool for classifying the data points into sets. Where as other systems only consider frequency, the newly developed system considers the characteristics of discontinuities, such as water, waviness, roughness, aperture, type and continuity when determining the dominant discontinuity sets in a geological area. This is a very important consideration, as joint sets, such as the 'flat dipper' at CSA, which a low frequency may have significant influence on stability of the rock mass. Studies in the two mining operations also reveal that the objective function can be used effectively to evaluate the fitness of the results of clustering analysis. Whilst the Bingham's distribution of the data orientations may not be well suited to the situation where the number of data points in the groups in the clustering analysis is insufficient for statistical purpose.

8.1.2 Applicability of Initial Design of Rock Bolting System

The field investigations show that rock failure is principally relevant to geological structures, i.e. discontinuities and the stress field. This research work focused on the influence of discontinuities and the stress field on the stability of a rock mass by assessing the quality of the rock mass and defining potentially unstable wedges and the actual mode of failure. The overall objective of this research was to develop a method of rock bolting design for underground excavation in mining so that hazards to personnel and operational interruptions can be identified, and minimised. This study firstly discussed the geological data required to design a rock bolting system. A modified geomechanics classification system, which considers the dominant discontinuity sets, the local stress field and the geometry of the excavation, was established to assess the quality of the rock mass. Using the modified RMR an initial pattern of rock bolting can be proposed. This pattern may then be adjusted after analysis to determine if there is the potential for unstable wedges to exist.

8.1.3 Evaluation of the Computerised Stereographic Projection Technique in Rock Bolting Design

A computerised stereographic projection technique was developed to identify potentially unstable tetrahedral or polyhedral wedges. The geometric parameters of these wedges was then determined, from which the volume of the wedges was found. This method eliminates the limitations of traditional stereographic projection techniques which can only be used to determine the maximum possible wedge defined by three discontinuity sets in an excavation. Kinematic analysis was carried out to determine the removability of the wedges. If any removable

wedge exists, a bolting pattern which suggests the number of bolts or cables of particular length and installation plunge, to control the wedge is proposed. In the particular case of two-face sliding, the number of bolts required is related to the area of the faces on which the wedge slides. The proposed design method take this into consideration, which makes it particularly suitable for the situation of reinforcing large wedges which consist of a number of small wedges.

The sizes and shape of wedges are heavily dependent upon the dip and the spacing of the discontinuities. Wedges created by steeply dipping discontinuity sets are relatively large and blocky and require more supports. Studies in both the Pasminco Mining Southern Operations, Broken Hill and the CSA Mine, Cobar showed that although flat dipping discontinuity sets have a significant bearing on stability, reinforcing these wedges is comparatively easy due to their flatter shape, i.e. large base area. In these two mines the drill and draw drives are generally require only rock bolts only for supports, but in some cases mesh will be required to control small blocks. The crown pillars must be reinforced by cable bolting installed prior to stoping. The effective thickness of the reinforced crown pillars is 12 m in 9 pillar upper stope in the NBHC mine, and 10 m in 69NE2 stope in the CSA Mine.

8.2 SUGGESTIONS FOR FUTURE RESEARCH

To verify the applicability of the design method to all situations it is necessary to build up a data base to record the application history. This will help to identify any drawbacks in the method, which may lead to improvements of the method. It is impractical at this stage to suggest that the proposed method will be versatile in

every situation due to the complexity of mining conditions and variable geological environments.

It is noted that there are some limitations in using the developed method. First of all, deformation of the wedges is ignored due to the rigidity assumption which may cause some problems in soft rock masses. Solving the problem may involve a study on the deformation behaviour of the rock wedge under a stress field to reveal the interaction between the wedges. Moreover a static loading situation is merely considered in the method. This may lead to an under-design due to the negative influence of dynamic loads generated by blasting or earthquakes on the stability of rock wedges. On some occasions seismic waves are the main cause of for roof collapse, therefore, it is important to understand the behaviour of rock wedges under dynamic loads. In addition, further work should be done to extend the application to more complex mining environments.

REFERENCES

Bao D. and Yang L., 1986; Rock mechanics studies in strip-fill mining in the Xiangxi Gold Mine. Hunan Metallurgy, Vol. 12, No.2, PP1-12.

Barron K. and Larocque E., 1962; Development of a model for mine structures. Proc. Canadian Rock Mechanics Symp., Montreal, PP145-190.

Barton C. M., 1977; A geomechanical analysis of rock structure and fabric in CSA Mine, Cobar, NSW. CSIRO Aust., Division of Applied Geomechanics, Technical Paper No. 24.

Barton N., 1973; A review of the shear strength of filled discontinuities in rock. Fjellsprengningsteknikk, Bergmekanikk, Oslo, Tapir Press, Trondheim, PP19.1-19.38.

Barton N., Lien R. and Lunde J., 1974; Engineering classification of rock masses for the design of tunnel support. Rock Mechanics, Vol. 6, No. 4, PP189 - 236.

Barton N., 1976; Recent experiences with the Q-system of tunnel support design. Proc. of Symp. on Exploration for the Rock Engineering, Johannesburg, Vol. 1, PP107-115.

Barton N. and Choubey V., 1977; The shear strength of rock joints in theory and practice. Rock Mechanics, Springer, Vienna, No. 1/21, PP1-54.

Bawden W. and Milne D., 1987; Geomechanical mine design approach at Noranda Minerals Inc., 6th Int. Congr. on Rock Mechanics, Canada, Vol. 2, PP799-803.

Beer G. and Watson J., 1989; Infinite boundary elements. Int. J. Num. Meth. Engrg., Vol. 28, PP1233-1247.

Bergman Sten A. and Bjurstrom Sten, 1983; Swedish experience of rock bolting - A keynote lecture. Proc. Int. Symp. on Rock Bolting, Abisko, PP243-255.

Bieniawski Z. T. and Van Tonder C. P. G., 1969; A photo-elastic model study of stress distribution and rock fracture around mining excavations. Experimental Mechanics, Vol. 9, PP75-81.

Bieniawski Z. T., 1973; Engineering classification of jointed rock masses. The Civil Engineer in South Africa, Vol. 15, No. 12, PP335-344.

Bieniawski Z. T., 1974; Geomechanics classification of rock masses and its application in tunnelling. Proc. 3rd Int. Congr. on Rock Mechanics, ISRM, Denver, Colo., Vol. IIA, PP27-34.

Bieniawski Z.T., 1976; Rock mass classification in rock engineering. Proc. Symp. on Exploration for Rock Engineering, Johannesburg, Vol. 1, PP97-106.

Bieniawski Z. T., 1976; Rapid site appraisal for dam foundations by the Geomechanics Classification. Proc. 12th Congr. on Large Dams, ICOLD, Mexico City, PP483-501.

Bieniawski Z. T., 1979; Tunnel design by rock mass classifications. U.S. Army Corps of Engineers, Waterways Experiment Station, Technical report, GL-79-10, P133.

Bieniawski Z. T., 1984; Rock Mechanics Design in Mining and Tunnelling. A. A. Balkema.

Bieniawski Z.T., 1991; In search of a design methodology for rock mechanics. Proc. 32nd U.S. Symp. on Rock Mechanics as a Multidisciplinary Science, PP1027-1036.

Bingham C., 1964; Distributions on the sphere and on the projective plane. PhD Dissertation, Yale University. New Haven. P93.

Bischoff J. A. and Smart J. D., 1975; A method of computing a rock reinforcement system which is structurally equivalent to an internal support system. Proc. 16th Symp. on Rock Mechanics, PP179-184.

Bjurstrom S., 1974; Shear strength of hard rock joints reinforced by grouted untensioned bolts. Proc. 3rd Congr. on Rock Mechanics, ISRM, Denver, Vol. II B, PP1194-1199.

Brady B. H. G. and St. John C. M., 1982; The role and credibility of computational methods in engineering rock mechanics. Proc. 23rd U.S. Symp. on Rock Mechanics, AIME, New York, PP571-586.

Bray J. and Goodman R., 1981; The theory of base friction models. Int. J. Rock Mech. Min. Sci. , Vol. 18, No. 6, PP453-469.

Brook N. and Dharmaratne P. G. R., 1985; Simplified rock mass rating system for mine tunnel support. Transactions, Institution of Mining and Metallurgy, Vol 94, PPA148-A154.

Brown E. T., 1981; Putting the NATM into perspective. Tunnel and Tunnelling, Vol. 13, No. 11, PP13-17.

Chio S. K. and Coulthard M., 1990; Modelling of jointed rock masses using distinct element method. Proc. Int. Conf. on Mechanics on Jointed and Faulted Rock. Institute of Mechanics, Technical University of Vienna. PP471-477.

Chio S. K. and Yang J. L., 1991; Computer simulation of rock structural effects for the design of mine pillars. Proc. 2nd Australian Conference on Computer Applications in the Mineral Industry. The University of Wollongong, NSW, PP153-158.

Choquet P. and Charette F., 1988; Applicability of rock mass classifications in the design of rock bolt support in mines. 15th Canadian Rock Mechanics Symposium. Toronto, PP39-48.

Cook N. G. W. and Schumann E. H. R., 1965; An electrical resistance analogue for planning tabular mining excavations. Chamber of Mines Research Report No. 72165, Johannesburg, PP21.

Cording E. J. and Deere D. U., 1972; Rock tunnel supports and field measurements. Proc. 1st North American Rapid Excavation and Tunnelling Conference, AIME, New York, PP601-622.

Cording E. J., Hendron A. J. and Deere D. U., 1972; Rock engineering for underground Caverns. Proc. Symp. on Underground Rock Chambers, Arizona, PP567-600.

Croney P. Legge T. and Dhalla A., 1978; Location of block release mechanisms in tunnels from geological data and the design of associated support. Computer Methods in Tunnel Design. Institute of Civil Engineers. London, PP97-119.

Cruden D. M., 1977; Describing the size of discontinuities. Int. J. Rock Mech. Min. Sci. & Geomech. Abstr., Vol. 14, No. 2, PP133-137.

CSIRO, 1992; Rock stress measurements, Pasminco Mining. Internal Report (CSIRO Report Investigation), PP19-21.

Cundall P. A. and Strack O. D. L., 1979; A discrete numerical model for granular assemblies. Geotechnique, Vol. 29, PP47-65.

Cundall P. A., 1980; UDEC - A generalised distinct element program for modelling jointed rock. Peter Cundall Associates, Report PCAR-1-80.

Cundall P. A., 1988; Formulation of a three-dimensional distinct element model - Part I: A scheme to detect and represent contacts in a system composed of many polyhedral blocks. Int. J. Rock Mech. Min. Sci. & Geomech. Abstr., Vol. 25, PP107-116.

Cundall P. A. and Hart R. D., 1989; Numerical modelling of discontinua. **Keynote** Address, Proc. 1st U.S. Conf. on Discrete Element Methods, Colorado, PP1-17.

Daws G., 1992; The use of the geomechanics rock mass classification system in the design of coal mine roofbolting systems. Geomechanics, Department of Mining Engineering, Nottingham University. PP57-61.

Deere D. U., 1964; Technical description of rock cores for engineering purposes. Rock Mechanics and Engineering Geology, Vol. 1, No. 1, PP17-22.

Everling G., 1964; Model test concerning the interaction of ground and roof support in gate roads. Int. J. Rock Mech. Min. Sci., Vol. 1, PP319-326.

Gaziew E. G. and Lapin L. V., 1983; Passive anchor reaction to shear stress in a rock joint, Proc. Int. Symp. on Rock Bolting, Abisko, PP101−108.

Golser J., 1981; Tunnel design and construction with NATM in weak rock. Proc. Int. Symp. on Weak Rock, Tokyo, Vol. 2, PP933-938.

Goodman R. E. Taylor R. L. and Brekke T. L., 1968; A model for the mechanics of jointed rock. J. Soil Mech. Found. Division, ASCE, Vol. 94, No. 3, PP637-659.

Goodman R. E., 1976; Methods of Geological Engineering. West Publishing Co., St. Paul.

Goodman R. E., and St. John C., 1977; Finite element analysis for discontinuous rocks. Numerical Methods in Geotechnical Engineering (C.S. Desai and J.T. Christian, eds), McGraw-Hill, New York, PP148-155.

Goodman R. E. and Shi G., 1985; Block Theory and Its Application to Rock Engineering. Englewood Cliffs, New Jersey.

Habenicht H., 1983; The anchoring effects - our present knowledge and its shortcomings - A key note lecture. Proc. of Int. Symp. on Rock Bolting, Abisko, PP253 - 268.

Hanna T. M., 1982; Foundation in Tension - Ground Anchors. Trans Book Company, P573.

Hibino S. and Motojinia M., 1983; Behaviour of rocks around large caverns during excavation. Proc. 5th Int. Congr. on Rock Mechanics, Melbourne, Vol. 2, PPD199-D202.

Hobbs D. W., 1968; Scale model studies of strata movement around mine roadways. Int. J. Rock Mech. Min. Sci. Vol. 5, PP219-235.

Hoek E., 1963; Experimental study of rock stress problems in deep level mining. Proc. 1st Congr. on Experimental Mechanics, New York, PP177-193.

Hoek E. and Bray J. W., 1979; Rock Slope Engineering. The Institution of Mining and Metallurgy, London.

Hoek E. and Brown E. T., 1980; Underground Excavations in Rock. The Institution of Mining and Metallurgy, London.

Hoek E., 1986; Practical rock mechanics - developments over the past 25 years. Proc. of the Conf. on Rock Engineering and Excavation in an Urban Environment, Hong Kong, PPix-xvi.

ISRM, 1978; Suggested methods for the quantitative description of discontinuities in rock masses. Int. J. Rock Mech. Min. Sci. & Geomech. Abstr., Vol. 15, PP319-368.

ITASCO Consulting Group INC., 1993; UDEC Manual, Vesion 1.8.

Jacobi O., 1980; The strata control system - retrospect and prospect. Gluckauf Translation, Vol. 116, PP454-460.

Kendorski F. S. and Cummings R. A., 1982; Prediction of caving mine drift deformations. Proc. 1st Int. Conf. on Stability in Underground Mining, University of British Columbia, Vancouver.

Kendorski F. S., Cummings R., Bieniawski Z. and Skinner E., 1983; Rock mass classification for block caving mine drift support. Proc. 5th Int. Congr. on Rock Mechanics, ISRM, Melbourne, PPB101-113.

Krauland N., 1983; Rock bolting and economy. Proc. Int. Symp. on Rock Bolting, Abisko, PP499-507.

Krauland N., Soder P. and Agmalm G., 1989; Determination of rock mass strength by rock mass classification - some experiences and questions from Boliden Mines. Int. J. Rock Mech. Min. Sci. & Geomech. Abstr. Vol. 26, PP115-123.

Lang T. A., 1961; Theory and practice of rock bolting. Trans. AIME, Soc. of Mining Engineers, Vol. 220, PP333-348.

Larsson H., 1984; Modelling of bolt action in jointed rock. Licentiate Thesis, Lulea University, Sweden.

Laubscher D. H. and Taylor H. W., 1976; The importance of geomechanics classification of jointed rock masses in mining operations. Proc. Symp. on Exploration for Rock Engineering, Johannesburg, A A Balkema, Vol. 1, PP119-128.

Laubscher D. H., 1977; Geomechanics classification of jointed rock masses - mining applications. Trans. Institute of Mining and Metallurgy, Vol. 86, PPA1-A8.

Laubscher D. H., 1990; A geomechanics classification system for the rating of rock mass in mine design. J. South African Institute of Mining and Metallurgy. Vol. 90, No. 10, PP257-273.

Lauffer H., 1958; Gebirgsklassifizierung fur den stollenbau. Geologie und Bauwesen, Vol. 24, No. 1, PP46-51.

Lin Y., Li Z., Zhang J. and Wang W., 1985; Dynamic cluster analysis applied to engineering stability classification of rock mass. Proc. Int. Symp. on Mining Technology and Science, China, PP731-736.

Lin Y., 1988; A study of computer engineering classification methods. Proc. 6th Int. Conf. on Numerical Methods in Geomechanics, Innsbruck, Vol. 3, PP1971-1979.

Ludvig B., 1983; Shear test on rock bolts. Proc. Int. Symp. on Rock Bolting, Abisko, PP113-123.

Maconochie D., Friday R. G. and Thompson I. R., 1981; Application of monitoring and numerical modelling in open stope mining. Proc. 4th Australian Tunnelling Conference, Melbourne, PP1-14.

Mark C. A., 1982; A physical model study of coal-mine roof using the base-friction technique. M. Sc. Thesis, The Pennsylvania State University, P139.

Merritt A. H., 1972; Geologic predictions for underground excavations. Proc. 1st North American Rapid Excavation and Tunnelling Conference, AIME, New York, PP115-132.

Nguyen V. U. and Ashworth E. A., 1985; Rock mass classification by fuzzy sets. Proc. 26th U.S. Symp. on Rock Mechanics, PP937-945.

Ord A., Cheung L., Hobbs B. and Blanc D., 1991; Automatic mapping of rock exposures for geotechnical purposes. Proc. 2nd Australian Conference on Computer Applications in the Mineral Industry, PP205-210.

Pahl P. J., 1981; Estimating the mean length of discontinuity traces. Int. J. Rock Mech. Min. Sci. & Geomech. Abstr., Vol. 18, PP221-228.

Panek L., 1962; The combined effects of friction and suspension in bolting bedded mine roof. U. S. Bureau of Mines, RI6139, P31.

Pasminco Mining Broken Hill Operation, 1990; Geological Review. Broken Hill, File No. 1943.

Piteau D., 1970; Geological factors significant to the stability of slopes cut in rock. Symp. on the Theoretical Background to the Planning of Open Pit Mines With Special Reference to Slope Stability, PP33-53.

Price I. and Fuller P., 1979; Case history study - 63E3/1 stope, the CSA Mine, Cobar. Technical Report, Mining Research Associates, P37.

Priest S. D. and Hudson J. A., 1981; Estimation of discontinuity spacing and trace length using scanline surveys. Int. J. Rock Mech. Min. Sci. & Geomech. Abstr., Vol. 18, No. 2, PP183-197.

Priest S., 1985; Hemispherical projection methods in rock mechanics. George Allen & Unwin, London.

Public Works Department, Hong Kong, 1981; Geotechnical Manual (for Slopes). Geotechnical Control Office.

Rabcewicz L. V., 1964; The New Austrian Tunnelling Method. Water Power, Vol. 16, No. 11, PP453-457 (Part 1); Vol. 16, No. 12, PP511-515 (Part 2).

Rabcewicz L. V., 1965; The New Austrian Tunnelling Method. Water Power, Vol. 17, No. 1, PP19-24 (Part 3).

Rabcewicz L. V. and Golser J., 1973; Principles of dimensioning the supporting system for the New Austrian Tunnelling Method. Water Power, Vol. 25, No. 3, PP88-93.

Rabcewicz L. V. and Golser J., 1974; Application of the NATM to the underground works at Tarbelar. Water Power, Vol. 26, No. 9, PP314-321 (Part 1); Vol. 26, No. 10, PP330-335 (Part 2).

Salamon M. D. G. and Oravecz K. I., 1970; The electrical analogue solution for determining the elastic response of strata surrounding tabular mining excavations. Proc. 2nd Int. Congr. on Rock Mechanics, ISRM, Belgrade, PP4-18.

Sakurai S., 1981; Direct strain evaluation technique in construction of underground openings. Proc. 22th U.S. Symp. on Rock Mechanics, MIT, PP278-282.

Sakurai S., 1983; Field measurements for the design of the Washuzan Tunnel in Japan. Proc. 5th Int. Congr. on Rock Mechanics, Melbourne, Vol. 1, PPA215-A218.

Schach R., Garshot K. and Heltzen A. M., 1979; Rock Bolting - A practical handbook. Pergamon Press, New York.

Shanley R. and Mahtab M., 1975; A computer code for analysis of clusters defined on the unit hemisphere. U.S. Bureau of Mines, Information Circular 8671.

Shi G. H., 1977; The stereographic method of stability analysis of rock mass. Scientia Sinica, Vol. XX, No. 3, PP290-296.

Shi G. H., 1982; A geometric method of stability analysis of discontinuity rocks. Scientia Sinica, Vol. XXV, No. 1, PP125-143.

Shi G. H. and Goodman R. E, 1983; Key block bolting. Proc. Int. Symp. on Rock Bolting, Abisko, PP143-165.

Singh R. N., Buddery P. S. and Wells B. T., 1982; Geotechnical investigation and appraisal of ground control practice for roof support design. Proc. 1st Int. Conf. on Stability in Underground Mining, PP396-427.

Singh R. N. and Eksi M., 1987; Empirical design of pillars in gypsum mining using rock mass classification systems. Journal of Mines, Metals & Fuels, Vol. 34, PP16-22.

Singh R. N., Porter I. and Chen D., 1991; Integrated computer aided stability analysis and rock bolting design for underground excavations. Proc. 12th Science & Technology Congress, Turkey, PP245-258.

Smith I. and Spreadborough M. J., 1993; Underground Mining at Pasminco Mining Limited's Broken Hill Southern Operations into the 21st Century. The AUSIMM Bulletin, No. 3, PP57-64.

St. John C. M., Christianson M., Petersen D. L. and Hardy M. P., 1979; Geotechnical analysis of underground mining methods for the copper - nickel ore bodies of N. E. Minnesota. Proc. U.S. 20th Symp. on Rock Mechanics, University of Texas, Austin, PP87-94.

Steffen O., Kerrich J. and Jennings J., 1975; Recent developments in the interpretation of data from joint surveys in rock masses. 6th Reg. Conf. for Africa on Soil Mech. and Found., Vol. II, PP17-26.

Stillborg B., 1986; Professional Users Handbook for Rock Bolting. Series on Rock and Soil Mechanics, Clausthal-Zellerfeld, Germany, Trans Tech.

Stini I., 1950; Tunnelbaugeologie. Springer - Verlag, Vienna, P336.

Sun X., 1983; Grouted bolts used in underground engineering in soft surrounding rock or highly stressed regions. Proc. Int. Symp. on Rock Bolting, Abisko, PP345-351.

Sun Y. and Gu S., 1982; Application of stereographic projection in geomechanics. (in Chinese). Scientific Publisher, China.

Takano A., Kitahara S., Kurosawa H. and Ueno M., 1981; The tunnelling by NATM in squeezing pressure zone and the study on the ground arch around tunnel - As to construction records of Nabetachiyama Tunnel. Proc. Int. Symp. on Weak Rock, Tokyo, PP939-944.

Tavakoli M., 1994; Underground Metal Mine Crown Pillar Stability Analysis. PhD Thesis, University of Wollongong.

Terzaghi K., 1946; Rock defects and loads on tunnel support. Rock Tunnelling with Steel Supports, Editors. R. V. Proctor and T. White, Commercial Shearing Co., Youngstown, Ohio, PP15-99.

The CSA Mine, 1990; Regional geology. Internal Report, the CSA Mine, Cobar.

Tyler D. B., Truman R. and Pine R. J., 1991; Rockbolt support design using a probabilistic method of key block analysis. Proc. 32th U.S. Symp. on Rock Mechanics as a Multidisciplinary Science, PP1037-1046.

Tyler D. B., Truman R. and Pine R. J., 1991; A probabilistic method for the formation of key blocks. Mining Science and Technology, Vol 13, PP145-156.

Unal E., 1983; Design guidelines and roof control standard for coal mine roofs. PhD Thesis, The Pennsylvania University.

Vervoort A., 1990; A statistical analysis of falls of ground in South African collieries. Proc. 9th Int. Conf. on Ground Control in Mining, Morgantown, West Virginia, U.S.A.

Vutukuri V. S. and Hassaini S. M. F., 1991; Assessment of applicability of four empirical strength criteria for intact coal. Proc. 6th Australian - New Zealand Conf. on Geomechanics (Geomechanical Risk Identification, Evaluation and Solutions), PP280-285.

Vutukuri V. S. and Hassaini S. M. F., 1992; A critical review of predictive methods for estimation of compressive strength of pillars. Int. Conf. Reliability, Production and Control in Coal Mines, Wollongong, PP262-271.

Warburton P. M., 1981; Vector stability analysis of an arbitrary polyhedral block with any number of free faces. Int. J. Rock Mech. Min. Sci. & Geomech. Abstr. Vol. 18, PP415-427.

Warburton P. M., 1983; Application of a new computer model for reconstructing blocky rock geometry, analysing single block stability and identifying keystones. Proc. 5th Int. Congr. on Rock Mechanics, Melbourne, Vol. 1, PPF225-F230.

Warburton P. M., 1985; A computer program for reconstructing blocky rock geometry and analysing single block stability. Computer and Geosciences, Vol. 11, PP707-712.

Warburton P. M., 1987; Implications of keystone action for rock bolt support and block theory. Int. J. Rock Mech. Min. Sci. & Geomech. Abstr. Vol. 24, PP283-290.

Wickham G. E., Tiedemann H. R. and Skinner E. H., 1972; Ground support prediction model - RSR concept. Proc. Rapid Excavation and Tunnelling Conf., PP43-64.

Worotnicki G. and Denham D., 1976; The state of stresses in the upper part of the earth's crust in Australia according to measurements in mines and tunnels and from seismic observations. Proc. Symp. on Investigations of Stress in Rock - Advances in Stress Measurement. ISRM, Sydney, PP71-82.

Worotnicki G., 1979; Local stress patterns and variations of stresses with depth at Broken Hill and Cobar, NSW. Bur. Min. Research Symp. on Crust and Upper Mantle of S.E. Aust. Australian National University, Canberra (Abstract Only).

Wullschlager D. and Natan O., 1983; Studies of the composite system of rock mass and non-prestressed grouted rock bolts. Proc. Int. Symp. on Rock Bolting, Abisko, PP75–85.

Yoshimoto K. and Doi Y., 1981; Results of a tunnel excavation by means of NATM. Proc. Int. Symp. on Weak Rock, Tokyo, PP963-968.

Zhang S. and Tong G., 1988; Computerised pole concentration graphs using the Wulff stereographic projection. Int. J. Rock Mech. Min. Sci. Geomech. Abstr., Vol. 25, No. 1, PP45-51.

Zhu W. and Wang P., 1986; The experiment on the reinforcement of rockbolts. Proc. Conf. on Rock Mechanics, Suzhu, (in Chinese).

Zienkiewicz O. C., 1977; The Finite Element Method. McGraw-Hill, London, P785.

BIBLIOGRAPHY

Atkinson T., 1985; Mining research and economics. Mining Technology, Vol. 67, No. 776, PP189-191.

Atkinson T. and Richards M. J., 1988; Developments in longwall mining. Mining Magazine, Vol. 159, No. 3, 4p.

Baczynski N. R. P., 1980; Application of various rock mass classifications to unsupported openings at Mount Isa, Queensland: a case study. Proceedings 3rd Australian - New Zealand Conference on Geomechanics, Wellington, Vol. 2, PP131-138.

Barton N., 1988, Rock mass classification and tunnel reinforcement selection using the Q-System. Rock Classification System for Engineering Purposes, ASTM STP 984, Louis Hirkaldie, Ed., American Society for Testing and Materials, Philadelphia, PP59-88.

Bawden W., Sauriol D. and Germain P., 1989; Practical rock engineering stope design case histories from Noranda Minerals Inc. CIM Bulletin, Vol. 82, No. 927, PP37-45.

Bieniawski Z. T., 1992; Principles of engineering design for rock mechanics. Pro. 33rd U.S. Symp. on Rock Mechanics, Rotterdam, PP1031-1040.

Brady B. H. G. and Brown E. T., 1985; Rock mechanics for underground mining. George Allen & Unwin, London.

Brown E. T. and Windsor C. R., 1990; Near surface in situ stresses in Australia and their influence on underground construction. Proc. 7th Australian Tunnelling Conf., Sydney, PP18-48.

Brown E. T., 1992; Australian mining geomechanics - development, achievements and challenges. Western Australian Conference on Geomechanics in Mining, Kalgoorlie, Western Australia, PP1-13.

Bulitchev N. S. and Kolin D. I., 1983; Theoretical aspects of rockbolt system and rock massif interaction. Proc. Int. Symp. on Rock Bolting, Abisko, PP109-112.

Chio S. K., Wold M. B., Crotty Sission J. M. and Lee M.F., 1991; 3-dimensional analysis of underground excavations -two new programs applied to a mining problem. Proceedings of 2nd Conference on Computer Methods and Advances in Geomechanics, Cairns.

Desouza E. M. and Archibald J. F., 1987; Rock classification as an influence in mine design operation. Mining Science & Technology, Vol. 6, No. 1, PP1-8.

Dhar B., Ratan S. Reddi H. and Mehta R., 1983; Laboratory study for the design of optimum rock-bolting in bedded strata. Proc. of Int. Symp. on Rock Bolting, Abisko, PP219-223.

Dight P. M. and Fry P. J., 1992; Support in underground drifts. Western Australian Conference on Geomechanics in Mining, Kalgoorlie, Western Australia, PP67-75.

Everling G., 1985; The West German strata control system and its application in mining. Proc. Int. Symp. on Mining Technology and Science, PP3-15.

Fuller P. G., 1983; The potential for cable support of open stopes. Proc. 5th Int. Congress of Rock Mechanics, Melbourne, PPD39-D44.

Gale W. J. and Blackwood R. L., 1986; Design consideration for reinforcement of coal mine roadways in the Illawarra coal measures. Ground Movement and Control Related to Coal Mining Symposium, Wollongong, PP89-92.

Gale W. J. and Blackwood R. L., 1987; Stress distributions and rock failure around coal mine roadways. Int. J. Rock Mech. Min. Sci. & Geomech. Abstr. Vol. 24, No.3, PP165-173.

Gale W. J., 1991; Strata control utilising rock reinforcement techniques and stress control methods, in Australian coal mines. Mining Engineer, Institution of Mining Engineering, Vol. 150, No. 352, PP247-253.

Herget G., 1982; Probabilistic slope design for open pit mines. Rock Mechanics, Supplement, Vol. 12. PP163-178.

Herget G., 1988; Stress in rock. A.A. Balkema, Rotterdam, P197.

Houghton D. A., 1976; The role of rock quality indices in the assessment of rock masses. Proc. Symp. on Exploration for Rock Engineering, Vol. 1, PP129-135.

Hutchins W. R., Bywater S., Thompson A. and Windsor C. R., 1990; A versatile grouted cable dowel reinforcing system for rock. Proc. Australian Institute of Mining and Metallurgy. 295: PP25-29.

Indraratna B. and Kaiser P. K., 1990; Design for grouted rock bolts based on the convergence control method. Int. J. Rock Mech. Min. Sci. & Geomech. Abstr., Vol. 27, No. 4, 1990, PP269-281.

Indraratna B. and Kaiser P. K., 1990; Analytical model for the design of grouted rock bolts. Int. J. for Numerical and Analytical Methods in Geomechanics, Vol. 14, PP227-251.

Jaeger J. C. and Cook N. G. W., 1979; Fundamentals of rock mechanics. 3rd edition, Chapman and Hall, London, P593.

Jeremic M. L., 1979; Ground Mechanics in Hard Rock Mining. Rotterdam.

Khair A. W., 1983; Physical and analytical modelling of the behaviour of truss bolted mine roof. Proc. Int. Symp. on Rock Bolting, Abisko, PP125-142.

Laubscher D. H., 1984; Design aspects and effectiveness of support system in different mining conditions. Trans. Inst. Min. Metall., Section A, Vol. 93, PA70-A81.

Lokin P., Nijajilovic R. and Vasic M., 1983; An approach to rock mass classification for underground works. Proc. 5th Int. Congr. on Rock Mechanics, Melbourne, Vol. 1, PPB87-B92.

Londe P. and Bonazzi D., 1974; Reinforced rock. Proc. 3rd Congr. on Rock Mechanics, ISRM, Denver, Vol. 2, PP1208-1211.

Lucus J. M., 1980; A general stereographic method for determining the possible mode of failure of any tetrahedral rock wedge. Int. J. Rock Mech. Min. Sci. & Geomech. Abstr. Vol. 17, No.1, PP57-61.

Nakao K., Lihoshi S. and Koyama S., 1983; Statistical reconsideration on the parameters for geomechanics classification. Proc. 5th Int. Congr. on Rock Mechanics, Melbourne, Vol. 1, PPB13-B16.

Shapiro A. and Delport J., 1991; Statistical analysis of jointed rock data. Int. J. Rock Mech. Min. Sci. & Geomech. Abstr., Vol. 28, No. 5, PP375-382.

Sheorey P. R., 1991; Experiences with application of the NGI classification to coal measures. Int. J. Rock Mech. Min. Sci. & Geomech. Abstr. Vol. 28, No. 1, PP27-33.

Shi G. H. and Goodman R. E., 1981; A new concept for support of underground and surface excavations in discontinuous rocks based on a keystone principle. Proc. 22nd U.S. Symp. on Rock Mechanics. Massachusetts Institute of Technology, Cambridge, Massachusetts, PP290-296.

Shi G. H. and Goodman R. E., 1989; The key blocks of unrolled joint traces in developed maps of tunnel walls. Int. J. Num. & Anal. Methods in Geomech., Vol. 13, PP131-148.

Singh R. N. and Buddery P. S., 1983; An assessment of the efficiency of roofbolt anchorage based on laboratory and field experimentation. Proc. Int. Symp. on Rock Bolting, Abisko, PP445-456.

Sinha R. S. and Schoeman K. D., 1983; Rock tunnels and rock reinforcement. Proc. Int. Symp. on Rock Bolting, Abisko, PP333-344.

Smaniotto L., Solomons S. S. and Tillman V. H., 1981; The evolution in design of longhole open stoping at the Zinc Cooperation Limited/New Broken Hill Consolidated Limited with particular reference to sloped wall mining. Design and Operation of Caving and Sublevel Stoping Mines, Editor D. R. Stewart, PP547-558.

Stacey T. R., 1986; Practical Handbook for Underground Rock Mechanics. Trans. Tech. Publication.

Stimpson B., 1970; Modelling materials for engineering rock mechanics. Int. J. Rock Mech. & Min. Sci., Vol. 7, PP77-121.

Stimpson B., 1983; The Influence of rock bolt location on the reinforcement of horizontally bedded roofs by full column grouted bolts. Proc. Int. Symp. on Rock Bolting, Abisko, PP195-204.

Terzaghi K., 1965, Sources of error in joint surveys. Geotechnique, Vol. 15, PP287-304.

Trueman R. and Tyler D. B., 1992; Hardrock excavation support design using a probabilistic key block and associated risk analysis. Western Australian Conference on Geomechanics in Mining, Kalgoorlie, Western Australia, PP143-148.

Unal E. and Ergur K., 1990; PC based modelling of rock reinforcement requirements in mine roadways. Rock Mechanics Contribution and Challenges, Proc. 31th U.S. Symp. on Rock Mechanics, Colorado, PP761-767.

Vutukuri V. S. and Katsuyama K., 1994; Introduction to Rock Mechanics. Industrial Publishing & Consulting, Inc., Tokyo.

Xu D., Chowdhury R. N. and Chen D., 1991; A computer system for clustering analysis. Proc. 2nd Australian Conf. on Computer Applications in the Mineral Industry, Wollongong, Australia, PP137-145.

Young D. S. and Hoerger S. F., 1990; Probabilistic prediction of keyblock occurrences. Proc. 31st U.S. Symp. on Rock Mechanics, PP229-236.

APPENDIX-1

RESULTS OF SCANLINE SURVEY FROM THE PASMINCO MINING SOUTHERN OPERATION, NBHC

Location: The 9 pillar upper stope

Data: 21/10/91

Rock Type: 2-Lens Lead Lode

Gangue minerals: calcite, rhodonite

Scanline Orientation: S140°E (horizontal)

No.	D(m)	L (m)	T	Orientation	C	R	Comments
1	0.40	0.41	SL.	322/24	1	3	2-7-1-1
2	0.42	OOR	OOR	150/75	2	3	2-6-8-1 Q
3	0.95	4.00	A	145/85	2	3	2-7-1-1
4	1.30	OOR	A	136/84			
5	1.62	4.00	A	141/76	2	3	2-6-1-1
6	2.00	OOR	OOR	350/74	2	3	2-6-8-1
7	2.30	0.50	A	144/68	2	3	2-6-8-1
8	2.50	1.00	A	141/80	5	3	2-6-8-1
9	2.95	OOR	OOR	134/84	2	3	2-4-8-1
10	3.15	0.40	A	126/50	4	3	2-7-1-8
11	3.50	OOR	OOR	315/90	3	3	2-7-1-1
12	4.50	OOR	OOR	140/89	4	3	2-7-1-1
13	4.88	-	-	-	-	-	ORE
14	6.10	0.50	A	136/45	4	4	2-7-1-1
15	7.17	0.30	A	293/75	3	2	2-7-1-1
16	7.30	OOR	OOR	304/80	2	3	2-3-8-1 Q
17	7.49	0.30	I	298/82	2	2	2-7-1-1
18	9.34	OOR	O	316/15	2	3	2-6-8-1 Q
19	9.95	0.70	I	294/08	2	3	2-7-1-1

* OOR = out of ore; A = terminate at another discontinuity; I = terminate in rock material; O = obscured or extending past exposure; Q = quartz.

20	0.00	OOR	O	232/20	2	3	2-5-8-1 Q
21	0.10	0.40	A	205/69	2	3	2-7-1-1
22	0.55	0.45	A	266/38	2	3	2-7-1-1
23	0.90	OOR	O	055/20	2	3	2-5-8-1 Q
24	1.50	-	-	108/42	2	3	
25	1.76	0.80	A	048/67	2	3	2-5-8-1
26	2.00	0.38	A	045/72	2	3	2-7-1-1
27	2.40	0.75	A	225/67	2	3	2-5-8-1
28	3.00	OOR	O	044/60	2	3	2-5-8-1
29	3.05	1.10	A	220/55	3	3	2-6-8-1
30	3.46	-	-	032/70			
31	3.53	0.80	A	0.11/75	2	3	2-7-1-1
32	3.67	0.80	A	022/60	2	3	2-7-1-1
33	3.80	0.84	A	058/65	2	3	2-7-1-1
34	4.40	0.75	A	055/60	2	3	2-6-8-1
35	4.40	0.76	A	030/62	2	3	2-6-8-1
36	4.50	0.52	A	050/60	2	3	2-6-8-1
37	4.14	1.20	A	190/34	2	3	2-6-8-1
38	4.85	1.50	A	018/82	2	2	2-6-8-1
39	1.15	OOR	O	057/63	4	3	2-7-1-1
40	5.17	OOR	O	284/40	2	3	2-4-8-1
41	5.37	OOR	O	044/84	2	3	2-6-8-1
42	5.75	OOR	O	150/75	2	3	2-4-8-1
43	0.66	0.40	A	252/65	2	3	2-7-1-1
44	0.84	0.90	A	264/65	2	3	2-7-1-1
45	1.30	0.80	A	277/68	2	3	2-7-1-1
46	2.03	OOR	O	270/65	3	4	2-7-1-1
47	2.55	OOR	O	305/10	2	3	2-6-1-1
48	2.95	0.10	A	014/65	-	-	-
49	3.20-7.40						lead lens
	7.57						2-7-1-1
50	7.75	1.50	I	325/15	4	3	2-7-1-1
51	8.24	0.20	A	026/65	3	3	2-7-1-1
52	8.75	1.10	A	045/30	4	3	2-6-1-1

53	9.40	2.00	A	330/15	2	2	2-6-1-1
54	9.55	OOR	O	342/75	2	3	2-7-1-1
55	9.55	0.80	I	226/30	2	3	2-7-1-1
56		-	O	266/30	2		
57	0.00	OOR	O	166/70	2	3	-
58	0.20	0.20	A	090/65	3	3	2-6-1-1
59	0.28	OOR	O	085/85	2	3	2-6-1-1
60	0.48	OOR	O	150/75	2	3	2-7-1-1
61	0.58	0.35	A	268/75	2	2	2-7-1-1
62	1.20	OOR	O	160/77	4	3	2-7-1-1
							Crushed zone
63							2-7-1-1
64	2.60	-	-	190/35	3	3	-
65	3.00	2.10	A	268/50	-	-	-
66	3.05	-	-	256/40	-	-	-
67	3.63	0.50	I	137/85	-	-	-
68	4.77	0.30	A	262/75	-	-	rich orebody
69	5.20						2-5-8-1 Q
70							2-5-8-1 Q
71	5.70	OOR	O	280/75	3	3	2-7-1-1
72	6.37	0.40	A	275/75	3	2	2-7-1-1
73	6.94	-	A	048/85	4	3	End of
74	7.22	-	A	048/80	4	4	orebody
75	9.90						2-7-1-1
76							2-7-1-1
77	10.05	0.15	A	242/70	2	2	2-7-1-1
78	10.09	0.25	A	265/75	2	2	2-7-1-1
79	10.15	-	A	260/70	2	2	2-7-1-1
80	10.28	0.70	I	259/75	2	2	2-7-1-1
81	10.65	1.20	A	265/75	2	2	2-7-1-1
82	10.97	0.25	A	272/70	2	2	2-7-1-1
83	11.03	0.30	A	270/60	2	2	2-7-1-1
84	11.07	0.45	A	270/65	2	3	2-7-1-1
85	11.34	1.50	I	316/15	2	4	2-7-1-1

86	11.55	1.50	I	245/65	3	3	
87	11.85	0.50	A	238/62	3	3	
88	0.31	-	I	009/80	3	3	2-7-1-2
89	1.75	0.50	A	350/08	3	3	2-7-1-2
90	2.85	0.45	A	359/56	3	4	2-7-1-2
91	3.55	>2.00	A	335/67	4	4	2-5-1-2
92	4.90	1.95	I	340/75	4	4	2-6-1-1
93	5.44	1.65	I	350/77	3	3	2-6-1-2
94	6.75	-	I	302/08	3	2	2-7-1-2
95	7.60	-	I	232/20	3	3	2-7-1-1
96	8.10	1.05	A	167/45	3	2	2-7-1-2
97	8.22	1.00	A	167/45	3	2	2-7-1-2
98	8.40	0.50	A	235/55	3	2	2-7-1-2
99	9.31	OOR	O	172/55	3	3	2-7-1-2
100	9.90	2.00	A	216/48	3	3	2-7-1-2
101	10.20	0.40	A	178/60	3	3	2-7-1-2
102	10.50	0.40	A	020/05	2	2	2-7-1-2
103	11.55	0.20	A	200/75	2	2	-
104	12.25	0.40	A	340/84	2	2	2-7-1-2
105	12.44	OOR	O	164/80	3	3	2-7-1-2
106	12.66	-	I	358/86	-	-	-
107	12.96	0.25	A	010/75	3	3	2-7-1-1
108	14.06	0.60	A	210/05	2	2	2-7-1-1
109	12.10	0.30	A	140/80	2	2	2-7-1-1
110	12.14	OOR	O	140/80	2	2	2-5-8-1 Q
111	12.37	1.05	A	262/82	2	2	2-7-1-1
112	12.45	1.00	A	275/80	3	3	2-7-1-1
113	12.70	OOR	O	266/87	3	3	2-5-8-1 Q
114	12.95	0.50	A	270/70	3	2	2-7-1-1
115	13.30	OOR	O	262/77	2	2	2-7-1-1
116	13.60	0.46	I	302/25	3	3	2-7-1-1
117	13.60	OOR	O	302/88	3	2	2-7-1-1
118	13.69	1.00	A	108/50	4	3	2-7-1-1

119	14.30	2.06	A	264/75	3	3	2-7-1-1
120	14.80	OOR	O	140/70	2	3	2-7-1-1
121	15.00	0.20	A	105/60	2	2	2-7-1-1
122	15.10	0.35	A	264/70	2	2	2-7-1-1
123	15.48	2.50	I	138/62	2	3	2-7-1-1
124	15.61	0.20	A	0.82/80	2	2	2-7-1-1
125	15.80	1.00	A	268/75	2	2	2-7-1-1
126	15.80	OOR	O	018/05	2	2	2-7-1-1
127	15.90	0.20	A	272/80	2	2	2-7-1-1
128	16.40	0.50	A	256/75	3	2	2-7-1-1
129	16.90	1.00	A	236/70	3	2	2-7-1-1
130	0.00	-	I	289/25	1	2	2-7-1-1
131	0.26	0.50	-	278/14	4	2	2-7-1-1
132	0.55	2.20	A	261/15	2	2	2-6-8-1
133	0.72	0.47	A	300/35	2	2	2-7-1-1
134	1.40	1.40	O	340/66	3	3	2-5-8-1
135							
136	0.35	0.50	A	140/45	2	2	2-7-1-1
137	0.47	0.47	A	270/38	2	2	2-7-1-1
138	0.66	0.76	A	310/81	2	2	2-7-1-1
139	0.85	0.51	-	215/81	2	2	2-7-1-1
140	0.38	2.90	-	185/65	-	-	2-7-1-1
141	0.85	3.10	A	120/81	3	3	2-7-1-1
142	0.85	2.00	A	220/10	3	3	2-7-1-1
143	1.15	1.20	I	190/05	3	3	2-7-1-1
144	0.20	1.86	I	235/28	2	2	2-7-1-1
145	0.40	0.60	I	028/35	3	3	2-7-1-1
146	0.45	0.85	A	150/05	3	3	2-7-1-1
147	0.70	2.07	A	262/79	3	3	2-7-1-1
148	1.20	1.05	A	160/08	2	2	2-7-1-1
149	1.20	1.50	A	340/62	3	2	2-7-1-1

150	0.55	3.40	I	272/22	3	3	2-6-8-1 Q
151	1.90	-	-	334/18	3	3	2-5-8-1
152	0.10	0.75	A	235/25	2	2	2-7-1-1
153	0.19	0.7	A	080/05	2	3	2-7-1-1
154	0.30	0.50	I	248/40	2	2	2-7-1-1
155	0.48	0.42	I	276/58	2	2	2-7-1-1
155	0.70	0.82	I	040/28	2	2	2-7-1-1
156	0.75	2.45	I	213/40	2	2	2-5-1-1
157	0.85	1.0	I	083/31	2	2	2-7-1-1
158	1.20	1.50	I	250/15	2	2	2-7-1-1
159	1.50	0.50	I	2285	2	2	2-7-1-1
160	1.80	OOR	O	224/47	2	3	2-7-1-1
161	1.50	3.10	I	283/63	2	3	2-6-8-1Q
162	0.55			072/73	3	3	2-7-1-1
164	1.0	1.90	I	230/11	3	3	2-7-1-1
165	1.20	OOR	I	254/30	3	3	2-7-1-1
166	1.30	4.04	OOR	230/15	3	3	2-5-8-1
167	.17	2.45	I	246/28	2	2	2-7-1-2
168	0.35	1.02	I	305/07	2	2	2-7-1-1
169	0.50	0.70	A	192/53	2	2	2-7-1-1
170	0.95	OOR	OOR	242/38	3	2	2-5-1-2
171	1.60	OOR	OOR	330/83			
172	0.00	OOR	OOR	217/56	2	2	2-7-1-2
173	0.40	OOR	OOR	294/15	2	2	2-7-1-2
174	0.65	0.90	A	355/85	2	3	1-7-1-1
175	1.25	3.00	A	336/0	2	3	2-7-1-2
176	1.40	3.00	A	024/10	2	3	2-7-1-2
177	1.30	1.00	I	286/14	2	2	2-7-1-2
178	1.45	OOR	OOR	046/88	2	2	2-7-1-1
179	0.60			330/74			

180	1.60	1.00	A	298/70	2	2	2-5-8-1
181	1.909	OOR	OOR	146/82	2	2	2-7-1-1
182	1.05	2.25	A	206/30	2	2	2-7-1-1
183	0.46	0.60	I	300/25	2	2	2-5-8-1
184	0.55	1.60	I	300/25	2	2	2-7-1-1
185	0.72	0.85	I	300/25	3	3	2-7-1-1
186	0.95	OOR	OOR	338/72	3	3	2-7-1-1
187	0.17	OOR	OOR	268/82	2	2	2-5-8-1
188	0.75	0.27	I	294/25	2	3	2-7-1-1
189	0.95	0.30	I	024/63	3	2	2-7-1-1
190	1.95			278/85	3	2	2-6-8-1
191	0.40	0.55	I	135/0	2	2	2-7-1-1
192	0.20	0.55	I	135/0	2	2	2-7-1-1
193	0.55	1.25	A	136/70	2	2	2-5-8-1
194	1.32	1.52	OOR	133/80	3	3	2-5-8-1
195	1.70	1.30	I	118/78	3	3	2-7-1-1
196	1.55	O	O	090/0	3	3	2-7-1-1

APPENDIX-2

RESULTS OF SCANLINE SURVEY FROM THE CSA MINE, COBAR

Location: the 69NE2 stope
Data: 18/07/91
Rock Type: Siltstone -Black chlorite
-Talc
-Ore (mainly chalcopyrite)
Scanline Orientation: N024°E (horizontal)

NO.	D(m)	L(m)	T	Orientation	C	R	Comments
1	0.12	0.70	I	092/80	1	1	3-7-1-1
2	0.31	0.67	I	074/80	1	1	3-7-1-1
3	0.55	0.94	I	090/79	1	1	3-7-1-1
4	0.85	0.76	A	102/80	1	1	3-7-1-1
5	1.05	2.05	I	098/75	4	1	3-7-1-1
6	1.13	0.50	A	108/82	1	1	3-7-1-1
7	1.16	2.26	I	257/56	4	-	3-4-8-1 Q
8	1.20	0.04	A	240/75	3	3	3-7-1-1
9	1.38	0.26	A	116/67	4	1	3-7-1-1
10	1.43	0.24	A	115/84	2	2	3-7-1-1
11	1.51	0.85	I	226/63	2	2	3-7-1-1
12	2.08	OOR	O	098/70	4	1	3-7-8-1 Q
13	2.20	0.45	O	288/76	4	2.5	3-7-1-1
14	2.29	1.10	A	116/80	2	1	3-9-1-1
15	3.00	0.22	A	095/75	2	1	3-7-1-1
16	3.23	OOR	O	091/90	2	1	3-7-1-1
17	3.23	OOR	O	083/80	1	2	3-9-1-1
18	3.43	OOR	O	298/65	3	2	3-7-1-1
19	3.61	OOR	O	114/80	3	2	3-9-1-1
20	3.68	0.48	A	286/89	2	2	3-7-1-1
21	3.82	0.02	A	114/80	3	1	3-9-1-1
22	3.83	OOR	O	102/85	2	1	3-7-1-1

23	4.01	OOR	O	346/68	4	1	3-9-1-1
24	4.12	OOR	O	132/67	4	2	3-9-1-1
25	4.25	OOR	O	125/90	4	1	3-7-1-1
26	4.43	OOR	A	071/80	1	1	3-7-1-1
27	4.73	OOR	A	094/82	3	1	3-7-1-1
28	4.84	0.55	O	274/90	3	1	3-7-1-1
29	4.86	0.45	O	094/87	1	1	3-7-1-1
30	4.93	OOR	A	250/74	1	1	3-7-1-1
31	5.04	OOR	O	106/89	1	1	3-7-1-1
32	5.05	0.46	I	094/90	2	1	3-7-1-1
33	6.10	OOR	A	118/86	2	1	3-7-1-1
34	6.15	1.20	O	100/89	2	1	3-7-1-1
35	6.48	1.00	A	110/89	2	1	3-7-1-1
36	6.52	OOR	A	242/76	3	1	3-7-1-1
37	6.61	0.60	I	008/87	2	1	3-7-1-1
38	6.71	1.10	I	094/89	2	1	3-7-1-1
39	7.06	1.00	A	216/69	3	1	3-7-1-1
40	8.95	0.77	A	120/68	3	1	3-7-1-1
41	9.07	0.08	A	245/75	3	1	3-5-1-1
42	9.49	0.30	O	248/75	3	1	3-5-1-1
43	9.57	OOR	A	090/88	3	1	3-7-1-1
44	9.65	0.28	A	090/83	3	1	3-7-1-1
45	0.45	-	O	073/90	2	2	3-7-1-1
46	1.27	3.65	A	184/20	3	3	2-7-1-1
47	1.27	0.90	O	138/82	3	2	3-7-1-1
48	1.42	0.70	O	122/84	3	2	3-7-1-1
49	1.84	0.20	O	084/86	3	2	3-7-1-1
50	o.23	1.50	A	102/88	2	2	3-7-1-1
51	1.01	1.60	O	120/79	3	3	3-7-1-1
52	1.01	1.60	O	244/66	3	3	3-7-1-1
53	1.29	0.45	I	102/82	3	2	3-7-1-1
54	1.54	0.90	O	296/90	3	3	3-7-1-1

55	1.54	0.90	O	231/72	3	3	3-7-1-1
56	1.65	0.55	O	102/75	3	3	3-7-1-1
57	1.89	0.70	O	0.90/87	2	2	3-7-1-1
58	1.89	0.70	O	090/85	3	2	3-7-1-1
59	0.49	0.53	-	022/60	3	3	3-7-1-1
60	0.54	1.95	-	256/75	2	2	3-7-1-1
61	0.61	1.85	-	248/75	3	2	3-7-1-1
62	0.73	0.13	I	120/12	2	2	3-7-1-1
63	0.98	1.50	-	100/85	2	2	3-7-1-1
64	1.81	0.70	O	230/55	2	2	3-7-1-1
65	2.24	-	O	270/85	3	3	3-7-1-1
66	2.59	-	O	270/85	2	2	3-7-1-1
67	1.04	0.28	I	057/76	2	1	3-7-1-1
68	1.57	-	O	032/10	3	3	2-7-1-1
69	1.74	0.43	A	210/62	1	1	3-7-1-1
70	1.84	0.20	A	214/68	2	3	3-7-1-1
71	0.63	0.62	O	145/66	2	2	3-7-1-1
72	0.83	0.56	O	235/66	2	2	3-7-1-1
73	0.59	1.30	O	285/85	3	2	3-7-1-1
74	1.20	0.65	A	293/05	2	2	3-7-1-1
75	2.40	0.22	O	246/72	2	2	3-7-1-1
76	0.40	0.15	A	332/86	2	2	3-7-1-1
77	0.45	0.27	A	141/73	2	2	2-6-8-1 Q
78	0.50	0.22	A	320/48	2	1	-
79	0.50	1.45	O	068/60	3	2	2-4-8-1
80	0.55	0.22	A	104/73	2	1	2-6-8-1
81	0.56	0.20	A	102/73	2	1	2-6-8-1
82	0.57	1.45	A	100/76	2	2	2-4-8-1
83	0.59	0.10	A	288/84	2	1	2-6-8-1
84	0.63	0.16	I	259/75	2	1	2-5-8-1

85	0.64	0.11	I	130/85	2	1	2-6-8-1
86	0.65	0.08	I	132/75	2	1	2-6-8-1
87	0.70	0.75	A	088/66	2	1	2-5-8-1
88	0.75	0.08	A	078/83	2	1	2-6-8-1
90	0.76	0.12	A	104/71	2	1	2-6-8-1
91	0.84	0.26	I	275/75	2	1	2-4-8-1
92	0.86	0.26	I	275/75	2	1	2-4-8-1
93	0.89	1.10	O	122/68	2	2	2-3-8-1
94	1.01	0.46	A	120/75	2	1	2-6-8-1
95	1.04	0.30	A	118/74	2	1	2-6-8-1
96	1.05	-	-	118/75	-	-	-
97	1.06	-	-	130/68	-	-	-
98	1.07	-	O	112/73	-	-	2-1-8-1
99	1.44	0.50	A	112/73	2	1	2-5-8-1
100	1.46	0.50	A	100/68	2	1	2-5-8-1
101	1.52	0.66	A	100/68	2	1	2-4-8-1
102	1.54	0.05	-	-	-	-	-
103	1.61	1.44	I	084/75	2	1	2-4-8-1
104	1.67	0.38	A	253/75	1	1	3-7-1-1
105	1.71	0.32	I	244/80	1	1	3-7-1-1
106	1.72	0.34	I	110/82	2	1	2-5-8-1
107	1.88	1.04	I	108/77	1	2	3-7-1-1
108	2.00	0.80	I	106/84	2	2	2-7-8-1
109	2.20-						Ore Zone
	2.80						
110	2.89	0.42	I	242/82	1	1	3-7-1-1
111	3.02	0.93	I	242/85	1	1	3-7-1-1
112	3.08	0.66	I	097/84	2	1	2-5-8-1 Q
113	3.11	0.11	A	260/89	1	1	3-7-1-1
114	3.12	0.13	A	260/89	2	1	3-7-1-1
115	3.18	0.21	A	247/85	1	1	3-7-1-1
116	3.32	0.40	A	246/83	1	1	3-7-1-1
117	3.45	0.40	O	230/89	1	1	3-7-1-1
118	3.48-						Shear zone

119	3.90						3-7-1-1
120	4.00	0.24	A	248/90	1	1	3-7-1-1
121	4.08	0.56	A	080/90	2	1	3-7-1-1
122	4.10	0.44	A	258/88	2	1	3-7-1-1
123	4.13	1.24	A	258/86	2	1	3-7-1-1
124	4.22	1.24	A	252/86	2	1	3-7-1-1
125	4.29	0.15	I	092/78	1	1	3-7-1-1
126	4.30	0.27	A	250/85	2	1	2-6-8-1
127	4.32	0.70	I	090/76	1	1	3-7-1-1
128	4.38	2.50	A	250/85	2	1	3-7-1-1
129	4.38	-	O	098/80	2	1	3-7-8-1 Q
130	4.44	0.38	A	094/80	1	1	3-7-1-1
131	4.52	0.50	A	102/80	1	1	3-7-1-1
132	4.58	0.97	A	266/88	1	1	-
133	4.65	0.72	A	098/84	1	1	-
134	4.70	0.18	A	078/90	3	1	-
135	4.70	0.87	A	090/75	2	1	-
136	4.73	0.65	I	104/86	2	1	-
137	4.82	0.90	O	262/32	2	2	-
138	4.82	-	O	068/89	-	-	3-7-1-1
139	4.94	0.42	O	079/84	2	1	2-6-8-1
140	5.18	1.00	A	260/30	1	1	3-7-1-1
141	5.20	0.50	O	100/80	2	1	2-5-8-1
142	5.20	0.92	I	082/90	2	1	3-7-1-1
143	5.21	0.49	O	100/80	2	2	2-5-8-1
144	5.25	1.45	A	261/32	2	1	3-7-1-1
145	5.35	0.60	A	082/86	1	1	3-7-1-1
146	5.41	0.62	A	090/82	1	1	2-6-8-1
147	5.45	0.75	A	070/90	1	1	3-7-1-1
148	5.56	1.05	I	096/80	1	1	3-7-1-1
149	5.68	1.15	A	074/86	2	1	3-7-1-1
150	5.70	0.90	I	246/29	1	1	3-7-1-1
151	5.70	-	O	296/76	1	1	2-4-8-1
152	5.72	2.50	I	088/66	1	1	2-5-8-1

153	5.78	2.57	I	080/78	2	1	2-5-8-1
154	5.78	2.05	A	265/30	2	1	3-7-1-1
155	5.80	0.82	I	076/86	2	1	2-6-8-1
156	5.86	1.00	I	290/86	2	1	2-6-8-1
157	5.92	0.50	A	278/25	1	1	3-7-1-1
158	5.93	-	O	078/88	1	1	3-7-1-1
159	5.95	2.80	I	062/60	2	1	2-4-8-1
160	6.09	1.50	I	072/75	1	1	2-5-8-1
161	6.16	-	O	078/76	2	1	2-4-8-1
162	6.23	-	O	068/84	3	1	2-4-8-1
163	6.23	1.52	I	260/29	1	1	3-7-1-1
164	6.45	-	O	068/84	1	1	3-7-1-1
165	6.49	-	O	068/84	1	1	3-7-1-1
166	6.50	-	I	260/90	1	1	3-7-1-1
167	6.69	-	O	066/90	1	1	3-7-1-1
168	6.79	0.30	A	102/78	2	1	2-5-8-1
169	6.80	0.30	A	102/78	2	1	2-5-8-1
170	6.80	0.82	A	265/30	1	1	3-7-1-1
171	6.85	0.46	A	260/32	1	1	3-7-1-1
172	6.90	0.73	A	098/76	4	2	2-5-8-1
173	6.95	0.87	A	090/72	4	2	2-5-8-1
174	7.15-						Q
	7.36						
175	7.36-			089/88			#
176	7.59						
177	7.60	1.00	A	086/70	2	2	2-4-8-1
178	7.65	-		088/68	2	2	
179	7.65			069/78			
180	7.95	0.50	O	262/32	1	1	3-7-1-1
181	8.10	1.80	A	264/31	1	1	3-7-1-1
182	8.20	1.85	A	262/34	1	1	3-7-1-1

parallel small joints.